

FINAL PROGRAM

PMP III



Third International Conference
Processing Materials for Properties

*The Materials Processing
Technology Forum*

December 7-10, 2008
Bangkok, Thailand

Sponsored by

TMS



MTEC 
a member of NSTDA

WELCOME TO PMP III...

...The Materials Processing Technology Forum

This Third International Conference on Processing Materials for Properties provides you with the opportunity for information exchange and fruitful collaborations on state-of-the-art materials processing technologies being developed around the globe. In addition to the technical sessions, we hope you will take advantage of all this conference offers you:

Special Presentations

Monday

“Sustainable Nanofoundation for Green Society”
by Professor Somsak Panyakaew,
Chulalongkorn University, Thailand

“New Development in Natural Rubber Processing”
by Professor Krisda Suchiva, MTEC, Thailand

Tuesday

“Physical Chemistry of Aqueous Processing
on Materials Surface”
by Professor Yasuhiro Awakura, Kyoto University;
President, MMIJ, Japan

“Separation Process of Precious Metals”
by Professor Junji Shibata, Kansai University, Japan

Wednesday

“Materials Science for the New Generation”
by Professor David Olson, Colorado School of Mines,
United States

“Innovations in Processing of Lightweight Metal
Matrix Composites”
Professor Ramana G. Reddy, University of Alabama,
United States

Exhibition

Hours: Monday through Wednesday, 9 a.m. to 6 p.m.

Be sure to visit the exhibition to learn about the latest products and services in materials processing technologies.

Networking and Social Events

Network with colleagues at these special events!

- Welcome Reception (Sunday)
- Coffee Breaks (Monday through Wednesday)
- Lunch (Tuesday and Wednesday)
- Conference Banquet (Monday)

These events are included as part of your registration. Guests may purchase tickets at the conference registration desk.

Table of Contents	Page
Schedule of Events.....	3
Floor Plans	4
Conference Organizers.....	6
Technical Program	10
Proceedings.....	71

Schedule of Events

Key: SCP = Sofitel Centara Plaza / BCC – Bangkok Convention Center

Sunday	Time	Building / Room
Registration	4:30 to 8 p.m.	SCP / Sala Thai, Lower Lobby
Welcome Reception	6 to 8 p.m.	SCP / Sala Thai, Lower Lobby

Monday	Time	Building / Room
Registration	8:30 a.m. to 4 p.m.	BCC / Auditorium B2, 4th Floor
Opening Ceremony	9:30 to 9:50 a.m.	BCC / Auditorium B2, 5th Floor
Plenary Lecture	9:50 to 10:35 a.m.	BCC / Auditorium B2, 5th Floor
Coffee Break/Poster Session.	10:35 to 11 a.m.	BCC / Regency Area, 4th Floor
Technical Session	11 a.m to 12:40 p.m.	BCC / 4th and 5th Floors
Keynote Speech	2 to 2:45 p.m.	BCC / Auditorium B2, 5th Floor
Technical Session	2:45 to 4:05 p.m.	BCC / 4th and 5th Floors
Coffee Break/Poster Session.	4:05 to 4:30 p.m.	BCC / Regency Area, 4th Floor
Technical Sessions	4:30 to 5:50 p.m.	BCC / 4th and 5th Floors
Cocktail Reception.	6 to 6:30 p.m.	SCP / Vibhavadee Ballroom B, Lobby Level
Conference Banquet	6:30 to 8 p.m.	SCP / Vibhavadee Ballroom B, Lobby Level

Tuesday	Time	Building / Room
Registration	8:30 a.m. to 4 p.m.	BCC / Auditorium B2, 4th Floor
Plenary Lecture	9:30 to 10:15 a.m.	BCC / Auditorium B2, 5th Floor
Coffee Break/Poster Session.	10:15 to 10:40 a.m.	BCC / Regency Area, 4th Floor
Technical Sessions	10:40 a.m. to 12:20 p.m.	BCC / 4th and 5th Floors
Lunch.	12:20 to 2 p.m.	BCC / Auditorium A2, 5th Floor
Keynote Speech	2 to 2:45 p.m.	BCC / Auditorium B2, 5th Floor
Technical Sessions	2:45 to 4:05 p.m.	BCC / 4th and 5th Floors
Coffee Break/Poster Session.	4:05 to 4:30 p.m.	BCC / Regency Area, 4th Floor
Technical Sessions	4:30 to 5:50 p.m.	BCC / 4th and 5th Floors

Wednesday	Time	Building / Room
Registration	8:30 to 11 a.m.	BCC / Auditorium B2, 4th Floor
Plenary Lecture	9:30 to 10:15 a.m.	BCC / Auditorium B2, 5th Floor
Coffee Break/Poster Session.	10:15 to 10:40 a.m.	BCC / Regency Area, 4th Floor
Technical Sessions	10:40 a.m. to 12:20 p.m.	BCC / 4th and 5th Floors
Lunch.	12:20 to 2 p.m.	BCC / Auditorium A2, 5th Floor
Keynote Speech	2 to 2:45 p.m.	BCC / Auditorium B2, 5th Floor
Technical Sessions	2:45 to 4:05 p.m.	BCC / 4th and 5th Floors
Coffee Break/Poster Session.	4:05 to 4:30 p.m.	BCC / Regency Area, 4th Floor
Technical Sessions	4:30 to 5:30 p.m.	BCC / 4th and 5th Floors
Closing Address	5:30 to 6 p.m.	BCC / Auditorium B2, 5th Floor

Note: A tour desk is located near registration (BCC / Auditorium B2, 4th Floor).

Meeting Policies



Americans With Disabilities Act

TMS strongly supports the federal Americans with Disabilities Act (ADA) which prohibits discrimination against, and promotes public accessibility for, those with disabilities. In support of ADA, we ask those requiring specific equipment or services to see a TMS representative at the PMP registration desk.

Audio/Video Recording Policy

TMS reserves the right to all audio and video reproductions of presentations at TMS sponsored meetings. Recording of sessions (audio, video, still photography, etc.) intended for personal use, distribution, publication or copyright without the express written consent of TMS and the individual authors is strictly prohibited.

Refund Policy for PMP Conference Registration

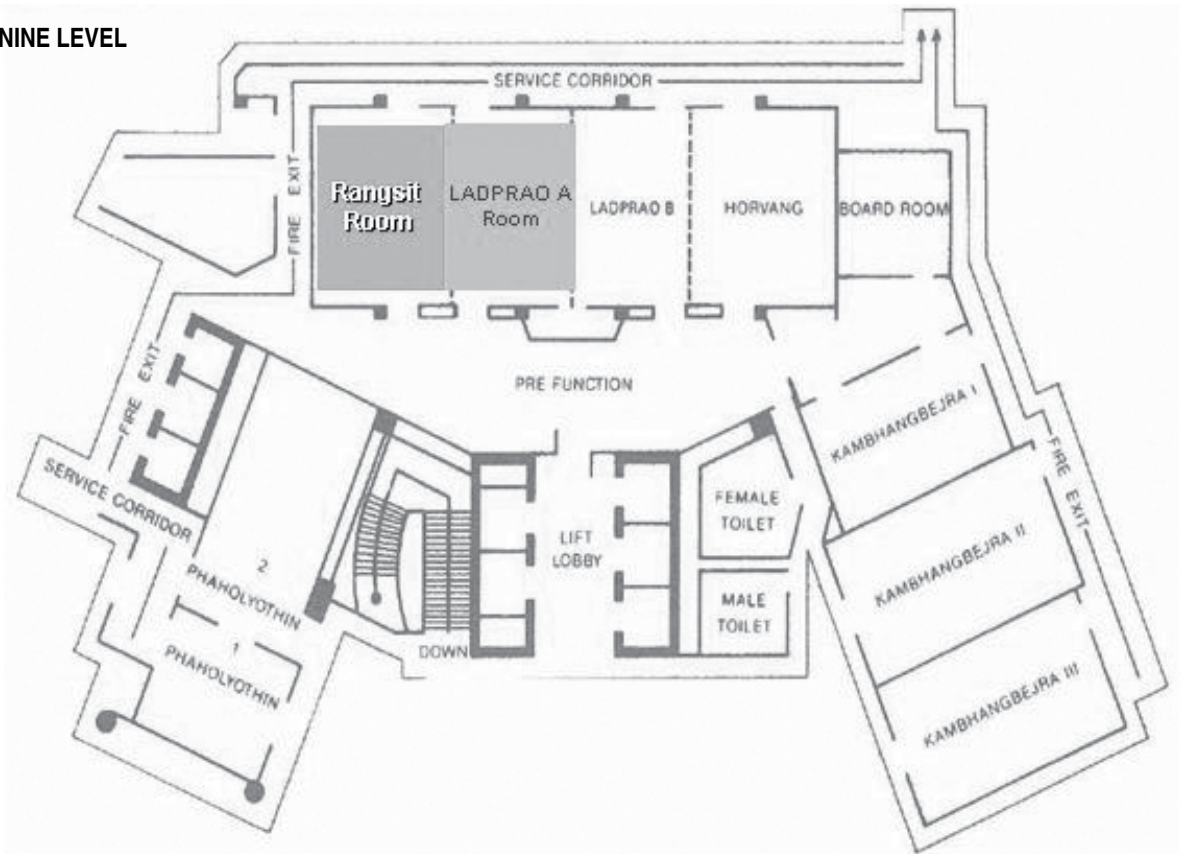
The deadline for all refunds was November 3, 2008. No refunds are issued after the deadline. All fees and tickets are nonrefundable.

Sofitel Centara Plaza

LOBBY LEVEL

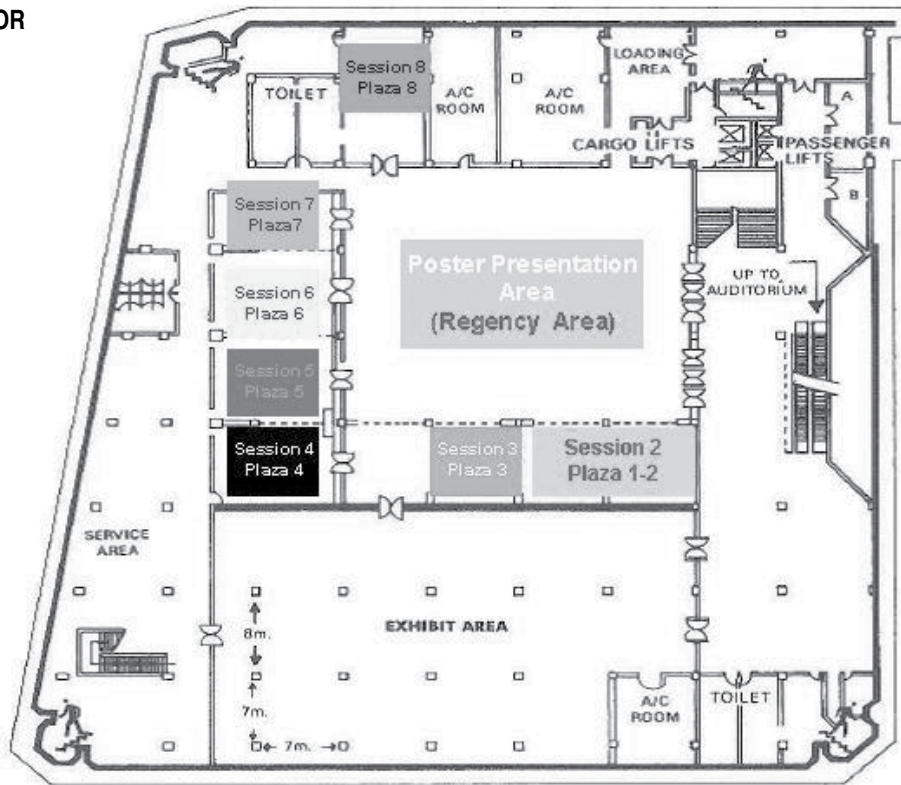


MEZZANINE LEVEL

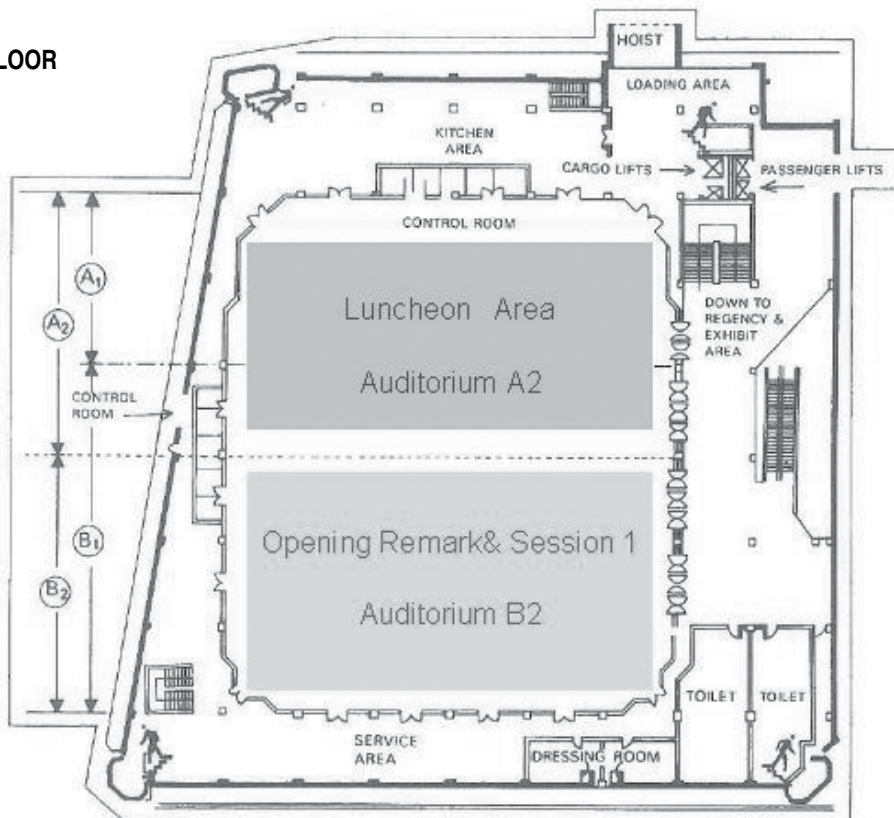


Bangkok Convention Centre

4th FLOOR



5th FLOOR



PMP thanks the following individuals and organizations for making this international conference possible.

Conference Co-Chairs

Dr. Paritud Bhandhubanyong, National Metal and Materials Technology Center
Professor Akio Fuwa, Waseda University
Professor Brajendra Mishra, Colorado School of Mines

Organizational Sponsors

The Minerals, Metals & Materials Society
Mining and Materials Processing Institute of Japan
National Metals and Materials Technology Center of Thailand

Organizational Co-Sponsors

ASM International
Canadian Institute of Mining & Metallurgy
Ceramic Society of Japan
Indian Institute of Metals
Institute of Materials Science, Vietnamese Academy of Science & Technology
Japan Institute of Metals
Materials Australia
Minerals, Metals & Materials Technology Centre, National University of Singapore
Society of Mining, Metallurgy, Resource, and Environmental Technology (Germany)
South African Institute of Mining and Metallurgy
The Korean Institute of Metals and Materials

International Organizing Committee

Professor Somsak Panyakaew, Chulalongkorn University
Professor Thiraphat Vilaithong, Chiangmai University
Professor Sukit Limpijumngong, Suranaree University of Technology
Professor Wiwut Tantapanichkun, National Nanotechnology Center
Professor Toshiharu Fujisawa, Nagoya University
Professor Takashi Nakamura, Tohoku University
Professor Junji Shibata, Kansai University
Mr. Susumu Okabe, MMIJ Secretary General
Dr. John Smugeresky, Sandia National Laboratory
Professor Sreeramamurthy Ankem, University of Maryland
Professor Eric Taleff, University of Texas
Dr. Patrice Turchi, Lawrence Livermore National Laboratory

International Steering Committee

Professor Supot Harnnongbua, Chulalongkorn University
Professor Fumitaka Tsukihashi, The University of Tokyo
Professor Tawee Tunkasiri, Chiangmai University
Professor Tetsuji Hirato, Kyoto University
Professor Narongrit Sombatsompop, King Mongkut's University of Technology Thonburi
Professor Diran Apelian, Worcester Polytechnic Institute
Professor Joydeep Dutta, Asian Institute of Technology
Dr. Subodh Das, Phinix LLC
Professor Shinya Matsuo, Osaka University
Dr. Edgar Vidal, Colorado School of Mines
Professor Masayasu Kawahara, Kumamoto University

International Advisory Committee

- Professor Sakarindr Bhumiratana, National Science and Tech. Development Agency
 Professor Katsuhiko Kaneko, Hokkaido University
 Dr. Nongluck Pankurdee, Thailand Institute of Scientific and Technological
 Dr. Haruhiko Asao, Mitsubishi Materials Corporation
 Dr. Veerapong Pae-suwan, The National Synchrotron Research Center
 Mr. Toshio Kurikami, Toho Zinc Co. Ltd.
 Dr. Veera Pholawat, Thai Army and MTEC Board
 Mr. Masaki Kohno, Dowa Holdings Co. Ltd.
 Professor Krisda Suchiva, MTEC and Mahidol University
 Professor Yoshio Waseda, Tohoku University
 Professor Pramote Dechaumphai, MTEC and Chulalongkorn University
 Professor Takateru Umeda, Chulalongkorn University
 Professor Lerkiat Vongsarnpikoon, National Science and Tech. Development Agency
 Mr. Naoaki Ogawa, Mitsui Mining and Smelting Co. Ltd.
 Professor Siriluck Nivitchanyong, National Metal and Materials Technology Center
 Professor Barry Muddle, Materials Australia
 Dr. Somnuk Sirisoonthorn, National Metal and Materials Technology Center
 Dr. Dongwha Kum, Korean Institute of Metals & Materials
 Dr. Krissanapong Kiratikorn, Commission on Higher Education
 Professor Chris Pistorius, South African Institute of Mining and Metallurgy
 Mr. Wikrom Vajragupta, Iron and Steel Institute of Thailand
 Mr. Michael Stelter, Society for Mining Metallurgy Resource and Environmental Technology
 Dr. Chatchai Somsiri, Thainox Stainless Public Co. Ltd.
 Dr. Srikumar Banerjee, Indian Institute of Metals
 Dr. Narong Akkrakitayakoon, Suranaree University of Technology
 Dr. Robert Shull, National Institute of Standards & Technology
 Professor Werusak Udomkichdecha, National Metal and Material Technology Center
 Dr. Garry Warren, University of Alabama
 Professor Chikabumi Yamauchi, Chubu University
 Dr. Warren Hunt, The Minerals, Metals & Materials Society
 Professor Yasuhiro Awakura, Kyoto University
 Mr. Kazuo Oki, Nippon Mining Holdings Inc.
 Dr. Anthony Pengidore, S/D Engineers
 Professor Masafumi Maeda, The University of Tokyo
 Dr. Joy Hines, Ford Motor Company
 Professor Emeritus Takeo Oki, Nagoya University
 Dr. Wolfgang A. Schneider, Hydro Aluminium GmbH
 Mr. Koichi Fukushima, Sumitomo Metal Mining Co. Ltd.
 Dr. Robert L. Stephens, Teck Cominco Metals Ltd.
 Professor Hisaaki Fukushima, Kyushu University
 Professor Diran Apelian, Worcester Polytechnic Institute
 Professor Emeritus Kimio Itagaki, Tohoku University
 Dr. James C. Foley, Los Alamos National Laboratory
 Mr. Yasuo Tamura, Japan Mining Industry Association
 Dr. Ray D. Peterson, Aleris International Inc.

International Scientific Committee

- Professor Supatra Jinawat, Chulalongkorn University
 Dr. Rittirong Pruthitkul, National Metal and Materials Technology Center
 Dr. Pradip, Tata R&D Design Center and Tata Consultancy Service Ltd.
 Professor Supasarote Muensit, Prince of Songkla University
 Dr. Pasaree Laokijcharoen, National Metal and Materials Technology Center
 Professor Yasuo Uchiyama, Nagasaki University
 Dr. Noppawan Tanpipat, National Nanotechnology Center

International Scientific Committee Continued

- Dr. Kuljira Sujiroj, National Metal and Materials Technology Center
Professor Yukihiko Sakamoto, Chiba Institute of Technology
- Dr. John T.H. Pearce, National Metal and Materials Technology Center
Professor Sirithan Jiemsirilers, Chulalongkorn University
Professor Kazuharu Yoshizuka, The University of Kitakyushu
- Dr. Anchalee Manonukul, National Metal and Materials Technology Center
Dr. Thanakorn Wasanapiarnpong, Chulalongkorn University
Professor Masato Kakihana, Tohoku University
Assistant Professor Ashutosh Tiwari, University of Utah
Professor Tawatchai Charinpanitkul, Chulalongkorn University
Associate Professor Yasushi Sasaki, Tohoku University
- Dr. Sumittra Charojrochkul, National Metal and Materials Technology Center
- Dr. Julathep Kajornchaiyakul, National Metal and Materials Technology Center
Associate Professor Tomio Takasu, Kyushu Institute of Technology
- Dr. Pongsak Dulyapraphant, National Metal and Materials Technology Center
- Dr. Pavadee Aungkavattana, National Metal and Materials Technology Center
Professor Yuichi Ikuhara, The University of Tokyo
Professor Narin Sirikulrat, Chiang Mai University
- Dr. Nuwong Chollacoop, National Metal and Materials Technology Center
Professor Norihiko Fukatsu, Nagoya Institute of Technology
- Dr. Siriporn Rojananan, King MongKut's University of Technology Thonburi
- Professor Nuchthana Poolthong, King MongKut's University of Technology Thonburi
Professor Hideyuki Yasuda, Osaka University
- Dr. Tippaban Palathai, King MongKut's University of Technology Thonburi
Dr. Saisamorn Niyomsoan, Burapa University
Professor Masahiro Yoshimura, Tokyo Institute of Technology
- Dr. Sukasem Kangwantrakoon, Suranaree University of Technology
Professor Vissanu Meeyoo, Mahanakorn University of Technology
Associate Professor Kenji Mishima, Fukuoka University
- Dr. Nakorn Srisukhombavornchai, King MongKut's University of Technology Thonburi
- Dr. Nutthita Chuankrerkkul, Metallurgy and Material Science Research Institute
Professor Naoyuki Kanetake, Nagoya University
- Dr. Nukul Euaphantasate, National Metal and Materials Technology Center
- Dr. Yuttanant Boonyongmaneerat, Metallurgy and Material Science Research Institute
Professor Atsushi Muramatsu, Tohoku University
Dr. Robert Molloy, Chiang Mai University
Professor Masakata Shimizu, Kyushu University
Professor Yasuhiro Konishi, Osaka Prefecture University
- Dr. Ekkarat Viyanit, National Metal and Materials Technology Center
Professor Manabu Iguchi, Hokkaido University
Professor Makio Naito, Osaka University
- Dr. Panadda Niranatlumpong, National Metal and Materials Technology Center
Professor Takahiko Okura, Akita University
Professor Shu Yamaguchi, The University of Tokyo
Dr. Rattikorn Yimnirun, Chiang Mai University
Professor Ryosuke O. Suzuki, Hokkaido University
Associate Professor Tetsuya Uda, Kyoto University
- Dr. Uraivan Leela-adisorn, Chulalongkorn University
Professor Katsunori Yamaguchi, Iwate University
Professor Shinji Hirai, Muroran Institute of Technology
- Dr. Sirapat Pratontep, National Nanotechnology Center
Associate Professor Toru H. Okabe, The University of Tokyo
Professor Tatsuya Kawata, Tohoku University
- Dr. Chanchana Thanachayanont, National Metal and Materials Technology Center
Associate Professor Kenichi Ohsasa, Hokkaido University

Professor Yuichi Setsuhara, Osaka University
 Professor An-Pang Tsai, Tohoku University
 Professor Hideo Nakae, Waseda University
 Dr. Sirirat Rattanachan, Suranaree University of Technology
 Professor Masazumi Okido, Nagoya University
 Professor Hiroyuki Fukuyama, Tohoku University
 Dr. Sutham Srilomsak, Suranaree University of Technology
 Professor Satoshi Yamashita, Chiba Institute of Technology
 Professor Takaaki Tsurumi, Tokyo Institute of Technology
 Dr. Yuntian Zhu, Los Alamos National Laboratory
 Professor Hiroyuki Sugimura, Kyoto University
 Professor Tetsuya Nagasaka, Tohoku University
 Dr. Asira Fuongfuchat, National Metal and Materials Technology Center
 Professor Fumio Saito, Tohoku University
 Professor Toyohisa Fujita, The University of Tokyo
 Dr. Wuttipong Rungseesantivanon, National Metal and Materials Technology Center
 Professor Hiroshi Umakoshi, Osaka University
 Professor Sohei Shimada, The University of Tokyo
 Dr. Iver Anderson, Iowa State University
 Mr. Corbett Battaile, Sandia National Laboratory
 Dr. Thomas P. Battle, Dupont Co.
 Professor Renato G. Bautista, University of Nevada
 Dr. Robert Biefeld, Sandia National Laboratory
 Dr. Carl Cady, Los Alamos National Laboratory
 Dr. Srinivas Chada, Medtronic
 Dr. Y. Austin Chang, University of Wisconsin
 Professor Narendra Dahotre, University of Tennessee
 Dr. Adrian Deneys, Praxair Inc.
 Professor Diana Farkas, Virginia Polytechnic Institute & State University
 Dr. David Field, Washington State University
 Professor Tadashi Furuhashi, Tohoku University
 Dr. John Hager, Colorado School of Mines
 Dr. Hani Henein, University of Alberta
 Mr. Darrel Herling, Pacific Northwest National Laboratory
 Dr. Elizabeth Holm, Sandia National Laboratory
 Dr. John Hryn, Praxair Inc.
 Mr. William Jarosinski, Praxair Surface Technologies
 Dr. Lynne Karabin, Aluminum Consultants
 Mr. Todd Leonhardt, Rhenium Alloys Inc.
 Assistant Professor Dan Lewis, Rensselaer Polytechnic Institute
 Professor Ben Q. Li, University of Michigan
 Dr. Jian Li, Natural Resources Canada
 Dr. Marvin McKimpson, Michigan Technological University
 Professor Marc Meyers, University of California, La Jolla
 Dr. Amit Misra, Los Alamos National Laboratory
 Dr. James Morris, Oak Ridge National Laboratory
 Professor Mihriban Pegguleryuz, McGill University
 Dr. Bruce Pint, Oak Ridge National Laboratory
 Dr. Adam Powell, Veryst Engineering
 Dr. Jud Ready, Georgia Tech Research
 Dr. Cathy Rohrer, Alcoa Technical Center
 Professor Judy Schneider, Mississippi State University
 Dr. Jeff Simmons, U.S. Air Force
 Dr. Morton Sorlie, Elkem Aluminum
 Professor Douglas Swenson, Michigan Technological University
 Professor Sammy Tin, Illinois Institute of Technology

Aqueous/Electrochemical Processing I.....	Mon PM.....	18
Aqueous/Electrochemical Processing II.....	Tues PM.....	33
Aqueous/Electrochemical Processing Poster Session.....	Mon AM-Wed PM.....	54
Closing Ceremony.....	Wed PM.....	53
Composites Processing I.....	Mon AM.....	12
Composites Processing II.....	Tues AM.....	27
Composites Processing III.....	Tues PM.....	34
Composites Processing IV.....	Wed PM.....	47
Composites Processing Poster Session.....	Mon AM-Wed PM.....	54
Energy Materials Processing I.....	Mon AM.....	13
Energy Materials Processing II.....	Tues AM.....	28
Energy Materials Processing III.....	Wed AM.....	42
Energy Materials Processing Poster Session.....	Mon AM-Wed PM.....	55
Environmental Protection Processing I.....	Mon AM.....	13
Environmental Protection Processing II.....	Mon PM.....	18
Environmental Protection Processing III.....	Tues AM.....	28
Environmental Protection Processing Poster Session.....	Mon AM-Wed PM.....	56
Materials Processing I.....	Mon AM.....	14
Materials Processing II.....	Mon PM.....	19
Materials Processing III.....	Mon PM.....	21
Materials Processing IV.....	Mon PM.....	22
Materials Processing IX.....	Wed PM.....	48
Materials Processing Poster Session.....	Mon AM-Wed PM.....	57
Materials Processing V.....	Tues PM.....	35
Materials Processing VI.....	Tues PM.....	36
Materials Processing VII.....	Tues PM.....	37
Materials Processing VIII.....	Wed AM.....	42
Materials Processing X.....	Wed PM.....	49
Materials Processing XI.....	Wed PM.....	50
Modeling Material Processing I.....	Tues PM.....	38
Modeling Material Processing II.....	Wed PM.....	51
Modeling Material Poster Session.....	Mon AM-Wed PM.....	60
Monday Keynote Lecture.....	Mon PM.....	18
Nanomaterials Processing I.....	Mon AM.....	15
Nanomaterials Processing II.....	Mon PM.....	23
Nanomaterials Processing III.....	Tues AM.....	29
Nanomaterials Processing IV.....	Tues PM.....	39
Nanomaterials Processing V.....	Wed AM.....	43
Nanomaterials Processing Poster Session.....	Mon AM-Wed PM.....	60
Opening Ceremony and Monday Plenary Lecture.....	Mon AM.....	12
Powder Preparation/Processing I.....	Mon AM.....	15
Powder Preparation/Processing II.....	Mon PM.....	24
Powder Preparation/Processing III.....	Tues AM.....	29
Powder Preparation/Processing IV.....	Wed AM.....	44
Powder Preparation/Processing Poster Session.....	Mon AM-Wed PM.....	62
Processing of Ceramics I.....	Wed AM.....	40
Processing of Ceramics II.....	Wed PM.....	44

Processing of Ceramics Poster Session.....	Mon AM-Wed PM.....	63
Processing of Electronic Materials and Devices I	Mon AM.....	16
Processing of Electronic Materials and Devices II.....	Tues AM.....	30
Processing of Electronic Materials and Devices III.....	Wed AM.....	45
Processing of Electronic Materials and Devices Poster Session	Mon AM-Wed PM.....	64
Solidification Processing I	Mon PM.....	17
Solidification Processing II.....	Tues AM.....	25
Solidification Processing III.....	Tues PM.....	31
Thin Film Coating Processing I.....	Tues AM.....	32
Thin Film Coating Processing II.....	Wed AM.....	46
Thin Film Coating Processing III	Wed PM.....	52
Thin Film Coating Processing Poster Session	Mon AM-Wed PM.....	64
Tuesday Keynote Lecture	Tues PM.....	33
Tuesday Plenary Lecture.....	Tues AM.....	27
Wednesday Keynote Lecture	Wed PM.....	47
Wednesday Plenary Lecture.....	Wed AM.....	42

Opening Ceremony and Monday Plenary Lecture

Monday AM
December 8, 2008

Room: Auditorium B2, Bangkok Convention Centre
Location: Sofitel Centara Grand Bangkok

Session Chair: Paritud Bhandhubanyong, National Metal and Materials Technology Center

9:30 AM Opening Ceremony

9:50 AM Plenary

Sustainable Nanofoundation for Green Society: *Somsak Panyakaew*¹;

¹Chulalongkorn University

Abstract not available.

10:35 AM Break

Composites Processing I

Monday AM
December 8, 2008

Room: Plaza 5
Location: Sofitel Centara Grand Bangkok

Session Chair: Naoyuki Kanetake, Nagoya University

11:00 AM

A Study of Characteristics and Mechanical Properties of Natural Rubber Filled Coir Composites: *Montip Lawsuriyont*¹; ¹Rajamangala University of Technology Thanyaburi

Coconut husk being a local raw material in Thailand could be used for develop natural rubber filled with coir. This research was focused on a study of forming the finishing materials from coir composites with rubber filler (grade STR 20) compound were prepared by incorporation of different loadings (0-30 phr) of coir. This is a unique blend of coir and natural rubber. The coir/rubber compound blends were composited using to improve the compatibility of coir/rubber compound blended and shaped into tested specimens by a compression molding machine. The composite samples were characterized for their mechanical properties. It was found that coir/NR compound blends provided to increase in density, 100% modulus and hardness properties. Also tensile, tear strength, and abrasion resistance properties were increased up to an optimum point (15 phr). Natural rubber filled coir composites will be much in demand, because of its environmentally friendly characteristic.

11:20 AM

Composites Made with Spin Polarized Compounds: *Viorel Sandu*¹; Stelian Popa¹; Elena Sandu²; Nicolae Hurduc³; Iulian Nor³; Ion Stamatin⁴; Adriana Andronic⁴; ¹National Institute of Materials Physics; ²National Institute for Nuclear Physics and Engineering; ³Technical University; ⁴University of Bucharest

Ferromagnetic compounds CrO_2 and $\text{La}_{2/3}\text{Sr}_{1/3}\text{MnO}_3$ were embedded in different polymer matrices. As matrix, we investigated copolymers of poly(methyl methacrylate) made either with styrene or butadiene. The use of copolymers is designed to provide better elastic properties to the composite at room temperatures when prepared as thick film. Magnetic and transport properties of the composites are presented as a function of the ratio of the two members of the copolymer.

11:40 AM

Development and Characterization of Magnesium Composites Using Nano-Size Oxide-Based Reinforcement: *Mui Hoon Brenda Nai*¹; *Mui Ling Sharon Nai*¹; *Manoj Gupta*¹; ¹National University of Singapore

Magnesium based nanocomposites containing an oxide-based reinforcement were successfully fabricated using powder metallurgy technique incorporating microwave assisted two-directional sintering. The sintered specimens were hot extruded and characterized in terms of microstructure (grain morphology, porosity and distribution of particulates) and mechanical properties (hardness and tensile properties). The results revealed a marked effect of reinforcement in nano length scale on the tensile properties of magnesium. An attempt is made in the present study to interrelate the tensile behavior of Mg with the presence of nano-size reinforcement.

12:00 PM

Effect of Graphite Particles on the Damping Behavior of ZA-27 Alloy Composite Materials: *Prakash Kupparavalli*¹; B. Girish¹; B. Satish¹; K. Niranjana Rao¹; ¹East Point College of Engineering and Technology

The objective of present work is to investigate the effect of macroscopic graphite particles on damping behavior of ZA-27 alloy composites. Liquid metallurgy technique will be used to prepare the composites, in which the graphite particulates will be used to reinforce ZA-27 alloy with varying fractions (1-7% by weight in steps of 2%). The idea is to arrive at an optimum graphite reinforcement content for structural applications and establish a correlation of experimental data with numerical values obtained using Finite Element Analysis. The experimental method uses free decay techniques to evaluate damping properties. Standard strips are of size 65mm x 7 mm x 0.8mm thick and are tested in cantilever method of vibration tests at various temperatures. It was observed that the damping capacity of the material increased with increasing fractions of macroscopic graphite particulates. ANSYS software will be used to carry-out the FEA analysis.

12:20 PM

Fabrication of Lotus-Type Porous Metals through Thermal Decomposition of Compounds: *Hideo Nakajima*¹; M. Tane¹; S. Suzuki¹; ¹Osaka University

Lotus-type porous metals with directional pores are fabricated by unidirectional solidification in a pressurized hydrogen gas called as High Pressure Method (HPM). The pores are evolved when the gas atoms dissolved into the melt from the gas atmosphere are precipitated in the solidification process. However, this method has two obstacles for mass-production of the lotus metals; hydrogen is flammable and explosive when a small amount of oxygen is mixed in the chamber, and the use of high-pressure chamber is expensive and its handling is laborious. In order to overcome those shortcomings, we developed a novel method called as "Thermal Decomposition Method (TDM)" of compounds involving gas elements. Hydrogen or nitrogen is dissolved in the melt of metals by addition of the compounds such as hydrides or nitrides, respectively. During the solidification the gas pores are evolved in the same way as HPM. Moreover, when the compounds are decomposed in the melt the metallic elements form some different compounds in the melt which serves as nucleation sites to evolve the pores with more uniform pore size and distribution. The fabrication method is superior to the conventional HPM.

Energy Materials Processing I

Monday AM
December 8, 2008

Room: Plaza 1
Location: Sofitel Centara Grand Bangkok

Session Chair: Tetsuya Uda, Kyoto University

11:00 AM Invited

Oxidation Behavior of Nanocrystalline Coatings for Fossil-Fired Steam Turbine Boiler Tubes: *N. Cheruvu*¹; Ronghua Wei¹; G. Rao²; David Gandy³; ¹Southwest Research Institute; ²Karta Technologies; ³Electric Power Research Institute

Nanocrystalline MCrAl coatings with aluminum ranging 4 to 10 wt. % were deposited on the substrate samples using the magnetron sputtering technique. Cyclic oxidation behavior of the nanocrystalline coatings has been investigated at two temperatures, 1010°C and 750°C. At the peak temperature 1010°C, the scale showed excellent spallation resistance for over thousand one-hour thermal cycles. At the lower peak temperature, the coating failed to provide protection and the results showed evidence of internal (runaway) oxidation. The as-coated and exposed specimens were characterized for the coating microstructure, grain size and the oxide scale using X-ray diffraction (XRD) and optical and scanning electron microscopy techniques. These results are used to discuss the effect of temperature and aluminum content in the coating on cyclic oxidation behavior of nanocrystalline MCrAl coatings.

11:20 AM

Improvement of Grain-Boundary Conductivity of Trivalent Cation Doped Barium Zirconate: *Susumu Imashuku*¹; Tetsuya Uda¹; Yositaro Nose¹; Yasuhiro Awakura¹; ¹Kyoto University

Trivalent cation doped barium zirconate has a relatively high proton conductivity under the wet conditions. It, therefore, has a great potential for electrolytes used in fuel cells. Yttrium-doped barium zirconate is known to have the highest bulk conductivity among trivalent cation doped barium zirconates. However, the grain-boundary conductivity is still low. To improve the low grain-boundary conductivity, it is necessary to reduce the density of grain-boundary in the electrolytes. The microstructure of yttrium-doped barium zirconate electrolyte consists of mixtures of large (1 micrometer) and fine (50 nanometers) grains. Therefore, it is desirable to obtain the electrolyte with microstructure of large grains. We found that the grain size of barium zirconate electrolyte becomes larger due to doping scandium. However, the bulk conductivity of scandium-doped barium zirconate is still very low. Thus, we co-doped scandium and yttrium into barium zirconate and investigated the relationship between the grain-boundary conductivity and doping.

11:40 AM

Effects of Cold Rolling and Final Polishing Directions on the Adhesion Energy of Thermal Oxide Scales on an AISI 441 Stainless Steel Interconnect Oxidised in a Cathode Atmosphere of Solid Oxide Fuel Cells Measured by a Tensile Test: Somrerak Chandra-ambhorn¹; *Thanasak Nilsonthi*¹; Alain Galerie¹; ¹King Mongkut's University of Technology North Bangkok

The tensile test operating in a SEM chamber was applied to investigate the adhesion behaviour of the oxide scale on AISI 441 stainless steel used as interconnect in solid oxide fuel cells (SOFCs). The samples were prepared by aligning the cold rolling and final polishing directions parallel and perpendicular to the loading one, and oxidised in synthetic air at 800°C as a simulated cathode atmosphere. Changing the final polishing direction from parallel to perpendicular to the loading direction reduced the spallation ratio in function of strain. When the polishing direction paralleled to the loading one, changing the rolling direction from parallel to perpendicular to the loading one reduced the spallation ratio in function of strain. The adhesion energies of scales on the studied samples were in the range of 80 – 360 J.m⁻².

12:00 PM

Effect of ZnO Particle Solid Content on Performance of MEH-PPV/ZnO Hybrid Solar Cells: *Kasin Kasemsuwan*¹; Chanchana Thanachayanont¹; Varong Pavarajarn²; ¹National Metals and Materials Technology Center of Thailand; ²Chulalongkorn University

Hybrid solar cells base on p-type semiconductor polymer poly(2-methoxy,5-(2'-ethylhexyloxy)-p-phenylene vinylene (MEH-PPV) and n-type zinc oxide (ZnO) particles were fabricated and investigated. Increasing the ZnO solid content was found to increase power conversion efficiency but decrease shunt resistance of the blend solar cells. A transmission electron microscopy (TEM) investigation of the ZnO particles showed a mixture of sphere and rod shape particles, ranging from 20-600 nm in size. An increase in ZnO content resulted in an increase in size of isolated ZnO particle agglomerates. From absorption spectra measurement we found that the absorption range of the blend solar cells was widened by the incorporation of the ZnO particles. With an increase in ZnO particle solid content, photoluminescence quenching was found to increase, indicating that charge separation and charge transfer had occurred and interfaces between a semiconductor polymer and inorganic particles could be used to provide efficient charge separation.

Environmental Protection Processing I

Monday AM
December 8, 2008

Room: Plaza 6
Location: Sofitel Centara Grand Bangkok

Session Chair: Toyohisa Fujita, The University of Tokyo

11:00 AM

Carbon Dioxide Adsorption by MCM-41 Synthesized from Rice Husk: *Anusorn Boonpake*¹; Siriluk Chiarakorn¹; Navadol Laosiripojana¹; Sirintornthep Towprayoon¹; Amnat Chidthaisong¹; ¹King Mongkut's University of Technology Thonburi

Carbon dioxide (CO₂) adsorption at various temperatures by the hexagonal ordered mesoporous synthesized from rice husk silica (R-MCM-41) was studied. The synthesized R-MCM-41 was confirmed by X-ray diffraction pattern and micrograph. FTIR analysis indicated the presence of well arranged siloxane bonding. R-MCM-41 showed type IV adsorption isotherm with hysteresis loop according to IUPAC classification. BET surface area, pore volume, and pore size distribution was 602.28 m²/g, 0.486 cm³/g, and 2.43 nm, respectively. The CO₂ adsorption capacity of R-MCM-41 was investigated by using thermogravimetric analyzer (TGA) with temperatures varying from 30 to 150°C. The maximum adsorption capacity (23.32 mg-CO₂/g-adsorbent) was obtained at 30°C. The adsorption capacity was decreased significantly when the adsorption temperature was increased. Furthermore, R-MCM-41 showed high stability in absorption-desorption reuse cycle. These results indicate that rice husk can be used as a source of silica for MCM-41 synthesis and further applied for CO₂ adsorption in carbon capture technology.

11:20 AM

Development of New Steels to Reduce Lifecycle Costs of Steel Bridges: *Fumio Yuse*¹; Takenori Nakayama¹; Naohiro Furukawa¹; Kengo Abe¹; Shigeo Okano¹; ¹Kobe Steel, Ltd.

The cost reduction of maintenance has been required especially for recent years in the steel structure product such as bridge. The development of new weathering steel which has an advanced corrosion resistance in atmosphere with chloride (airborne salt from the sea and deicing salt) has been carried out by Kobe Steel. The newly developed steel contains Cu, Ni, and Ti. The corrosion resistance of developed steels has been investigated by cyclic corrosion tests and exposure tests with salt spray once a week for three years. The developed steel showed advanced corrosion resistance in both investigations and it is suggested to contribute the cost reduction of maintenance. It is revealed by XRD that protective rust was formed and it could be barrier against corrosive environment in order to achieve the

advanced corrosion resistance. The alloy elements; Cu, Ni, and Ti could be effected to produce protective rust.

11:40 AM

Development of Pt-Ir-Hf Modified Aluminide Coatings and Their Deterioration Process: *Murakami Hideyuki*¹; Akihiro Yamaguchi¹; Yoko Mitarai¹; Rachel Thomson²; Geoff West²; ¹National Institute for Materials Science; ²Loughborough University

The effects of Hf addition to Pt-Ir modified aluminide containing alloy coatings were investigated. Cyclic oxidation tests revealed that while Hf addition did not drastically affect the mass change kinetics, it retarded the surface rumpling and microstructural changes in the substrate. Internal voids formed by oxidation test were drastically retarded by the trace Hf addition. It is anticipated that a more undulated surface may lead to form a surface oxide scale with localized internal stress, resulting in the scale spallation or crack formation in the scale. Spallation of surface oxides consumes Al in the coated layer for reheating the surface scale, which could lead to the formation of voids caused by the outer diffusion of Al. Hf addition seems to retard the process described above. Hot corrosion tests also confirmed the advantageous effect of Hf addition, which promotes the formation of Al₂O₃ thus retarding the salt attack.

12:00 PM

Is Hydrotalcite Effective for Toxic Ion Removal?: Junji Shibata¹; Norihiro Murayama¹; Daisuke Sakamoto¹; Mitsuhiro Okada¹; ¹Kansai University

Hydrotalcite-like compounds (HT), which have layered structure of Mg-Al complex hydroxide, are one of inorganic anion exchangers. Removal of various toxic anions composed of As(III), As(V), Se(IV), Cr(VI), B(III) was conducted using the powder and granular HTs. The feasibility to use HT as an anion exchanger was investigated. Various toxic metal ions can be removed by the anion exchange reaction in the pH region where anionic species such as AsO₂⁻, HAsO₄²⁻, CrO₄²⁻ and SeO₃²⁻ are formed. Almost all anion exchange isotherms for toxic ions can be correlated with Langmuir equation. Anion exchange selectivity of HT is mainly based on the hydration ionic radius and the valence of electric charge. The HT powder can be granulated by using polyvinylalcohol as a binder, and the toxic ions can be removed continuously with the granular HT by a column method. Hydrotalcite is effective for toxic ion removal.

12:20 PM

Optimization of Post Combustion in an Electric Arc Furnace for Advanced Steelmaking: *Wu Zhonghua*¹; Dipak Mazumdar²; Arun S. Mujumdar¹; ¹Minerals, Metals, and Materials Technology Centre (M3TC); ²Indian Institute of Technology-Kanpur

In the state-of-the-art electric arc furnace (EAF) flat-rolled steelmaking plant, about 1.5 kmol of CO is generated per ton of steel, which if combusted to CO₂, represents 425 MJ of energy recovery. Efficient transfer of the heat energy from the post combustion (PC) to the molten steel bath can reduce production costs and improve productivity. A comprehensive CFD model was developed to simulate the process. It was applied to the PC process in an industrial scale EAF furnace. Different PC system designs and operational strategies were evaluated e. g energy transfer efficiency, emission reduction ratio, oxygen usage efficiency. It was observed that only a simple modification of the PC system can improve greatly the system performance and hence reduce the steelmaking cost due to reduced energy consumption and decreased melting time in the EAF furnace. This CFD model can be used as a tool to optimize existing industrial EAF furnaces.

Materials Processing I

Monday AM

December 8, 2008

Room: Plaza 3

Location: Sofitel Centara Grand Bangkok

Session Chair: Takahiko Okura, Akita University

11:00 AM Invited

Effects of Surface Roughness on Superplastic Carburizing of Duplex Stainless Steel: *Sharidah Abdul Aziz*¹; Iswadi Jauhari¹; ¹University Malaya

Superplastic carburizing (SPC) is a carburizing process that combines carburizing with superplastic deformation. Since SPC involves direct interaction between the superplastically deformed surface and the solid carbon medium, the effect of surface roughness on the process cannot be disregarded. This paper presented the study of surface roughness effects on superplastic carburizing of duplex stainless steel (DSS). SPC was conducted under four different surface roughness (R_a) conditions of 0.9, 0.3, 0.1 and 0.03 μ m. The microstructure, surface hardness, and carburized layer thickness were studied. Comparisons also were done on non-superplastic material. The results showed that the surface roughness strongly affected the properties of the superplastically carburized duplex stainless steel while its effects on the non-superplastic material were not that obvious.

11:20 AM

A Study on Effect of Machining Variables on Hardness of EDMed SKD 11 and DC53 Tool Steels: *Kannachai Kanlayasiri*¹; ¹King Mongkut's Institute of Technology Ladkrabang

Electric-discharge machining (EDM) is a non-traditional machining method that is widely used to pattern tool steels for die manufacturing. This paper is to investigate the hardness induced by EDM process in SKD11 and DC53 tool steels. The machining variables are electrical discharge pulse (ON) and electrical discharge peak current (IP). Copper alloy is used as the electrode. Vickers micro hardness tests were performed to obtain the hardness of specimen at various depths from the EDMed surface. The results from analysis of variance at the confidence level of 95% showed that the hardness near the surface increased with the increase of ON and IP, and the effect of electrical discharge pulse was more influential to the hardness changes than that of the electrical discharge peak current. An empirical model and response surface of the induced hardness were also developed in this study.

11:40 AM

Effect of Process Parameters on Powering Characteristics of Galvannealed Materials: *R. J. Singh*¹; Khursid Alam Khan²; Shantanu Chakrabarti²; ¹National Institute of Technology; ²Tata Steel

Globally, the use of metallic coated steel sheets in the automobile industry is increasing. The sheet should have excellent formability, weldability, paintability and corrosion resistance. Since bare cold rolled steel sheets have certain limitations, application of galvanised steel sheets is steadily expanding. Galvannealed steel sheet fulfills all requirements and has become of major interest in the automobile industry. The success of Galvannealed (GA) steels in the body-in-white depends upon material design and parameters of various processes involved, like cold rolling, continuous annealing, hot dipping and galvannealing. In the present work, powdering resistance, one of the important product characteristics of GA, has been studied and a relation is established between the process parameters and the powdering value. The product obtained through optimisation of the process parameters has been successfully used by major automotive producers without any powdering problem, for internal as well as external automotive applications.

12:00 PM

Arsenic and Antimony Elimination from Iron Base Complex Materials by Using Pig Iron: *Leandro Voisin*¹; Takahiko Okura¹; Kimio Itagaki²; ¹Akita University; ²Tohoku University

Novel pyrometallurgical processes related to the use of pig iron in nonferrous metallurgy are proposed for treating iron base complex materials

containing arsenic or antimony such as furnace residues and secondary Fe-Cu alloys produced in reducing smelting and recycling. In this study, based on the data reported by the authors for the phase relations and distribution of minor elements between the liquid iron base alloy and coexisting liquid phases in the Fe-Pb-M, (M = As, Sb), Fe-Cu-M and Fe-Cu-S-M systems saturated with carbon at 1473K material balance calculations were made on some processes using pig iron. The processes are focused on the elimination or fixation of arsenic and antimony and the recovery of precious metals when the Fe-Pb composite byproduct produced in lead smelting, the Fe-Cu furnace residue recovered in copper smelting and recycling, and the copper matte recovered in slag cleaning are treated.

Nanomaterials Processing I

Monday AM
December 8, 2008

Room: Plaza 7
Location: Sofitel Centara Grand Bangkok

Session Chair: Yasuhiro Konishi, Osaka Prefecture University

11:00 AM Invited

Effect of Synthesis Condition on Photocatalytic Activity of TiO₂ Nanoparticles: *Withaya Panpa*¹; Supatra Jinawath¹; ¹Chulalongkorn University

Photocatalytic activities of TiO₂ nanoparticles prepared by the hydrolysis of titanyl sulphate in the presence of different precipitating agents (NaOH and urea) were investigated. The different synthesis conditions led to the different physical properties of TiO₂ powders, such as crystal size and surface area which consequently affected their photocatalytic activities. It was found that pure anatase phase with low crystallinity could be easily formed when using urea at a synthesis temperature of 95°C. The characteristic properties of TiO₂ powders were analyzed by XRD, SEM, BET and N₂ adsorption techniques. The photocatalytic activity of the obtained TiO₂ powders was carried out through the decolorization of reactive red 243 dye (Drimarene Red X-6BN, Clariant Co., Ltd.) in aqueous solutions at pH 5.8 under UV-irradiation. The photocatalytic activity of TiO₂ powder prepared using urea was much higher than that using NaOH and close to those of the commercial TiO₂, P-25 and ST-01.

11:20 AM

Behavior of Nanosilica Filled Epoxy Resins: *Peerapan Dittanet*¹; ¹Lehigh University

Nanosilica filled diglycidyl ether of bisphenol A (DGEBA), diglycidyl ether of bisphenol F (DGEBF), and cycloaliphatic epoxy resins were examined to improve their mechanical and thermal properties. Dynamic mechanical analysis (DMA) and thermal mechanical analysis (TMA) directly measured the modulus and coefficient of thermal expansion (CTE), respectively, of nanosilica-epoxy composites. It was revealed that by increasing the wt% of nanosilica particles, the CTE for DGEBA, DGEBF, and cycloaliphatic nano-filled system clearly decreased. On the other hand, the modulus and fracture toughness were found to increase with increasing nanosilica content. A good agreement was found for the measured modulus and CTE and theoretical models. Similarly as the wt% of the silica content increase for any epoxy, the fracture toughness also increases. The moisture absorption for cycloaliphatic nano-filled system is clearly reduced with the addition of wt% content, however, the moisture absorption is unaffected by addition of filler contents for DGEBA nano-filled system.

11:40 AM

Carbon Nanotubes and Titanium Oxide Nanocomposite: Controlling Syntheses and Photoelectronic Application: *Yaodong Yang*¹; Liming Dai²; Jiefang Li¹; Dwight Viehland¹; ¹Virginia Tech; ²University of Dayton

Titanium dioxide (TiO₂) and Carbon nanotubes (CNT) are both very important materials at present. TiO₂ has very good photoelectronic property and CNT has mechanical stability, high thermal/electrical conductivity, and large surface area. Using electrophoresis for coating titanium dioxide

on aligned/nonaligned carbon nanotubes, we prepared TiO₂-CNT coaxial nanowires, TiO₂ nanomembranes, TiO₂ modified CNT-polymer film and any other interesting TiO₂-CNT composite nanostructures. These TiO₂-CNT nanostructures combine the advantages from TiO₂ and CNT together which were demonstrated fast photocurrent responses and possessed unique photo-induced electron transfer properties of practical significance. After introducing them into polymer, we can make transparent and flexible device. Our work represents a significant advance in the development of various new photoelectronic nanomaterials attractive for a wide range of optoelectronic applications.

12:00 PM

Development of Low-Current Arc Plasma Process with Ultrasonic Cavitations for Synthesizing Metal-Filled Carbon Nanocapsules in Organic Solution: *Ruslan Sergiienko*¹; Etsuro Shibata¹; SungHoon Kim¹; Takashi Nakamura¹; ¹Institute of Multidisciplinary Research for Advanced Materials, Tohoku University

Nanoparticles of metal carbides (Fe₃C, χ -Fe_{2.5}C, Co₃C, TiC) wrapped in multilayered graphitic sheets, called as carbon nanocapsules (CNCs), were synthesized by a new method in which low-current arc plasma was generated even in organic solutions due to an ultrasonic irradiation. In this process, ultrasonic horn was utilized not only for ultrasonic irradiation but also for cathode electrode. An anode electrode material such as iron and cobalt was optionally selected. Ultrasonic cavitation bubbles were induced between the gap of cathode and anode electrodes in the organic solution. Consequently, an electric arc plasma can be generated even in insulating organic solutions such as benzene and ethanol at power as low as around 45~165 W (DC 30~55V, 1.5~3 A). The structure, morphology and phases of CNCs were characterized by HR-TEM, Raman spectroscopy and XRD. The magnetic properties of the CNCs samples were measured by VSM.

12:20 PM

Applications of Black Conductive Powders to High Transmittance Solar Control Windows: Takeshi Chonan¹; Atsushi Tofuku¹; Kenichi Fujita¹; *Kenji Adachi*²; ¹Sumitomo Metal Mining Company, Ltd.

Highly conductive black powders such as ruthenium dioxide, titanium nitride and lanthanum hexaboride have been found as possibly transformed into high transmittance and high clarity solar filters by a nano-particulate processing using a media agitation mill. With decreasing particle size to a nano-scale, it is found that a haze of the dispersion decreases and a visible light transmittance increases, while a new property of absorption in the near-infrared range emerges and increases depending on the materials. This near-infrared absorption is considered to arise from the surface plasmon resonance of conduction electrons, and the absorption profile is found as simulated well by using the Mie scattering theory with bulk optical constants of those materials. Those nano-particulate dispersions can be processed into coating liquids and functional powders for the applications to solar control windows.

Powder Preparation/Processing I

Monday AM
December 8, 2008

Room: Plaza 8
Location: Sofitel Centara Grand Bangkok

Session Chair: Tetsuji Hirato, Kyoto University

11:00 AM

A Method for Synthesizing Large Quantities of Metal Oxide Nanowires: *Miran Mozetic*¹; Uros Cvelbar¹; ¹Jozef Stefan Institute

A method for synthesizing large quantities of metal oxide nanowires is presented. Metal foils are exposed to highly reactive oxygen plasma. Due to interaction of oxygen atoms on the foil surface a thin oxide film grows spontaneously. In a limited range of plasma parameters the growth of the oxide is heavily unisotropic, leading to a formation of bundles of well-oriented nanowires with the length of several 10 μ m and the diameter of the

order of 10 nm. The diameter depends on the flux of neutral oxygen atoms on the sample surface. The growing phenomenon is demonstrated for the case of niobium oxide. Possible mechanisms involved in the formation of nanowires during oxygen plasma treatment are presented and discussed.

11:20 AM

Aspect Ratio of Green MIM Parts on Shrinkage during Sintering: *Suttha Amaranan*¹; Anchalee Manonukul¹; ¹Thailand National Metal and Materials Technology Center

Metal injection moulding (MIM) is a process that can produce small, complex, and near-net-shape parts with excellent mechanical properties. The shrinkage during sintering in MIM parts is one of the most important parameters in production. In this research, stainless steel 316L feedstock was injection moulded to form three different shapes which are tensile test specimen, three-step specimen and square-donut specimen. Three-step specimen and square-donut specimen are specially designed for observation of shrinkage behaviour. In addition, nine sets of square-donut specimens with different aspect ratios were investigated. The result shows that the anisotropic shrinkage was observed, which affected by the gravitational force, frictional force between specimens and setters, and the aspect ratio of the specimen. The domination of each factor is dependent on the geometry of green parts. Hence, the relationship between shrinkage and aspect ratio can be established.

11:40 AM

Composite Metal Powder Coated with Un-Bundled Carbon Nanotube (CNT) and Characteristics of Its Extruded Material: *Hisashi Imai*¹; Katsuyoshi Kondoh¹; Hiroyuki Fukuda¹; Bunshi Fugetsu²; ¹Osaka University; ²Hokkaido University

CNT is a very useful reinforcement for composites because of its high strength and Young's modulus, and excellent heat and electrical characteristic. It is, however, very difficult to uniformly distribute CNT in a metal matrix because CNT is easy to be bundled by van der Waals force. In this paper an effective method to cover metal powder with un-bundled CNTs has been suggested. Pure copper, Mg and Al alloy powder coated by CNTs were prepared by using a few kinds of the surfactants (surface active agent), having both hydrophobic and hydrophilic groups via wet process. The un-bundled CNTs exist on the powder surface by dipping the raw powder into the above solution and drying at elevated temperature. In employing Mg powder, yield stress and tensile strength of the composite with CNTs could be remarkably increased via the above process.

12:00 PM

Effect of Processing Parameters on Nanostructured Cr₃C₂-Ni₂₀Cr Powder and Coating Characteristics: Armando Padial¹; Cecilio Cunha¹; Olandir Correa¹; Jose Martinelli¹; Nelson Lima¹; *Lalgudi Ramanathan*¹; ¹Instituto de Pesquisas Energéticas Nucleares - IPEN

This paper presents the effects of high energy milling parameters on characteristics of Cr₃C₂-Ni₂₀Cr powder prepared as feed-stock for nanostructured HVOF coatings on steel surfaces. It also presents the influence of the powders on coating features. The crystallite size of powders milled in nitrogen was about 65 nm and significantly smaller than that milled in hexane, which were about 100nm. Further studies in which the hexane content was reduced progressively from 100 to 10 mL revealed marked decrease in particle size to 3 μm and crystallite size to 50 nm with decrease in hexane. This was attributed to the cushioning effect of hexane. Details about powder particle morphology and phase constituents as well as the microstructure and mechanical properties of the nanostructured HVOF coatings will be presented and discussed.

12:20 PM

Energy Efficient Sintering of Al/Cu Nanocomposites Using Different Microwave Power Levels: Eugene Wong¹; *Shashank Nawathe*²; Manoj Gupta¹; ¹National University of Singapore; ²Indian Institute of Technology-Bombay

Pure aluminum and Al/Cu nanocomposites were fabricated by integrating pure aluminum with nano copper reinforcement using powder metallurgy route incorporating energy efficient microwave assisted rapid sintering

technique. The composites were subjected to different microwave power levels during the sintering. Microstructural characterization studies revealed the presence of minimal porosity and reasonably uniform distribution of the reinforcement in the nanocomposites. Mechanical characterization revealed that the maximum strength is achieved for composite sintered at 50% power level while the highest ductility is achieved for composite sintered at 30% power level. The best overall combination of mechanical properties assessed in terms of work of fracture was realized in the composite sintered at 100% microwave power level. An attempt is made in the present study to correlate the effect of different microwave power levels on the characteristics of the Al/Cu nanocomposites.

Processing of Electronic Materials and Devices I

Monday AM
December 8, 2008

Room: Plaza 4
Location: Sofitel Centara Grand Bangkok

Session Chair: Hiroyuki Fukuyama, Tohoku University

11:00 AM

Ultra Thin Profile Free Copper Foil for Fine Line Patterning: *Kensuke Nakamura*¹; ¹Mitsui Mining & Smelting Co., Ltd

There is an increasing number of IC substrate designed with the finer line patterns than ever. But a conventional practice that relies on the use of a copper foil with a profile has apparently negative impact on stabilizing etching process to attain the ultra fine line and space such as 10um/10um. This report presents a new type of copper foil; namely, MultiFoil-G, the ultra thin and flat copper foil with the high performance primer resin that works as a chemical bonding agent to a dielectric material. The patterning process and bonding reliability with this new technology have been tested and found to be greatly improved compared with the conventional approach. Moreover the wider bonding compatibilities with various types of die-electric materials and a high yield to form 2 layer BVH using CO₂ laser have been attained.

11:20 AM

Effect of Nano-Size Copper Addition on the Tensile Properties of Tin: *Md. Alam*¹; Mui Ling Sharon Nai¹; Manoj Gupta¹; ¹National University of Singapore

In the present study, varying volume fraction of nano-size copper (0 vol. %, 0.2 vol. % and 0.35 vol. %) particulates were incorporated into tin using powder metallurgy method with microwave assisted sintering. Microstructural characterization studies conducted on the extruded samples showed reasonably uniform distribution of secondary phase, near equiaxed grain morphology and the presence of minimal porosity in all cases. Room temperature tensile test results revealed that strength level increases with the addition of nano copper while ductility decreases. An attempt has been made to correlate the effect of copper addition on the tensile properties of tin.

11:40 AM

Effect of Sputtering Pressures and RTA Conditions on Properties of Ta₂O₅ Thin Films: *Jicheng Zhou*¹; Di-hui Huang¹; ¹Central South University of Forestry and Technology

Ta₂O₅ thin films were deposited by DC reactive magnetron sputtering, and rapid thermal annealing (RTA) was performed. Influence of sputtering pressures and annealing temperature on surface characteristics, microstructure and optical properties of Ta₂O₅ thin films were discussed in this paper. The results indicate that the refractive index of Ta₂O₅ thin films ranged from 2.04 to 2.16 (at λ = 550 nm), decreased with the increasing of sputtering pressure; As-deposited Ta₂O₅ thin films are amorphous; Surface roughness was decreased after annealed at low temperature, refractive index n and extinction coefficient k decreased with the increasing of annealing temperature a hexagonal structure (δ-Ta₂O₅) was identified after annealed at 800, another transition from δ-Ta₂O₅ to low temperature orthorhombic structure (L-Ta₂O₅) occurred at 900-1000°.

12:00 PM

Effect of Sub-Micron Alumina Particulates on the Properties of a Sn-0.7Cu Lead-Free Solder Alloy: Xiangli Zhong¹; Manoj Gupta¹; Sharon Nai¹; ¹National University of Singapore

Sn-0.7Cu lead-free solder alloy reinforced with sub-micron size alumina particulates in different volume percentage was synthesized using powder metallurgy technique incorporated with microwave sintering. Following synthesis, the extruded materials were characterized in terms of physical and mechanical properties. The density values of the composite solder materials were found to decrease with an increase in volume percentage of alumina particulates. The results of room temperature tensile test revealed that yield stress and ultimate tensile stress of the composite solder materials show an increase with increase in volume percent of alumina particulates. Particular emphasis is placed to interrelate the effect of volume fraction of sub-micron size alumina particulate added in the Sn-0.7Cu alloy with the physical and tensile properties of the resultant composite solder materials.

12:20 PM

Role of Acetonitrile for Copper via Filling: Toshiaki Ono¹; Yasuo Komoda¹; Mitsui Mining and Smelting Company, Ltd.

The electroplating of copper was carried out in the bath composed of acid copper sulfate and acetonitrile (AN bath). The influence of current density and fluid-flow conditions on the current efficiency was investigated by a rotating disk electrode. It was found that the current efficiency decreased with the increase of the rotation rate and the decrease of current density. On the basis of those results, AN bath was applied to a copper via filling. Full filling with the copper in the vias can be achieved by the selection of the proper fluid-flow and current density.

of nucleation density. The influence of these nucleation parameters on the microstructure was investigated. By choosing the reliable parameters of mold surface and bulk liquid respectively, the calculation microstructures were good correspond to real casting magnets. The suitable mold casting design was determined by this CAE system.

11:40 AM

Electric-Field Modified Crystal Growth from Thermodynamic and Kinetic Aspects: Satoshi Uda¹; Xinming Huang¹; ¹Tohoku University

An external electric field is applied on a crystallization process deliberately in order to modify the growth mechanism. This has two distinct consequences: (i) a thermodynamic effect and (ii) a growth-dynamic effect. The former pertains to the modification of the chemical potentials of both solid and liquid phases in equilibrium, which could convert the incongruent-melting state into congruent-melting state. Langasite ($\text{La}_2\text{Ga}_2\text{SiO}_{14}$) is an example. While the latter modifies the solute transport, growth kinetics, surface creation and defect generation related to crystal growth. The nucleation rate of YBCO growth via a peritectic reaction was controlled. The electric field required for these effects were analyzed to be on the order of $10^4\text{--}10^5$ V/cm which occurred in the electric double layer between melt and platinum crucible as well as at the solid-melt interface.

12:00 PM

High Thermal Gradient Directional Solidification and Its Application in the processing of Nickel-Based Superalloys: Lin Liu¹; Taiwan Huang¹; Jun Zhang¹; Hengzhi Fu¹; ¹Northwestern Polytechnical University

The present contribution attempts to introduce several high thermal gradient directional solidification techniques through overheating the melt, enhancing heat extrusion from the solidified part of ingots and selecting proper thermal baffles, which can realize thermal gradient up to 1000K/cm in front of liquid/solid interface. The microstructure and tensile properties at elevated temperature of single crystal superalloys CMSX-2 and DD-3 were studied over a range of cooling rate with large variations in withdrawal speeds in directional solidification. The superfine dendrite with restrained side branches was obtained under both high thermal gradient and fast withdrawal rate up to 0.1mm/sec. The high thermal directional solidification results in reduction in primary and secondary dendrite arm spacing, refinement of γ' phase, reduced microsegregation of alloying elements and smaller size of $\gamma\text{-}\gamma'$ eutectics. Rupture life and ductility in fine structure samples at 1323K increase significantly than that in conventional high rate solidification (HRS) process.

12:20 PM

A New Approach to Producing Super-High Strength Al-10Zn-2.3Mg-2.4Cu-Zr Aluminum Alloy Billets: Jianzhong Cui¹; Haitao Zhang¹; Hiromi Nagaumi²; ¹Key Laboratory of Electromagnetic Processing of Materials, Ministry of Education, Northeastern University; ²Nippon Light Metal Company Ltd., Nikkei Research and Development Center

Low frequency electromagnetic casting process (LFEC) is used to produce the super-high strength aluminum alloys in this research. Moreover, the effects of low frequency electromagnetic field on the macro-physical fields during the semi-continuous casting process of aluminum alloys and the microstructure and crack in the billets are studied and analyzed. Comparison of the results for the macro-physical fields in the LFEC process with that in the conventional DC casting process indicate the following characters: a vigorous forced convection of the melt; an entirely changed direction of melt flow; a remarkably increased velocity of melt flow; a uniform distribution of temperature; a decreased gradient of temperature; the elevated isothermal lines; the reduced sump depth; the decreased stress and plastic deformation. Further, the microstructure of the billet is refined remarkably and the crack in the billets is eliminated in LFEC process because of modification of the macro-physical fields.

Solidification Processing I

Monday AM
December 8, 2008

Room: Plaza 2
Location: Sofitel Centara Grand Bangkok

Session Chair: Kenichi Ohsasa, Hokkaido University

11:00 AM Invited

Cast and Homogenized Structures of Al-Zn-Mg-Cu Alloys by Low Frequency Electromagnetic Direct Chill Casting: Takateru Umeda¹; Pramote Thirathipviwat¹; Kaekwan Koesuko¹; Mawin Supradist¹; ¹Chulalongkorn University

As cast and homogenized structures of super high strength aluminum Al-Zn-Mg-Cu alloys produced by low frequency electromagnetic casting (LFEC) were discussed. Solidification structure constituents of alloys were first discussed, in particular, boundary phases formed mostly by eutectic reaction were discussed: MgZn₂ included with Cu is a major eutectic phase in boundaries. Secondly microsegregation of Al-9.8Zn-2.5Mg-2.3Cu-0.14Zr was reported. Microstructure evolution homogenized for 10 hr at 460°C was lastly discussed.

11:20 AM Invited

Prediction of Solidification Microstructure of Alnico Magnets Using Cast CAE System: Masakatsu Fukuda¹; Choochart Chaiyakot²; Charkorn Khomnotai²; ¹Mitsubishi Steel Manufacturing Company, Ltd.; ²MSM Thailand Company, Ltd.

Alnico magnets are well-known for typical casting magnets having high remanence and good temperature stability. The excellent magnetic properties of these magnets arise from directional solidification using chill plates in the shell mold casting. We applied fluid flow analysis and solidification analysis before the prediction of microstructure for columnar Alnico-5 magnet (MK-5DG). The solidification microstructure were calculated by coupling of the finite differential method and Cellular Automaton method in 2-dimension. The heterogeneous nucleation rate was expressed as Gaussian distribution by a function of undercooling which has three parameters namely the average undercooling, the maximum nucleation density and the deviation

Monday Keynote Lecture

Monday PM
December 8, 2008
Room: Auditorium B2, Bangkok Convention Centre
Location: Sofitel Centara Grand Bangkok

Session Chair: Paritud Bhandhubanyong, National Metal and Materials Technology Center

2:00 PM Keynote

New Development in Natural Rubber Processing: *Krisda Suchiva*¹;

¹National Metal and Materials Technology Center (MTEC)

Abstract not available.

Aqueous/Electrochemical Processing I

Monday PM
December 8, 2008
Room: Plaza 1
Location: Sofitel Centara Grand Bangkok

Session Chair: Kazuya Koyama, National Institute of Advanced Technology

2:45 PM Invited

Lamination Interface of the Wax-Less Permanent Cathode Process in Copper Refinery: *Kimihiko Shimokawa*¹; Tuneso Maruyama¹; Masamichi Oida¹; Makoto Narita¹; Ikunobu Sumida¹; ¹Hibi Kyodo Smelting and Refinery Company, Ltd.

There are a wax type and a wax-less type in a permanent cathode process in the copper electrorefining. The copper deposit can be separated from the cathode in two pieces as crack progresses by notch effect from the cavity generated through the deposition under the V-groove which is located at the bottom of stainless cathode. The wax-less type is superior to the wax type on the quality. However, there is the problem of remarkably increased stripping cycle when the power supply is shut down for several hours because the crack progress is opened at the lamination interface generated during the power failure. It is necessary to investigate the interface initiation mechanism on the copper deposition to take measures to control the lamination. In this paper, we would like to present the results of the investigation of the interface initiation mechanism during the power failure.

3:05 PM

Photocatalytic Properties of TiO₂(B) Synthesized from Water-Soluble Titanium Complex: *Makoto Kobayashi*¹; Valery Petrykin¹; Masato Kakihana¹; Koji Tomita²; ¹Institute of Multidisciplinary Research for Advanced Materials, Tohoku University; ²Tokai University

Titanium dioxide (TiO₂) has been used as a photocatalyst for decomposition of harmful organic compounds. Until now eight polymorphs of titania have been described. Among them, only anatase and rutile are well studied because their synthesis is easy and well-established. Recently TiO₂(B), one of TiO₂ polymorphs, has attracted a lot of attention as a prospective lithium electrode, sensor material, and a photocatalyst. Generally, synthesis procedure of TiO₂(B) consists of three steps. We developed a one-step synthesis method based on hydrothermal treatment of water-soluble titanium complexes leading to single phase TiO₂(B) nanoparticles. The obtained TiO₂(B) powders were characterized by XRD, TEM, Raman spectroscopy. The samples had high specific surface area and demonstrated high photocatalytic activity. Photocatalytic activity of TiO₂(B) was also compared against rutile and anatase nanoparticles.

3:25 PM

Increase Production and Quality Improvement of Electrolytic Copper at Tank House in Naoshima Smelter and Refinery: *Hideki Zen*¹; Tatsuo Ishida¹; Makoto Takagi¹; ¹Mitsubishi Materials Corporation

Operation of copper tank house in Naoshima Smelter & Refinery started in 1969. Increase of electrolytic copper production had been mainly carried out

in the past by installing more tank house cells and raising cell current density. However this time increase of production and improvement of quality was achieved without big amount of capital investment, as follows. 1) 22 cells which were used at lead refinery were converted to stripper cells for copper refinery. 2) To improve verticalness of starter sheets, 48 hours electrolysis to produce starter sheets was adopted. 3) Starter sheet preparation machine was modified. 4) Flow amount of electrolyte was controlled at commercial cells. As a result, 750t/month electrolytic copper was increased and tank house capacity reached to 19,500t/M. Furthermore current efficiency at commercial cells was kept over 96.5%.

3:45 PM

Effect of Processing Parameters on Properties of Nanocrystalline FeCrP

Electrodeposits: *Lalgudi Ramanathan*¹; Clarice Kunioshi¹; Olandir Correa¹;

¹Instituto de Pesquisas Energéticas Nucleares - IPEN

Many nanocrystalline alloys have exhibited higher corrosion resistance than their crystalline counterparts and are therefore being used as protective coatings. Electrodeposition from aqueous solutions has rendered a variety of nanocrystalline alloy coatings. The effects of electroplating bath additives, aging of the bath and use of an ion selective membrane on the composition, morphology and corrosion resistance of nanocrystalline Fe-Cr-P deposits have been investigated. Deposits with the desired levels of Cr and P were obtained from baths containing formic acid as a complexant and with the use of a membrane. Surfactant additions and aging of the bath improved further the deposit characteristics. Electrochemical measurements carried out in sulfuric acid indicated increased corrosion resistance of SAE 1020 steel coated with nanocrystalline Fe-Cr-P deposits.

4:05 PM Break

4:30 PM

Electrolytic Deposition and Thermoelectric Characteristics of Bi₂Te₃

Compound Using Basic Ammonia Solution: Takanori Hiramoto¹; *Shingo*

*Sugiyama*¹; Akio Fuwa¹; ¹Waseda University

In this study, Bi₂Te₃ compound film has been successfully electrochemically deposited using basic ammonia solution containing Bi(NO₃)₃, TeO₂ and Nitrilotriacetic acid (NTA), whereby electrochemical deposition cathode potential and solution composition have been varied for the compound stoichiometry, morphology and thermoelectric power characteristics investigation. The deposited film has also been heat-treated, which has shown much improvement on thermoelectric power characteristics, equivalent with other synthetic methods for Bi₂Te₃ compound material.

Environmental Protection Processing II

Monday PM
December 8, 2008
Room: Plaza 6
Location: Sofitel Centara Grand Bangkok

Session Chair: To Be Announced

2:45 PM

Isothermal and Cyclic Oxidation Behavior of Y₂O₃ Coated Fe₂₀Cr

Alloy: Marina Pillis¹; Edval Araujo¹; Olandir Correa¹; *Lalgudi Ramanathan*¹;

¹Instituto de Pesquisas Energéticas Nucleares - IPEN

This paper presents the effect of Y₂O₃ coating on long term isothermal and cyclic oxidation behavior of Fe₂₀Cr alloy. The oxidation tests were carried out for periods of up to 200 hours and the oxidation behavior was evaluated gravimetrically. The oxidation curves revealed that surface addition of Y₂O₃ reduced considerably the mass gain of the alloy after extended oxidation periods. EDS analysis of sections of oxidized Y₂O₃ coated specimens revealed a Cr rich layer close to the metal/oxide interface and the presence of Y and Cr near the oxide/air interface, suggesting diffusion of Cr through the Y₂O₃ layer. XRD analysis indicated the existence of Y₂O₃ and YCrO₃ phases. Macroscopic observations revealed that the Y₂O₃ coating, initially white before oxidation had turned green after oxidation, corroborating diffusion of substrate Cr through the Y₂O₃ layer.

3:05 PM

Metals Recycling and Waste Treatment Businesses of Nippon Mining and Metals Group: *Junzo Hino*¹; *Takehisa Aoki*²; *Juichi Yoneda*³; *Makoto Narisako*⁴; *Susumu Akagi*¹; ¹Nippon Mining and Metals Company, Ltd.; ²Nikko Environmental Service Company, Ltd.; ³Tomakomai Chemical Company, Ltd.; ⁴Nikko Mikkaichi Recycle Company, Ltd.

Nippon Mining and Metals company (NMM) group carries out its metal recycling business, which recovers copper, precious metals and other valuable metals from recycling materials, and environmental services business, which manages detoxification of industrial waste and recovery of valuable metals, basing on its long year experiences and advanced technologies with mining and smelting operations. It collects approximately 100,000 tons per year of copper and precious metal scraps from waste sources such as electronic parts, mobile phones, catalytic converters, print circuit boards and gold plated parts. These items are recycled through the smelting and refining operations of Saganoseki smelter and Hitachi plant of the NMM affiliate NIKKO Smelting Company. In addition, environmental services are provided through four other affiliates: Nikko Environmental Services, Tomakomai Chemical, Nikko Mikkaichi Recycle and Nikko Tsuruga Recycle. Outline of the the recycling and environmental service operations of Nippon Mining and Metals group is introduced in this paper.

3:25 PM

Novel Gas-Fired Pulse Combustors-Design Evaluation via Simulation: *Wu Zhonghua*¹; *Arun S. Mujumdar*¹; ¹Minerals, Metals, and Materials Technology Centre (M3TC)/National University of Singapore

Pulse combustion is known to offer better combustion and energy efficiency but at the cost of higher nosier level relative to steady combustion. Conventional cylindrical geometries are not the only ones that can be used for gas-fired pulse combustors although conventionally this is the practice. Some novel concepts such as use of a “heart” shape combustion chamber, fractional and spiral tailpipes, etc can be potential design innovations. They are simulated using a CFD model that was validated earlier with published experimental data. Operational characteristics such as the specific impulse, thrust output-to-power input ratio, noise level, etc are computed and compared. It was found that the novel geometric designs produce distinct advantages e.g. compact structure, low noise, high specific impulse etc. An optimal geometry design is suggested based on our numerical results. Such studies are expected to yield better designs of the pulse combustor leading to more industrial applications in future.

3:45 PM

Rare Earth Chromite Coatings for Increased H.T. Oxidation Resistance of Metallic SOFC Interconnects: *Lalgudi Ramanathan*¹; *Marina Pillis*¹; ¹Instituto de Pesquisas Energéticas Nucleares - IPEN

The high costs and manufacturing difficulties associated with dense lanthanum chromite based ceramic interconnects presently used in solid oxide fuel cells (SOFC) and the concerted efforts to reduce SOFC operating temperatures to below 1000°C has increased the search for metallic interconnects. Chromium dioxide or alumina forming iron based alloys are potential materials for interconnects. Coatings and/or surface treatments are options to further extend the useful life of these potential SOFC interconnect alloys. This paper presents details of ‘in situ’ formation of lanthanum chromite at high temperatures from powder mixtures and the effects of such ‘in situ’ coatings on the oxidation behavior of Fe-20Cr and Fe-20Cr-4Al alloys at SOFC operating temperatures. The oxidation measurements and the results of SEM/EDS as well as XRD analyses indicated that lanthanum chromite coatings increased significantly the oxidation resistance of the alloys, even more so than other rare earth oxide coatings.

4:05 PM Break

4:30 PM

Preparation of Chemically Modified Lignophenol Gels from Biomass Wastes and Its Application to the Recovery of Precious Metals: *Katsutoshi Inoue*¹; *Durga Parajuli*¹; *Kanjana Khunathai*¹; *Masamitsu Funaoka*²; ¹Saga University; ²Mie University

Lignin contained in all plants is a refractory material. In recent years, Funaoka developed a simple method to extract lignin as a new material named

“lignophenol” without changing its original nature from various biomass wastes such as wasted woods. It is expected as environmentally benign biodegradable plastics. It is possible to prepare various kinds of lignophenol compounds with a variety of functions by simple chemical modifications. In the present work, we investigated its application as adsorbents for precious metals. It was found that gold(III) is very selectively adsorbed from hydrochloric acid on the lignophenol gel with very high capacity while other noble metals like platinum and palladium as well as base metals are not practically adsorbed. By immobilizing various amino groups on the matrices of lignophenol, platinum and palladium were also adsorbed while practical adsorption of base metals was not observed, but the adsorption of gold was much enhanced.

4:50 PM

Preparation of Polyaniline Derivatives for Anticorrosive Coating: *Dusadee Supcharoen*¹; *Krongkan Sirinukulwattana*¹; *Somboon Sahasithiwat*²; *Suppalak Angkaew*¹; ¹King Mongkut’s University of Technology Thonburi; ²National Metal and Materials Technology Center

Our research aims to prepare polyaniline (PANI) derivatives that are more soluble in common organic solvents and having conductivity and anticorrosive properties similar to PANI. Six derivatives; namely poly(N-methylaniline), poly(N-ethylaniline), poly(o-anisidine), poly(o-toluidine), poly(2,3-dimethylaniline), and poly(2,5-dimethylaniline), were prepared by oxidative polymerization. All of them were soluble in tetrahydrofuran, chloroform, and toluene. The derivatives with larger side-group, i.e. poly(2,3-dimethylaniline) and poly(2,5-dimethylaniline), showed higher solubility than other derivatives. Solution of 2% polymer (PANI or the derivatives) and 2% PVC in NMP was spray-coated onto steel testing panels. The coated panels were doped with 1-M HCl to convert the polymer into its conductive form. Anticorrosive testing was performed by immersing the polished steel panels into 3.5% NaCl solution and the extent of rust formation was followed over time. The results showed that all of the derivatives exhibit anticorrosion protection similar to PANI, especially poly(2,5-dimethylaniline), poly(o-anisidine) and poly(o-toluidine) gave slightly better protection than PANI.

5:10 PM

Zeolitic Adsorbent for the Separation of Strontium and Cesium: *Erika Sonohara*¹; *Syouhei Nishihama*¹; *Kazuharu Yoshizuka*¹; ¹University of Kitakyushu

Separation of strontium and cesium has been investigated with zeolitic adsorbents. The zeolite A type adsorbent has large specific surface area (562 m²/g) and the particle size is 1.16 μm. The conventional batchwise experiments indicate the adsorption mechanism for both metal ions are Langmuir type. The maximum adsorption amounts at equilibrium pH of 4.00 are 3.32 mmol/g for strontium and 1.66 mmol/g for cesium, and at equilibrium pH of 6.00 are 3.69 mmol/g for strontium and 3.64 mmol/g for cesium. Since the pH dependencies of the adsorption of strontium and cesium are different, selective separation of the metals can be achieved. Based on the batch studies, the column operation for the separation of the two metals is conducted.

Materials Processing II

Monday PM
December 8, 2008

Room: Plaza 3
Location: Sofitel Centara Grand Bangkok

Session Chair: Ryosuke Suzuki, Hokkaido University

2:45 PM

Lead Solubility in FeOx-CaO-SiO2-NaO0.5 and FeOx-CaO-SiO2-CrO1.5 Slags at Iron Saturation: *Katsunori Yamaguchi*¹; *Dai Matsuura*¹; *Toshiko Kon*¹; ¹Iwate University

The sodium and chromium contents in copper or lead smelting slags are increasing with the increase in waste recycling. The lead solubility in the slag is important from both an economical and environmental perspective.

As a fundamental study, experiments have been carried out to determine the equilibria between FeOx-CaO-SiO₂-5mass%NaO_{0.5} or FeOx-CaO-SiO₂-5mass%CrO_{1.5} slags and lead metal in iron crucibles at 1573K. It has been found that addition of soda decreases the lead solubility in SiO₂ rich side of the slag, while soda increases the solubility in CaO rich side. Chromium in the slag decreases the lead solubility in the FeOx-CaO-SiO₂ slag. The activity coefficients of PbO in the FeOx-CaO-SiO₂-5mass%NaO_{0.5} or FeOx-CaO-SiO₂-5mass%CrO_{1.5} slags were compared with those of the CaO-SiO₂-FeOx ternary system.

3:05 PM

Calciothermic Reduction and Simultaneous Electrolysis of CaO in the Molten CaCl₂: *Ryosuke Suzuki*¹; ¹Hokkaido University

The author's group proposed the electrolysis of CaO to produce Ca in molten CaCl₂ in order to use Ca for the reduction of TiO₂ in the molten CaCl₂ and to supply the by-product CaO for further electrolysis. In the lab-scale test, 1.0 g TiO₂ powder was successfully reduced and deoxidized to produce 2000 ppm of oxygen for 3 h at 1173 K. For application to the industry, it is the key to separate the CO/CO₂ gas bubbles at the carbon anode from the dissolved Ca generated near the cathode. The usage of ceramic membrane such as porous MgO or ZrO₂ anode were effective to minimize the carbon contamination. The dissolution of CO₂ gas in the molten CaCl₂ was measured under the equilibrium with the atmospheric pressure of CO₂ gas. The precipitation of CaCO₃ was expected when the CaO concentration was >10 mol%CaO at 1173K.

3:25 PM

Casting Practice for High-Carbon Nitrogen-Alloyed Chromium-Manganese Austenitic Stainless Steels: *Meredith Heilig*¹; Brajendra Mishra²; Manuel Marya²; Dave Olson¹; ¹Colorado School of Mines; ²Schlumberger Reservoir Completions Center

A development regarding carbon additions in nitrogen-alloyed stainless steels presents intriguing possibilities for the future of chromium-manganese based stainless steels. With proper levels of carbon and nitrogen, a cast material can be made that will not form carbides or nitrides, alleviating concern over localized corrosion. The metallurgical requirements to achieve enhanced properties will be considered. Work has been done to economically produce austenitic stainless steel alloys with improved mechanical properties and corrosion resistance. The combination of a series of casting practices is crucial in manufacturing high-carbon nitrogen-alloyed austenitic stainless steel castings with minimal inclusions. The practices to economically produce these castings at atmospheric pressure will be discussed. Alloys of moderate to high nitrogen and carbon concentrations have been produced and examined in comparison to commercially available stainless steels. A review of melting trials, microstructural features, and the results of mechanical testing and corrosion resistance assessment will be presented.

3:45 PM

Cryogenic Processing –Your Flexible Friend: *Paul Stratton*¹; ¹Linde Gas

Cooling to cryogenic temperatures has many uses in the processing of materials, some of which are focussed on changing their properties. During steel processing, components are quenched to convert the soft high temperature austenite content to hard martensite. However, in some steels the process can only go to completion below room temperature. Cooling to temperatures in the range -70 to -150°C is used to complete the conversion and obtain optimum properties. Cryogenic processing is environmentally friendly and uses less energy than the alternative multiple tempering route. If, after quenching, components are immediately cooled to an even lower temperature in liquid nitrogen and held for at least 24 hours, nucleation sites for eta-carbides are formed. The nano-scale carbides precipitate during post-processing tempering and improve wear resistance. Again, the process is environmentally friendly and saves resources by increasing the life of treated tools.

4:05 PM Break

4:30 PM

Corrosion Resistance of Si-Al Bearing Ultrafine Grained Weathering Steel in Saline Environment: *Toshiyasu Nishimura*¹; ¹National Institute for Materials Science

High Si-Al type ultrafine grained (UFG) weathering steel was created by the grain refinement and weathering guidance. This steel showed excellent properties in strength and corrosion resistance. The samples were made by the multi-pass warm rolling process. The grain size rolled at 873K was 1 μm, and TS and EL was 800MPa and 20%, respectively. The corrosion tests using chloride ions confirmed that the developed steel exhibited excellent corrosion resistance than SM. The EPMA and TEM analyses showed that Si and Al were existing in the inner rust. Si and Al were identified as Si₂⁺ and Al₃⁺ state in the nano-scale complex oxides of inner rust. The EIS measurement showed that the corrosion resistance (R_t) of the developed steel was much larger than that of SM. In the developed steel, the nano-scale complex oxides were made in inner rust, and increased R_t, and showed high corrosion resistance.

4:50 PM

Challenges of Obtaining Reliable High Temperature Measurements in PTAW Processing: *Tonya Wolfe*¹; *Hani Henein*¹; ¹University of Alberta

High temperature measurements of PTAW (plasma transferred arc welding) coatings deposited in-situ are required in order to optimize the process. There is wide interest in obtaining high temperature measurements for other high temperature processes using infrared thermography. However, the reliability of the quantitative data is often in question. Changes in emissivity with temperature, surface condition and phase change challenge the credibility of infrared results. In this paper, the methodology developed and applied to PTAW in order to generate reliable temperature measurements of the surface of the deposit upon cooling after the arc is extinguished, will be described. The methodology applies the coupled use of differential scanning calorimetry, laser reflectance pyrometry, infrared thermography and mathematical modeling.

5:10 PM

Effect of Blank Holder Force on the Depth of Ears in Deep Drawn AA1017 Cups: *Sanmbo Balogun*¹; *David Esezobor*¹; *Samson Adeosun*¹; ¹University of Lagos

Blank holder pressure is generally 0.7 to 1.0% of the total sum of the yield and ultimate tensile strength of the sheet metal. A very high blank holder force (BHF) will result to tearing of the cup wall while, a low BHF will lead to wrinkling of the flange. The relationship between the BHF and the cup heights (CH) is studied in this paper. It presents the effects of sheet properties on the formability of AA 1017 during cup forming. The results of the study indicate a linear relation between BHF and CH for thinner gauge hot rolled material (0.7 to 1.6 mm thick). The CH increases slowly as the BHF rises. This could be attributed to substantial recovery obtained during annealing process. However, CH increase significantly with BHF when the material is hot worked prior to annealing.

5:30 PM

Boronizing: Surface Modification of Metal/Alloy with Boron: *Naruemon Suwattananont*¹; *Roumiana Petrova*¹; *Sittinun Tawkaew*²; ¹New Jersey Institute of Technology; ²Srinakharinwirot University

Boronizing (Boriding) is a thermo-chemical surface modification in which boron atoms diffuse through metal/alloy substrates and form metallic boride phases on the substrate surface. The conventional powder pack boronizing method is presented. In this research, the boronizing of different metal/alloy substrates (carbon steel, stainless steel, nickel-alloy, titanium alloy and transition metals) was treated at 800 – 1100°C for 4 – 8 h. under an inert atmosphere. The microstructure and phase identification of metallic boride coatings were observed. The microhardness of coatings is more than 2000 HK, depending on types of metallic boride coatings. The corrosion resistance of boronized low carbon steel is approximately 100 times higher than that of unboronized low carbon steel. The oxidation resistance of boronized coating is also improved and stands up to 800°C. The friction coefficient of boronized coating is between 0.2 - 0.4.

Materials Processing III

Monday PM
December 8, 2008

Room: Plaza 4
Location: Sofitel Centara Grand Bangkok

Session Chair: Toru Okabe, University of Tokyo

2:45 PM

Development of an Advanced Semi-Solid Forming Process: *Perakit Viriyarattanasak¹; Masao Kikuchi²; Masayuki Itamura²; Takumi Maeda²; Koichi Anzai³; Eisuke Niyama⁴; ¹National Metal and Materials Technology Center; ²Nanocast Corporation; ³Tohoku University; ⁴Nagoya Institute of Technology*

In conventional semi-solid casting both thixocasting and rheocasting, there has a limit in use of alloy and a difficulty in controlling a globular microstructure and its grain size that will lead to a lower mechanical properties. Furthermore, the inefficiency in production cost and productivity are still a disadvantage in commercialization. In this paper, a quick and easy semi-solid slurry manufacturing process called "Nanocast method" will be introduced. By this method, various alloy systems ex. ADC5, ADC6, ADC10, AC4C and AC2A etc. can be used. Furthermore, tool life ex. shot sleeve, plunger tip and die life will be extended because of low melt temperature and slow shot speed injection. Resulting in working environment improvement and energy saving. The application of this method in die casting and forging will be introduced also.

3:05 PM

Development of Nickel-Base Foams for Energy and Functional Applications: *Yuttanant Boonyongmaneerat¹; Markus Chmielus²; David Dunand³; Peter Müllner⁴; ¹Metallurgy and Materials Science Research Institute, Chulalongkorn University; ²Hahn-Meitner-Institut, Smart Magnetic Materials Group; ³Department of Materials Science and Engineering, Northwestern University; ⁴Department of Materials Science and Engineering, Boise State University*

Owing to a combination of appealing properties including high surface area and high specific strength, metallic foams have recently received much interest both in research and industrial contexts. Here, we develop for the first time open-cell shape-memory Ni-Mn-Ga foams and closed-cell syntactic Ni-Cr-Mo foams via the replication casting technique for possible use in actuator and solid oxide fuel cell interconnect applications, respectively. Several important properties, including magnetoplasticity and creep response, which critically determine the performance of the foam alloys for such applications are experimentally evaluated. With the uniqueness of their cellular microstructures, comprising networks of dense struts and porosity, the Ni-base foams exhibit exceptional magnetic-induced-strain and high-temperature mechanical responses, which are markedly superior to those of conventional solid alloy counterparts. Combining these qualities with their light weight and relatively low production cost, the developed Ni-Mn-Ga replicated foams and Ni-Cr-Mo syntactic foams are very attractive for sensor and energy applications, respectively.

3:25 PM

Effect of Austenite on the Drawing Limit of Ferrite-Austenite DP Steel Wire: *Hu-chul Lee¹; Seung-Hyun Lee¹; ¹Seoul National University*

The effect of austenite on the drawability of ferrite-austenite DP steel wires was investigated. Low carbon alloys were solution treated and tempered at between 525°C and 700°C. The volume fraction of austenite was varied from 20% to 40% depending on the alloy composition, tempering temperature, and tempering time. The drawability of the wire was also decreased with the increase in the austenite volume fraction and the decrease of the mechanical stability of austenite. The interface of the martensite and ferrite was identified as the void nucleation site and the number density of voids was increased with the increase in the austenite volume fraction. Plastic incompatibility at the interface was assumed to be the main reason of void nucleation. Ferrite-austenite DP steels could be drawn to the true strain of 8.0 at maximum

without intermediate heat treatment. Tensile strength of the wire was varied with the volume fraction of transformed martensite.

3:45 PM

Effect of CaF₂ on the Interfacial Behavior of Al-Alloy and Monolithic Refractories: *Pramod Koshy¹; Sushil Gupta¹; Veena Sahajwalla¹; Phil Edwards²; ¹University of New South Wales; ²Shinagawa Refractories Australasia Pty. Ltd.*

The interfacial phenomena between Al-alloy and refractory was investigated as a function of varying silica/alumina ratios at 1250°C. Dynamic contact angles were measured using sessile drop technique, while interfacial phases were characterized using X-ray diffraction (XRD) and Electron Probe Micro Analyzer (EPMA). This paper also reports the effect of CaF₂ on the modification of the wetting resistance of the refractory samples. The effect of non-wetting agent concentrations in improving wetting resistance is shown to be dependent on silica/alumina ratio of the refractory. The interfacial behaviour and their associated mechanisms related to the intensity of reactions with the alloy are discussed.

4:05 PM Break

4:30 PM

Effect of Filler Alloys on a Gas Tungsten Arc Dissimilar Weldment between AISI 304 Stainless Steel and AISI 1020 Carbon Steel in NaCl and H₂SO₄ Solutions: *Somrerak Chandra-ambhorn¹; Wichan Choypan¹; Wikornake Tanespolake¹; ¹King Mongkut's University of Technology North Bangkok*

A gas tungsten arc welding (GTAW) was applied to weld an AISI 304 stainless steel and an AISI 1020 carbon steel with AISI 308L (Fe-20Cr), 309L (Fe-23Cr), 316L (Fe-19Cr-2.6Mo) fillers. The corrosion behaviour of the weld metal was investigated in 3500-ppm NaCl solution and 1-M H₂SO₄ solutions at room temperature by potentiodynamic method. In NaCl solution, the corrosion potential of weld metals produced by AISI 316L and 309L fillers exhibited the similar value and higher than that produced by AISI 308L filler. The pitting potential of weld metal produced by AISI 316L filler was higher than that of AISI 309L filler. In the H₂SO₄ solution, transpassive and corrosion potentials of weld metal produced by AISI 316L filler exhibited the superior values to those of weld metals produced by AISI 308L and AISI 309L fillers. Microstructure and discussion in term of pitting resistance equivalent number (PREN) were described in the paper.

4:50 PM

The Processability Study on Polyethylene/Low Molecular -Weight Natural Rubber Blends: *Songkot Utara¹; Ploenpit Boochatham¹; ¹King Mongkut's University of Technology Thonburi*

The LLDPE/NR blends were prepared by melt mixing at 150°C. The molecular weights of natural rubbers used were in the range of $M_w = 8.30 \times 10^5 - 1.45 \times 10^6$ g/mol, $M_n = 2.62 \times 10^5 - 4.48 \times 10^5$ g/mol and MWD = 2.3 - 3.3. The processability study of LLDPE/NR blends at different strains and temperatures showed that adding NR having $M_w = 8.30 \times 10^5$ g/mol, $M_n = 2.62 \times 10^5$ g/mol and MWD = 3.3 slightly reduced the processability ($\tan\delta$) of LLDPE. In addition, loading NR up to 40 (%w/w) slightly changed the processability of LLDPE whereas higher molecular weights as well as loading remarkably reduced processability of polyethylene as lower $\tan\delta$ values were observed. Among these, 60/40 blends showed the processability closed to those of virgin polyethylene. Morphology study showed that the higher loading of NR, the stronger intramolecular interaction among rubber molecules was observed resulting in the flow resistance of polyethylene.

5:10 PM

Theoretical and Experimental Investigation of Significant Quantities in Designing Electron Gun for Applying in a SEM System: *Hanieh Yazdanfar¹; ¹Tarbiat Modares University*

In this study, several quantities which are most important and effective in the performance of an electron gun have been investigated. For the purpose of designing an electron gun, investigations and calculations for electron production from tungsten, lanthanum hexaboride, Th-w and Re-w filaments by thermionic emission and for controlling the electron beam current have been accomplished here. Lifetime, evaporation rate, current density right

above the cathode and over the anode, structural impurity contamination effect, electron beam divergence angle and the required pressure were calculated and the diagram of these quantities have been illustrated versus temperature of filament, accelerating voltage and distance between cathode and anode. In our calculations the motion of electrons was considered maxwellian. The correlation between some of the above quantities such as pressure effect on beam current and its relationship with brightness has also been investigated. Space charge effect has been considered obtaining beam current value.

5:30 PM

Titanium Production Process by Disproportionation of Titanium Dichloride in MgCl₂ Molten Salt: *Taiji Oi*¹; Toru Okabe¹; ¹Institute of Industrial Science, University of Tokyo, Okabe Laboratory (Fw-301)

In order to establish a new titanium production process, the synthesis and disproportionation of TiCl₂ in molten salt were investigated. This process comprised (1) the synthesis of TiCl₂ by reacting TiCl₄ with titanium metal in MgCl₂ molten salt at 1073-1273 K and (2) the formation of titanium by the disproportionation of TiCl₂ in molten MgCl₂ at 1273 K. The results revealed that TiCl₂ was successfully obtained in the synthesis step and that the efficiency of TiCl₂ formation was drastically improved by using molten MgCl₂ as the reaction medium. Some preliminary experiments demonstrated that titanium powder of over 99% purity was produced by disproportionation of TiCl₂ in MgCl₂ molten salt. The titanium production methods investigated in this study can be applied to a new titanium production process such as high-speed Ti production or to Ti coating on steel. This process can also be used for recycling titanium metals from scraps.

Materials Processing IV

Monday PM
December 8, 2008

Room: Plaza 5
Location: Sofitel Centara Grand Bangkok

Session Chair: Brajendra Mishra, Colorado School of Mines

2:45 PM

Effect of Quenching Media on Mechanical Properties of Aluminum 6063 Alloy: Sanmbo Balogun¹; David Esezobor¹; Samson Adeosun¹; *Atinuke Oladoye*¹; Fidelia Ochulor¹; ¹University of Lagos

Average quench rates are useful to compare experimental results from various quench methods. Quench-factor analysis can be used to predict or optimize quantitatively the property of materials. In this paper, the quench sensitivity of AA 6063 is studied. Air, water, brine, spent automobile engine oil and palm olein oil are used as the cooling media. Artificial aging of five of the samples after solution treatment (5600C, at 1 hour) is done at 1750C for 8 hours. The study reveals that the volume and size of the intermetallic Mg₂Si formed, which is dependent on the severity of the quenchants affects the mechanical properties of AA 6063. Optimum combination of hardness, tensile strength and ductility over the extruded properties can be obtained with cooling in brine solution after solution treatment. It is also observed that artificial aging does not significantly improve these properties.

3:05 PM

Effect of the Simultaneous Phase on Polymer Adhesions during Coinjection Molding: *Wuttipong Rungseesantivanon*¹; Gordon Smith²; ¹National Metal and Materials Technology Center; ²University of Warwick

The co-injection molding process was studied. The experiment has led to an understanding of the mechanism of dual injection processing. Emphasis has been focussed the relationship between the simultaneous times and the minimum skin thickness fractions and the effect of the simultaneous times on the polymers adhesion level. In the presence of compatibiliser, the chemical reaction between active functional groups of skin and compatibiliser in the core occurred. Suitable conditions were necessary to produce good bonding between skin and core. The greater thickness of skin layer and greater simultaneous injection times led to more probability for the skin and core

active functional groups to react with each other before the skin became no-flow layer. Methods available to achieve these thicknesses and simultaneous injection times were possible by controlling the molding parameters, such as lengths of simultaneous phase which could affect the skin-core thickness formations and their adhesion to different degrees.

3:25 PM

Effects of A3 Steel Shielding Layer on the Stable Magnetic Field: *Yu Liang*¹; Jiang Yanli¹; Feng Naixiang¹; Cui Jianzhong¹; ¹Northeastern University

In this work, the influence of A3 steel on the stable magnetic field have been predicted theoretically with ANSYS and confirmed experimentally. The shield effectiveness of steel shield layers were compared in the same and different stable magnetic fields, The results showed that the magnitude and the distribution of the stable magnetic field were influenced greatly by the shape and thickness of the shielding layer, the current intensity and the positions of the bus bar. And the measured and simulative data were consistent well, which proved the suitability of software ANSYS to simulate the magnetic field of aluminum reduction cells.

3:45 PM

Extrusion of Cu Powder Feedstock: Ruangdaj Tongsri¹; Rattana Wichianrak²; Nuchthat Poolthong²; *Nandh Thavarungkul*²; ¹National Metal and Materials Technology Center; ²King Mongkut's University of Technology Thonburi

In this study, mixtures of Cu powder (representative of metal powders) with flow-assisting polymers were prepared. The Cu powder-polymer mixtures, also known as "feedstock", were expected to be extrudable with low pressure and temperature. Different shape Cu powders were mixed with low density polyethylene (LDPE), paraffin wax and stearic acid. Different ingredients of these polymers were prepared and each formula was mixed with 60% by volume of Cu powder. Experimental results showed that the polymer ingredients of LDPE:wax: acid of 40:55:5 and 45:50:5 could make enough green strength of the extrudates. However, the 45:50:5 formulas gave extrudates with smooth surface. The extrudates showed neither distortion nor warpage. Further processing steps of the extrudates, including solvent debinding and sintering were also performed. The results will be shown and discussed.

4:05 PM Break

4:30 PM

Enrichment of Phosphorous from Low-Grade Resources: *Daisuke Sato*¹; Lipang Wang¹; Gjergj Dodbiba¹; Jun Sadaki¹; Toyohisa Fujita¹; Hideaki Tanno²; ¹University of Tokyo; ²Eriez Magnetics Japan Company, Ltd.

Phosphorus is an element, which is primarily being used in the agricultural sector. Nevertheless the phosphorous resources are limited. Therefore, this study is focused on the enrichment of phosphorus from low-grade resources, such as slug or sand that include apatite. In order to increase the grade of phosphorus, the sample was grinded and screened (-32mesh). Then, the resulting powder was processed by using a magnetic separator at various magnetic flux densities. The concentration of phosphorus was analyzed by inductively coupled plasma spectrometer (ICP). The experimental result showed that a high-grade of P₂O₅ product was recovered in the non-magnetic fraction. The grade of the a P₂O₅ product was relatively high (32wt%), while the magnetic flux density was kept at 0.2T. The experimental results suggested that the recovered high-grade P₂O₅ product can be used as raw materials in the fertilizer industry since its grade is higher than 30 wt%.

4:50 PM

Extending Fatigue Life of McKibben Artificial Muscle Actuators: *Nattapong Nithi-Uthai*¹; Sathaporn Laksanacharoen²; ¹Prince of Songkla University; ²King Mongkut's Institute of Technology North Bangkok

The McKibben artificial muscle is a pneumatic actuator which has a high force to weight ratio. This artificial muscle consists of the inner rubber bladder and the braided outer sleeve. Repeated contraction of the muscle leads to fatigue and failure of the actuator at the inner rubber bladder. In this paper, fatigue lives of the actuators are investigated. Natural rubber is used to make the inner rubber bladder via dipping process. Effect of rubber compounding

formulas and processing conditions are studied. Klute-Hannaford model is used to predict life cycles of the actuators. Experiment results reveal that we are able to develop natural rubber bladder which possess superior life cycle of 50000 cycles at 30% contraction, a decade over that of previously reported. Material constant, beta, is found to be 1.77 which is closer to classically reported for natural rubber at 2 than empirically used by Klute and Hannaford at 3.

5:10 PM

Effects of Cold-Rolling and Martensite Volume Fraction on Microstructures and Mechanical Properties of Dual-Phase Steels:

*Chaichan Duengkratok*¹; Somrer Chandra-Ambhorn²; Witthaya Eidhed²; ¹Materials and Metallurgical Engineering Program, Thai-Germa Graduate School, King Mongkut's University of Technology North Bangkok; ²Department of Production Technology, Faculty of Engineering, King Mongkut's University of Technology

Nowadays, high strength and excellent formability of sheet steels are required to reduce the weight of automobile in order to save the energy consumption. The dual-phase steels are the attractive ones to produce the high performance automotive parts. Normally, the dual-phase steels are produce from the hot-rolled steel. In this paper, the effects of the cold-rolling and martensite volume fraction (MVf) on microstructures and mechanical properties of the dual-phase steels were investigated. In the experimental procedure, two types of the hot-rolled steels (Fe-0.11%C-0.52%Mn and Fe-0.11%C-1.41%Mn) were selected to develop the dual-phase steels. The samples are deformed using cold-rolling with 25, 35, 45 and 65% cold-rolling, respectively. Then, the samples were heated to the different intercritical temperatures in order to produce the martensite volume fractions, approximately 10, 20, 30 and 40%MVf. The temperatures were examined by using the software "Thermo-Calc". After quenched, the microstructure shows that the martensite phase formed at the ferrite grain boundaries. It is clearly that the smaller ferrite grain sizes were obtained in the 65% cold-rolled samples compared with 25, 35, and 45% cold-rolled samples, respectively. Moreover, finer and uniformly distributed martensite phases are also obtained. It should be noted that cold-rolling is strongly effect on size and morphology of martensite in the 20%MVf samples compared with the 40%MVf samples. The effects of MVf and Mn content on the mechanical properties are also presented.

5:30 PM

Effects of Heat Treatment Parametres on Microstructure and Corrosion Properties of Dual-Phase SAPH 440 Steel: Somrer Chandra-ambhorn¹; Kittisak Lraorprasertsuk¹; Withaya Eidhed¹; ¹King Mongkut's University of Technology North Bangkok

A SAPH 440 carbon steel containing 0.13% carbon and 1.4% manganese were heated to 780 and 830°C and held at these temperatures for 40, 80 and 120 minutes before quenching to cool water. It was found that the dual phase of martensite island in ferrite matrix could be obtained in the range of 30 to 42%. The amount martensite increased with the decreased holding period at the same soaking temperature, and increased with the increased soaking temperature at the same holding period. The increase of martensite went along with the increase of Vickers hardness of the dual phase steel. The immersion test 70% nitric acid at room temperature was conducted in function of time up to 6 minutes. It was found that the corrosion rate decreased with the increased amount of martensite. The corrosion results obtained by potentiodynamic method was described and discussed in the paper.

Nanomaterials Processing II

Monday PM
December 8, 2008

Room: Plaza 7
Location: Sofitel Centara Grand Bangkok

Session Chair: To Be Announced

2:45 PM Invited

Functional Ceramics Nano-Composites via Solidification and Annealing of Eutectic Melts in Al_2O_3 - HfO_2 - Gd_2O_3 and Al_2O_3 - Y_2O_3 - CaO Systems: Masahiro Yoshimura¹; Naonori Sakamoto¹; Shunji Araki¹; Daisuke Ogasawara¹; Tomoaki Watanabe¹; ¹Tokyo Institute of Technology

We are challenging to develop novel processing to fabricate shaped and sized ceramics without sintering of molded powders. In addition to Soft Processing using aqueous solutions,^{1,2} we have studied solidification of eutectic and/or near eutectic melts in binary and ternary systems non-containing network former oxides, that is, HfO_2 - Al_2O_3 - MOx (M=rare earths, etc.).^{3,4} In their developments, we have found that transparent amorphous phases can be obtained by just simple solidification of near eutectic melts without splat quenching. We have successfully fabricated an amorphous bulk ceramics in the ternary system HfO_2 - Al_2O_3 - $GdAlO_3$. It has the near eutectic composition of HfO_2 (14 mol%), Al_2O_3 (63 mol%) and Gd_2O_3 (23 mol%) and highly transparent, >85%, in the visible region after the cooling of around 200-500 K/s for 2-5 mm f globules. The sample had kept amorphous up to 1073K but crystallized above 1273K keeping its transparency when it contained 5-10 nm hafnia and 5-10 nm $GdAlO_3$ grains. The formation of an amorphous phase could be discussed by the equilibrated temperature (T_e) lines in meta-stable phase diagram.⁵ Similar Amorphous phase could be obtained in the system Al_2O_3 - CaO - Y_2O_3 .^{6,7} It gives crystalline $12CaO \cdot 7Al_2O_3$ phase by annealing at 1273K without cracking during crystallization due to controlled nano-structures with another crystalline phase $CaYAlO_4$.⁸ Numerical Simulation of the rapid solidification for the spherical samples were studied.⁹ The present study suggests possible formation of crystalline and non-crystalline bulk ceramics by the melt-solidification of eutectic melts in various ternary or multiple phase systems. [References] ¹M. Yoshimura, J. Mater., Sci., 41 [5] 1299-1306 (2006). ²M. Yoshimura and R. Gallage, J. Solid State Electrochem., in press. ³S. Araki and M. Yoshimura; Int. J. Appl Ceram. Technol., 1, 155 (2004). ⁴A. Sugiyama, S. Araki, N. Sakamoto, T. Watanabe, and M. Yoshimura; J. Electroceramics, 17, 71-74 (2006). ⁵S. Araki and M. Yoshimura; J. Euro. Ceram. Soc., 26 3295-3299 (2006). ⁶N. Sakamoto, T. Watanabe, and M. Yoshimura; J. Electroceramics, 17, 1075-1078 (2006). ⁷N. Sakamoto, T. Watanabe, and M. Yoshimura; Int. J. Applied Ceramic Technology, 3 [4] 266-271 (2006). ⁸N. Sakamoto, K. Suda, T. Watanabe, N. Matsushita, and M. Yoshimura; J. Euro Ceram. Soc. (accepted, Jan. 12, 2008). ⁹Z. S. Nikolic and M. Yoshimura; J. Mater. Sci., 42 [18], 7729-7737.

3:05 PM

Electrochemical Preparation and Properties of Nanocrystalline Ni-W Alloys: A.S.M.A. Haseeb¹; K. Bade²; M. A. Satter¹; ¹University of Malaya; ²Forschungszentrum Karlsruhe

Nanocrystalline nickel-tungsten alloys are considered to have good potential for the fabrication of LIGA based micro electro mechanical systems. In this study, Ni-6.7at% W alloy was galvanostatically prepared from ammoniac-citrate bath at 348 K. Ni-W alloy samples were then characterized by SEM, EDX, x-ray diffractometry and microhardness measurements. The specimens were annealed at 473-773 K for 3-48 hours. The Ni-6.7at% W alloy possessed an as-deposited grain size of 18 nm which did not change significantly upon annealing. Annealing caused only a slight decrease in the lattice parameter of the Ni-W alloy sample. Microhardness values of the sample increased with annealing duration at 473 and 573 K, reaching peak hardnesses of 1155 and 1185 HV respectively from an initial value of 640 HV. No significant change in hardness was found at 673 K, while a decrease was observed at 773 K. The structure property relationship in nanocrystalline Ni-W alloy is discussed.

3:25 PM

Fabrication and Investigation of ZnO/Multi-Walled Carbon Nanotubes (CNTs) Nanocomposites: *Maolin Pang*¹; *Kexin Yao*¹; *Hua Chun Zeng*¹; ¹National University of Singapore

Nanoparticles can be assembled on a one-dimensional (1D) nanostructures to form unique and interesting hybrid nanomaterials. The as-obtained nanocomposite materials have attracted intensive interest because they may exhibit new optical and electrical properties. Recently, carbon nanotubes (CNTs) have been used as templates for the hybrid assembly of nanoparticles. ZnO as an important functional materials, has been widely investigated and prepared into various nanostructured morphologies. However, there are limited reports on ZnO nanoparticles integrated with CNTs as hybrid structures. In the present work, we report a hybrid system of ZnO nanoparticles on multi-walled CNTs synthesized by a simple method. The results showed that the original smooth multi-walled CNTs were decorated by ZnO nanoparticles, and the ZnO nanoparticles have well-distributedly attached to the multi-walled CNTs to form chain-like structures. Our results highlight opportunities for integrating CNTs with other functional oxide nanoparticles, and for exploring the collective properties of nanoparticles/CNT hybrid materials.

3:45 PM

Microbial Synthesis of Gold Nanotriangles Using the Metal-Reducing Bacterium *Shewanella algae*: *Takashi Ogi*¹; *Tomoyuki Tachimi*¹; *Norizoh Saitoh*¹; *Toshiyuki Nomura*¹; *Yasuhiro Konishi*¹; ¹Osaka Prefecture University

Microbial synthesis of gold nanotriangles was achieved at room temperature using Fe(III)-reducing bacterium *Shewanella algae*. Cell extracts prepared by sonicating a cell suspension as well as *S. algae* cells were capable of reducing 1 mM aqueous Au(III) ions into elemental gold within 10 min when H₂ gas was provided as the electron donor. The reaction time was found to be an important factor in controlling the morphology of biogenic gold particles. At an early stage of reaction, well dispersed spherical gold nanoparticles below 10 nm in size were synthesized, and gold nanotriangles 100 nm in size started to synthesize after 6 h. After 1 day, 60% of the total nanoparticle population using the cell extracts was due to gold nanotriangles, and was markedly higher than that using the resting cells. The absorption peak of the suspension of gold particles was also investigated to clarify the size and morphology of the prepared gold particles.

4:05 PM Break

4:30 PM

Microbial Preparation and Catalytic Activity of Palladium Nanoparticles on the Metal-Reducing Bacterium *Shewanella oneidensis*: *Yasuhiro Konishi*¹; *Shuji Shimanaka*¹; *Norizoh Saitoh*¹; *Toshiyuki Nomura*¹; ¹Osaka Prefecture University

An environmentally friendly method using the metal ion-reducing bacterium *Shewanella oneidensis* was proposed to deposit palladium nanoparticles on the bacterial cells. Microbial reduction and deposition of palladium nanoparticles was achieved at room temperature and pH 7 using resting cells of *S. oneidensis*, when either formate or lactate was provided as the electron donor. The bioreductive deposition of palladium was a fast process: 5 mM aqueous Pd(II) ions were completely reduced to crystalline solid Pd(0) within 60 min. Biogenic palladium nanoparticles 5-10 nm in size were located on the bacterial cells. The biomass-supported Pd(0) nanoparticles were tested for catalytic activity in the chemical reduction of 0.5 mM soluble Cr(VI), achieving 90% conversion to Cr(III) at room temperature and pH 4 for 30 min.

4:50 PM

Fabrication of Thermal Insulative Thin Film Encapsulating Nano-Sized Hollow Silica Particles: *Hideo Watanabe*¹; *Masayoshi Fuji*¹; *Minoru Takahashi*¹; ¹Nagoya Institute of Technology

There have been interests in hollow particles with size of micrometer or nanometer since they have unique properties as compared to dense ones. In this study, we have suggested an application of nano-sized hollow silica particles, prepared by inorganic bead template method we developed, for

thermal insulative film. The film in which nano-sized hollow silica particles are encapsulated is fabricated by spraying the mixture of a polymer resin, the hollow particles and solvents onto a substrate followed by drying to be solidified. Thermal conductivity of the film is quite low and can be correlated with content and dispersibility of the particle in the film. To disperse the hollow particle in the resin solution as well as in the film, affinity between the particle surface and the resin has to be enhanced. For this reason, surface modification on surface of the hollow silica particle has been extensively carried out.

5:10 PM

Disinfection of E.coli by Nanosized MWNT/TiO₂ Photocatalyst: *Kornkanok Ubongchonlakat*¹; *Lek Sikong*¹; ¹Prince of Songkla

MWNT/TiO₂ powders prepared by sol-gel method were characterized by XRD, SEM, EDS and TEM. Photocatalytic reactions of the synthesized powder were determined by degradation of methylene blue solution under visible light condition. Disinfection test of E.coli bacteria mean of photocatalytic reaction of MWNT/TiO₂ powder was also investigated. It was found that MWNT/TiO₂ enhances the photocatalytic reaction under a visible light and the disinfection efficiency of E.coli bacteria.

5:30 PM

Ultrafine Grain Structure Development in Steels with Different Carbon Content Subjected to Severe Plastic Deformation: *Jozef Zrnik*¹; *Sergey Dobatkin*²; *Jan Dzugan*¹; *Tomas Kovarik*³; ¹COMTES FHT s.r.o.; ²Baikov Institute of Metallurgy and Materials Science; ³West Bohemian University

The present work focuses on the results received from severe plastic deformation (ECAP) of low carbon (LC) steel and medium carbon (MC) steel performed at increased temperatures. The high straining ($\epsilon \sim 4$) in LC steel resulted in extensively elongated ferrite grains with dense dislocation network randomly recovered. The warm ECAP deformation of MC steel in dependence of the increased effective strain ($\epsilon \sim 2$) resulted in more advanced recovery process. In interior of the elongated ferrite grains the subgrain structure prevails. As straining increases ($\epsilon \sim 4$) the dynamic recovery and RX became advanced to form mixture of subgrain and submicrocrystalline structure. The straining and increased ECAP temperature caused the cementite lamellae fragmentation and spheroidization as number of passes increased. The tensile behaviour of the both deformed steels was characterized by strength increase however the absence of strain hardening was found stronger at low carbon steel.

Powder Preparation/Processing II

Monday PM

December 8, 2008

Room: Plaza 8

Location: Sofitel Centara Grand Bangkok

Session Chair: To Be Announced

2:45 PM

Effects of Setters on Sintering Metal Injection Moulded Commercially Pure Titanium: *Nattapol Muenya*¹; *Anchalee Manonukul*¹; ¹National Metal and Materials Technology Center of Thailand

Titanium is an expensive material with high strength-to-weight ratio and excellent corrosion resistance. Metal injection moulding of titanium requires more attention than iron and stainless steel. Setter is one of many factors that is important to titanium sintering. The setter is used to support specimens and allows binders to permeate during thermal debinding and sintering. Titanium usually reacts rapidly especially at high temperature. Hence, the setter must be stable during sintering to obtain high-quality titanium parts. Therefore, this work investigated the physical and mechanical properties of specimens after sintering using five different setters. The objective is to determine the most suitable setter for pure titanium. The five setters are made from yttria, zirconia, calcium oxide and the combination of these materials which are generally known to be stable for sintering titanium. The results show similar tensile strength but very different elongation.

3:05 PM

Effects of TiO₂ Powder and Film Preparation on Photo-Degradation of Cyanide: *Chabaiporn Junin*¹; Chanchana Thanachayanont¹; Pimpa Limthongkul¹; ¹National Metal and Materials Technology Center (MTEC)

Cyanide contamination in wastewater has posted an important problem to the environment. Various methods for cyanide wastewater treatment have been used including physical, chemical and biological processes. Among these methods, breaking down cyanide using TiO₂ as photocatalyst has caught many interests due to its high performance and environmental friendliness. In this work, the effects of synthesis and preparation processes of TiO₂ in the form of powder and film on degradation of cyanide have been investigated. The properties of the synthesized samples were characterized using XRD, SEM and TEM and UV-vis. It has been found that the TiO₂ synthesized in this work is very effective for the treatment of cyanide. Calcination temperature has been found to have the most profound effect on the phase, crystallite size and effectiveness in cyanide degradation compared to other synthesis variables. Details on the effect of processing conditions on the material properties will be presented.

3:25 PM

Electro-Discharge Compaction of Fe-Ni-W Powders: *Evgeny Grigoryev*¹; ¹Moscow Engineering Physics Institute

Composition of Fe-Ni-W powders was consolidated by electro-discharge compaction process. The formation of high density and high strength structure of W-Ni-Fe composite materials was investigated and optimal process parameters were defined. The structure of Fe-Ni-W composite material reaches top strength at certain magnitudes of applied pressure and high voltage electrical discharge parameters. We studied densification process of powder material during electro-discharge compaction by means of high-velocity filming. Pulse current parameters were measured by Rogovsky coil. The temperature evolution during electro-discharge compaction process was measured by means of thermocouple method. We have installed the wave nature of powder densification process in electro-discharge compaction. We defined wave front velocity of densification process and pressure amplitude in wave front subject to parameters of electro-discharge compaction.

3:45 PM

Injection Moulding of 316L Stainless Steel Powder for Biomedical Application Using a Palm Oil Derivatives Binder System: *Rosdi Ibrahim*¹; Shamsul Muhamad²; Roila Awang³; ¹AMREC, SIRIM Berhad; ²Institute of Medical Research (IMR); ³Malaysian Palm Oil Board (MPOB)

This paper focuses on the investigation to produce sintered parts of stainless steel 316L using vertical injection molding process. The stainless steel 316L medical grade powder was mixed using z-blade mixer with the thermoplastic binder system comprising of polyethylene, paraffin wax, stearic acid, palm stearin and palmitic acid at different volume percent (%). The feedstock then was studied in term of viscosity and shear rate using capillary rheometer. The feedstock was molded using vertical injection molding machine. After molding, the green molded part was immersed into the solvent to extract partly of the binder system. The parts then were sintered under vacuum atmosphere at the temperature of 1360°C. The physical and mechanical properties of the sintered part such as density, hardness, shrinkage, ultimate tensile strength and elongation were measured. Bio-compatibility study of in-vitro test using cell osteosarcoma MG-63 was observed and discussed.

4:05 PM Break

4:30 PM

Influence of Phosphorus Addition on Sintering Behavior and Mechanical Properties of TiC-Ni Composites: *Nawarat Wora-uaychai*¹; Nuchthana Poolthong¹; Ruangdaj Tongsrir²; ¹King Mongkut's University of Technology Thonburi; ²National Metal and Materials Technology Center

TiC-Ni composites are promising for cutting tool applications. They have excellent combination of hardness, wear resistance, and toughness. These composites are possibly produced by liquid phase sintering via dissolution/re-precipitation process. The sintering temperature of this process is higher than eutectic temperature of the metal binder. Sintering can be enhanced by formation of a liquid phase when a sintering activator in metal binder is added.

Sintering activation is evidenced by sintering temperature lowering. In this study, the effect of phosphorus as sintering activator on sintering behavior of TiC-Ni and TiC-P-Ni composites has been investigated. The TiC-Ni powders were mixed, compacted and then sintered at 1000-1300°C. Microstructures, physical and mechanical properties of the sintered TiC-Ni specimens were observed and tested. Relationship between phosphorus content, sintering temperature and mechanical properties is given in the paper.

4:50 PM

Microstructure and Porosity as a Result of Sintering Time and Temperature in Pre-Alloy and Mixed Powders Ti-6Al-4V Specimens: *Khuntong Songsiri*¹; *Anchalee Manonukul*¹; Prasert Chalermkarnnon¹; Hideki Nakayama²; Motoi Fujiwara²; ¹National Metal and Materials Technology Center, MTEC; ²CASTEM (Thailand) Company, Ltd.

Two types of Ti-6Al-4V powders were used in this investigation, pre-alloy Ti-6Al-4V powders and mixed Ti-6Al-4V powders which contain the combination of commercially pure titanium and 60Al-40V powders. Both powders were injected to form tensile test specimens and sintered at 1050-1300°C for 2 and 8 hours. Sintered specimens were subjected to tensile and hardness tests, microstructure investigation and porosity characterisation. The results show that the plate-like α phase is thicker and longer when the sintering temperature increases. The plate-like α phase of pre-alloy powders is thinner and shorter than that of the mixed powders. In addition, the pre-alloy powders have less porosities than the mixed powders at the same sintering condition. The microstructure of pre-alloy powders is more homogeneous than the mixed powders. The microstructure and porosities influence the mechanical properties of sintered parts. Therefore, the pre-alloy powder specimens have better mechanical properties than the mixed powder specimens.

5:10 PM

NiO-GDC Nano-Composite Prepared via Co-Precipitation and Combustion Synthesis: *Mayuree Sansernnivet*¹; Watinee Kijboon²; Sumittra Charojrochkul¹; Pimpa Limthongkul¹; ¹National Metal and Materials Technology Center; ²Chiangrai Rajabhat University

Current activities on SOFCs have been focusing on the reduction of operating temperature to an intermediate temperature range of 500-800°C. Improvements on the material and microstructure of the anode part are important to reach the targeted operating temperature. A composite between NiO and Gd doped CeO₂ (GDC) have typically been used as the material of choice. Preparation of the NiO-GDC composite has typically been done through a regular mixing process of the NiO and GDC powders. However, agglomeration and poor distribution of the two phases when fine particles are used have been limiting the cell performance. Preparations of the fine and good dispersion of the NiO and GDC phases starting anode powder have included high energy milling and sol-gel processes. In this work, co-precipitation and combustion processes are proposed. Effects of preparation routes and synthesis conditions on the microstructure and dispersion of the powders were investigated and will be presented.

Solidification Processing II

Monday PM
December 8, 2008

Room: Plaza 2
Location: Sofitel Centara Grand Bangkok

Session Chair: Surendra Tewari, Cleveland State University

2:45 PM Invited

Development of Aluminum Semi-Solid Slurry Maker for Rheo-Diecasting Process: *Nuchthana Poolthong*¹; *Kanokkan Srimuang*¹; *Worawit Jirattiticharoen*²; ¹King Mongkut's University of Technology Thonburi; ²Department of Industrial Promotion

In the high-pressure die casting (HPDC) process, the melt is forced into a die cavity at very high speed causing turbulent flow. As a result, air is trapped within the cavity, forming porosities in the components, which

reduces its strength. The porosity due to turbulent could be reduced or even eliminated if the viscosity of the metal flow could be increased with the solid fraction of semi-solid slurry. The objective of this research is to provide an apparatus and method which is specially adapted for producing semi-solid metal alloys and improve die-casting system suitable for production of high integrity component. The rheo-diecasting (RDC) process innovatively adapts the cooling slope to creation of semi-solid slurry followed by direct shaping of the semi-solid slurry into a component using the existing high-pressure die-casting process. Using this technique the porosity due to turbulent mould filling and shrinkage porosity can be reduced.

3:05 PM

Influence of Solidification Rate on Graphite Morphological Change in Cast Iron: *Hideo Nakae*¹; ¹Waseda University

There are many graphite morphologies in cast iron, not only flake and spheroidal. For example, the morphologies of the flake graphite are classified from type A to type E and the graphite shapes are from type I to type VII by ASTM A247. We would like to study the influence of solidification rate or cooling rate on the graphite morphological change from type A to type D for flake graphite and from spheroidal (type I) to chunky (similar to the type V) for spheroidal graphite based on the micro solidification rate, namely the solidification rate of eutectic cell using one directional solidification rate and the three dimensional solidification rate. The undercooling of eutectic solidification was discussed using the three dimensional solidification rate for the basics of the heat balance.

3:25 PM

Integrated Design of Casting and Heat Treatment for Al-Si-Cu-Mg Casting Alloys: *Harold Brody*¹; ¹University of Connecticut

As part of a program to develop computer assisted models for the integrated design of casting and heat treating processes, the evolution of microstructure (OEM, SEM, and TEM) and solute redistribution are being followed through solidification, post-solidification cooling, solution heat treatment, and quenching of Al-Si-Cu-Mg alloys. Particular attention is paid to the influence of chemical nonuniformity on microstructure and tensile properties in these multicomponent and multiphase alloys. Processing parameters, microstructural features, and tensile properties are correlated to obtain predictive relations. Work has been sponsored by DOE and CHTE.

3:45 PM

Microstructure Formation in Al-Alloy High Pressure Die Castings for Ductile Applications: *Somboon Otarawanna*¹; Christopher Gourlay²; Hans Laukli³; Arne Dahle²; ¹CAST CRC; ²ARC CoE for Design in Light Metals; ³Hydro Aluminium, Research and Technology Development

The use of lightweight alloy parts manufactured by high pressure die casting (HPDC) in structural automotive components can significantly reduce cost and decrease vehicle mass. The presence of porosity, which has an adverse effect on mechanical properties and pressure tightness of components, limits the extent of use of HPDC castings in these ductile applications. Therefore, it is necessary to develop better understanding of microstructure formation during HPDC, which is a very complex process, to enable improvements in mechanical properties of as-cast components and reduce scrap rates. In this work, microstructural characterization of Al-based alloy HPDC castings for ductile applications was carried out by optical and electron microscopy. The influence of casting shape and alloy composition to the as-cast microstructure is demonstrated. Also, the formation of salient as-cast microstructural features is then discussed by considering the influence of flow and solidification during each stage of the process.

4:05 PM Break

4:30 PM

Study on the Microstructure and Properties of 7050 Aluminum Alloy made by LFEC: *Yubo Zuo*¹; Jianzhong Cui¹; ¹Northeastern University

7050 aluminum alloy ingots were made by the low frequency electromagnetic casting (LFEC) and DC casting process, respectively. Effects of electromagnetic field frequency and current intensity on microstructure were investigated. The results showed that LFEC has significant effects on macrostructure and microstructure refinement, and can improve as-cast

mechanical properties. The microstructure of LFEC ingot from the border to the center on the cross section shows fine equiaxed or nearly equiaxed grains which are much finer and more uniform than that of DC cast ingot. It was found that electromagnetic field frequency and current intensity play important roles on the microstructure refinement. In the range of experimental parameters, the optimum current intensity and electromagnetic field frequency for LFEC process is found to be 9600 to 12800AT and 20 to 25Hz.

4:50 PM

The Effect of Low Frequency Electromagnetic Field on Crack Formation of the Super-High Strength Al-10Zn-2.3Mg-2.4Cu-Zr Aluminum Alloy Billets: *Haitao Zhang*¹; Jianzhong Cui¹; Hiromi Nagaumi²; ¹Key Laboratory of Electromagnetic Processing of Materials, Ministry of Education, Northeastern University; ²Nippon Light Metal Company Ltd., Nikkei Research and Development Center

In DC casting of aluminum ingots uneven cooling rates at different regions of the ingot generate thermal stresses, which cause solidification cracks that might propagate to failure. In this research, the effects of low frequency electromagnetic field on the crack formation of the super-high strength aluminum alloy billets are studied and analyzed by measuring the mechanical properties in the mushy zone, observing the fracture of crack and inter-metallic phase by SEM and the numerical modeling. The experimental results show that the cracks are easily found in DC ingots but not in LFEC ingots. The reason for restraining crack generation by applying electromagnetic field lies in: the stress and plastic deformation generated in casting processes is decreased due to the reduced temperature variation between interior and exterior of ingots; moreover, the amount of the residual liquid phase at grain boundary is reduced, and also the brittle inter-metallic phase is refined remarkably.

5:10 PM

Convection Due to Changing Cross-Section during Directional Solidification and Its Influence on the Dendritic-Array Morphology: Kunal Pandit¹; Xiaolei Wu¹; *Surendra Tewari*¹; ¹Cleveland State University

The morphology and distribution of primary dendrites have been examined in Pb-Sb alloy samples directionally solidified in ampoules shaped like an hour-glass to examine the influence of convection due to the varying cross-section on the cellular/dendritic interface. This sample design increases the flow towards the interface as the liquid-solid interface enters the neck of the ampoule and decreases the flow as the interface exits the neck. It is observed that increased flow towards the growth front suppresses the extent of side-branching and decreases the primary dendrite spacing. It can suppress the side-branching completely and yield a cellular array. It can even produce a planar liquid-solid interface when the morphology in its absence would have been dendritic.

5:30 PM

In-situ Observation of Microstructure Evolutions during Solidification of Sn-Cu Alloys: Hisao Esaka¹; *Yoshiko Miyauchi*¹; ¹National Defense Academy

The Sn-Cu Alloy is one of candidate alloys for lead-free solder. It is important to understand the solidified structure of this alloy, but such reports are few. Therefore, this study has been carried out to make in-situ observation by a laser confocal microscope and to understand the solidification process by the interruption test. Three alloys, hypo-eutectic, eutectic and hyper-eutectic alloys have been prepared. In the case of hypo-eutectic and eutectic, primary Sn dendrite and interdendritic eutectic were observed, which agreed with the coupled growth concept. In the case of hyper-eutectic alloy, fibrous primary Cu₆Sn₅ grew and then Sn dendrite grew as halo, and finally eutectic structure formed. It was not necessary to be undercooled to form the primary Cu₆Sn₅. However, it was necessary to be undercooled to form halo, since there was no halo in the undercooled state below eutectic temperature.

Tuesday Plenary Lecture

Tuesday AM
December 9, 2008

Room: Auditorium B2, Bangkok Convention Centre
Location: Sofitel Centara Grand Bangkok

Session Chair: Akio Fuwa, Waseda University

9:30 AM Keynote

Physical Chemistry of Aqueous Processing on Materials Surface:
*Yasuhiro Awakura*¹; ¹Kyoto University

Electroplating of metals, alloys and metal compounds from aqueous media is an important soft process for manufacturing thin-films materials in high-tech industry, metal plating in surface finishing, and electrowinning and electrorefining in extractive metallurgy. Therefore, many studies have been carried to develop new plating methods with high functional and fine structure materials as well as processes with high rate. Electroplating is substantially based upon reduction-oxidation reactions on substrates while it also concerns with acid-basis reactions in terms of stability of ionic species in plating bath; selection of complexing agents for metal ions and pH buffer capacity of plating bath. Thermodynamics is useful to understand these issues; Eh-pH diagram is available to consider them in a bird's eye view. On the other hand, some aspects, i.e. what determines plating rates, what is the limiting to it and how the current distribution is determined, are of interest in industrial processes. They have relations with the balance between electrode reaction and ionic mass transfer in electroplating. It is, therefore, necessary to understand the electromigration and diffusion of ionic species in plating bath. In this lecture, physical chemistry of aqueous processing on materials surface is discussed from the view points of thermodynamics and transport phenomena, which involves applicability of Eh-pH diagrams for electroless plating, alloy plating, thin film plating of semiconductors and some aspects of electrical conductivity and diffusivities of aqueous solutions and concentration boundary layer in the vicinity of plating substrates.

10:15 AM Break

Composites Processing II

Tuesday AM
December 9, 2008

Room: Plaza 5
Location: Sofitel Centara Grand Bangkok

Session Chair: Julie Schoenung, University of California

10:40 AM

Effect of Nickel Particle Size on Microstructure and Properties of Zirconia-Nickel Composites: *Zhong-Chun Chen*¹; Kazuhito Andoh²; Shin-Ichi Kikuchi²; Takenobu Takeda²; Fumio Fujita¹; ¹Tohoku University; ²Yamagata University

Zirconia-nickel composites have attracted much attention in various structural and functional applications, because of their good mechanical, electrical, and thermal properties and in particular, good compatibility due to similar elastic moduli and coefficients of thermal expansion. In this research, ZrO₂-Ni composites with different Ni particle sizes were prepared via a powder metallurgy route, and the effect of Ni particle size on microstructure and mechanical and thermal properties has been investigated. The morphology of second phase in the composites depends on the size ratio between matrix and second-phase powders. The Ni phase has an equiaxed morphology and is discretely dispersed in ZrO₂ matrix, while the ZrO₂ phase exhibits a branching cluster structure in Ni matrix. A larger size ratio easily results in coarsening of both matrix and second phase. The composites obtained from finer Ni powder show lower percolation threshold, higher bending strength and hardness.

11:00 AM

Effect of Tungsten-Carbide Particles on the Mechanical Properties of Copper Alloy Composites: B. Girish¹; B. Satish¹; *Basawaraj Karabasappa*¹; H. Siddesh¹; ¹East Point College of Engineering and Technology

Copper matrix composites with tungsten carbide particle reinforcements prepared using liquid metallurgy technique will be investigated for their mechanical properties. The content of the reinforcement in the composite will be varied from 1-7% by weight with an increment of 2% with an objective to achieve higher dimensional stability. Such composites may find applications in thermal, electrical and structural components. The idea is to arrive at an optimum tungsten carbide reinforcement content for high temperature, high strength applications. The focus is on developing a material having high thermal conductivity along with high strength. In this present study, the mechanical properties like ultimate tensile strength, compression strength, ductility, hardness, etc. The microstructure study will also be evaluated to study the distribution of the reinforcement in the copper alloy matrix.

11:20 AM

Empirical Formulas for Predicting the Stable Location of Crack in Foam-Core Sandwich Beam Specimens: *Paiboon Limpitpanich*¹; ¹Burapha University

The objective of this study is to obtain the empirical formulas that are used to predict the stable location of crack in foam-core sandwich beam specimens. The specimens are typically used for determining fracture toughness of the interface layer and the core of foam-core sandwich panels. The proposed formulas are constructed by performing a non-linear regression from results of finite element (FE) modeling. FE analysis in combination with the virtual crack-closure technique is used in the current study. Various FE models are obtained by varying material and thickness of the top and the bottom faces of the sandwich models. Results show that the stable location can be in either the core or the face and core interface layer. The proposed formulas are also validated by experimental results of foam-core sandwich beam specimen with good agreement.

11:40 AM

Formation of L-Poly(Lactic Acid) Microcomposites Using Supercritical CO₂: *Kenji Mishima*¹; ¹Fukuoka University

L-poly(lactic acid)(PLA) microspheres were produced by expansion of CO₂ saturated polymer suspensions. The suspensions of CO₂ saturated polymer solution containing ethanol were depressurized and PLA micro-composites were obtained. To control the particle morphology, the gas saturated polymer suspensions were expanded. After spraying solutions through a nozzle to the atmosphere, polymeric fibers and/or coalesced particles were obtained. The expansion of polymer suspensions to water impedes particles growth and agglomeration. The particles do not tend to agglomerate after expansion, since the ethanol used as cosolvent on the surface of particles diffuse through the water phase. Furthermore, the interfacial tension between the polymer droplets and water phase contributes the microspheres formation. The changing the pre-expansion pressure, and injection distance between the nozzle and water interface, controls the particle size distribution and morphology of microparticles.

12:00 PM

Fatigue and Fracture Properties of Tungsten Carbide Particles Reinforced Copper Alloy Composites: *Siddesh Holehonnur*¹; *Basawaraj Karabasappa*¹; B. Satish¹; B. Girish¹; B. Shivakumar¹; ¹East Point College of Engineering and Technology

In the present study, tungsten carbide particle reinforced copper alloy composite materials will be investigated for their fatigue and fracture behaviour. The composites will be prepared using liquid metallurgy technique. The content of the reinforcement in the composite will be varied from 1-7% by weight with an increment of 2% with an objective to achieve higher dimensional stability. Such composites may find applications in thermal, electrical and structural components. The idea is to arrive at an optimum tungsten carbide reinforcement content for high toughness, wear resistance and high strength applications. The focus is on developing a material having high toughness along with high fracture and fatigue strength. In this present study, properties like fracture toughness, energy release rate,

ductility, hardness, etc. will be investigated. Scanning electron microscope investigations will also be carried out in order to explain the observations made.

Energy Materials Processing II

Tuesday AM
December 9, 2008

Room: Plaza 1
Location: Sofitel Centara Grand Bangkok

Session Chair: Asako Hirai, University of California, Santa Barbara

10:40 AM

Low Stress Viscous Creep in a Ti3Al2.5V Tubing under Internal Pressurization: Srikant Gollapudi¹; Korukonda Murty¹; Indrajit Charit²; ¹North Carolina State University; ²University of Idaho

Hoop creep behavior of a thin-walled Ti3Al2.5V tubing was studied under closed-end internal pressurization with emphasis at low stresses of interest to in-service conditions. The creep-rates varied linearly with the applied stress at these low stresses at temperatures between 823K and 873K. An activation energy close to that for grain boundary diffusion was identified. Predictions based on Coble creep are 3 orders of magnitude lower than the experimental strain-rates. The slip bands observed in TEM have a mean spacing of 250 nm and the predictions based on the Spingarn and Nix model of the climb of dislocations at the grain boundaries in the slip bands were noted to be close to the experimental results. This is the first time that the slip band model was found to be operating in the viscous creep regime. This work is supported by the National Science Foundation grant #DMR-0412583.

11:00 AM

Experimental Investigation on Energy Efficiency of Fired Clay Brick Incorporated with Sugarcane Bagasse Ash: Danupon Tonnyayopas¹; Perapong Tikasakul¹; Saravut Jaritngam¹; ¹Prince of Songkla University

Characterization in behavior of the clay material used in construction clay brick industry due to additions of sugarcane bagasse ash (SBA) was investigated. Mixtures of clayey soil and BA (10-50wt. %) were uniaxially pressed and sintered at optimized temperature of 1050°C. Experimental results of partial replacement of the SBA specimens from chemical and mineralogical analysis (XRF and XRD), thermal analysis (DTA, TG), bulk density, water absorption and cold crushing strength. It is displayed that the SBA can be directly affected on the properties of the sintered brick products. It influenced as a flux agent, becoming the energy efficiency of the lightweight fired clay brick.

11:20 AM

Freeze-Drying—Electrophoretic Deposition of Titanium Dioxide for Fabrication of Dye-Sensitized Solar Cells: Eugene Olevsky¹; Evan Khaleghi¹; ¹San Diego State University

In dye-sensitized solar cells (DSSCs), titanium dioxide plays a crucial role. Many methods are used to produce the titanium dioxide surface for dye-sensitized solar cells, including electrophoretic deposition (EPD), screen printing, and doctor blade deposition. Each of the methods has its advantages and disadvantages, but none come close to the “ideal” surface morphology. The ideal morphology has a large surface area for dye attachment, but also does not impede electron flow to the conduction layer. A technique is developed, utilizing freeze drying and electrophoretic deposition, to produce a superior surface morphology for DSSCs, that increases surface area for dye attachment. Analysis of the freeze-dried solar cell’s performance shows a significant increase over traditional deposition methods.

11:40 AM

Separation of Rare-Earths from Nuclear Fuel by Selective Sulfurization: Toshifumi Nihei¹; Nobuaki Sato¹; Soichi Sato²; ¹Tohoku University; ²Japan Atomic Energy Agency

For the recovery of nuclear materials from oxide fuel, a novel reprocessing process by selective sulfurization method was proposed with three steps

of 1) voloxidation for decladding, 2) selective sulfurization of FPs and 3) selective acid dissolution of sulfurized FPs. Sulfurization behavior of uranium oxides and FPs such as rare-earths (Ln₂O₃) in CS₂ was examined by thermogravimetry and XRD analysis. At voloxidation step, UO₂ was oxidized to U₃O₈ by the heat treatment in air at 1273K, while a part of U₃O₈ changed to rare-earth doped UO₂ solid solution. Rare-earth doped UO₂ solid solution was selectively sulfurized by CS₂ at temperatures lower than 723K, while U₃O₈ was reduced to UO₂ without sulfurization. Cerium doped UO₂ solid solution showed similar behavior to UO₂. Then the sulfurized rare-earths selectively dissolved into nitric acid, while UO₂ did not. Rare-earths in spent oxide fuel could be separated from nuclear materials by selective sulfurization method.

Environmental Protection Processing III

Tuesday AM
December 9, 2008

Room: Plaza 6
Location: Sofitel Centara Grand Bangkok

Session Chair: To Be Announced

10:40 AM

Removal of Arsenic with Jarosite in Acid Mine Drainage: Hiroshi Nakazawa¹; Wataru Haruyama¹; Tomoyuki Shinohe¹; ¹Iwate University

The acid mine drainage in abandoned Horobetsu mine in Hokkaido, Japan, contains arsenic and iron ions; total arsenic 10ppm, arsenite 8.5ppm, total iron 379ppm, ferrous iron 266ppm, pH1.8 in average. The mine drainage is neutralized up to pH7.5 and arsenic is removed by co-precipitating with iron hydroxide. It is known that iron ion precipitates as jarosite during the oxidation of ferrous ion by Acidithiobacillus ferrooxidans in sulfuric acid solution. We found that arsenic was removed with the formation of jarosite resulting from microbial oxidation of ferrous ion at pH2.0. In order to remove arsenic with less iron ion before the neutralization process, we have examined the effects of several factors such as pH, coexistence of cationic ions, species of arsenic (arsenite, arsenate), oxidation rate of ferrous ion and so forth on the removal of arsenic by the formation of jarosite in acid mine drainage.

11:00 AM

Separation and Recovery of Valuable Metals from Copper Smelting Dust with High Arsenic Content: Hiroyuki Sano¹; Takashi Nozawa¹; Akihiro Ogawa¹; Victor Montenegro¹; Toshiharu Fujisawa¹; ¹Nagoya University

Most of the dust generated from the copper smelting process in Chili has been stored after the stabilization by hydrometallurgical process because it contains high concentration of arsenic. However, in recent years, the dust generation has increased because of degrading the quality of concentrate. In addition, the environmental regulations become stricter. On the other hand, valuable metals such as copper and zinc are contained in the dust at high concentrations and it is desirable to recover them. In this study, separation and recovery process of valuable metals from the dust was developed. In this process, copper and zinc in the dust were recovered by dissolving in water after the sulfating roasting. Harmful elements in the dust such as arsenic and lead were separated by stabilization or evaporation.

11:20 AM

Surface Modification of Plastics of Shredder Residue for Hybrid Jig: Mayumi Ito¹; Maiko Akatsuka¹; Yutaka Kuwayama¹; Kunihiko Hori¹; Naoki Hiroyoshi¹; Masami Tsunekawa¹; ¹Hokkaido University

The authors had reported that RETAC jig is very useful to separate relatively low density particles such as plastics, and demonstrated that the highly efficient jig separation for plastic components used in waste office machines and home appliances could be possible in pilot-scale test. To further improve the separation efficiency, a hybrid jig (RETAC jig with air bubbler under particle bed) was developed by the authors, which can separate plastics having similar specific gravities using difference in wettability produced by a pretreatment. This study presents the wettability control of plastics (PP, PE, ABS, PU) of shredder residue for hybrid jig treatment using organic

solutions or surfactant solutions. The effect of the solutions on the wettability of the plastics was determined by measuring the contact angle and the critical surface tension of the plastics in the solutions. The effect of surface oxidation on the plastics was also investigated.

11:40 AM

Technology Development and Plant Practice of the Recycling of Nickel from Spent Electroless Nickel Plating Baths Using Solvent Extraction:

*Mikiya Tanaka*¹; Yukinori Saiki²; Ryuji Kojima²; Kazuhiro Hagsawa³; Hirokazu Narita¹; Ying Huang¹; ¹National Institute of Advanced Industrial Science and Technology; ²Japan Kanigen Company, Ltd.; ³Kanigen (Thailand) Company, Ltd.

Although electroless nickel plating is an important surface finishing technology, the treatment of a large amount of its spent baths should be established from the environmental and economical viewpoints. The present authors have developed a recycling process of nickel in the spent baths using solvent extraction in which the impurities of iron and zinc are initially removed by an acidic organophosphorous reagent and then nickel is extracted with a mixture of LIX84I and a small amount of an acidic organophosphorous reagent. This process was introduced into a plating plant of Japan Kanigen Co., Ltd. in 2007 and is now contributing to the emission reduction from the plant. In this paper, the laboratory-scale experimental results and practical operation data will be presented.

nanocomposites was investigated. A basic understanding of thermodynamics of synthesis of nanocomposites, temperature profile and velocity distribution within reactor and vapor saturation of carbides and nitrides is essential for quantitative predictions of characteristics of in-situ synthesized nanocomposites. Thermodynamic analysis for predicting conditions of synthesis of nanocomposites were made. A mathematic model was developed for describing temperature profile and velocity distribution within the plasma reactor. The model is applied to predict feeding rate, design *in situ* processing of nanocomposites. The thermal plasma technique in producing nanocomposites and the various process parameters that influence the final product are discussed. The model predictions were found to be in reasonable agreement with experimental data for nanocomposites.

11:40 AM

Self-Catalyzed Growth of Silica Nanowires: *Guang Zhu*¹; ¹Beijing Information Technology Institute

Simple method base on thermal evaporation of silica nanoparticles has been discovered to synthesis silica nanowires. The as-grown product was characterized by scanning electron microscopy, transmission electron microscopy, and energy-dispersive X-ray spectroscopy. The obtained silica nanowires had no metal contaminations, ultralong lengths of millimeters, the diameters of about 50 nm, and smooth surface. However, the morphologies and microstructures of silica nanowires are affected by synthesis conditions, such as the synthesis temperature and the vapor concentration of the SiO_x. On the basis of these experimental results, a self-catalyzed growth mechanism of silica nanowires is proposed.

12:00 PM

Nanoparticle Dispersed Gels for Direct Writing of Ceramic Structures:

Akira Kondo¹; *Hiroya Abe*¹; Makio Naito¹; Jun Akedo²; ¹Osaka University; ²National Institute of Advanced Industrial Science and Technology

Direct Writing allows one to design and rapidly fabricate materials in complex 3D shapes without the need for expensive tools, dies or lithographic masks. In this study, nanoparticle dispersed colloidal gels were newly prepared for filamentary-based technique of the direct writing. 2D and 3D ceramic patterns were very flexibly written by the rapid solidification of the colloidal gels after its exclusion from nozzle. Possibilities of the present soft-colloidal gels for ceramic microsystems/interconnect will be discussed.

Nanomaterials Processing III

Tuesday AM
December 9, 2008

Room: Plaza 7
Location: Sofitel Centara Grand Bangkok

Session Chair: To Be Announced

10:40 AM Invited

One-Step Fabrication of TiO₂ Nanoparticles Deposited on Hydroxyapatite Crystals by Mild Hydrothermal Synthesis: *Pornapa Sujaridworakun*¹;

Dujreutai Pongkao²; Anwar Ahniyaz²; Tomoaki Watanabe²; Masahiro Yoshimura²; ¹Chulalongkorn University; ²Tokyo Institute of Technology

TiO₂ nanoparticles deposited on hydroxyapatite (HAp) have been successfully synthesized by direct (one step) hydrothermal treatments of a CaCO₃ suspension in a H₃PO₄ solution with 10 vol% TAS-FINE (titanium amine complex) at 150°C for 6 h or 120°C for 12-24 h under nearly neutral pH conditions. The obtained products were characterized by XRD, SEM-EDX, visible, Raman, and TEM. The XRD and Raman results showed the formation of HAp and TiO₂ anatase phases under these hydrothermal conditions. SEM and TEM observations revealed that anatase TiO₂ nanoparticles with the size of about 10 nm width and 150 nm length were deposited on the surfaces of the HAp crystals with the micron sizes. The anatase nano-crystals seem to be formed by heterogeneous nucleation on the surfaces of HAp crystals.

11:00 AM

Photocatalytic Activities of Carbon Black Doped TiO₂ Nanoparticles by Sol-Gel Method: *Weerachai Sangchay*¹; Lek Sikong¹; ¹Prince of Songkla University

The purpose of this study to investigate the photocatalytic activities of carbon black doped TiO₂ nanoparticles prepared by sol-gel method and calcinations at various temperatures. The synthesized powders were characterized by XRD, SEM, EDS and DTA. The photocatalytic reaction of synthesized powders was done by means of the degradation of methylene blue solution under UV and visible light irradiation. It was found that carbon black doped in to the TiO₂ powders enhances the photocatalytic activity.

The purpose of this study to investigate the photocatalytic activities of carbon black doped TiO₂ nanoparticles prepared by sol-gel method and calcinations at various temperatures. The synthesized powders were characterized by XRD, SEM, EDS and DTA. The photocatalytic reaction of synthesized powders was done by means of the degradation of methylene blue solution under UV and visible light irradiation. It was found that carbon black doped in to the TiO₂ powders enhances the photocatalytic activity.

11:20 AM

Plasma Processing of Nanocomposites: *Ramana Reddy*¹; ¹University of Alabama

Nanocomposites exhibit significantly improved properties over conventional monolithic metallic alloys. Thermal Plasma *in situ* processing of

Powder Preparation/Processing III

Tuesday AM
December 9, 2008

Room: Plaza 8
Location: Sofitel Centara Grand Bangkok

Session Chair: To Be Announced

10:40 AM

Processing of Ultrafine-Grained WC-Co Hardmetals for Property Enhancements: *Sukunthakan Ngermbamrung*¹; Kannigar Dateraksa¹;

Yuttanant Boonyongmaneerat²; Nutthita Chuankrerkkul²; Kuljira Sujirote¹; ¹National Metal and Material Technology Center, National Science and Technology Development Agency; ²Metallurgy and Materials Science Research Institute, Chulalongkorn University

Hardmetals comprising tungsten carbide (WC) and cobalt (Co) are powder metallurgy products employed in many important manufacturing applications, including cutting tools and drawing dies. Due to recent development of new machining technologies, demands for enhanced mechanical properties and prolonged service life of the materials are growing rapidly. One approach to achieve these is through a reduction of hardmetals' grain size, using ultrafine powders in the fabrication. This however must be accompanied by good understanding of sintering protocols and uses of grain growth inhibitors, due to the increased activity of the fine crystallite size. In this study, we systematically investigate the influence of material compositions and sintering parameters on microstructures and mechanical properties of WC-Co compacts. A focus is made on how grain size and properties, including

hardness and toughness, are related to WC powder size, the additives¹ and Co contents, and firing parameters, and the optimum processing conditions are determined.

11:00 AM

Production of Titanium Foam by Lost Carbonate Sintering Process for Hard Tissue Engineering: *Nasser Barakat*¹; Abd El-Nasser Omran²; Hak Kim³; ¹Minia University; ²El Azhar University; ³Chonbuk National University

Titanium is one of the most common used metals in the biomedical field. In this study the titanium foam is produced using potassium carbonate powder to be exploited as scaffold in the hard tissue engineering. The obtained foam has porosity of more than 60%. The mechanical properties of the foam have been estimated and compared with the calcined bovine bone. The results confirmed that titanium foam might be used as scaffold in the hard tissue engineering.

11:20 AM

Rapidly Solidified Magnesium Alloy Coarse Powder by SWAP and Characteristics of Its Wrought Alloy: *Katsuyoshi Kondoh*¹; Hiroyuki Fukuda¹; Hisashi Imai¹; Hiroshi Izaki²; Isamu Otsuka²; ¹Osaka University; ²EPSON Atomix

SWAP (spinning Water Atomization Process) promises to serve coarse magnesium alloy powder, being significantly safe in handling, with fine microstructures via rapid solidification process. The conventional magnesium alloy, AZ31B (Mg-3%Al-1%Zn-0.3%Mn) powder are prepared by SWAP, and compacted at room temperature. The green compact with a relative density of about 85% is rapidly heated at 473 - 673K in nitrogen gas atmosphere, and immediately consolidated by hot extrusion. Microstructures observation and evaluation of mechanical properties of the wrought AZ31B powder metallurgy (PM) alloy are carried out. As-atomized powder indicates fine grains with 2-5 micron, and its wrought alloy also shows remarkably uniform microstructures with refined grains less than 1-2 micron via dynamic recrystallization during hot extrusion. A wrought AZ31B alloy extruded at 573K reveals 330 MPa tensile yield stress and 18% elongation at room temperature, which are superior to the materials in using the coarse powders machined from AZ31B ingot.

11:40 AM

Solvothermal Synthesis of Raspberry-like $YVO_4:Eu$ Nanoparticles in Methanol-Water System: *Sulawan Kaowphong*¹; Kouichi Nakashima¹; Valery Petrykin¹; Somchai Thongtem²; Masato Kakihana¹; ¹Tohoku University; ²Chiang Mai University

Synthesis of phosphor powders with sub-micron particle size and controllable morphology currently attracts considerable attention. Eu-doped YVO_4 is a well-known red phosphor in television and cathode ray tubes (CRTs) due to its high luminescent intensity. In this work, $YVO_4:Eu$ nanoparticles with controllable size were successfully fabricated by the original solvothermal method at 300°C for 3 hours employing methanol-water solution. The effect of the solution pH on sizes and morphology of the $YVO_4:Eu$ particles was examined. SEM micrographs have revealed that the powders are composed of raspberry-like particles with diameter of 400-600 nm, which comprise the primary spherical particles in the range of 12-15 nm. The sizes of the primary particles decrease with the increase of pH. Post-annealing at 1000°C improves the luminescence intensity of the $YVO_4:Eu$ red phosphor, and the raspberry-like shapes of the powders prepared in acidic solutions are retained. The powders prepared under basic conditions experience considerable sintering.

Processing of Electronic Materials and Devices II

Tuesday AM

December 9, 2008

Room: Plaza 3

Location: Sofitel Centara Grand Bangkok

Session Chair: To Be Announced

10:40 AM

Effects of Indium Addition on Properties and Wettability of Sn-0.3Ag-0.7Cu Solder Alloy: *Kannachai Kanlayasiri*¹; ¹King Mongkut's Institute of Technology Ladkrabang

The Sn-Ag-Cu family of alloys is a very attractive family of Pb-free solder alloys. Sn-0.3Ag-0.7Cu solder alloy, a member of the Sn-Ag-Cu family, is a widely used solder alloy in Thailand. This research was aimed to study effects of indium (In) addition on solidus and liquidus temperatures, hardness, wetting force and wetting time of Sn-0.3Ag-0.7Cu solder alloy. Effects of adding In from 0.5-3.0 wt% to Sn-0.3Ag-0.7Cu were investigated. Results showed that In has a strong influence on solidus and liquidus temperatures, hardness, wetting force and wetting time of Sn-0.3Ag-0.7Cu solder alloy. The solidus and liquidus temperatures of the alloys were decreased as the In content increased, and the melting range was wider with the increase of In content. The hardness of the solder alloys was increased as the amount of In increased. Addition of In also improved wettability of the alloys.

11:00 AM

Electrical and Mechanical Properties of Ternary Rubber Composites for Electronic Sensors: *Benjaporn Nooklay*¹; Pitsanu Bunnaul¹; Wiriyu Thongruang¹; Kanadit Chetpattananondh¹; Pruittikorn Smithmaitrie¹; ¹Prince of Songkla University

Electrical and mechanical properties of conductive rubber composites made of natural rubber filled with carbon black (Vulcan XC-72) and multiwall carbon nanotube were studied. The AC electrical conductivity was measured at the frequency range of 0.001-1MHz. The threshold composition of the binary composite of carbon black filled rubber was found at the carbon black content of 30 phr. The multiwall carbon nanotube was added as the third composition of binary composites for bridging of electrons across carbon black aggregates. Compressive strength and compression set of rubber composites were tested for mechanical property investigations. It was found that both compressive strength and compression set increased with the increment of carbon black contents. From the results, it could be considered that the ternary composites can be selectively used as an electronic sensor in their elastic ranges of 20-40% due to their low compression set of 10-15%.

11:20 AM

Electrospun Polyaniline Derivative-Polystyrene Composite Fibers: Surface Morphology and Chemical Vapor Sensing: *Darunee Aussawasathien*¹; Somboon Sahasithiwat¹; Laongdao Menbangpung¹; ¹National Metal and Materials Technology Center

The electrospinning technique was utilized to produce camphorsulfonic acid (HCSA) doped polyaniline (PANI) derivative-polystyrene (PS) composite fibers in the non-woven mat form with different fiber characteristics, depending on the proportion of components in spinning solutions. HCSA doped PANI derivative-PS composite fibers were fabricated on the interdigitated gold (Au) substrates for use as chemical vapor sensors. This work opens up the possibility of using the derivative of polyaniline as a component in composite fibers for chemical sensing applications by taking advantages of its good solubility in common solvents as well as detectable electrical changes for small amount of composite fibers used.

11:40 AM

Enhancing Mechanical Response of a 96.5Sn-3.0Ag-0.5Cu Solder Using Energy Efficient Microwave Assisted Sintering Route: *Mui Ling Sharon Nai¹*; Joshua VM Kuma¹; Manoj Gupta²; ¹Minerals, Metals and Materials Technology Centre; ²National University of Singapore

In the present study, the effects of conventional sintering and two-directional microwave assisted rapid sintering on the microstructure and tensile properties of a commercial lead-free solder (96.5Sn-3.0Ag-0.5Cu) are investigated. Conventional sintering was conducted on solder samples in an inert Argon atmosphere, whilst microwave sintering was carried out on the samples under ambient conditions. Two sintering temperatures of 150°C and 210°C were investigated. Microwave sintered samples exhibited lower porosity and more refined matrix grain size. Tensile results of microwave sintered samples also revealed superior strength (0.2% YS and UTS) when compared to conventionally sintered samples. Furthermore, results showed that samples microwave sintered at 210°C yielded the best combination of mechanical properties.

12:00 PM

Thermo-Kinetics Analysis of Ge₂Sb₂Te₅ Amorphous Materials Containing Nb, Mo and W Elements: *Mitsuaki Fujita¹*; *Shou Otaka¹*; Akio Fuwa¹; ¹Waseda University

Ge₂Sb₂Te₅ has been used in DVD disk memory devices where phase transition phenomena between amorphous(glassy) and crystalline state has been utilized reflecting its optics characteristics in laser illumination. In this study, Ge₂Sb₂Te₅ amorphous glassy film was firstly synthesized on glass substrate by a magnetron sputtering device and, then, crystallization kinetics from the amorphous state to crystalline state was investigated during heating treatment using a DSC(differential scanning calorimetry) and its behavior was studied by the Kissinger kinetics. The effect of Nb, Mo and W addition to Ge₂Sb₂Te₅ during its crystallization has been also investigated for improved performance.

11:00 AM Invited

Effect of Iron and Silicone on Hot Tearing of Al-5.8%Cu Alloy: *Hiromi Nagami¹*; Satoru Suzuki¹; ¹Nippon Light Metal Company, Ltd

The effect of Fe and Si addition on hot tearing tendency of Al-5.8%Cu alloy was systematically investigated by a hindered hot tearing test, "I-beam test". Insulator was pasted on the middle of the mold wall, in order to locate tears only in the middle of the test bars. It was found that the hot tearing tendency of Al-5.8%Cu alloy was most increased at 0.2 to 2% Si addition. When the Si addition was exceed 3%, the hot tearing tendency was decreased. The crack sensitivity was highest at 0.2% Fe addition, and it tended to a little improve the crack sensitivity, when the Fe quantity was increased to 0.5%. When the Fe addition was exceed 2%, the crack sensitivity was remarkable improvement. It was found that the solidifying eutectic and the intermetallic compounds play an important role in hot tearing by the observation results of the microstructure.

11:20 AM

Observation of Nucleation and Fragmentation during Solidification by Time Resolved X-Ray Imaging Technique: *Tomoya Nagira¹*; *Hideyuki Yasuda¹*; Yosuke Yamamoto¹; Noriaki Nakatsuka¹; Masato Yoshiya¹; Akira Sugiyama²; Itsuo Ohnaka²; Keiji Umetani³; Kentarou Uesugi³; ¹Osaka University; ²Osaka Sangyo University; ³Japan Synchrotron Radiation Research Institute

Nucleation and development of dendrites are important issue for controlling microstructure during solidification. However, there are few studies on the in-situ observation of the solidification phenomena. The 3rd generation type synchrotron radiation facility enables us to observe the solidification of metallic alloys in-situ. The in-situ observation was performed for Sn-based alloys and Al-based alloys. In this presentation, we would show fragmentation of dendrite arms and nucleation of Sn-Bi alloys and Al-Cu alloys. In addition, effect of Ti and B addition on nucleation and fragmentation will also presented.

11:40 AM

Spatial Orientation of Dendrite in Chill Zone: *Hisao Esaka¹*; ¹National Defense Academy

In general, many fine grains nucleate on the surface and many dendrites grow their preferred growth direction, in case of alloy casting. Solidified structure is usually observed on the cross section which is parallel to the heat flow direction. Since the growth direction of dendrites are not always parallel to the cross section, the solidified structures exhibit quite complex patterns. In this study, the observed shape of dendrite has been investigated experimentally using Al-20 mass% Cu alloy. Furthermore, the solidified structure has been analyzed assuming that dendrite has simple, plate-like secondary arms. Here, 3D-CAD and solid analytical geometry has been applied.

12:00 PM Break

12:25 PM

Monte Carlo Simulation of Grain Growth Taking into Account the Influence of Temperature: *Shigeaki Ogibayashi¹*; ¹Chiba Institute of Technology

The grain growth behavior in Monte Carlo simulation taking into account the influence of temperature has been studied based on the original Potts model proposed by Anderson et al. It has been revealed that the influence of temperature in Monte Carlo simulation could be introduced through the correspondent relationship between Monte Carlo Step and real time. A new equation for the relationship between Monte Carlo Step and real time has been derived based on the idea of the law of similitude in grain growth. The grain growth during cooling for the actual time-length system has been estimated using newly derived equation and the estimated grain size as a function of temperature showed quantitatively good agreement with the observed results reported in the literature when lattice constant in the calculation system was set to be 0.015cm which was a half of the initial grain diameter in the real system.

Solidification Processing III

Tuesday AM
December 9, 2008

Room: Plaza 2
Location: Sofitel Centara Grand Bangkok

Session Chair: Harold Brody, University of Connecticut

10:40 AM Invited

Directional Solidification of Ni-Based Superalloy with Melt Superheating Treatment: *Jun Zhang¹*; Changshuai Wang¹; Lin Liu¹; Hengzhi Fu¹; ¹Northwestern Polytechnical University

The mechanical property of Ni-based superalloy used in advanced aeroengine is mostly decided by the solidification microstructure. Although the relationship between the solidification microstructure and the solidification processing parameter has been studied for several decades, the influence of the melt characteristics on the solidification microstructure hasn't been paid much attention. In this paper, the melt superheating treatment is carried out for Ni-based superalloy during directional solidification processing. With appropriate superheating treatment regulation, the thermal gradient of solidification interface remains constant for different melt superheating temperatures in order to accurately investigate the relationship between the solidification microstructure and the melt state. The research results show that the dendrite growth has obvious change and the grain orientation becomes quite well with the melt superheating temperature increased from 1500° to above 1700° although the thermal gradient of solidification interface is unchanged. It can be concluded that the melt structure change has influence on the solidification processing.

12:45 PM

Numerical Simulation of Columnar-to-Equiaxed Transition during Solidification of Aluminum Base Alloy: *Kenichi Ohsasa*¹; Kiyotaka Matsuura¹; ¹Hokkaido University

The columnar to equiaxed transition (CET) during the unidirectional solidification of Al-Si alloy was numerically simulated by using the cellular automaton (CA) method. In the simulation, molten alloys were unidirectionally solidified in an adiabatic mold from a steel chill block located at the bottom of the mold. The top of the mold was maintained at certain temperature for preventing the alloy from the nucleation at the melt surface. In the simulation, columnar to equiaxed transition (CET) and subsequent equiaxed to columnar transition (ECT) were observed. The condition of CET was examined and compared with theoretical predictions. It was shown from the simulation that the CET occurred when the fraction of solid of equiaxed crystals in front of the columnar crystals reached at certain value of 0.1. This value disagreed with the value of the theory proposed by Hunt.

Thin Film Coating Processing I

Tuesday AM
December 9, 2008

Room: Plaza 4
Location: Sofitel Centara Grand Bangkok

Session Chair: Kazuharu Yoshizuka, The University of Kitakyushu

10:40 AM

Anatase TiO₂ Thin Film for Decomposing Aldehydes in Water: *Kazuharu Yoshizuka*¹; Kyoko Izumi¹; Naoko Ishibashi¹; Syouhei Nishihama¹; ¹The University of Kitakyushu

Anatase TiO₂ nano particles were synthesized in neutral aqueous media. The particle size of the anatase TiO₂ could be controlled from 20 nm to 60 nm by changing the preparation procedures of Ti(OH)₄ gel, which is a precursor of amorphous TiO₂. The temperature of hydrothermal synthesis of amorphous TiO₂ also affected crystallinity of anatase TiO₂, while synthesis time scarcely affected. The TiO₂ thin film under 1 μm was prepared by casting anatase TiO₂ gel on the glass beads. The TiO₂ thin film can effectively decompose acetaldehyde and formaldehyde in water by the photocatalyst function of anatase TiO₂.

11:00 AM

Application of Spray-Drying Method for Synthesis of BaAl₂S₄:Eu Blue Emission Electroluminescent Phosphor Powders and Ceramics.: *Valery Petrykin*¹; Masato Kakihana¹; ¹Tohoku University

BaAl₂S₄:Eu is the high brightness electroluminescent material for the thick dielectric electroluminescent (TDEL) flat panel displays. Prospective display assembling process involves fabrication of phosphor thin films by RF sputtering using Ba-Al-Eu alloy as a target and annealing of the metal film in the H₂S atmosphere. Thus, application of a BaAl₂S₄:Eu ceramics could be a convenient alternative to the three metals alloy. Usually synthesis of bulk BaAl₂S₄:Eu relies on solid-state interaction between individual sulfides which can not provide homogeneous distribution of Eu activator. We developed partial solution synthesis of BaAl₂S₄:Eu phosphor based on spray-drying method. Compared to the other solution techniques explored in this work, such as polymerizable complex method, freeze-drying and co-precipitation methods, spray-drying yields powders with excellent mouldability to form ceramic targets. The prepared ceramic samples have excellent phase purity and exhibit internal quantum efficiency of 38% with the emission intensity of ≈60% compared to commercial BAM.

11:20 AM

Co-Sputtering Deposition and Characterization of Ti-Cu Thin Film Metallic Glass: *Jianjun Pang*¹; *Ming Tan*¹; Christopher Shearwood¹; ¹Nanyang Technological University

Metallic glasses (MGs) have attracted increasing attention due to their excellent properties such as high yield strength, large elastic strain limit and enhanced elastic energy-storage density. Among various MGs Zr-, Ti-, Pd-

and Cu-based exhibit superior glass forming ability (GFA) to make them candidates for microelectromechanical system (MEMS) materials. In this article, the Ti-Cu binary system was investigated based on the following: (i) has not yet been studied thoroughly, (ii) relatively cost-effective, and (iii) free of toxic elements for biomedical application. Co-sputtering method was used to form Ti-Cu thin films. The amorphization and compositional proportion of thin films were characterized by X-ray diffraction (XRD), differential scanning calorimetry (DSC) and energy dispersive spectroscopy (EDS). Nanoindentation was employed to measure the mechanical properties. The effect of composition on the GFA of Ti-Cu thin films will be discussed by combining the analysis of resulting data and presently proposed glass forming theory.

11:40 AM

Control of Tarnishing and Corrosion of Copper Alloys: *Hyung Joo*¹; Da-Quan Zhang²; Young Park¹; Kang Lee¹; Jae Uk Jung¹; ¹Yonsei University; ²Shanghai University of Electric Power

The wide copper strip splits usually into several strips of smaller width. At the time, to reduce the temperature during the splitting process, a coolant is applied. It usually contains a mixture of mineral spirit, mineral oil, toluene, xylene etc. After splitting process, the coolant is wiped with absorbents and the cleaned strips are wound, packed, covered and transported. In transport containments, when the temperature is higher than around 60°C in summer, the strip coil tarnishes due to humidity and other factors; some stains and black residues form on the copper-alloy surface. To inhibit such a tarnishing and corrosion of the copper strip is the purpose of this study. In the present work, the tarnish film of copper caused by surface oil residues was investigated by SEM measurement and EDX analysis. The protection for copper tarnish was developed by surface treatment method and VCI technology.

12:00 PM

Preparation of Carbon Nitride Using Microwave Plasma CVD and Its FE Property: *Sakamoto Yukihiko*¹; Komizo Shunichiro¹; Hamamura Naoki²; Takaya Matsufumi¹; ¹Chiba Institute of Technology; ²Musashi Institute of Technology

Investigation was carried out on the preparation of carbon nitride using microwave plasma CVD and the effect of synthesis condition on FE properties of carbon nitride. The microwave plasma CVD apparatus was used. Mixture of CH₄ and N₂ was used for the reaction gas system. The estimation of the deposits was carried out by SEM, AES, ESCA, XRD, and Raman spectroscopy. The surface morphologies of the deposits were changed from crystals to whiskers with increasing of CH₄ concentration. Si, C, N and O peaks were observed in AES spectra of all samples. Composition of the deposit at CH₄ concentration; 1% calculated from the AES spectrum, nitrogen concentration was 57.5%. C-N and C=N bonding were obtained in XPS spectra. FE properties of the deposit synthesized in optimum synthesis condition (CH₄ flow rate; 4SCCM, synthesis pressure; 6.0kPa, growth time; 5h) was showed the highest current density at low electric field.

Tuesday Keynote Lecture

Tuesday PM
December 9, 2008
Room: Auditorium B2, Bangkok Convention Centre
Location: Sofitel Centara Grand Bangkok

Session Chair: Akio Fuwa, Waseda University

2:00 PM Keynote

Separation Process of Precious Metal: Junji Shibata¹; ¹Kansai University
Separation process of precious metal was briefly discussed; basic idea for separation process, basic idea for dissolution process, separation with solvent extraction and separation with solvent impregnated resin were explained in this manuscript. If it is possible to collect separately each precious metal, the separation and recovery are easily operated. However, the process for separation and purification becomes complicated, when precious metals are contained simultaneously in the solids like electronic wastes and anode slime. Solvent extraction and solvent impregnated resin processes are considered to be effective for the aqueous solutions containing precious metal ions at the concentration as high as 0.5 g/dm³ and the concentration lower than several hundred ppms, respectively.

Aqueous/Electrochemical Processing II

Tuesday PM
December 9, 2008
Room: Plaza 1
Location: Sofitel Centara Grand Bangkok

Session Chair: To Be Announced

2:45 PM Invited

Zinc Electrowinning by Using Leaching Solution of Secondary Zinc Oxide: Masatami Sakata¹; Hiroshi Hata¹; Kenji Haiki²; ¹Mitsui Mining and Smelting Company, Ltd.

In zinc smelting, most of the secondary zinc oxide contains fluoride ion (F⁻) in large quantities. Fatal troubles at the zinc electrowinning process are occurred by the cathode corrosion caused by F⁻, so we developed the iron compounds as F⁻ adsorbents used in zinc sulfate solution. The iron compounds can be reused repeatedly as F⁻ adsorbents because they can adsorb and desorb F⁻ alternatively depending on the pH. Moreover, if the adsorptive capacity of the adsorbents decreases, we can dissolve and re-synthesize them to recycle iron contents. In this paper, results of the experimental process which consists of five circuits (leaching, F⁻ removal, chloride removal, purification, and electrowinning) to produce high purity electrolytic zinc from the secondary zinc oxide are reported.

3:05 PM

Manufacturing of the Ferrate Using the Electrolytic Process in High-Dense Alkaline Solution and Its Applications: Hidehiko Ohtsu¹; Satoshi Yamashita¹; ¹Chiba Institute of Technology

Because the oxidizability of ferrate (FeVI) is so strong, it is very difficult to manufacture as industrial materials for practically use. In this study, manufacturing of the ferrate (FeVI) using the electrolytic process in high-dense alkaline solution and its application of surface treatment for magnesium alloys were investigated. The steel-wool was used as the anode for an iron source, and the platinum was used as the cathode. To produce ferrate solution, the potassium hydroxide and the sodium hydroxide of the 4, 8, 12M were used for electrolytes, and current of electrolytic was kept to 4A. The ferrate solution can be obtained easily by electrolyzing using the steel-wool as an iron source in high-dense sodium hydroxide solution in the atmosphere. Moreover, this ferrate was effective for the surface treatment for magnesium alloys.

3:25 PM

Optimization of Environment-Friendly Electrochemical Polishing Process for Titanium Plate Electrode: Masatoshi Sakairi¹; Misaki Kinjyo¹; Tatsuya Kikuchi¹; ¹Hokkaido University

Electro or mechanical polishing is essential technique for electrode preparation. Therefore, there are many studies related to polishing especially for electrochemical polishing. A new environment-friendly NaCl ethylene glycol type electrochemical polishing solution for titanium has been developed. This solution can be used around room temperature and does not contain toxic chemical ions such as fluoride and sulfate ions. However, it is not clear electrochemical polishing condition for titanium plate electrode, which is used localized electrochemical test. The purpose of this study is to decide optimum electrochemical polishing condition for titanium plate electrode, which is used for localized corrosion test. Best polishing was obtained double voltage, at the initial 25 V for 120 s then 10 V for 900 s at room temperature in 1.7 kmol/m³ NaCl ethylene glycol solution.

3:45 PM

Oxidation Behavior of Sensitized AISI 310 Steel in KNO₃ and K₂CO₃ at 1123 K: M. Misbahul Amin¹; Che Mohd. Ghazali¹; Neelofar Amin¹; ¹University Malaysia Perlis

Sometimes the operating temperature is such that the stainless steel can become sensitized, i.e. chromium carbide can precipitate at grain boundaries. The behavior of sensitized stainless steel is quite different from that of the solution-treated stainless steels in corrosive environments. The oxidation behavior of sensitized austenitic AISI 310 stainless steel were carried out in KNO₃ and K₂CO₃ at 1123 K. The oxidation rate was appreciably higher as well as the alloy severely attacked by nitrate and carbonate salts due to evolution of nitrogenous and CO₂ gases respectively. The decomposition of nitrate and carbonate takes place leading to passivity break down, resulting evolution of gases. The microstructural evolution and chemical analysis of the oxide films grown by oxidation were performed by SEM and EDX.

4:05 PM Break

4:30 PM

Synergistic Effect of Polymer Additives and Chloride Ions and Their Degradation in Copper Electrorefining: Hiroaki Nakano¹; Satoshi Oue¹; Hiroshi Kuboyama¹; Hisaaki Fukushima¹; Yutaka Hayashibe²; ¹Kyushu University; ²Mitsubishi Materials Corporation

The cathode potential for Cu deposition was greatly polarized in solutions containing both chloride ions and gelatin or PEG, showing evident synergistic effect of polymer additives and chloride ions on Cu deposition. The rotating ring-disk electrode technique revealed that Cu deposition in solutions containing small amounts of chloride ions proceeded with initial formation of adsorbed intermediate CuCl_{ad}. The Cole-Cole plots obtained by AC impedance techniques suggest that the reduction of CuCl_{ad} is suppressed by polymer additives. The polarization caused by the additives gradually decreased with increasing the electrolysis duration. Gel permeation chromatography showed that the molecular weight of gelatin in electrolyte decreased with increasing the electrolysis duration. The decrease in molecular weight of gelatin by electrolysis brought about the shift of the cathode potential to noble direction, showing that the molecular weight of degraded gelatin was related with the deposition potential of Cu.

4:50 PM

The Effect of Acid Addition on the Preparation of Carbon-Supported Platinum Nanoparticles by Alcohol Reduction: Yoshitatsu Kano¹; Mutsuko Komoda²; Yuji Mizuta¹; Yoiti Yoichi¹; Seizo Kakimoto²; Tetsuji Hirato¹; ¹Kyoto University; ²Sharp Corporation

Carbon-supported platinum nanoparticles are used for PEFC (Polymer Electrolyte Fuel Cell) as an electrode catalyst. In this paper, platinum nanoparticles were synthesized at 369 K by using n-propanol as a reducing agent, and the influence of acid addition before reduction process was examined. It was found that an appropriate amount of acid addition improved the dispersion property of platinum particles on carbon support. The effect of acid addition on the solution conditions was examined. The results obtained

suggest that the acid addition reduced the activity of dispersing agent and increased the adsorption of platinum ions on carbon support.

5:10 PM

The Electrodeposition of Zn-Al Alloys from Dimethylsulfone Electrolytes: *Yuji Mizuta*¹; Kazumi Takenaka¹; Tetsuji Hirato¹; Shuhei Kunishige²; ¹Kyoto University; ²Tohoku University

The electrodeposition of Zn-Al alloys was investigated from AlCl₃-ZnCl₂-dimethylsulfone (DMSO₂) electrolytes. The electrodeposition was done at 110°C and at current densities between 3 and 10 A/dm². The aluminum contents of electrodeposits obtained were ranged from 1 to 20 at%. In the X-ray diffraction profiles, Bragg diffraction peaks of Zn were observed, while those of Al not. With a decrease in ZnCl₂ concentrations of the electrolyte, the intensity of the diffraction peaks of Zn decreased. These results suggest the supersaturation of Al in Zn solid solution and/or the formation of a Zn-Al amorphous phase.

Composites Processing III

Tuesday PM

Room: Plaza 5

December 9, 2008

Location: Sofitel Centara Grand Bangkok

Session Chair: To Be Announced

2:45 PM

Mechanical Properties of Nanocrystalline Co-Cu Alloy with a Nanoscale Multilayer Structure: *Motohiro Yuasa*¹; Hiromi Nakano²; Yoshiaki Nakmoto¹; Kouta Kajikawa¹; Hiromu Kusuda¹; Youqing Chen¹; Mamoru Mabuchi¹; ¹Kyoto University; ²Ryukoku University

Co/Cu multilayer systems have been investigated for giant magneto resistance (GMR), and Co-Cu alloy films provide an alternative for GMR applications such as magnetic sensor. In the present paper, nanocrystalline Co-Cu alloy with a nanoscale multilayer structure has been fabricated by electrodeposition method and its mechanical properties have been investigated by tensile tests at room temperature. The grain size of the Co-Cu alloy was 110 nm, and the grains contained a nanoscale multilayer structure with a narrow spacing of 3 nm. as a result of tensile tests, the Co-Cu alloy exhibited very high strength of about 2 GPa and large strain rate dependence. The notable mechanical properties were related to the nanoscale multilayer structure.

3:05 PM

Refinement Behavior of Second Phase Particles in Hypereutectic Al-Si Alloy by Compressive Torsion Processing: *Yuji Kume*¹; Shotaro Tahara¹; Makoto Kobashi¹; Naoyuki Kanetake¹; ¹Nagoya University

Refinements and distribution of second phase particles in hypereutectic Al-Si alloy are important to improve the mechanical property of that alloy. Severe Plastic Deformation (SPD) process enables to refine not only matrix grain but also second phase particles. In the present work, the compressive torsion processing (CTP), which was developed by us, was applied to refine second phase particles, primary and eutectic silicon phases, in hypereutectic Al-Si alloy. Effects of processing conditions (rotation number and processing temperature) on the refinement were investigated. The second phase particles were successfully refined and homogeneously distributed by the CTP. The primary and eutectic silicon particles were broken to pieces and dispersed in a matrix alloy during the CTP, then resulted in homogeneous distribution of fine silicon particles.

3:25 PM

Processing and Physical Properties of High Porosity Metal Foam Using EPS Bead: *Toru Shimizu*¹; Kunio Matsuzaki¹; ¹National Institute of Advanced Industrial Science and Technology

To produce metal foam over 95% porosity, the process using foamed polystyrene sphere as space holder is developed. And this process can use low cost metal powder and process itself is simple. Using this process, the

production cost of high porosity metal foam can be decreased. In this process, slurry of metal powder and water solution of PVA are used, and EPS beads are used as space holder. Using stainless powder for metal injection molding, the metal foams from 90 to 96% porosity are produced, and the pore size and the porosity can be controlled by the size and quantity of using EPS beads. Using this process, high porosity and large size steel foam can be produced by reasonable cost, and physical properties of the foam are measured to consider the applications.

3:45 PM

Microstructure and Mechanical Properties of a Ti-Ti₂AlNb Multilayer Composite Plate: *Rafail Galeev*¹; *Oleg Valiakhmetov*¹; *Rinat Safiullin*¹; *Marat Shagiev*¹; ¹Institute for Metals Superplasticity Problems

Intermetallic alloys and composites based on the ordered orthorhombic Ti₂AlNb phase are of a great interest for aerospace applications. They demonstrate much better resistance to creep and burn than conventional titanium-based alloys, enabling operation up to 700°C. Furthermore, these intermetallics do not suffer from the very poor ductility and fracture toughness usually associated with titanium aluminides. Nevertheless, for commercial application of Ti₂AlNb-based alloys and composites the problem of workability improvement is still very important. It may be overcome by development of the multilayer composite material consisting of the alternating layers of an orthorhombic intermetallic and commercial high temperature titanium alloy. In the present work, such composite sandwiches were produced and their mechanical properties were studied. The composite material exhibited improved mechanical properties both at room and elevated temperatures. Its ductility was found to be higher than that of orthorhombic alloy while the strength considerably exceeded the strength of titanium alloy.

4:05 PM Break

4:30 PM

Metal Matrix Composites Processing: Multiscale Modelling and Property Extraction: *Fionn Dunne*¹; Hua-Xin Peng²; ¹Oxford University; ²Bristol University

A multiscale approach is presented for the process modelling of locally reinforced metal matrix composite shaft components. Micro-mechanical models are first developed for both hexagonal and square packed titanium alloy foil-SiC fibre-foil (FFF) composite materials, which are used to investigate the dependence of densification on pressure. The possible use of titanium alloy matrix coated fibres (MCFs) within the FFF consolidation process is also investigated and it is shown that densification rates are considerably higher. The F-MCF-F processing route also offers the advantage of careful control of fibre spacing and the reduced likelihood of fibre damage during processing. The densification results obtained at the micro-level are used to develop homogenized porous plasticity constitutive equations for the densification of the composite which are implemented with finite element software. Analyses of component processing then become possible, and the processing of a locally reinforced shaft is then investigated. It is shown that higher processing rates are achievable using hexagonal packing, and that during processing, a radial variation in relative density exists until full densification is achieved in the composite reinforced region of the shaft. The combinations of loading rate and fibre array type giving rise to full densification during processing are investigated.

4:50 PM

Gas Barrier and Adhesion Properties of EVOH/Glass Composite for Glass Sealing: *Hidetoshi Yamabe*¹; ¹Sumitomo Metal Mining Company, Ltd.

Over the years, the use of lead-containing sealants in the electronics industry has come under increasing environmental pressure. Recently, the toxicity of this material to humans has also become an area of concern in Japan. Polymeric materials offer an environmentally benign alternative to the glass sealants. From this point of view, polymeric composite material based on EVOH (ethylene-vinyl alcohol copolymer) was developed as an alternative to lead-containing glass sealants. This material showed sufficient gas and vapor barrier properties for the sealing with good adhesion to the

glass sheets. Barrier properties were affected by its polymeric structure and dispersion aspect of the glass flake.

5:10 PM

Microstructure and Thermal Expansion Behavior of Magnesia-Magnesium Aluminate Spinel Composites: *Wantanee Buggakupta*¹; Julie Yeomans²; ¹Chulalongkorn University; ²University of Surrey

While the coefficient of thermal expansion (CTE) of a ceramic material can be measured, it would be more useful to be able to predict it on the basis of microstructural information. To investigate this possibility, magnesia-magnesium aluminate spinel (MMAS) particulate composites were studied. Corn starch was used to make porous microstructures. The microstructures were analysed using scanning microscopy and quantitative data were collected and reported in the form of the contiguity. Thermal expansion behaviour and the CTE were determined using dilatometry and compared with the predicted CTE values obtained from a traditional rules-of-mixtures (ROM). A new approach modified from the conventional ROM in order to take account for quantitative microstructural information of solid contiguity was introduced. A good agreement between the predictions and the measured data suggests that such quantitative information may be a useful parameter in the prediction of the CTE values of ceramic materials with complex microstructures.

5:30 PM

Influence of Distribution of Oxide Contaminants on Mechanical Properties of Recycled Mg Alloy by Solid-State Recycling: *Yasumasa Chino*¹; Mamoru Mabuchi²; ¹National Institute of Advanced Industrial Science and Technology; ²Kyoto University

Recently, "solid-state recycling" has been proposed as a new recycling method, where magnesium scraps such as machined chips are directly extruded in order to attain strong solid state bonding between them. The recycled specimen from machined chips exhibits high strength at room temperature. The superior strength of the recycled specimen is due to dispersed fine oxide contaminants which are originated from scraps surfaces. On the other hand, the recycled specimen often shows low elongation, in particular, at elevated temperature. The low elongation of the recycled specimen is attributed to excessive cavity formation induced by oxide contaminants. In the first half of the paper, effects of distribution and size of oxide particles on high strength of the recycled specimen are described. In the latter half, critical conditions for cavity nucleation in the recycled specimen are discussed using existing theoretical models.

Materials Processing V

Tuesday PM
December 9, 2008

Room: Plaza 3
Location: Sofitel Centara Grand Bangkok

Session Chair: David Olson, Colorado School of Mines

2:45 PM Invited

Study of Superplastic Boronizing on Duplex Stainless Steel (DSS): Strain Effect: *Nur Hafizah Abd Aziz*¹; Iswadi Jauhari¹; ¹Faculty of Engineering, University Malaya

Boronizing has long been used to improve the surface properties of metals. A study on superplastic boronizing through compression method was conducted focusing mostly on the effect of sample's surface asperities deformation. Thus, the effect of the bulk material's superplastic deformation (strain) on boronizing was studied. This process was conducted on thermo-mechanically treated duplex stainless steel (DSS) with fine grain microstructure which can exhibit superplasticity. Boronizing was conducted at temperature of 1223 K and compression rate of 1×10^{-3} s for various strain conditions. Metallographic, hardness and layer thickness of the boronized materials were investigated revealed a uniform and dense boronized layer. The formation of boronized layer was confirmed through XRD analysis. Hardness and boride layer thickness up to 1961 HV and 28.8 μm were obtained. The overall

results suggested that through this superplastic boronizing method hard and thick boride layer can be formed at a very fast rate.

3:05 PM

Reduction in Unit Energy Consumption at Saganoseki Smelter and Refinery: Yuji Shimizu¹; Toshihiro Kamegai¹; ¹Nikko Smelting and Refining Company, Ltd.

In 1996 Saganoseki Smelter and Refinery integrated its two flash furnaces to one while maintaining the smelting capacity. Since then, the smelting capacity had been expanded. As a result, the smelting capacity reached 450,000mtpy in 1999. Afterwards, SPI (Saganoseki Process Innovation) project had been executed in the smelter and the refinery from 2003 to 2007. It had aimed at the further cost reduction and the maintenance of the production under the conditions that the copper content of the concentrate had become lower. The unit energy consumption change by these improvements and modifications was verified from the energy consumption data and the production data. The unit supplied energy for smelting has been reduced by 50% compared with 1995.

3:25 PM

Improvement of Mechanical Properties of Phynox Superalloy Using Continuous Bending: *Hasan Sheikh*¹; Seyed Masoud Hashemi¹; ¹Malek Ashtar University of Technology

In this work, the yield strength and hardness of phynox superalloy have been improved using applied strain in continuous bending process. For this purpose, the strip of phynox superalloy with cross section dimensions of 2.5x0.9mm² has been passed through a die channel with corner angle of 145°. Under this working conditions, a negligible value of strain is applied on material per each pass. By repetition of this process, a high value of strain is applied and the mechanical properties improve.

3:45 PM

Gypsum Formation in the CaO-FeOx-Cu2O Slags at Copper Saturation: *Katsunori Yamaguchi*¹; Shiichi Sato¹; Fumito Tanaka²; ¹Iwate University; ²Mitsubishi Materials Corporation

Continuous converting of copper matte using calcium ferrite slag of the CaO-FeOx-Cu2O system is an attractive technology for copper converting. This slag sometimes tends to separate out gypsum under a high oxygen potential required to produce blister copper. Experiments have been carried out to determine the precipitation of CaSO₄ in the CaO-FeOx-Cu2O slag with equilibrating with molten copper under the SO₂ partial pressures of 0.2, 0.4, 0.6 and 1.0 atm at temperature range from 1473 to 1573K. The results have revealed that CaSO₄ tends to precipitate from slag when the temperature lowers, the CaO content increases, the SO₂ pressure increases, or blister copper is oxidized excessively.

4:05 PM Break

4:30 PM

High Strain Rate and High Temperature Tensile Test of Lead Free Copper Alloy Castings; Machinability Evaluation: Takateru Umeda¹; Wantanee Sithilor¹; Mawin Supradist¹; *Toshimitsu Okane*²; Takahiko Fujii³; ¹Chulalongkorn University; ²National Institute of Advanced Industrial Science and Technology (AIST); ³Fuji Technical and Consulting Service Company, Ltd.

Lead free copper alloy castings are now commonly used for water supply equipments according to the WHO guideline. One of the most serious problems in producing final products is a poor machinability of all lead free copper alloys comparing with JIS CAC406. To understand the machinability of lead free copper alloy, high temperature tensile testing at high strain rate was carried out to simulate machinability. Tensile strength and elongation of lead free bronze tested alloys at strain rate of 1 s⁻¹ were decreased sharply when temperature was increasing above 100°C, while CAC406 had an enough strength and elongation around 100°C and decreased above 300°C. On the other hand, tensile strength of Si brass test alloys were much higher than CAC406.

4:50 PM

Various Improvements for the Zinc Roasting and Sulfuric Acid Process at Onahama Refinery: *Tatsuya Suzuki*¹; Masaru Suzuki¹; ¹Toho Zinc Company, Ltd.-Onahama Refinery

Toho Zinc Onahama Refinery presently produces approximately 150,000 t/y of zinc calcine and 151,000 t/y of sulfuric acid, treating zinc concentrates by a fluosolid roaster. This plant started its operating in 1968. Recently, it became necessary to modify the operation method and to strengthen the equipment function at the roasting and sulfuric acid process, because the function of equipments became inefficient through long-term use, and the physical property and quantity of contained impurity in zinc concentrates have changed. We report the various improvements at each process and the results that carried out to improve the roasting and sulfuric acid operation.

5:10 PM

Fabrication of Separately Formed Electro-Spun Fibers: *Hirohisa Tamagawa*¹; Minoru Taya²; ¹Gifu University, Department of Human and Information Systems, Faculty of Engineering; ²University of Washington, Center for Intelligent Materials and Systems, Department of Mechanical Engineering

As one of fine fiber fabrication techniques, electrospinning is a quite efficient and simple technology. Electrospinning enable us to fabricate fine fibers consisting of a number of different type of polymers. Diameter of fiber fabricated is extremely small, and sometimes it reaches as small as nano level. It is a quite attractive technology. Nowadays, this technology comes to be adopted not only for the textile engineering field but also totally different field such as tissue engineering. However, it was not until these days that the recognition to the electrospinning technology was widely made in its quite long existence period. Therefore, still this technology has enormously large room to be investigated. Fabricating a non-woven mat consisting of fine fibers is a subject that the electrospinning can display its usefulness most efficiently. For example, a two-dimensional durum filter with superior functionality can be fabricated quite easily by the electrospinning. However, extracting the electro-spun fibers individually is a difficult task for the electrospinning technology, since electro-spun fibers are inevitably entangled and stick together. Extraction of single fiber is quite difficult task, and establishing a single fiber extraction technique is a challenging theme in this field. We found a quite simple technique to extract electro-spun fibers separately. This technique simply employs a paper mesh which is to be placed between the needle tip and counter electrode of electrospinning unit. Polymer solution stuffed in a syringe in the electrospinning unit is spewed out toward the counter electrode by the high electric field applied. Part of polymer solution spewed out is trapped by the paper mesh and stretched, during its travel toward the counter electrode. Consequently, the stretched fine fibers are formed between paper mesh and counter electrode separately.

Materials Processing VI

Tuesday PM
December 9, 2008

Room: Plaza 4
Location: Sofitel Centara Grand Bangkok

Session Chair: N. Cheruvu, Southwest Research Institute

2:45 PM Invited

Effect of Ca Addition on Microstructure and Mechanical Properties of AZ31B/nano-Al₂O₃ Composite: *Nguyen Bau*¹; Manoj Gupta¹; ¹National University of Singapore

In this study, different amounts of Ca (1 wt. %, 2 wt. % and 3 wt. %) were incorporated into a AZ31B/nano-Al₂O₃ magnesium alloy composite using the disintegrated melt deposition (DMD) technique followed by hot extrusion. The samples were characterized in terms of physical, microstructural and mechanical properties. Microstructural characterization studies revealed that with increasing Ca addition, the matrix grain size and the presence of Mg₁₇Al₁₂ phase reduced. On the contrary, it was observed that the presence

of Al₂Ca phase increased. Furthermore, the presence of Ca significantly assisted in improving 0.2% yield strength (YS) and ultimate tensile strength (UTS) while failure strain (FS) was dramatically reduced. An attempt is made to correlate the effect of increasing amount of Ca on the microstructure and mechanical properties of AZ31B/nano-Al₂O₃ composite.

3:05 PM

Investigation of Microstructure and Mechanical Properties of Joining of Semi Solid (SSM) A356 by Friction Stir Welding Process: *Prapas Muangjumburee*¹; Abdul Binraheem¹; ¹Prince of Songkla University

The butt joints of semi solid A356 (SSM A356) were produced in as cast conditions by friction stir welding process (FSW). The effect of tool rotational speed and welding speed on the microstructure and mechanical properties was investigated using various techniques. The variations of welding parameters produced different joints properties. It was found that the integrity of the joint contributed for the mechanical properties of the joint. The combination of 1,750 rpm and 160 mm/min reveals the sound microstructure. The hardness of the weld zone, thermo-mechanical affected zone (TMAZ) and the base metal (BM) indicates more uniform distribution than that of other combinations. The tensile strength of the joint is also elevated.

3:25 PM

Iron-Carbide Composites Prepared by P/M: *Ruangdaj Tong Sri*¹; Sainathee Chakthin²; Nandh Thavarungkul²; *Nuchthana Poolthong*²; ¹National Metal and Materials Technology Center; ²King Mongkut's University of Technology Thonburi

The iron-carbide composites have been prepared using a simple powder metallurgy (P/M) processing route, which includes compacting and sintering of mixed powders. Sintered composites were designated to have nominal composition of Fe-5 wt. % carbides (SiC, TiC and WC). Two carbide particle sizes, -20 μm and 20-32 μm, were mixed with Fe powder. The compacted specimens were sintered at 3 different temperatures, 1100, 1150 and 1200°C. Preliminary study revealed that stability of carbide particles under sintering conditions showed its effects on microstructures and properties of the sintered Fe-carbide composites. Microstructures and mechanical properties of sintered Fe-5 wt. % carbide composites will be presented and discussed.

3:45 PM

Influence of Milling Parameters on Residual Stress in Nickel Base Super Alloy Udimet 720: *B. R. Sridhar*¹; S. V. Joshi¹; S. Paul Vizhian²; K. Jayaram¹; ¹Gas Turbine Research Establishment; ²University Visvesvaraya College of Engineering

Machining parameters such as speed, feed and depth of cut play an important role in determining the residual stress as well as the surface roughness of any material. The material used for the present study is a nickel based superalloy Udimet 720. The alloy finds applications for the manufacture of gas turbine engine components like shafts, discs and blades. Specimens extracted from a test forging of this alloy were machined by milling using different combinations of milling parameters (speed, feed and depth of cut). Residual stress and surface roughness measured on the specimens showed different magnitudes for different combinations of milling parameters. The variations did not reveal any definite trend with respect to milling parameters. In several cases the increase in the magnitudes of residual stress and surface roughness could be attributed to different degrees surface working undergone by the specimens during the milling operation. Analytical relationships were developed between the magnitudes of residual stress and surface roughness and milling parameters. Experimental and analytical data suggested that the combined effects of milling parameters influence both residual stress and surface roughness.

4:05 PM Break

4:30 PM

Kinetic Study on Oxidation, Chlorination and Evaporation Reactions for Chloride-Based Fluxes: *Yang Cui*¹; Canguo Wang²; Xiaojun Hu²; Naoya Takahashi³; *Hiroyuki Matsuura*³; Fumitaka Tsukihashi³; ¹Shougang Research Institute of Technology; ²University of Science and Technology Beijing; ³University of Tokyo

The present study is focused on the refining processes with utilization of chlorine. Generally, melting points of metal chlorides are lower, and vapor

pressures are higher than those of oxides and sulfides. Therefore, the refining using chlorides could be carried out at lower temperatures compared to conventional metal refining processes. Metal refining by using chlorine is advantageous for development of environmental-friendly processes. Firstly, evaporation kinetics of $\text{FeCl}_2\text{-ZnCl}_2$ and $\text{PbCl}_2\text{-ZnCl}_2$ melts were measured and the effects of temperature, initial compositions and oxygen partial pressure were studied. The evaporation rate of ZnCl_2 was larger than that of other components and oxygen partial pressure had a great effect for the evaporation rate. Secondly, removal of impurities such as antimony and lead in copper melts by CuCl , CuCl-CaO and $\text{CuCl-Na}_2\text{CO}_3$ fluxes were observed. Impurities were removed efficiently with chloride-based fluxes. The role of simultaneous chlorination and oxidation reactions for impurity removal was discussed.

4:50 PM

Liquidified Natural Rubber Processing with Supercritical Carbon Dioxide: Surat Areerat¹; Pongpapaat Piyamanocha¹; ¹King Mongkut's Institute of Technology Ladkrabang

Natural rubber (NR) always contains ultra high molecular weight up to 10^6 which causes energy consuming in the processing line. Therefore, liquidified NR processing with molecular weight reduction technique allows us to utilize its as an alternative feedstock. After liquidifying process, the effective controlling of its molecular weight is important. Thus, this present utilizes the advantage of supercritical carbon dioxide (sc-CO_2) as a plasticizer for reducing of NR molecular weight. While sc-CO_2 dissolving into NR solution revealed the minimization of chemical peptizing agent (used Pentachlorothiophenol as low as 0.1 phr). The NR-Mw measurement was performed by using a GPC. Experimental result showed that NR-Mw is reduced about 63.4% compared with the ordinary NR. Moreover, the visualized observation of NR/ sc-CO_2 solution at temperature ranging from 303 to 333 K and pressure ranging from 0.1 to 15 MPa were investigated by using a high-pressure view cell.

5:10 PM

Influence of Pin Configuration on Movement of Beads in a Stirred Mill: Rikio Soda¹; Junya Kano¹; Fumio Sato¹; ¹Institute of Multidisciplinary Research for Advanced Materials, Tohoku University

This work has clarified motion of beads in a stirred mill with different configuration of pins in a stirred mill operated under wet condition, suspending gibbsite powder as a sample ground. The mill was run experimentally at constant speed, besides the beads motion is simulated by Discrete Element Method. The simulated data were checked by the experimental ones taken through transparent vessel by using video-camera. As clarified before, the specific impact energy of beads calculated from the simulated data is well correlated with the grinding rate constant of the ground product. It was found that the beads velocity reaches the maximum value when the number of the pin is changed from 2 to 12. The number of pins plays a significant role to control the grinding performance for a beads mill under wet condition.

Materials Processing VII

Tuesday PM Room: Plaza 6
 December 9, 2008 Location: Sofitel Centara Grand Bangkok

Session Chair: R. J. Singh, National Institute of Technology

2:45 PM Invited

Development of High Fatigue Resistent Electrical Steels for High Frequency Motors: Sam Chang¹; Hee Park¹; ¹Pohang University of Science and Technology

Morden motors have been advanced as previous AC motors are changing to new structure motors as high efficient DC brush motors or magnetic resistant motors. These motors exhibit very high efficiency at a high revolution of motor and have advantages of simplicity and high recycling. Therefore electrical steels using for cores of rotor must endure the centrifugal force

during high speed rotation. Present work was performed to design alloying and process parameters to achieve a good fatigue strength and yield strength without deterioration of magnetic properties.

3:05 PM

Microscopic Study of Slags from a Secondary Lead Blast Furnace: Fumito Tanaka¹; Yusuke Kimura¹; Mikio Watanabe²; ¹Mitsubishi Materials Corporation; ²Hosokura Metal Mining Company, Ltd.

Hosokura Metal Mining Co., Ltd. processes spent lead-acid battery to produce electrolytic lead, while leaving acceptable influences on the environment. The company derives noticeable competitiveness from proven technologies for operating the blast furnace, which was developed jointly with Mitsubishi Materials Corp. Emerged businesses to recycle various lead-bearing materials have also been enhancing the bullion production. Processing lead-bearing materials, however, impacts on the slag chemistry or energy balance of the blast furnace, thereby misleading the operators occasionally. Microscopic examination of slag samples from the blast furnace revealed the metallurgical cause of the operational difficulties and helped to identify secondary materials whose feeding rate should be optimized. Among impurities included in secondary materials, the present paper will focus on the metallurgical impact of soda. It will also discuss the furnace controls under the influence of soda, applying slag chemistry of the state of the art.

3:25 PM

New Era of Onahama Smelter with New "O-SR Process" - Onahama Type Direct Laundered S-Furnace and Reverb Furnaces: Haruhiko Asao¹; Masao Hirano²; Osamu Iida¹; Shousaku Hayashi²; ¹Mitsubishi Materials Corporation; ²Onahama Smelting and Refining Company

Onahama Smelter has been maintained its profitability over 40 years by developing innovatory technology, while it employs conventional process, such as huge energy-consuming reverberatory furnace (RFs). In 80's, concentrate injection into PS-converters was developed to increase production drastically. New development of combustible waste treatment in RFs was followed in 90's, which realized drastic fuel saving and accompanying metals recovery. In December 2007, new S-furnace of the Mitsubishi Process was installed. Concentrate is solely treated in S-furnace, which is directly laundered to RFs for continuous and automatic delivery of melts. RFs are dedicated to slag/matte separation and combustible waste treatment. This new "O-SR process" realized, not only high productivity and more flexibility for raw materials, but also more combustible waste treatment and less fuel consumption in RFs. This paper introduces good example that the combination of new technology and existing process makes a conventional smelter revived as the most cost-efficient smelter.

3:45 PM

Physical Chemistry of Oxidative Roasting Complex Oxides with Alkali and Water Leaching Reactions for the Extraction and Beneficiation of Metal Oxides: Animesh Jha¹; Abhishek Lahiri¹; ¹University of Leeds

The paper aims to discuss the molten salt chemistry of sodium carbonate based liquids, which form during alkali roasting of minerals (e.g. chromite, ilmenite, and bauxite) above 400°C. The alkali oxide reacts with the decomposition product of mineral constituents and forms a complex liquid which plays an important role in determining the disproportionation of constituent minerals. For example during roasting of chromite minerals the sodium carbonate combines with sesquioxides (Fe, Cr, Al) and forms water soluble sodium complexes: Na(Al,Fe)O_2 , $\text{Na}_2(\text{Fe,Cr})\text{O}_4$, and insoluble $\text{Na}_2\text{Cr}_2\text{O}_4$. Here we also explain the physical chemistry and thermodynamics of the overall reactions, together with the structural analysis of complexes using the X-ray powder diffraction and scanning electron microscopy. After alkali roasting, the leaching reactions were analysed to separate the soluble phases, leaving the insoluble material (e.g. COPR in $\text{FeO.Cr}_2\text{O}_3$) and sodium titanate, which we have examined in detail for producing high-grade sodium chromate and titanate.

4:05 PM Break

4:30 PM

Microstructure and Mechanical Properties of Electron Beam and Tungsten Inert Gas Welded Burn Resistant (BuRTi) Ti-25V-15Cr-2Al-0.2C Alloy: *Tapany Udomphol*¹; Paul Bowen²; ¹Suranaree University of Technology; ²University of Birmingham

Mechanical properties of EB and TIG welds of a burn resistant titanium alloy have been assessed via tensile, fracture toughness, fatigue strength and fatigue crack growth resistance tests. The welds suffered from mechanical property degradation and were susceptible to brittle failure due to excessively large columnar beta grains in the weld fusion zone. The presence of the second phase precipitates changed the weld fracture mechanism from a transgranular cleavage fracture to an intergranular fracture at grain boundaries. Columnar beta grains orientated normal to the applied tensile stresses are prone to intergranular fractures along the weakened beta grain boundaries. Decreased beta grain size is believed to give enhanced fracture and fatigue resistance of the welds.

4:50 PM

Understanding the Application of the LENS® Technology to the Fabrication of WC-Co Cermets: Yuhong Xiong¹; John Smugeresky²; Enrique Lavernia¹; *Julie Schoenung*¹; ¹University of California; ²Sandia National Laboratories

In this study, two types of WC-Co powder (submicron-sized and nanostructured) were used to make bulk cermets by the Laser Engineered Net Shaping (LENS®) process. It was found that decomposition and decarburization of WC was limited during laser deposition. The effects of working distance, laser power, powder feed rate, and traverse speed on microstructure were studied in detail. Thermal behavior leading to the different microstructures that result from the variations in processing parameters was also investigated. Relevant environmental burdens for the fabrication of WC-Co cermets were quantified to compare the LENS® process and the conventional powder metallurgy process. The manufacturing costs for WC-Co cermets were also investigated for these two processes to fully evaluate the application of the LENS® technology to WC-Co cermets.—Work by UC Davis is supported by the NSF under Grant DMI-0423695. Work by Sandia is supported by the US Department of Energy under contract DE-AC04-94AL85000.

5:10 PM

An Investigation of Arc Spray Formed Rapid Tooling on Homopolymer Substrate: *Peerawatt Nunwong*¹; Chatchapol Chungchoo¹; Suparek Sirivedin²; Panadda Niranatlumpong³; ¹Department of Mechanical Engineering, Kasetsart University (KU); ²Department of Mechanical Engineering Technology, College of Industrial Technology, King Mongkut's University of Technology North Bangkok (KMUTNB); ³Thermal Spray Laboratory, National Metal and Materials Technology Center (MTEC)

Thermal spray-coated backing mold was fabricated by one of many commercially available rapid tooling techniques. The coating/substrate interface condition, and hence, the finished mold quality, depend on the surface properties of the master model (substrate). Characterizations of surface deformations of the model and the critical thickness of the homopolymer substrate were carried out in this work. The deformation of the master model made from polypropylene was simulated during the solidification of the spray droplets, using a finite element analysis (FEA). The mechanical properties of the substrate are important parameters. In order to clarify this effect, the spraying conditions were kept constant for all specimens in the experiment. From the FEA, the critical thickness of the substrate can be identified. This same method can then be performed on other components to establish the suitable thickness of the master model.

Modeling Material Processing I

Tuesday PM

December 9, 2008

Room: Plaza 8

Location: Sofitel Centara Grand Bangkok

Session Chair: Tomio Takasu, Kyushu Institute of Technology

2:45 PM

Computational Thermodynamics and Computational Kinetics as Powerful Tools for Modelling Fabrication Aspects of Materials: *Henrik Strandlund*¹; Xiao-Gang Lu¹; Qing Chen¹; Anders Engstrom¹; ¹Thermo-Calc Software AB

Computational thermodynamics has evolved over the past 40 years to become a powerful, flexible tool for the study of a variety of scientific and technological areas of industrial importance. For example, it has been successfully applied to alloy and process development for different kind of metallic and ceramic materials. The most widely used software package for this purpose is Thermo-Calc. During the last 20 years computational kinetics has become an important tool for predicting rate of transformations and temporal evolution of microstructure during processing in for example metallic alloys. One of the more well-known tools for this purpose is the commercial finite-difference code DICTRA. The purpose of this paper is to discuss how different computational tools, such as the two already mentioned software packages, can be applied to problems in materials processing. In addition, a completely new software package, TC-PRISMA, for simulating precipitation reactions in alloys will be presented.

3:05 PM

Computer Aided Design of Optimal Algorithms of Pulsed Control Ensuring Preset Operating Properties of Joints of Metals: *Oksana Shpigunova*¹; A. Glazunov¹; ¹Institute of Applied Mathematics and Mechanics of Tomsk State University

The essence and complicity of approach to computer design of an optimal pulsed arc welding technology is that programmed periodic action should be developed on the one hand to exert its effect on melting and transfer of an electrode metal, and on the other hand, to control over the molten pool fluidity, the structural formation of weld and heat-affected zone that appears as result of the weld pool crystallization whilst ensuring stability of the pulsed regime in welding in different spatial positions. The results of physical simulation and mathematical modelling permit to design optimal algorithms of pulsed control of energy characteristics of welding - arc current and voltage, arc heated efficiency, peak short-circuiting current. The results of computer experiments permit to establish pulsed welding controlled parameters - service properties of welded joints (such as the sizes of welds and heat-affected zone, quality and strength properties of welded joints) relation. The solution of the pulsed arc welding and surfacing processes optimizing problem is a matter of great significance because of continuously increasing requirements on quality and reliability of welded joints, saving in welding fabrication cost. The construction of welded structures has a number of special features. These are associated with the character of welding metallurgy and solidification processes in the weld metal, the welded joint heating and cooling conditions and others, influenced on the stability of parameters of the complex electrodynamic's system: "power source - electrode - arc - weld pool - welded joint". It is necessary to ensure the regulation of the penetration depth, welding in wider gaps and in different spatial positions, joining metals and alloys of dissimilar chemical composition, decreasing the degree of splashing of electrode metal, increasing the stability of arc ignition and arcing. Arc heating sources energy concentration is unable to solve these problems including increasing the productivity of welding operations and improving the welded joints quality parameters.

3:25 PM

Consolidation Enhancement in Spark-Plasma Sintering: *Eugene Olevsky*¹; ¹San Diego State University

Spark-plasma sintering (SPS) carries a potential for the rapid and efficient consolidation of a broad spectrum of powder materials. Possible mechanisms of the enhancement of consolidation in SPS versus conventional techniques of powder processing are categorized with respect to their thermal and non-thermal nature. A model for spark-plasma sintering taking into consideration various mechanisms of thermally and non-thermally-activated material transport is developed. The interplay of three mechanisms of material transport during SPS is considered: surface tension-, electromigration- and external stress-driven grain-boundary diffusion, surface tension- and external stress-driven power-law creep, and temperature gradient-driven thermal diffusion. Besides SPS, the obtained results are applicable to the ample range of powder consolidation techniques which involve high local temperature gradients and high heating rates. The results of modeling agree satisfactorily with the experimental data on SPS of a metal (aluminum) and ceramic (alumina) powders in terms of SPS shrinkage kinetics.

3:45 PM

Detailed Modeling of Electrodeposition Using the Phase Field Method: *Adam Powell*¹; ¹Opennovation

Pongsaksawad and Powell developed a phase field model of transport-limited electrodeposition capable of predicting the shape and topology evolution of dendrites or liquid streamers. The work presented here builds on that model in two ways. First, it adds ohmic interface resistance in order to capture mixed reaction/transport-limited deposition when overpotential is small. Second, it incorporates fluid-structure interactions using the mixed stress method in order to model dendrite breakage and transport in the liquid, and also to model dendrite shape evolution under shear flow in the electrolyte. Two applications of this work are: design of alternating current waveforms for fast and stable electrodeposition e.g. for electrowinning, and design of waveforms for powder synthesis. Though the formulation is generally applicable in two or three dimensions, only two-dimensional results will appear in this presentation.

4:05 PM Break

4:30 PM

Effect of Gate Design on Ingate Velocity: Pongsak Dulyappahant¹; *Prarop Kritboonyarit*¹; ¹National Metal and Materials Technology Center

A gating system is one of the major factors directly affecting quality of castings in High Pressure Die Casting (HPDC) processes. In this study, the effect of gate design to the ingate velocity and metal casting pressure is studied. The real gating system used in the production of an automotive part is used as a case study and a commercial casting process simulation is used as a tool. The experimental results show that, by changing only the gate design but still use the same runner system and process parameters setup, ingate velocity can be increased by 10 percent. The increased of ingate velocity would benefit in reducing the use of high plunger velocity, which results in less machine power, lower tool wear, less flash, and higher injection pressure.

4:50 PM

Finite Element Analysis for Match Mold Forming of Starch/Biodegradable Polyester Blend: *Arisara Chaikittiratana*¹; Chantaraporn Phalakornkule¹; Tanawit Thongwichean¹; ¹King Mongkut's University of Technology

The objective of this work is to study the sheet thermoforming process of a Tapioca starch-biodegradable polyester (Enpol™)blend with the mixing ratio of 50:50 by weight. The mechanical behavior of the material extruded in the form of thin sheet was studied by means of compression test at the temperature between 90°C to 120°C and at various strain rates. It was found that temperature of 120°C and strain rate of 0.5 s⁻¹ gave the most satisfying condition for the sheet stamping process and this condition. Hyperelastic and Elastic – Plastic material model were used to capture the compressive behaviour of the material. It was found that the second order polynomial hyperelastic model and Elastic – Perfectly Plastic model represented reasonably well the behavior of the material and the 2D Finite element

simulation with Elastic – Plastic material model gave the best representation of the real thermoforming process.

5:10 PM

Hyperspectral Imaging Based Techniques for Dimensional Stones Characterization: *Giuseppe Bonifazi*¹; Silvia Serranti¹; ¹Sapienza Università di Roma

Dimensional stone products are commercially classified on the market according to several factors related both to intrinsic lithologic-mechanical characteristics and to their pictorial attributes. Such attributes are influenced by working actions and are also influenced by time. Sometimes pictorial-aesthetic attributes can be correlated with a specific status of the stone in terms of surface alteration and sometimes in mechanical attributes. The study was addressed to develop an innovative set of imaging based procedures able to quantify the level of alteration of the surfaces through a detection and quantification of their physical and chemical characteristics.

Nanomaterials Processing IV

Tuesday PM

December 9, 2008

Room: Plaza 7

Location: Sofitel Centara Grand Bangkok

Session Chair: To Be Announced

2:45 PM Invited

Ultra Fine Grain Evolution in Cu-Zn Alloy by Coordinated Effects of Mechanical and Annealing Twins: *Hiromi Miura*¹; Shouji Maruoka¹; Taku Sakai¹; ¹University of Electro-Communications

A Cu-Zn alloy was rolled at 77 K followed by low temperature annealing. By the rolling, ultra fine mechanical twins evolved almost uniformly in the whole areas. Annealing at temperature lower than 543 K caused evolution of recrystallized ultra fine grains (UFGs), which were mainly composed of annealing twins. The average grain size was roughly about 200-300 nm. The UFGs, however, contained further finer annealing twins in side of them. The actual grain size, therefore, was supposed to be lower than 100 nm. UFGed Cu-Zn alloy sheet was, therefore, easily fabricated by simple processes of rolling and annealing. The evolution of recrystallized UFGs during low temperature annealing would be caused by high driving force for primary recrystallization due to high densities of mechanical twins and dislocation. Furthermore, coarsening after the primary recrystallization was hard because of low temperature and high thermal stability of annealing twins.

3:05 PM

Synthesis and Characterization of Uniform Copper Nanoparticles Obtained by a Polyol Process: *Kazuomi Ryoshi*¹; Hiroko Oshita¹; Yasumasa Hattori¹; ¹Sumitomo Metal Maining Company, Ltd.

A solution-phase approach has been demonstrated for the large-scale synthesis of uniform copper particles of about 40nm in diameter. The formed Pd nano-particles serve as seeds for the growth of copper produced by the reduction of Cu₂O with ethylene glycol heated up to around 160°. Under proper conditions, the adsorbed protective agent such as poly(vinylpyrrolidone) and poly(ethylenimine) on the copper particles inhibits coagulation of the particles during the growth. The aqueous copper dispersion concentrated to 60wt.% by ultrafiltration was stable in the refrigerator for more than 3 months. The copper layer exhibited a low electrical resistivity of about 60μΩcm after sintering at 220° for 1 hour in nitrogen gas atmosphere.

3:25 PM

Synthesis and Stability of Metallic Fluid Dispersing Ferromagnetic Fine Particles: *Toyohisa Fujita*¹; Hyun-Seo Park¹; Ling-Fei Cao¹; Gjergj Dodbiba¹; ¹University of Tokyo

Generally speaking, a liquid metal has a high thermal and electric conductivity as well as fluidity. When ultra fine particles are dispersed in a liquid metal, the functional fluid such as magnetic fluid and magneto-rheological fluid can be prepared. For many years the synthesis of the mercury-based magnetic

fluid has investigated, however, the liquid mercury is toxic and difficult to handle. In this research, the ferromagnetic fine particles are dispersed in the liquid gallium and its magnetic properties are measured. The fine particles of nickel, iron, and iron alloy have been coated by silica in order to increase the affinity to liquid gallium. The silica layer thickness on the surface of particles is adjusted. The effect of viscosity and temperature of liquid gallium when dispersing fine magnetic particles was also investigated.

3:45 PM

Synthesis of CuInS₂ Colloidal Nanocrystals and Their Optical Properties: *Katsuhiko Nose*¹; Yuki Soma²; Takahisa Omata¹; Shinya Otsuka-Yao-Matsuo¹; ¹Osaka University

Chalcopyrite-type CuInS₂ is a direct semiconductor possessing 1.53eV of energy bandgap. As decreasing of the crystal size, the optical bandgap of the semiconductor becomes larger due to the quantum size effect. The energy bandgap calculation of CuInS₂ using the effective mass approximation predicts that the emission wavelength of the exciton recombination is tunable by the crystal size. We succeeded in the synthesis of nonaqueous colloidal solution of CuInS₂ nanocrystals. The mixed solutions, CuI and InBr₃ dissolved in oleylamine, which was diluted by the 1-octadecene, and sulfur dissolved in triphenylphosphite, were used as source solutions. Trioctylphosphite was added in the source solutions. It was heated at 200 degree Celsius; the reaction time was varied from 30 s to 30 min. The crystal growth from 1.6nm to 3.1nm as increasing of the reaction time from 30s to 30 min was observed. The size dependent optical properties of CuInS₂ nanocrystals were investigated.

4:05 PM Break

4:30 PM

Thermolysis of Nickel Acetylacetonate in Organic Surfactant and Formation of Metallic Nickel, Nickel Carbide and Nickel Oxide Nanocrystals: Yuji Goto¹; Kota Taniguchi¹; *Takahisa Omata*¹; Shinya Otsuka-yao-Matsuo¹; Naoki Ohashi²; Shigenori Ueda³; Hideki Yoshikawa³; Yoshiyuki Yamashita³; Hirofumi Oohashi³; Keisuke Kobayashi³; ¹Osaka University; ²National Institute for Materials Science (NIMS); ³National Institute for Materials Science(NIMS), SPring-8

Nickel acetylacetonate was thermally decomposed in organic solvent and surfactant under inert atmosphere. The phases obtained were identified using XRD, laboratory XPS and hard-X-ray photoelectron spectroscopy. For the case using the oleylamine as a solvent and a surfactant, nanocrystals of two cubic phases and a hexagonal phase appeared. The hexagonal phase was a nickel carbide (Ni₃C) with ~50 nm grain size, which had been often identified as a hexagonal close-packed metallic nickel. One cubic phase was a face-centered metallic nickel with ~50 nm grain size, and the other was identified as novel cubic nickel carbide, which was characterized as an intermediate product of the carbidization of metallic fcc-Ni to the hexagonal nickel carbide. For the case using the 1-octadecene as a solvent and the fatty acid as a surfactant, nanocrystals of nickel oxide with 3~4 nm grain sizes appeared. The formation mechanism of these phases was discussed.

4:50 PM

TiO₂ Hollow Nanofibers Templated by Electrospun Polymeric Nanofibers: *Shinsuke Nagamine*¹; Yoshitaka Tanaka¹; Tetsuro Hoshino¹; Masahiro Ohshima¹; ¹Kyoto University

TiO₂ hollow nanofibers were fabricated by a newly developed method based on the electrospinning technique and the interfacial hydrolysis of alkoxide. A polymethyl methacrylate (PMMA) / water / acetone solution was electrospun and the formed PMMA nanofibers were directly carried into a solution of titanium tetraisopropoxide (TTIP) in hexane. The hydrolysis of TTIP at the interface of PMMA fibers and hexane resulted in the formation of sheaths of TiO₂ covering PMMA fibers. The hollow TiO₂ nanofibers with several hundreds of nanometer in diameter were obtained after the heat treatment to remove PMMA. The effects of preparation conditions including the composition of spinning solution, the applied voltage, and the concentration of TTIP, will be discussed.

5:10 PM

Superplastic Behavior of of Nanostructured Intermetallic Ti₂AlNb-Based Alloy: *Marat Shagiev*¹; Gennday Salishchev¹; ¹Institute for Metals Superplasticity Problems

Intermetallic alloys based on the orthorhombic Ti₂AlNb phase are considered as promising materials for high-temperature applications due to their superior balanced mechanical properties compared with conventional titanium alloys and titanium aluminides. In the present work, mechanical properties of an orthorhombic alloy both at room and elevated temperatures were considerably improved due to formation of the homogeneous microstructure with the average grain size of about 300 nm. It was produced by thermomechanical processing which included multistep isothermal forging at temperatures below the β-transus and intermediate annealings. At room temperature, nanostructured material exhibited elongations up to 25% and the ultimate strength of about 1400 MPa. The Ti₂AlNb-based alloy demonstrated superplastic behavior in the temperature range of 850-1000°C and at strain rates of 4.2×10⁻⁴-2.0×10⁻² s⁻¹. The maximum elongation of 930% and steady state flow stress σ₅₀ of about 125 MPa were obtained at 900°C and strain rate of 4.2×10⁻³ s⁻¹.

Processing of Ceramics I

Tuesday PM
December 9, 2008

Room: Plaza 2
Location: Sofitel Centara Grand Bangkok

Session Chair: Shinya Matsuo, Osaka University

2:45 PM Invited

Grain Growth Behavior of Agglomerated Nanocrystalline Zirconia Powder during High Temperature Heat Treatment: *Chunbo Liu*¹; ¹Central South University

Brittleness of nanostructured ceramic coatings can be reduced. Agglomerated nanocrystalline zirconia powder can be used to form nanostructured thermal barrier coating by plasma spraying. In this paper, agglomerated nanocrystalline ZrO₂-8%Y₂O₃ powder prepared by spray drying was heat-treated at the temperature from 1200°C to 1400°C for 2 hours. Scanning electron microscopy was used to examine the changes of particle size and morphology of the heat-treated powder. Nano-particle growth behavior was investigated. Experimental results show that the large agglomerates connect, nano-particles in the agglomerate grow and inhomogeneous growth of the nano-particles occurs when heat treatment temperature reaches 1300°C. This inhomogeneous growth phenomenon is related with the non-uniform distribution of Y₂O₃ in ZrO₂. Nano-particles grow through the mechanisms of gradual merge of nano-particles and sudden coalescence of nano-particles.

3:05 PM Invited

One-Step Fabrication of Functional Ceramic Patterns by Ink-Jet Deposition Method Using Precursor Solutions at Moderate Temperatures (<300°C): *Masahiro Yoshimura*¹; Ruwan Gallage¹; Atsushi Matsuo¹; Takeshi Fujiwara¹; Hajime Wagata¹; Tomoaki Watanabe¹; Nobuhiro Matsushita¹; ¹Tokyo Institute of Technology

Most ceramic films have been fabricated by high temperature firing of sol/gel and/or vacuum-gas processes like PVD, CVD, electron beam evaporation, etc. using sophisticated instruments and tremendous energies. Solution precursor processes such as sol-gel, pyrosol, spray, etc. are advantageous processing methods for ceramic film/pattern fabrication due to low cost and low temperatures. We have successfully employed ink-jet technique named as ink-jet reaction method to prepare ceramic films and patterns where two precursor solutions were reacted directly (on-site) on a substrate.^{1,2} CdS, PbS,² CaWO₄, BaWO₄,³ etc., have been fabricated on papers at RT. In the present study, we have used ink-jet and spray technology to fabricate ceramic films such as ceria, zirconia, titania, etc. at moderate temperatures around 300°C or lower. Transparent films of TiO₂⁴ and CeO₂^{5,6} with 200-700 nm thickness have

been fabricated on glass substrate at 275-350°C without any post-firing. PMP-III. In ink-jet method, a modified ink-jet printer was used. Precursor solution was prepared by dissolving the suitable salt depending on the material to be deposited appropriate solvents (water/ethanol). Cleaned glass substrate was kept on the hotplate and heated it up to a predetermined temperature. Empty ink cartridge/spray gun was filled with precursor solution and fabrication was continued. Droplets of the precursor solution produced through the nozzles of ink-jet head or spray gun were traveled at atmospheric pressure towards heated substrate. In ink-jet, when droplets hit on the heated substrate, precursor started to decompose and nucleation and growth of the oxide grain occurred to form a ceramic film. In the case of spray, flame heating was also used to make crystallized films. Obtained phases were characterized by X-ray diffraction (XRD) and surface morphology by Laser Microscopy and Scanning Electron Microscopy. The XRD patterns confirmed that formed phases were well crystallized. Adhesion property of fabricated film to the substrate was also good. Single-step patterning of BaTiO₂ and Carbon⁷ will also be presented. [References] ¹M. Yoshimura, J. Mater. Sci., 41 [5] 1299-1306 (2006). ²M. Yoshimura and R. Gallage, J. Solid State Electrochem., in press. ³R. Gallage, M. Yoshimura, et al., Mater. Sci. Eng. B, 137, 299-303 (2007). ⁴M. Yoshimura, R. Gallage, et al., J. Electroceram., 16, 533-536 (2006). ⁵R. Gallage, M. Yoshimura, et al., J. Am. Ceram. Soc. (accepted). ⁶R. Gallage, M. Yoshimura, et al., J. Electroceram., in press. ⁷T. Watanabe, M. Yoshimura, Thin Solid Film, 515, 2696-2699 (2006), Carbon, 44, 799-802 (2006)

3:25 PM

Fabrication of Fine-Grained Yttria-Stabilized Tetragonal Zirconia Polycrystals from Polycrystalline Beads: *Chiraporn Auechalanukul¹*; W. Roger Cannon²; ¹King Mongkut's University of Technology, Thonburi; ²Rutgers University

This research sought to study the fabrication of fine-grained yttria-stabilized tetragonal zirconia polycrystals (3Y-TZP) through particle deformation as a result of creep during hot pressing. The effect of particle size on the densification during hot pressing in the absence of a contribution from surface energy was investigated. Spherical polycrystalline particles were prepared by pre-sintering of spray-dried granules of 3Y-TZP at 1400°C for 2 hours. Three particle size fractions, nominally 25, 45 and 75 µm, were hot-pressed at 1350°C for 1 hour using pressures of 6, 10, 20 and 40 MPa. A nearly dense (>98%) 3Y-TZP monolith was produced at 40 MPa, while the fine grain size (0.3 µm) of the starting polycrystalline particles was retained. No particle size dependence on the hot-pressing densification rate was found for a particle size range of 10 to 100 µm, when the pressure was at least 10 MPa.

3:45 PM

High Temperature Flexural Strength of the Al₂O₃-YAG Eutectic Composite Produced by Using Transformation from Metastable Eutectic to Equilibrium Eutectic: *Tomoya Nagira¹*; Hideyuki Yasuda¹; Masato Yoshiya¹; Katou Takeharu²; ¹Osaka University; ²JFCC

The Al₂O₃-YAG equilibrium eutectic at 2099K and the Al₂O₃-YAP metastable eutectic at 1975K exist in the Al₂O₃-Y₂O₃ system. The heating the metastable eutectic up to temperatures above the metastable eutectic temperature produced undercooled melt. The solidification in the equilibrium path accompanied the melting of the metastable eutectic. The microstructure of Al₂O₃-YAG eutectic composite and the transformation from metastable eutectic to equilibrium eutectic depended on the Al₂O₃-YAP particle size. In this study, the temperature dependences of flexural strength of Al₂O₃-YAG eutectic composite produced by different Al₂O₃-YAP particles sizes were evaluated. Flexural strength of the casting produced by Al₂O₃-YAP particles with diameters less than 45 µm maintained up to 1073K and the temperature at which the flexural strength started to decrease shifted to higher temperature decreasing the Al₂O₃-YAP particles size. The influence of the microstructure on the high temperature flexural strength will be also discussed.

4:05 PM Break

4:30 PM

Enhanced Densification and Grain-Size Refinement in Cation-Doped Tetragonal Zirconia: *Keijiro Hiraga¹*; Byung-Nam Kim¹; Koji Morita¹; Hidehiro Yoshida¹; ¹National Institute for Materials Science

In tetragonal zirconia, possibility is investigated of densification with finer grain sizes under the combination of doping and sintering in air. The materials used are CIP'ed compacts of 3-mol%-yttria-stabilized tetragonal zirconia (3Y-TZP) doped with a small amount of metallic cations. For a given sintering temperature and initial density of the compacts, the effects of doped cations are similar in the enhancement of densification, but different in grain growth during densification: some cations enhanced grain growth, whereas others suppressed grain growth. As a result, the doping of the latter cations brings about a grain size finer than that of the undoped 3Y-TZP for a given relative density. It is also shown that the grain-size refinement by the doping is enhanced by two-step sintering.

4:50 PM

Perovskite-Type Oxynitride Dielectrics: *Jutharat Achcharattaworn¹*; ¹Newcastle University

Rare earth oxynitrides LaTiO₂N and NdTiO₂N have been synthesised by ammonolysis of complex oxide precursors, prepared by solid-state reaction between appropriate binary oxide powders. By XRD, it was found that almost pure LaTiO₂N had been obtained after 24 hours reaction time with less than 5% TiN as the only impurity, while NdTiO₂N needed more 24 hours to obtain the pure phase. To densify the samples, they were hot-pressed in graphite dies at 1250°C, 25 bar for 1 hour and whereas LaTiO₂N remained unchanged, NdTiO₂N sample was decomposed and oxidised. Dielectric properties have been investigated. Due to the conductivity of TiN, the overall LaTiO₂N sample showed metallic rather than dielectric behaviour. To further improve the purity, XRD showed that pure LaTiO₂N has been obtained after nitriding La₂Ti₂O₇ at 950°C for 16 hours with 10 wt% carbon powder added to the mix.

5:10 PM

Ultra Rapid Sintering of Ceramics: *Peter Hing¹*; ¹University of Brunei Darussalam

The pressureless sintering of ceramics to near theoretical density requires prolonged periods at elevated temperatures. For example, the sintering of polycrystalline alumina to translucency requires normally sintering time ranging from 8 to 10 hours between 1800C and 1900C in vacuum or hydrogen atmosphere. In this study, we have been able to sinter alumina to translucency within a few minutes in a low thermal mass furnace in a reducing atmosphere without distortion, discoloration and damage. The development has important bearing on energy conservation in a normally highly energy intensive ceramic and metal industry. The properties and microstructures of the sintered translucent alumina will be presented and discussed. The potential for applications of the technology for sustainable development of compact and high efficacy high intensity discharge light sources and for compact low cost planar and tubular solid oxide fuel cells will be discussed.

Wednesday Plenary Lecture

Wednesday AM
December 10, 2008
Room: Auditorium B2, Bangkok Convention Centre
Location: Sofitel Centara Grand Bangkok

Session Chair: Brajendra Mishra, Colorado School of Mines

9:30 AM Plenary

Materials Science for the New Generation: *David Olson*¹; ¹Colorado School of Mines

Abstract not available.

10:15 AM Break

Energy Materials Processing III

Wednesday AM
December 10, 2008
Room: Plaza 1
Location: Sofitel Centara Grand Bangkok

Session Chair: Sreeramamurthy Ankem, University of Maryland

10:40 AM

Synthesis and Electrical Property of La_{1.6}Sr_{0.4}NiO₄ to be Used for IT-SOFCs: *Thitirat Inprasit*¹; Pimpa Limthongkul²; Sujitra Wongkasemjit¹; ¹Chulalongkorn University; ²National Metal and Materials Technology Center

Recent worldwide interests in solid oxide fuel cells (SOFCs) research have been focusing on the intermediate temperature range cells (ITSOFCs). In this study, material with Ruddlesden-Popper structure having the composition of La_{1.6}Sr_{0.4}NiO₄ was focused due to its thermal expansion coefficient (TEC) matching with the commonly used gadolinia doped ceria (GDC) electrolyte. We found that La_{1.6}Sr_{0.4}NiO₄ was successfully synthesized via sol-gel process at room temperature using water as solvent in the presence of different templates, viz. ethanalamine (TEA) and triethylenetetraamine (TETA), and after calcination at 1050°C. Relationship between the synthesis routes, phase and microstructures was investigated using various techniques. Electrical properties measured using 4 point probe and impedance spectrometry were compared between the products prepared via the different routes.

11:00 AM

Recent Developments in Processing/Structure/Properties Relationships of Titanium Alloys: *Sreeramamurthy Ankem*¹; Paul Oberson²; ¹University of Maryland; ²U.S. Nuclear Regulatory Commission

While titanium has long been used as a structural material, the 21st century will see increasing demand for advanced titanium alloys to meet technological challenges for applications in the aerospace, biomedical, and energy fields, among many others. Variation of alloying elements and processing conditions of titanium alloys can be used to tailor the microstructures and hence properties such as strength, fracture toughness, creep resistance, corrosion resistance, and biocompatibility. This paper discusses recent findings regarding the effect of processing on microstructure and low-temperature (<0.25*T_m) creep behavior of single-phase and two-phase titanium alloys. In particular, the role of alloy chemistry, interstitial impurities, and phase morphology will be considered. These findings are useful to predict the creep behavior of presently used titanium alloys and to develop new processing techniques for advanced titanium alloys with enhanced creep resistance. This work is supported by the National Science Foundation under Grant Number DMR-0513751.

11:20 AM

Penetration of Water into Yttrium- and Scandium-Doped Barium Zirconate and Its Relation to Proton Conductivity: *Yoshitaro Nose*¹; Yusuke Okumura¹; Susumu Imasyuku¹; Koichi Suehiro¹; Tetsuya Uda¹; Yasuhiro Awakura¹; ¹Kyoto University

Trivalent cation doped barium zirconate shows protonic conduction under wet atmosphere, where proton is introduced into barium zirconate by dissolution and penetration of water. Since electric conductivity depends on concentration of proton, behavior of water in barium zirconate is very important to understand its proton conductivity. In this study, penetration rate of water and its content have been measured on yttrium- or scandium-doped barium zirconate. Furthermore, electric conductivity has been investigated to clarify its dependence to the content of water. The penetration rate of water was evaluated from the weight change of pellet using thermogravimetry, when changing atmosphere from dry to wet condition. The apparent diffusion coefficient of water calculated based on the penetration rates decreases with increasing grain size of barium zirconate, while it does not depend on the kind of dopant. The penetration mechanism of water and the relation between electric conductivity and proton concentration will be discussed.

11:40 AM

Preparation and Thermoelectric Properties of Nonstoichiometric NdGdS₃ with Gd Excess: *Michihiro Ohta*¹; Shinji Hirai²; ¹National Institute of Advanced Industrial Science and Technology; ²Muroran Institute of Technology

The ternary rare-earth sulfides NdGd_{1-x}S₃ have been prepared in order to determine their potential as high temperature thermoelectric materials. The binary sulfides Ln₂S₃ (Ln = Nd and Gd) were first prepared by the reaction of Ln₂O₃ with CS₂ gas. A mixture of powders of Nd₂S₃, Gd₂S₃ and GdH₃ was then consolidated by pressure-assisted reaction sintering to produce the desired composition of NdGd_{1-x}S₃. The electrical resistivity, Seebeck coefficient, and thermal conductivity of sintered samples were measured from 300 to 1000 K. All the Seebeck coefficients are n-type. The electrical resistivity and the magnitude of Seebeck coefficients decrease with increasing Gd content. Moreover, the NdGd_{1-x}S₃ compounds have low thermal conductivity.

Materials Processing VIII

Wednesday AM
December 10, 2008
Room: Plaza 3
Location: Sofitel Centara Grand Bangkok

Session Chair: Paul Stratton, BOC Gases

10:40 AM

Picklability of Tertiary Scales Formed on the Edge of Hot-Rolled Carbon Steel Strip: Effect of the Cooling Rate at the Edge of Strip Controlled by the Laminar Flow of Water: Somrerak Chandra-ambhorn¹; *Supattra Intarasakda*¹; ¹King Mongkut's University of Technology North Bangkok

This work produced the tertiary scales in the hot rolling line subjected to different cooling rates at the edge of carbon steel strips by controlling the amount of water spray, a laminar flow, on that area. The increase in cooling rate at the edge of the strip reduced the thickness of scale, which were 9.5 ± 0.9 and 10.15 ± 0.8 μm for scales on the edges of strip where the edges were faster and lower cooled respectively. The reduced scale thickness promoted the picklability of the tertiary scale from its substrate, as investigated by an immersion test in a 10% v/v HCl aqueous solution at 80°C and a potentiodynamic method. Kinetics of scale removal during pickling was discussed in the paper.

11:00 AM

Production of Vanadium Metal and V-Ti Alloys from Oxide Preforms: *Akihiko Miyauchi*¹; Toru Okabe¹; ¹Institute of Industrial Science, University of Tokyo, Okabe Laboratory (Fw-301)

In order to develop a new process for the effective production of vanadium metal or (V-Ti alloys) from vanadium pentoxide (V₂O₅), a fundamental study

on a preform reduction process (PRP) based on metallothermic reduction was investigated. The feed preforms were prepared by calcining a mixture of V₂O₅ and CaO in order to synthesize complex oxides (Ca_xV_yO_z) that have good mechanical strength at elevated temperatures and are suitable for handling during processing. The reduction experiments were conducted at a constant temperature between 1073 K and 1373 K by using either Ca or Mg vapor for 6 h. The feasibility of producing V metal or V-Ti alloys by PRP will be discussed based on the fundamental experiments.

11:20 AM

Porous Superelastic NiTi Produced by Sintering with NaCl Space-Holders: *Ampika Bansiddhi*¹; David Dunand²; ¹Department of Materials Engineering, Kasetsart University; ²Department of Materials Science and Engineering, Northwestern University

Highly-porous NiTi with ~50-70% porosity was fabricated by pressureless densification of Ni-rich NiTi powder with temporary NaCl space-holders. The porosity and pore characteristics (pore size, shape and connectivity) were controllable through the initial volume fraction and geometry of the space holders. The NiTi foams exhibited superelasticity at room temperature and body temperature. High compressive yield strength with low stiffness and large recovery strain were observed. Simple, cost-effective processing and post-processing procedures were demonstrated to achieve a desired porous structure, and hence a desired mechanical and shape recovery behavior. By combining the unique properties of NiTi with an adjustable foam architecture, NiTi foams can be custom-designed for multi-functional applications such as impedance-matching connectors between structural parts, energy-absorbing structures, actuators, and bone implants.

11:40 AM

Processing of Secondary Lead Raw Materials at Chigirishima Refinery: *Takafumi Kawamura*¹; Kazuma Morino¹; ¹Toho Zinc Company, Ltd.

Toho Zinc Chigirishima Refinery started up lead metal production in 1951. The production capacity of electrolytic lead is 90,000t/y by the sintering - blast furnace – electrolysis process. Recently, the conversion of raw materials from lead concentrates to secondary materials is advanced. By solving various problems that occur along with the raw materials conversion, productivity and efficiency of facilities and attached equipments are significantly improved. The processing ratio of secondary lead raw materials has been increased up to approximately 50% currently. We report about various problems which occur in the processing of secondary lead raw materials and the measures taken with their result.

12:00 PM

Prestressed and Improvement Impact Resistance on Ceramic Armour: *Kannigar Dateraksa*¹; Kuljira Sujirote¹; ¹National Metal and Materials Technology Center

Due to its high hardness and light weight, alumina ceramic has been extensively used as the preferred armour material. However, resultant debris from both fractured ammunition and from the ceramic itself may be unsafe. In this study, a three-axial pre-stressed armour insert with improved debris confinement has been developed using shrink fit technique. The armour insert was made by laying alumina hexagonal tiles on a stainless steel plate and then confining in aluminium sheet by heating up to approximately 800°C and cooling down. Calculation of pre-stress in ceramic tiles wrapped by metal is presented. The armour insert was tested in accordance with the NIJ standard, level 3 by placing in front of an armour jacket level 2A. The damage zones on witness clay, including ceramic fragmentation, were observed.

Nanomaterials Processing V

Wednesday AM
December 10, 2008

Room: Plaza 7
Location: Sofitel Centara Grand Bangkok

Session Chair: Ramana Reddy, The University of Alabama

10:40 AM Invited

Effect of Reaction Conditions on Synthesis of SiC Nanowires by Simple Thermal Evaporation: *Wasana Khongwong*¹; Masamitsu Imai¹; Katsumi Yoshida¹; Toyohiko Yano¹; ¹Research Laboratory for Nuclear Reactors, Tokyo Institute of Technology

The nanowires with SiC core was created by simple thermal evaporation method through reaction between evaporation of silicon nanopowders and decomposition of CH₄ gas. The effect of reaction time on synthesis of nanowires was investigated. The diameter of SiC nanowires synthesized under flowing CH₄ among Si nanopowder evaporation at 1350°C for 1 and 3 h was less than 100 nm and the length was several tens microns. X-ray diffractometry (XRD), field-emission scanning electron microscopy (FE-SEM), energy dispersive X-ray (EDX) spectroscopy, transmission electron microscopy (TEM), and high-resolution TEM (HRTEM) were used to characterize the nanowires. The results show that more complete reaction to form SiC nanowires was obtained from longer soaking time experiment.

11:00 AM

Fabrication of Non-Firing Ceramics Assisted by Particle Surface Activation Using a Planetary Ball-Milling: *Apiluck Eiad-ua*¹; Tomohiro Yamakawa¹; Hideo Watanabe¹; Masayoshi Fujii¹; Minoru Takahashi¹; ¹Nagoya Institute of Technology

We have proposed a novel ceramic fabrication method without firing and/or debinding processes, so that costs and energy for post-forming processes can be greatly reduced. In the proposed method, surfaces of a raw material powder are mechano-chemically activated using a planetary ball-milling, and mixture of activated powder with an alkaline solution can be solidified by chemical bonds among particles, which is induced by cations eluted from the particle surface due to the milling-assisted activation. In this paper, the non-firing ceramic was fabricated by the proposed method with use of a wasted resource from paper making industry. Effect of the operational conditions in the planetary ball-milling such as rotational speed and treatment time was investigated with respect to elution amount of cations as well as mechanical properties of the solidified body.

11:20 AM

Integrated Material Design for Bulk Nanocrystalline Ceramic: *Hiroshi Kimura*¹; ¹National Defense Academy

The materials design methodology is proposed for bulk nanocrystalline ceramics with superior mechanical property in widespread applications on the basis of new paradigm of materials science and technology that consists of the trinity of process, structure and function. Emphasis is placed on how to make a pathway between nanotechnology, nanochemistry and model mechanics in solid state powder method of bulk nanocrystalline ceramics. The instrumented reaction ball milling method is used to set up nano-mechano-chemistry for the solid state amorphization and the nanocrystalline synthesis of oxide, covalent and multi-component ceramics obtain by mechanical alloying and mechanical milling. Then, the pulse electric current discharge consolidation can provide a variety of in process nanocrystalline control densification in the absence of sintering additives. This article furthermore describes nanostructure-strength relationship, processing for nano-functionallizaion featuring superplastic zirconia, bioactive ceramics and high temperature covalent ceramics having high strength and high toughness.

11:40 AM

Silica Nanoparticle Agglomerates with Controlled Packing Structure and Their Dispersion Characteristics into Thermoplastics by Simple Melt-Compounding Method: *Mitsuru Tanahashi*¹; Yusuke Watanabe¹; Toshiharu Fujisawa¹; ¹Nagoya University

A novel and simple method for the fabrication of silica/thermoplastic nanocomposites was investigated, whereby silica nanoparticles were dispersed uniformly through breakdown of loosely packed agglomerates of silica nanoparticles with low fracture strength in a kneaded plastic melt during direct melt-compounding. Firstly, the packing structure and the fracture strength of the silica agglomerate were controlled by destabilizing an aqueous colloidal silica solution via pH control and salt addition. In the next place, silica/thermoplastic composites were fabricated by melt-compounding some thermoplastics with the prepared silica agglomerates of various packing structure. Using this method, submicron particles of silica without any complicated surface treatments of silica could be dispersed uniformly into various thermoplastic matrices. In particular, homogeneous distribution of silica particles with a diameter of around 50 nm was achieved successfully in polyethylene matrix. The relationship between the packing structure of the prepared silica agglomerates and their dispersion characteristics into various plastics was discussed.

11:20 AM

Synthesis of Tungsten and Tungsten Carbide Nanopowders from Ammonium Paratungstate in a Thermal Plasma Reactor: Taegong Ryu¹; Kyu Sup Hwang¹; *Hong Sohn*¹; Zhigang Fang¹; ¹University of Utah

Nanosized tungsten and tungsten carbide powders were synthesized by a thermal plasma process using ammonium paratungstate (APT) as the precursor. The injected precursor was vaporized in the plasma flame and the reactions of the vaporized precursor produced nanosized tungsten and tungsten carbide powder. The effects of the ratio of reactant gases, plasma torch power, and the flow rate of plasma gas on the product properties were investigated and the particle size was determined. Tungsten and tungsten carbide (WC_{1-x}) particles finer than 40 nm were obtained by the thermal plasma process. The produced tungsten carbide powder, which sometimes contained small amounts of W₂C and W phases, was further subjected to a heat treatment under hydrogen to produce fully carburized WC as well as to remove excess carbon. The particle size of WC thus obtained was less than 100 nm.

11:40 AM

The Effect of Uniform Alumina Coating on Copper Particles on Oxidation Resistance: *Yasumasa Hattori*¹; Keiji Kamada¹; Mika Okada¹; ¹Sumitomo Metal Mining

A new method is described for coating fine copper particles with a continuous aluminum oxide layer, which is produced by the hydrolysis of Al³⁺ ions in aqueous solution and the subsequent thermal decomposition. The hydrolysis reaction can be controlled by the addition of oxidizing agent, resulting in uniform coating without the precipitation of independent aluminum hydroxide particles. The aluminum oxide layer with thickness of around 20nm enhances the resistance of the copper particles to aerial oxidation, raising the temperature at which a detectable oxidation occurs from 100 to 230°.

Powder Preparation/Processing IV

Wednesday AM

Room: Plaza 8

December 10, 2008

Location: Sofitel Centara Grand Bangkok

Session Chair: To Be Announced

10:40 AM Invited

Graphite Particles Reinforced Fe-Al-X Alloy Composites for Slide Bearing Applications: *Se-Hyun Ko*¹; Wonsik Lee¹; Il Ho Kim¹; Jin Man Jang¹; Seoung Gun Shin²; ¹Korea Institute of Industrial Technology; ²Lubo Industries, Inc.

The Fe-Al-X(Ni, Cu, Sn and P) composites reinforced by graphite particles were fabricated employing the powder metallurgy process for slide bearing applications. The compositions of graphite were changed from 2 to 6 wt%. Elemental powders were mixed to specific compositions with a powder lubricant, and then the mixed powders were compacted at 300 and 500 MPa. The green compacts were heated to 450° to remove the lubricant and sintered at 1050 to 1150° for 1 h. The sintering was conducted in vacuum. The sintering of binary Fe-Al system showed low density and growth in dimension. The additions of Cu, Sn and P improved the sinterability of green compacts due to occurrence of partial liquid phases. The effect of the alloy compositions and the sintering conditions on microstructures and mechanical properties will be presented in this presentation.

11:00 AM

Surface Processing by Flat Sandblasting Nozzle: *Nobuo Ogawa*¹; ¹Tokyo University of Science

Sandblasting techniques have many applications for processing the works by means of various solid particles in the gas-solid jets. Recently, industrial worlds demand micro surface processing in wide range to process. However it is difficult to make two-dimensional flows of the gas-solid flows because of very large density of the solid particles compared with the gas flows. Now we make new type two-dimensional nozzles applying the axisymmetrical gas-solid flows through annular pipes. And we try to make high quality surface processing by the two-dimensional nozzle (flat nozzle). In general, only coarse finish is provided in sandblasting techniques. However we can get the high quality surface due to multi fluid flows.

12:00 PM

Ultrafine Mg-3%Al Alloy: Its Synthesis and Investigation of Its Tensile Properties at Elevated Temperature: *Ashis Mallick*¹; Srikanth Vedantam¹; Lu Li¹; ¹National University of Singapore

In this paper, we present temperature dependent studies of the tensile properties of ultrafine (UF) Mg-3%Al alloy. The bulk UF sample were synthesized from elemental powder via mechanical alloying (MA) and followed by isostatic pressing, sintering and hot extrusion. Tensile tests were performed at temperatures ranging from 25°C to 250°C. The UF sample exhibited two-fold increase in strength and ductility in comparison with their coarse-grain counter part at room temperature. Perfect elastic-plastic flow behavior with no apparent necking was observed for UF sample suggesting that deformation was homogeneous. The strain rate sensitivity (SRS) was calculated three times higher compared those of coarse-grain. With increase in temperature, the alloy shows additional hardening leading to an increase in the percentage of elongation. However, further increase of test temperature the true stress-strain curves displayed gradual decrease of elongation and hardening region. An alteration of fracture surface was observed in different testing environments.

Processing of Ceramics II

Wednesday AM

Room: Plaza 2

December 10, 2008

Location: Sofitel Centara Grand Bangkok

Session Chair: John Smugeresky, Sandia National Laboratories

10:40 AM Invited

Influence of Organic and Inorganic Additive on Microstructure and Porosity of Alumina Body: *Parawee Pumwongpitak*¹; Siriporn Larpiattaworn¹; ¹Thailand Institute of Scientific and Technological Research

Microstructure and porosity of sintered alumina body were studied concerning to the type of additive. In this work, a polyvinyl alcohol (PVA)

and aluminium hydroxide (Al(OH)₃) were used as organic and inorganic additives in alumina powder, respectively. The amount of PVA in alumina powder was varied from 5% to 20%, while 30% Al(OH)₃ was added into the mixture of 65% Al₂O₃ and 5% PVA. The green alumina body was formed by using two steps of pressing, first is uniaxial press and follow with cold isostatic press. The samples were then sintered at 1500°C for 1 h soaking time. The properties of sintered samples such as shrinkage, density, porosity, pore size, water absorption, and microstructure were investigated. It was found that sintered alumina contained Al(OH)₃ presented larger pore size and higher porosity than those without Al(OH)₃.

11:00 AM

Preparation of Transparent Alumina by Spark Plasma Sintering: *Byung-Nam Kim*¹; Keijiro Hiraga¹; Koji Morita¹; Hidehiro Yoshida¹; ¹National Institute for Materials Science

We fabricated fully-dense transparent alumina by spark plasma sintering at 1100-1600°C and at a pressure of 80 MPa. Fast densification occurred for pure and MgO-doped alumina powders without any pre-treatment. For the pure alumina sintered at 1300°C for 20 min, the average grain size is 1.4 μm and the total forward transmission is 75% for the red wavelength (640nm). In a range of 1150-1300°C, the total forward transmission increased, while the in-line transmission decreased with increasing sintering temperature. The transparency is sensitive to the porosity, but less sensitive to the grain size; the increasing sintering time yields higher transparency. We also examined the hardness, strength and other mechanical properties of the alumina.

11:20 AM

Spark-Plasma-Sintering of High Strength Transparent Spinel Polycrystals: *Koji Morita*¹; Byung-Nam Kim¹; Hidehiro Yoshida¹; Keijiro Hiraga¹; ¹National Institute for Materials Science

Fine-grained transparent spinel polycrystals can be fabricated only for a 20min soak at 1300°C by employing low heating rate spark-plasma-sintering (SPS) processing. For the low heating rates of 10°C/min, the spinel exhibits an excellent in-line transmission of about 47% for visible-wavelength of 550nm. In addition to the transparency, the low heating rate SPS processing has made it possible to fabricate a fine grained spinel with $d \approx 0.45 \mu\text{m}$ due to the low temperature sintering and short holding time. The fine grain size can improve the mechanical property of the spinel. The fracture strength of the fine grained spinel exhibits a large value of $\approx 500\text{MPa}$, which is two times greater than those (250MPa) of conventional coarse grained spinel polycrystals. Therefore, for engineering applications, the low heating rate SPS processing has a significant advantage over the high temperature HIP and HP techniques.

11:40 AM

Influence of Soda-Lime-Silica Cullet on the Properties of Porcelain Mixture: *Worapong Thiemsorn*¹; Puwanart Kaewthip²; ¹Chiangmai University; ²Sibelco Minerals (Thailand) Company, Ltd.

Influence of soda-lime-silica cullet on the properties of porcelain mixture was investigated. The batches were prepared with varying the powder cullet for 10-40 wt% and then were fired in the range of 1,050-1,250°C for 30 min. The results show that the fired samples containing higher content of cullet could vitrify at lower than 1,250°C. The whiteness tend to decrease but the translucency was reversed with an increase of cullet content at individual firing temperature. The microstructures indicated mullite, quartz and amorphous phases with pores dispersed in the amorphous phase. The mixture containing the cullet 40 wt% was used to produce prototype products. The slip properties showed the density, viscosity and casting rate as 1.83 g/cm³, 137 mPa.s and 0.72 mm./min, respectively. The green products were fired at 1,100°C. The prototypes show high translucency, 73.8% whiteness, 0.08 % water absorption and 1,218 kg/cm² of bending strength.

Processing of Electronic Materials and Devices III

Wednesday AM
December 10, 2008

Room: Plaza 5
Location: Sofitel Centara Grand Bangkok

Session Chair: To Be Announced

10:40 AM

Evolution of Interfacial Structure of the Sn-3.7Ag-1.0In-0.9Zn Lead-Free Solder: *Yongchang Liu*¹; Ronglei Xu¹; Zhiming Gao¹; ¹Tianjin University

The formation and evolution of intermetallic compounds (IMCs) layer between the Sn-3.7Ag-1.0In-0.9Zn lead-free solder and substrate were (Cu and Ni/Cu) investigated for different soldering periods. The structure of the IMCs layer in the soldered interface varies apparently with increasing the soldering time. The interface soldered on the Cu substrate is composed of a thick Cu₅Zn₈ layer and a thin Cu₆Sn₅ layer, which are separated by an intermediate solder layer. While in the soldered interface on the Ni/Cu substrate, a thin continuous Ni₃Sn₄ dissolved with small amount of Cu is firstly observed. As the reflow time going on, a thick Sn-Ni-Cu intermediate compound layer is formed at the interface after the plated Ni layer is consumed totally. Once the plated Ni layer disappears, the corresponding growth rate increases apparently. The evolution of the soldered interfacial structure was discussed in view of the governing factor for the atomic diffusion.

11:00 AM

Mechanism of AlN Formation by Sapphire Nitridation: *Hiroyuki Fukuyama*¹; T. Aikawa²; H. Kobatake²; K. Takada³; K. Hiraga¹; ¹Tohoku University; ²Institute of Multidisciplinary Research for Advanced Materials, Tohoku University; ³Tokuyama Corporation

Aluminum nitride (AlN) is an ideal candidate as a substrate for AlGaN-based nitride semiconductor devices for the deep-UV LED and LD. In the present study, high-quality single crystalline AlN films have been fabricated by nitriding sapphire by N₂-CO gas mixtures with a precise control of driving force (chemical affinity) of the nitridation reaction based on the phase stability diagram of the AlN-Al₂O₃-C-N₂-CO system at elevated temperatures. Figure 1 (Left) shows the phase stability diagram of the AlN-Al₂O₃-C-N₂-CO system under the condition of carbon activity, $a_C = 1$, and total activity of gas phase, $p_{CO} + p_{N_2} = 1$.

11:20 AM

Al-Doped ZnO Films Prepared by Spray Pyrolysis: Chanipat Euvananont¹; Supattra Pakdeesathaporn²; Pawilas Pratoomwan²; *Yot Boonthongkong*¹; Chanchana Thanachayanont¹; ¹National Metal and Materials Technology Center; ²Kasetsart University

ZnO films have been prepared by the spray pyrolysis method using 0.05M solution of zinc acetate dihydrate in methanol as the precursor. The films were grown at 430°C for 2.5 hrs, with Al doping achieved by the addition of AlCl₃. It was also shown that the ZnO film morphology evolves from a relatively dense structure comprising hexagonal platelets in the undoped film, towards a more porous structure comprising faceted particles with increasing AlCl₃ doping to 2.5%. The lowest electrical resistivity of 0.35 Ohm-cm was obtained in the 0.3% Al-doped film, but no simple relationship between Al doping and the electrical resistivity was observed. We postulate that doping ZnO films with AlCl₃ provides an influence that is equivalent to reducing the rate of precursor supply towards the growing film, which explains the observed trends of decreasing film thickness and increasing average crystallite size with increasing doping concentration.

11:40 AM

Producing of Bi₂Te₃-Sb₂Te₃ Pseudo Binary Alloys for Thermoelectric Applications and Study of Their Properties: *Sayed Rasoul Fallahian*¹; Saeed Safi²; ¹Islamic Azad University of Majlesi, New Town; ²Material and Energy Research Center (MERC)

The various Binary compounds of Bi₂Te₃-Sb₂Te₃ form a pseudo binary system. These compounds are semiconductor and are suitable for low

temperature thermoelectrics. In this investigation, various compounds of Bi₂Te₃-Sb₂Te₃ are synthesized (in polycrystalline form) with using of high purity Sb, Te and Bi in quartz ampoules. Then phase diagram, lattice parameters, density, band gap energy, thermal and electrical conductivity, thermoelectric power and figure of merit of these compounds were investigated with using of XRD, IR spectrophotometer and others instruments. Results indicated that this system has an ideal solid solution phase diagram. Lattice parameters and density increased linearly with increasing of Bi₂Te₃ content, but band gap energy decreased. These results confirm that this system is a continuous solid solution. With combining of Bi₂Te₃ and Sb₂Te₃, both thermal and electrical conductivity primarily decreased and then increased. But for thermoelectric power and figure of merit this was inverse. Results indicated that Sb₂Te₃-30%Bi₂Te₃ compound has maximum thermoelectric power and figure of merit. Thus this compound is the most effective compound for thermoelectrics applications.

Thin Film Coating Processing II

Wednesday AM
December 10, 2008

Room: Plaza 4
Location: Sofitel Centara Grand Bangkok

Session Chair: Yasuo Uchiyama, Department of Material Science and Engineering, Nagasaki University

10:40 AM

Deposition and Characterization of Cobalt Doped and Undoped BaTiO₃ Thin Films: Sara Borhani Haghighi¹; Thirumany Sritharan¹; ¹Nanyang Technological University

BaTiO₃ is one of the widely studied ferroelectric ceramics due to its extensive application in electronic industries. Its high dielectric constant coupled with its simple structure that allows hosting ions of different sizes is of interest. Thin films of doped and undoped BaTiO₃ were fabricated at room temperature using rf magnetron sputtering system on Pt/Ti/SiO₂/Si and SiO₂/Si substrates. Post annealing cycles were explored to produce crystalline crack free films. In most samples the films were made up of a combination of phases; BaTiO₃ with P4mm and Pm-3m crystal structure and TiO₂ (Brookite and orthorhombic structures). The formation of TiO₂ could be due to Ti precipitation or oxidation of Ti buffer layer. Rietveld refinement of the XRD data was conducted via TOPAS software. The lattice parameters were obtained from the rietveld refinement with good approximation (R -Bragg < 5). Surface topography and roughness were investigated with the aid of AFM and SEM.

11:00 AM

Effect of Sealing on the Surface Morphology and Electrochemical Property of Cerium-Based Conversion Coating on AZ31 Magnesium Alloy: Salah Salman¹; Ryoichi Ichino¹; Masazumi Okido¹; ¹Department of Material Science and Engineering, Nagoya University

The use of magnesium alloys in engineering applications has increased steadily in recent years. However the high chemical reactivity and the inadequate corrosion resistance limited their use. Proper surface treatments are required in order to increase the corrosion resistance. Commonly applied surface treatment is the chemical conversion in which chromate bath was traditionally applied; however, it is toxic to human and difficult to be recyclable. Non-chromate solutions have been recently developed; one of the most promising systems is based on cerium solution. In this paper, chemical conversion coating was performed onto AZ31 (3 % Al, 1 % Zn) magnesium alloy by immersion in 0.05 M Ce(NO₃)₃. Sealing of the film in 1 M NaOH and 10 g dm⁻³ Na₂SiO₃ solution further enhanced the anti-corrosion property and the surface properties of the film. The structure, morphology, and composition of the films were determined by optical microscope, SEM and EDS.

11:20 AM

Electrochemical Impedance of Intermetallic Titanium Nitride PVD Coating on AISI 316L in 3.5% and 12% NaCl at 25C and 70C: Kosit Wongpinkaw¹; Siriwan Ouampan¹; Piya Khumsuk¹; Ekkarut Viyanit¹; Wanida Pongsaksawad¹; ¹National Metal and Materials Technology Center

Austenitic stainless steel 316L is susceptible to environmental induced corrosion (EIC) under strong chemical concentration such as in pharmaceutical industry. To improve its corrosion resistance, physical vapor deposition (PVD) is applied to produce hard ceramic layers on the stainless steel surface. In this study, intermetallic titanium nitride thin film was coated on AISI 316L stainless steel by plasma-arc assisted physical vapor deposition. Electrochemical impedance tests were performed at 25C in 3.5% NaCl and 12% NaCl between 1 hour to 24 hours to evaluate the corrosion resistance of the coating under moderately and highly corrosive environments. The results show that the PVD coated sample was more resistant to corrosion than the uncoated sample immersed in 3.5% NaCl. Corrosion behavior of coated PVD sample in 12% NaCl compared to that in 3.5% NaCl at 25C and 70C will also be discussed.

11:40 AM

Growth of Cu Alloy Layers through Reduction-Diffusion Method Using Ionic Liquid Bath at Medium-Low Temperatures: Kuniaki Murase¹; Akira Ito¹; Yui Nishizaki¹; Takashi Ichii¹; Hiroyuki Sugimura¹; ¹Kyoto University

Electrochemical alloying of Cu substrates with Sn or Zn through a reduction-diffusion method was investigated using hydrophobic ionic liquids, trimethyl-*n*-hexylammonium bis[(trifluoromethyl)sulfonyl]amide and 1-ethyl-3-methylimidazolium bis[(trifluoromethyl)sulfonyl]amide, as a solvent for electrolytic baths. The use of the latter ionic liquid made it possible to raise the processing temperature up to 190°C and to form silver-gray Cu-Sn "speculum metal" layers faster than with an aqueous media. Cu thin layers, electrolessly deposited on a heat-resistant polymer, could also be alloyed with Sn. The resulting Cu-Sn layers were composed of Cu₆Sn₅ and Cu₃Sn intermetallic phases, while the Cu-Zn layers, which appears golden in color, involved CuZn and/or Cu₂Zn₉ phases. The layers obtained at 170–190°C showed clear composition gradients where the outer and inner parts of the Cu-Sn layer have compositions corresponding to Cu₆Sn₅ and Cu₃Sn phases, respectively.

12:00 PM

Stress Field Near Interface Edge of Thin Film Bi-Material under Creep: Kittikorn Ngampungpis¹; Takayuki Kitamura¹; ¹Kyoto University

The mechanics of thin film bi-material interface under creep is of interest in many advanced engineering disciplines including electronics, aerospace and nuclear engineering. Stress field and its complex singularity near an interface edge due to the nonlinearity and the time dependence of deformation were analyzed in this study by finite element method (FEM). The thin-film material and substrate considered are defined to creep with the different rate. The result indicated that during the transition, the stress near the interface edge has the stress singularity nearly $1/(n+1)$, where n is the creep exponent of the faster creeping material. The slower creeping material later time-dependently contributed the affects to the stress field near the interface edge. The collapse of stress singularity near the interface under creep can be observed when the material pairs have almost the same creep rate, though the different elastic properties are defined.

Wednesday Keynote Lecture

Wednesday PM
December 10, 2008

Room: Auditorium B2, Bangkok Convention Centre
Location: Sofitel Centara Grand Bangkok

Session Chair: Brajendra Mishra, Colorado School of Mines

2:00 PM Keynote

Innovations in Processing of Lightweight Metal Matrix Composites: *Ramana Reddy*¹; ¹The University of Alabama

Newly emerging chemical in situ process is economical and energy efficient for large scale manufacturing of particulate metal matrix composites compared to the conventional (physical ex situ) processes. This presentation concentrates on some of the key examples from the author's experience and others, application of engineering fundamentals on the in situ processing of nanoparticles of discontinuously reinforced Al and Mg alloys metal matrix composites. Aluminum and Magnesium alloys were reinforced with AlN nanoparticles using chemical in situ process. Thermodynamic analyses were made to identify the conditions for the in situ formation of the AlN in Al and Mg alloys. Effect of experimental processing parameters (i.e. time of gas injection, concentration of ammonia, and temperature of the melt) on the formation of AlN nanoparticles in alloy was determined. The AlN quantities in the composites varying from 5 to 51 wt % were produced. Increase in either injection time or flow rate of the ammonia gas increased the nitride content. AlN particles with an average size of 400 nm were produced. The measured Vickers hardness of the composites formed increased with increasing AlN content. The amount of AlN experimentally formed is in good agreement with the thermodynamically predicted data. A kinetic rate equation of in situ formation of AlN nanoparticulates in lightweight metal matrix composites was developed. A possible reaction mechanism of AlN formation was proposed. The industrial applications of this in situ manufacturing of composites by molten metal technology were discussed.

Composites Processing IV

Wednesday PM
December 10, 2008

Room: Plaza 5
Location: Sofitel Centara Grand Bangkok

Session Chair: Damion Dunne, BHP Billiton

2:45 PM

Nanoporous Metals Fabricated by Dealloying: Morphological Evolution and Properties: *Masataka Hakamada*¹; *Naobumi Saito*¹; ¹National Institute of Advanced Industrial Science and Technology (AIST)

Dealloying is the selective dissolution of less noble metal from binary alloys, and can fabricate the nanoporous metals. The fabricated metals are also regarded as composites made from the metals and nanopores. We fabricated nanoporous Au and Pt by the dealloying. The dispersed open nanopores offer significant surface area, inducing many interesting properties which are not seen in the macroscopic porous metals having pore size above micrometers. Self-organization of the morphology of nanopores in nanoporous Au and Pt, which was induced by thermal and acid treatments, will be reported in this presentation. The nanopore also affects the mechanical properties; the smaller the ligament size was, the higher the hardness was. This size dependence is also quite different from that for conventional porous metals.

3:05 PM

Natural Plant Fibre Based Green Composite for Automobile Application: *Ankur Gupta*¹; ¹Motilal Nehru National Institute of Technology

Environment-friendly, fully biodegradable green composites based on plant natural fibres and resins are increasingly used for various applications as replacements for non-degradable materials. They contain plant fibre as

reinforced or filler material and a matrix of thermosets or thermoplastics. Green composites made entirely from renewable agricultural resources could offer a unique alternative for building, construction, furniture and automotive application. Plant fibres are suitable to reinforce plastics due to relative high strength and stiffness, low density, low CO₂ emission, and biodegradability. A modern automobile requires recyclable or biodegradable parts because of the increasing demand for clean environment. A natural and biodegradable composite reinforced by natural fibres provides an important environmental advantage in automobile industry. In this paper, green-composites based on natural plant fibres discussed. The present work aims at to provide a short review on advance processing techniques and developments in the area of green composites made by natural plant fibres and their applications.

3:25 PM

Synthesis of Ceramic Particle Dispersed Metal Matrix Composites from Elemental Powders: *Kiyotaka Matsuura*¹; *Kenichi Ohsasa*¹; ¹Hokkaido University

TiB₂-FeAl, TiB₂-Fe, TiC-FeAl and TiC-Fe hard alloys have been produced by the combustion synthesis from the elemental powders under pseudo-isostatic pressure. When mixtures of iron, aluminum, titanium and boron powders, for example, were heated to a temperature just above the melting point of aluminum, the temperature of the sample suddenly increased to approximately 1600°C, which indicates that the combustion synthesis reaction occurred in the powder mixture. Metallographic investigation, an X-ray diffraction analysis and an electron probe microanalysis indicated that a TiB₂ particle dispersed FeAl-based composite was produced. The TiB₂ particle size increased with increasing TiB₂ volume fraction without preheating of the powder mixture. The TiB₂ particle size decreased with increasing preheating time, temperature and pressure before the combustion synthesis reaction. The Vickers hardness of the composite varied from 500 to 2000 depending on the microstructure. This method was applied to the production of other hard alloys.

3:45 PM

Synthesis of TiB₂-Al₂O₃/Fe Composites from Natural Ilmenite by Self-Propagating High-Temperature Synthesis: *Sutham Niyomwas*¹; ¹Prince of Songkla University

The TiB₂-Al₂O₃/Fe composites were obtained in situ by self-propagating high temperature synthesis (SHS) of FeTiO₃-B₂O₃-Al System. The reaction was carried out in a SHS reactor under static argon gas at the pressure of 0.5 MPa. The standard Gibbs energy minimization method was used to calculate the equilibrium composition of the reacting species. The effects of increasing aluminum mole ratio to the precursor mixture of FeTiO₃, B₂O₃ and Al were investigated. XRD and SEM analyses indicate complete reaction of precursors to yield TiB₂-Al₂O₃/Fe and TiB₂-Al₂O₃/Fe alloy as product composites.

4:05 PM Break

4:30 PM

Viability of Composite Materials in Current Design and Manufacturing Practices: *Pongtorn Prombut*¹; ¹Kasetsart University

Composite material technology has been under continuous development initially in response to the requirements of the aerospace and the sporting equipment industries, where material performance takes priority over the cost. However, composites have gained increasing acceptance in more general applications such as in automotive, marine, and construction industries due to an improvement in performance/cost ratio. This paper explores the viability of composite technology as an alternative to the more conventional metallic materials. The objective is to identify advantages offered by composites as well as principal obstacles to their acceptance. In many cases studied, some obstacles can be overcome by an integrated approach to product design. For composites, the production cost, the choice of feedstock, the choice of processing technologies, and the component geometry and performance are interdependent. The paper shows that composite structures can be produced at industry acceptable costs and production rates or at competitive total costs of ownership.

4:50 PM

Effect of Natural Fillers on Properties of Tapioca Starch/Rubber Latex Composite Foam: *Manisara Phiriyawirut*¹; Bumrung Lertloykulchai¹; ¹King Mongkut's University of Technology Thonburi

To improve the mechanical properties and water absorption of tapioca starch-based composite foams the addition of natural fillers was investigated. Starch-based composite foams were prepared from tapioca starch, natural rubber latex and natural filler by using a kitchen aid, and then starch batter was formed by thermal compression molding. To this mixture 5% natural rubber latex and 0-25% of cellulose, zein and soy protein isolate (SPI) were added. Various properties of the starch-based composite foams were investigated including morphology, flexural properties, density, water absorption, and enzymatic degradation. All of the samples were biodegradable by lipase enzyme. The flexural strength of cellulose and zein filled composite foam was higher than that of the unfilled one. Water absorption of natural filler filled composite starch foams were significantly decreased from unfilled one. There were slightly differences in water uptake of different filler type at high filler content.

Materials Processing IX

Wednesday PM
December 10, 2008

Room: Plaza 1
Location: Sofitel Centara Grand Bangkok

Session Chair: Hani Henein, University of Alberta

2:45 PM

Promotion of Recyclable Material Treatment at Mitsubishi Process in Naoshima Smelter and Refinery: Tetsuro Sakai¹; Norio Usami¹; *Masayuki Kawasaki*¹; ¹Mitsubishi Materials Corporation

The recyclable materials including valuable metals such as copper and precious metals had been treated at Mitsubishi Continuous Copper Smelting Furnace (Mitsubishi Process) in Naoshima Smelter and Refinery since the start of furnace operation. Early stage of recyclable material treatment was mainly focused on treating the copper bearing materials which did not contain inflammable materials due to a restriction on capacity of furnace waste heat boilers. As the environmental conservation awareness had been rapidly raised in recent years, establishing treatment systems for wide range of recyclable materials was demanded. To cope with the demand, Naoshima Smelter and Refinery started the operation of incinerating and melting plant of recycle waste in 2003. All of produced slag-metal generating from incinerating and melting plant of recycle waste is treated at Mitsubishi Process. Consequently new treatment system is established without secondary industrial waste by uniting two processes.

3:05 PM

Selective Extraction of Nd and Dy from Rare Earth Magnet Scrap into Molten Salt: *Sakae Shirayama*¹; Toru Okabe¹; ¹Institute of Industrial Science, University of Tokyo, Okabe Laboratory (Fw-301)

With the purpose of developing a novel recovery process of neodymium (Nd) and dysprosium (Dy) from rare earth magnet scrap, we investigated a selective extraction of Nd and Dy by using molten magnesium chloride (MgCl₂) or its vapor as a selective extracting agent. As a part of the preliminary experiments, Dy-containing Nd-Fe-B magnet alloys were immersed in molten MgCl₂ at 1273 K. Experimental results showed that the rare earth elements in the magnet alloys were successfully extracted into chloride salts by the substitution reaction between the rare earth elements and MgCl₂. After the removal of MgCl₂ by vacuum distillation, Nd and Dy can be separately recovered by either a wet process or a dry process (e.g., vacuum distillation). In this study, the effectiveness of MgCl₂ as an extracting agent was investigated in order to establish an effective recycling process for Nd-Fe-B magnet scrap.

3:25 PM

Recovering Gold Jewelry Scrap by Using Traditional Method: Process Revisited: *Saadiah Kaspin*¹; ¹Universiti Teknologi Mara

The gold scrap generated in jewellery production can be cleaned and recycled, but contaminated scrap and other wastes need to be collected and refined back to pure gold. The nitrogen dioxide produced from the traditional gold recovery process caused the air pollution and derived to the safety issues. This problem relates to the quality control of each methods used by the refiners. This research is keen to identify and develop a suitable new method that could be applied for in-house gold recovery process. An area of concern would be on the suitability of the proposed recovery method to be introduced and implemented by the traditional or small scale jewellery workshop with a good, innovative device to recover gold to avoid any losses with a safer and systematic system. A full cycle of physical and chemical testing via traditional and sophisticated means have been conducted to derive and validate findings and conclusions.

3:45 PM

Removing Arsenic from Low-grade Fluorite: *Koji Higashino*¹; Daisuke Fukuzawa¹; Gjergj Dodbiba¹; Toyohisa Fujita¹; Hiromitsu Takeyasu²; Takuya Arase³; Tsutomu Naganuma⁴; Kazuya Oharu⁴; ¹University of Tokyo; ²Japan Chemical Innovation Institute; ³Daikin Industries Ltd.; ⁴Asahi Glass Company, Ltd.

In this study, the low-grade fluorite ore was upgraded. The experimental work was primarily focused on removal of arsenic, which is difficult to be removed by conventional method. The fluorite ore was finely ground to less than 200 nm, in order to liberate particles that contain arsenic. Then, the sample was sulfurized by using a sodium hydrosulfide solution, in order to facilitate the removal of arsenic by flotation using potassium amyl xanthate (PAX) as collector. Considering that the particle size is very small, a microbubble flotation machine was employed, since it can generate micron-size bubbles. The main finding of this study is that arsenic was effectively removed, if the particle size was small (176nm), solvent pH was low (about pH 2) and the agitation time was long (16 hour). The experimental results suggested that 55% of arsenic can be removed.

4:05 PM Break

4:30 PM

Reduction of Titanium Oxide in the Presence of Nickel by Nonequilibrium Hydrogen Gas: *Hidehiro Sekimoto*¹; Tetsuya Uda¹; Yoshitaro Nose¹; Yasuhiro Awakura¹; ¹Kyoto University

It is difficult to reduce TiO₂ to metallic Ti with hydrogen gas under the usual condition because of the strong affinity between titanium and oxygen. Therefore, we tried the reduction of TiO₂ using nonequilibrium hydrogen gas, which could have the large apparent chemical potential of hydrogen. In this work, two kind of experimental conditions were employed as nonequilibrium hydrogen gas, including hydrogen plasma and supercooled monatomic hydrogen. The former was formed by RF microwave plasma generator. The latter was formed at 2273 K by hot-wire method. Furthermore, Ni powder was mixed with TiO₂ in the experiments. Nickel works as a monitor for the chemical potential of oxygen, which is estimated from titanium concentration in nickel phase obtained after reduction. The results of XRD analysis indicate that the different titanium oxide formed in each reduction condition. The effect of nonequilibrium hydrogen gas will be discussed in terms of thermodynamics and kinetics.

4:50 PM

Recent Operation of the Flash Smelting Furnace at Saganoseki Smelter and Refinery: Yutaka Yasuda¹; Mitsumasa Hoshi²; *Katsuya Toda*²; ¹Pan Pacific Copper Company, Ltd.; ²Nikko Smelting and Refining Company, Ltd./Saganoseki Smelter and Refinery

In 1996 Saganoseki Smelter and Refinery integrated its two flash furnaces to one while maintaining the smelting capacity in order to reduce the operating cost and maintain the global competitiveness. And then many improvements were carried out to expand the feeding capacity to the flash furnace to 160 t/h, attaining to 450,000 mtpy of the smelting capacity in 1999. However, the copper content in the concentrates had been decreased and we estimated

that the anode production was limited. Therefore, SPI (Saganoseki Process Innovation) project was carried out in order to expand the smelting capacity from 2003 to 2007. As the result of those modifications and improvements, the feeding capacity to the flash furnace attained to 212 t/h and the smelting capacity attained to 480,000 mtpy. This paper introduces the outline of expanding the smelting capacity and the recent operating conditions of the flash furnace.

5:10 PM

Recovery of Ni-Co Alloys from Spent Ni-MH Batteries: *Namfon Jittaseno*¹; Preecha Termsuksawad¹; ¹King Mongkut's University of Technology Thonburi

Nickel and cobalt can be extracted from spent nickel-metal hydride (Ni-MH) batteries by hydrometallurgical and electrochemical processes. The electrodes of spent battery are dissolved in 2 M sulfuric acid at 30, 45 and 60°C for 3, 4 and 5 hours. The experiments show that after dissolving at 30°C for 3 hours the leaching percentage of electrodes was about 75%. However, increasing time does not significantly increase leaching percentage of the electrodes. Nickel, cobalt, manganese, aluminum, zinc, lanthanum and cerium were detected in the leaching solution. Other metals except nickel and cobalt were extracted by 25% bis(2-ethylhexyl) phosphoric acid (D2EHPA) in kerosene at 20–80% of organic phase at 30°C and pH range of 1-3. Consequently, nickel cobalt alloys was deposited on cathode by electrowinning process with current densities ranging from 20 to 40 mA/cm², temperatures of 30, 45 and 60°C and pH of 2-4.

Mn dioxide structure when Mn(II) hydroxide was oxidized to Mn dioxide. As a result, incorporated Pt was scarcely dissolved by HCl in contrast to Au. According to these investigations, separation of Au and Pt was achieved by phase transformation of Mn(II) hydroxide to Mn dioxide, and the different coprecipitation and dissolution behaviors of nano-sized Au and coprecipitated Pt.

3:25 PM

Study of Metadynamic Recrystallization Kinetics in a Low Alloy Steel: *Y. C. Lin*¹; Jue Zhong¹; ¹Central South University

The metadynamic recrystallization behaviors in 42CrMo steel were investigated by isothermal interrupted hot compression tests. The kinetic equations have been proposed to describe or predict the metadynamic recrystallization behaviors of hot deformed 42CrMo steel. Comparisons between the experimental and predicted results were carried out. Results show that the effects of deformation parameters, such as strain rate and deformation temperature, on the softening fractions of metadynamic recrystallization for the two-stage hot deformation are significant. However, the strain (beyond the peak strain) has little influence. The predicted results are in good agreement with the experimental ones, which indicates that the proposed kinetic equations can give an accurate and precise estimate of the softening behaviors and microstructural evolutions for 42CrMo steel.

3:45 PM

Structure Uniformity and Creep Behavior of Modified Nickel Base Alloy NiMoCr: *Jozef Zrnik*¹; Libor Kraus¹; Panyawat Wangyao²; Stanislav Nemecek¹; ¹COMTES FHT s.r.o.; ²Metallurgy and Materials Science Institute, Chulalongkorn University

The thermomechanical (TM) processing of NiMoCr solid solution nickel base superalloy is a process to influence considerably the grain characteristics of the wrought structures. The initial as-cast ingot structure break down by hot working usually does not provide uniform recrystallized grain structure. In order to modify the structure heterogeneity in roughly forged ingot the conventional two step hot rolling was conducted. Post deformation annealing was applied expecting further contribution in modification of primary recrystallized microstructure. The uniformity of alloy microstructure increased as higher straining of slab was introduced. Nevertheless the deformation condition were applied the bimodal grain structure was typical applying the specific TM experimental schedules. The creep behavior of differently modified alloy structure after various hot working conditions and the annealing process were then investigated for considered testing condition. The results of creep tests showed that creep characteristics such as strain rate and lifetime are greatly dependent on resulting microstructure.

4:05 PM Break

4:30 PM

Structure of Oxide Scale Formed on Cr-Si-Ni Alloys: *Yoshio Suzuki*¹; Akira Yamauchi¹; Kenichi Ohsasa¹; Kiyotaka Matsuura¹; *Kazuya Kurokawa*¹; ¹Center for Advanced Research of Energy Conversion Materials, Hokkaido University

A double-layered SiO₂/Cr₂O₃ scale is expected to show excellent high-temperature corrosion resistance. For the formation of double-layered scale we proposed the Cr-Si-Ni alloys. The oxide scales formed on Cr-Si-Ni alloys with various Ni contents at 1273 K were observed and analyzed by TEM and TEM-EDS. These alloys consisted of CrSi₂ and (Cr,Ni)Si phases. It was found that CrSi₂-(5, 10, 20) mass% Ni alloys form the SiO₂/Cr₂O₃ scales and the ratio of SiO₂ thickness to Cr₂O₃ thickness in the oxide scale depends on the concentration ratio of CrSi₂ to (Cr, Ni)Si in the substrate. These alloys showed excellent high-temperature corrosion resistance in atmospheres containing sulfur and chlorine.

4:50 PM

Structure and Properties of Polypropylene/Polyethylene Terephthalate Blend: *Natee Srisawat*¹; Supaporn Thumsorn¹; Jessada Wong On²; ¹Rajamangala University of Technology Thanyaburi; ²Pathumwan Institute of Technology

This research studied in structure and properties of polypropylene (PP)/Polyethylene terephthalate (PET) blend. The PP/PET blends were prepared

Materials Processing X

Wednesday PM
December 10, 2008

Room: Plaza 3
Location: Sofitel Centara Grand Bangkok

Session Chair: B. R. Sridhar, Gas Turbine Research Establishment

2:45 PM Invited

Nonstoichiometric Pyrrhotites Heat Capacity: *Tatyana Chepushtanova*¹; *Vladimir Lukanov*¹; Brajendra Mishra²; ¹Kazakh National Technical University; ²Colorado School of Mines

To present day are staying undefined suppositions about pyrrhotites heat capacity values at low-temperature phase transitions. In this work was established in Curie point the value of synthetic pyrrhotites heat capacity depending on sulfur contention (from 53,05 before 53,27) and decrease from 73,42 before 73,30 J/mole•°C at 320–303°C. Heat capacity of Fe_{0,885}S and Fe_{0,888}S at 294–293°C consist 39,99 and 39,92 J/mole•°C accordingly. Heat capacity of pyrrhotites Fe_{0,855}S – Fe_{0,888}S is not depend from structure and equal at 550°C 73,30 J/mole•°C. Results were got by calorimeter STA PC/PG Luxx NETZSCH Company.

3:05 PM

Coprecipitation of Au(III) Complex Ions as Au Nanoparticles with Mn(II) Hydroxide for the Selective Recovery of Au and Pt: *Chompunoot Wiraseranee*¹; Kotaro Yonezu²; Satoshi Utsunomiya²; Dawan Wiwattanadate³; Akira Imai²; Koichiro Watanabe²; Takushi Yokoyama²; ¹Chulalongkorn University - and - Kyushu University; ²Kyushu University; ³Chulalongkorn University

The coprecipitation behavior of Au(III) complex ions with Mn(II) hydroxide was examined. Coprecipitated Au was stoichiometrically reduced to elemental gold by electron transfer via Au-O-Mn bonding. Au particles coprecipitated with Mn(II) hydroxide were nano-sized, and could be effectively dissolved by diluted HCl. To apply the advantages of this coprecipitation method to recovery of Au and Pt, the coprecipitation of Au in the presence of Pt(IV) complex ions with Mn(II) hydroxide was conducted. Compared to the coprecipitation of Pt(IV) complex ions in the absence of Au, the amount of coprecipitated Pt was remarkably enhanced in the presence of Au, which Au was considered as the oxidant for Mn(II), and Pt was coprecipitated as Pt(IV). These results suggested Pt(IV) incorporated into

in single screw extruder. The composition of PP/PET blends were 100/0, 90/10 and 80/20 with and without a compatibilizer. The compatibilizer was maleic anhydride grafted polypropylene (PP-G-MA). The effectiveness of the compatibilizer was evaluated using various techniques, such as mechanical analysis, scanning electron microscopy, and rheological analysis. The results show that the addition of PP-g-MA promotes a fine dispersed-phase morphology, and improves toughness of the blends. Shifts in the glass-transition temperature of the PET phase and the increase in the melt viscosity of the compatibilized blends indicated enhanced interactions between the discrete PET and PP phases induced by the compatibilizer.

5:10 PM

Catalytic Process for the Dehydrohalogenation of NiCl₂ Catalytic Process for the Dehydrohalogenation of NiCl₂ Supported on Al₂O₃: *Chartsak Chettapongsaphan*¹; ¹National Metal and Materials Technology Center

In the process for the preparation of catalysts for hydrogenation from oxides of nickel from the aqueous solution of the chlorides the solutions are introduced into a pyrohydrolysis unit, where the desired oxides are formed with specific surface areas of between 40 and 60 m²/g, agglomerate sizes from 1 to 4 micrometers and a mean particle size of between 2 and 3 micrometers, and the anions are combined with to hydrogen to give the corresponding acids. As a further process step, this can be followed by a reduction at high temperature not exceeding 1400°C. The catalytically active substances can also be deposited on support matrices such as aluminium oxide supports. Simple further processing to shaped forms (pellets etc.) is possible.

Materials Processing XI

Wednesday PM
December 10, 2008

Room: Plaza 7
Location: Sofitel Centara Grand Bangkok

Session Chair: Animesh Jha, University of Leeds

2:45 PM Invited

Influence of Copper on Microstructure and Mechanical Properties of Hypereutectic Ductile Irons: Tumrongsak Witchanantakul¹; *Usanee Kitkamthorn*¹; Sarum Boonme¹; Rattana Borrisuthhekul¹; Narong Akkarapattanaagoon¹; ¹Suranaree University of Technology

Hypereutectic ductile cast irons with the compositions of Fe-(3.3-3.5)C-(2.8-3.0)Si-xCu where x = 0-1.5 (in weight%) were cast into the cylindrical bars. The alloys were austenitized at 950°C for 0-3 hours, and then air-cooled. Austempering at 300°C for 2 hours after austenitizing were also carried out. Results show that increasing the levels of Cu promotes the pearlitic microstructure of the matrix in the as-cast alloys. Fully pearlitic microstructure of each alloy is obtained when austenitizing time for 0%, 0.5%, 1% and 1.5% Cu-added iron alloys are 2 hrs, 1.5 hrs, 1 hr and 45 minutes, respectively. Addition of Cu also improves mechanical properties of the as-cast alloys and those of the air-cooled samples. Results from the austempering experiment show that low levels of Cu (< 1.5wt%) do not significantly affect the microstructure and mechanical properties of the austempered irons. Relations among microstructure, mechanical properties and heat treatment conditions were discussed.

3:05 PM

The Investigation of Ultra-High Strength Steel by Quenching-Partitioning-Tempering (Q-P-T) Process: *Rong Yonghua*¹; Wang Xiaodong¹; Xu (Hsu) Zuyao (T.Y.); ¹Shanghai Jiao Tong University

By comparing quenching and partitioning(Q&P) process proposed by Speer et al with quenching-partitioning-tempering (Q-P-T) process proposed by Hsu, an ultra-high strength steel of Fe-0.485C-1.195Mn-1.185Si-0.98Ni-0.21Nb by the Q-P-T process was designed and the microstructure was characterized. The results indicate that this Q-P-T steel exhibits the tensile strength over 2000MPa combined with good elongation above 10%, and a steel with the carbon content less than 0.5wt% and with the tensile strength over 2000MPa accompanying elongation above 10% at heat treatment

state has not yet been reported. The modification of alloying elements was suggested to improve the mechanical properties of this steel.

3:25 PM

Synthesis of S and N Co-Doped TiO₂ Films by AC-PLD Method and Their Photo Properties: *Minoru Matsuda*¹; Masaki Yoshinaga¹; Nobuaki Sato¹; Atsushi Muramatsu¹; ¹Tohoku University

For the application of TiO₂ film to visible light active photocatalyst by anion doping, synthesis of S and N co-doped TiO₂ films was conducted by atmosphere controlled pulsed laser deposition (AC-PLD) method. In this method, anion doped TiO₂ film was formed on quartz substrate by the irradiation of pulsed Nd:YAG laser light on TiO₂ target in the presence of CS₂ and CH₃CN. Both S and N were found to be doped homogeneously in the obtained TiO₂ film. The co-doped film was visible light active and its absorption property was sensitive to the partial pressure of the gaseous reagents during the ablation. Furthermore, the co-doped film showed better catalytic performance than either sulfur or nitrogen doped TiO₂ film.

3:45 PM

Synthesis of Two Types of Adsorbents: A Comparison Study of Their Efficiencies and Environmental Impacts when Adsorbing Molybdenum from Wastewater: *Gjergj Dodbiba*¹; Teiji Nukaya²; Yuji Tanimura²; Toyohisa Fujita¹; ¹University of Tokyo; ²Nittetsu Mining Company, Ltd.

A comparison study was carried out in order to compare the adsorption efficiencies and the environmental impacts of two different methods for treatment of Mo contaminated wastewater. In other words, a FeCl₃-based adsorbent and a FeSO₄-based adsorbent were synthesized and their efficiencies in adsorbing Mo from wastewater were compared in terms of the adsorption capacity and the rate of adsorption. Here, it should be noted that the main material being used in the synthesis of the FeSO₄-based adsorbent is a waste product from the manufacturing process of titanium dioxide. Finally, the experimental results were used as input parameters in assessing the environmental impacts of these two different adsorption methods. In other words, both methods were compared in the context of the life cycle assessment (LCA). The environmental impacts were expressed in terms of resources depletion potential and global warming potential.

4:05 PM Break

4:30 PM

Synthesis of Slow Release Fertilizer by Means of Mechanochemical Method: *Solihin*¹; Qiwu Zhang¹; Fumio Saito¹; ¹Institute of Multidisciplinary Research for Advanced Materials, Tohoku University

The candidates of slow release fertilizer materials, such as KMgPO₄ and NH₄MgPO₄, have been synthesized by means of mechanochemical method, using a planetary mill to conduct solid-state reaction. It is found that rate of nutrient release depends on the rotational speed of the mill. The release performance of both KMgPO₄ and NH₄MgPO₄ in water is depending on mill speed. For example, small amount of KMgPO₄ and NH₄CaPO₄ formed on the surface of reactant powder particles decreases with an increase in mill speed of rotation. The nutrient release rate of phosphorous, potassium, ammonium from KMgPO₄ and NH₄MgPO₄ is decreased down to 10-20%, whereas magnesium can be dissolved slightly. Thus the mechanochemical method may be an effective synthesizing tool for controlling the release of fertilizer materials, such as KCaPO₄ and NH₄CaPO₄, in water.

4:50 PM

Synthesis of Metallic Nanoparticles by Hydrolysis of Magnides, Aluminides, and Sodides: Huabin Wang¹; *Derek Northwood*¹; ¹University of Windsor

The hydrolysis behaviour of magnides, aluminides, and sodides at room temperature has been systematically investigated. Ni, Cu, Au, Ag, Si, Ge, and Pt nanoparticles prepared by the hydrolysis of magnides and sodides were roughly spherical in shape with particle sizes below 20nm. The hydrolysis byproduct of magnides, Mg(OH)₂, has a very small solubility in water, and is easily removed by a dilute acid. The use of a dilute acid for the removal of Al(OH)₃, the hydrolysis byproduct of aluminides, leads to a fairly low pH, as a result, chemically active transition metal nanoparticles do not survive, especially when exposed to air. Only chemically inert transition metals,

Au and Ag, could be prepared by this method. The hydrolysis byproduct of sodides, NaOH, has a high solubility. Hence, preparation of metallic nanoparticles by hydrolysis of sodides does not need an acid-rinsing process, but there are difficulties in controlling the reaction rate.

5:10 PM

Characterization of Stamping Properties of Magnesium-Alloy Sheets: *Fuh-Kuo Chen*¹; Hsin-Hong Chen¹; ¹National Taiwan University

Due to its lightweight and high specific strength, magnesium alloy has been widely used for structural components, notably in the automotive industry. Although the principle manufacturing process has been die casting, the press forming has considerable potential because of its competitive productivity and performance. Among the fabrication processes of press forming, stamping of Mg-alloy sheets is especially important for the production of thin-walled structural components. In the present study, the stamping properties of various Mg-alloy sheets, AZ31, AZ61 and AM60 were investigated using the experimental approaches and the finite element analysis. Since the magnesium alloys usually exhibit limited ductility at the room temperature due to their hexagonal close-packed structure, the mechanical properties of magnesium-alloy sheets were examined at various temperatures. In the present study, the stress-strain relationship, *n*-value, and *r*-value of magnesium-alloy sheets at various temperatures ranging from room temperature to 400°C were obtained from experimental results, and were employed to the finite element analysis afterwards. In addition, the important stamping characteristics of magnesium-alloy sheets, such as limit drawing ratio (LDR), forming limit, springback and minimum bending radius, were also examined by experiments and the finite element analysis. The stamping properties obtained from experiments were then applied to the finite element analysis of a circular cup drawing process at various temperatures. The finite element simulation results agreed very well with the experimental data obtained from the actual drawing processes, and the accuracy of the stamping properties of magnesium-alloy sheets obtained in the present study was then confirmed.

Modeling Material Processing II

Wednesday PM Room: Plaza 8
December 10, 2008 Location: Sofitel Centara Grand Bangkok

Session Chair: Adam Powell, Opennovation

2:45 PM

Kinetic Description for Solid State Phase Transformation: *Feng Liu*¹; ¹Northwestern Polytechnical University

The progress of solid-state phase transformations can generally be subdivided into three overlapping mechanisms: nucleation, growth, and impingement. These can be modeled separately if hard impingement prevails. On that basis, numerical and analytical methods for determination of the kinetic parameters of a transformation have been proposed and focused on both isothermally and isochronally conducted transformations. To extend the range of transformations that can be described analytically a number of more or less empirical sub-models, which are compatible with experimental results, has been included in the discussion. It has been shown that powerful, flexible, analytical models are possible, once the concept of time or temperature dependent growth exponent and effective activation energy, in agreement with the existing experimental observations, has been adopted. Without recourse to any specific kinetic model, simple recipes have been given for the determination of the growth exponent and the effective activation energy from the experimental transformation-rate data.

3:05 PM

Modelling of Phase Transformation and Process Parameter Identification of Hot Rolled Dual Phase Steel: *Piyada Suwanpinij*¹; S. Benke¹; Christoph Keul²; Ulrich Prahl²; Wolfgang Bleck²; ¹ACCESS e.V., RWTH Aachen University; ²RWTH Aachen University, Department of Ferrous Metallurgy

The excellent combination of mechanical properties of dual phase steels arises from the distribution of hard martensite islands in the soft matrix of ferrite. The dual phase microstructure in lean steel can be achieved directly after hot rolling by a well-defined deformation and cooling schedule. Process parameters: degree of deformation, holding time and temperature, and cooling schedule are simulated by deformation dilatometer. It is indicated that large deformation is required to produce dual phase structure and the amount of alloying elements must be compromised to obtain high hardenability and small solute drag effect. The acceleration effect of hot rolling is coupled into the modelling in terms of nucleation density and elastic strain energy of dislocations. The mobility of grain growth must be proper adjusted in the modelling of such the case. The ferrite nucleation density and fraction increase with logarithm strain almost linearly.

3:25 PM

Numerical Simulation of Mass Transfer in Copper Electrorefining with Gas Injection: Yoshitsugu Hanada¹; Tomio Takasu¹; Hideyuki Itou¹; ¹Kyushu Institute of Technology

Electrorefining at higher current density is desirable due to the increase in productivity attained without expanding the size of a plant. However, increasing the current density in common commercial practice causes problems such as anode passivation, dendritic deposition, cathode impurities and energy consumption. In general, agitation of the electrolyte is effective in suppressing these problems. To apply the agitation to commercial practice effectively, the method of agitation is important. One possible method is agitation by gas injection. Quantitative understandings of phenomena are required to optimize operating conditions. In this study, two phase flow and mass transfer were numerically simulated. Effect of difference of turbulent models and grid size on the results were examined. Characteristics of fluid motion and copper concentration were investigated. Evaluations were done for mass transfer coefficient and the concentration on the electrodes which are important to overcome the problems at high current density.

3:45 PM

The Simulations of Tubular Solid Oxide Fuel Cells (SOFC): *Korakot Rattanakornkan*¹; Wanwilai Evans¹; Anotai Suksangpanomrung²; Sumittra Charojochkul³; ¹Srinakarinwirot University; ²Chulachomklao Royal Military Academy; ³National Metal and Materials Technology Center

The simulations of two types of tubular solid oxide fuel cell (SOFC) were carried out. The geometry of the single cell comprises an air channel, fuel channel, anode, cathode and electrolyte layers. The computational results were validated with experimental data. The current density, gas flow behavior, temperature and species concentration are analyzed. The effects of the gas temperature, gas flow rate and the dimension of fuel cell on the current density, power density and thermal efficiency were investigated. The results of this work can be used for studying the cell behavior of a tubular SOFC and used to help develop efficient fuel cell designs.

4:05 PM Break

4:30 PM

Thermal Analysis of Hot Strip Rolling Using Finite Element and Upper Bound Methods: *Hasan Sheikh*¹; ¹Malek Ashtar University of Technology

Thermal analysis of rolling possesses has been studied in this work. A Finite Element method has been coupled with an Upper Bound solution assuming, triangular velocity field, to predict temperature field during hot strip rolling operation. To do so, an Upwind Petrov-Galerkin scheme together with isoparametric quadrilateral elements has been employed for solving the steady-state heat transfer equation. A comparison has been made between the published and the model predictions and a good agreement was observed that shows the accuracy of the proposed model.

4:50 PM

Understanding Metastability and Phase Equilibrium in Mo-Rich Mo-Ti-Zr-C Alloys: *Voramon Dheeradhada*¹; ¹GE Global Research

Molybdenum-based alloys in the Mo-Ti-Zr-C family combine several metallurgical properties desirable for high temperature, non-oxidizing structural applications. Typically, Mo alloys are prepared by either powder metallurgy or vacuum arc melting routes, often followed by thermomechanical operations such as forging, extrusion, rolling, and/or swaging, with various intermediate and final annealing treatments. Differences in process histories result in distinct microstructural differences, and hence will affect the alloy properties. Alloys such as TZM (Mo-0.5Ti-0.08Zr-0.03C by weight) and TZC (Mo-1.2Ti-0.3Zr-0.1C) are believed to owe their high temperature strength and microstructural stability to a combination of solute strengthening and carbide phases. As such, the stability of the respective carbides, and the subsequent mechanical behavior of the alloys, are strongly dependent on the alloying additions and processing history. The effects of alloying elements on the phase equilibrium in the Mo-rich corner of the Mo-Ti-Zr-C system was investigated using a CALPHAD-based thermodynamic model. A diffusion multiple approach was employed to validate and refine the CALPHAD model. Key results from the CALPHAD model and diffusion multiple validation will be described and compared to experimental observations of commercially available and laboratory synthesized TZM-family alloys. The results are used to gain a better understanding as well as guide the development of TZM-family alloys.

5:10 PM

Eigenstrain Analysis of Residual Stresses Due to Welding and Post-Weld Heat Treatment of Aerospace Materials: *Alexander Korsunsky*¹; Tea-Sung Jun¹; ¹University of Oxford

Welding, surface treatment, plastic forming and other manufacturing processes generate residual stresses and introduce distortion in engineering components and assemblies. The knowledge of residual stress states is important for the ability to predict the subsequent in-service behaviour in response to thermo-mechanical loading, including the propensity to suffer further distortion, and particularly the initiation and propagation of fatigue cracks. Inertia friction welding between Ni-base superalloy components was considered in the present study. The process is increasingly used in the aerospace industry for butt joining of hollow cylindrical components, such as shafts and drums. Inverse eigenstrain framework was used for the interpretation of neutron diffraction measurements in order to find the underlying eigenstrain distributions. The advantage of this approach lies in the fact that limited sets of experimental residual strain data from neutron diffraction measurements can be used to obtain an approximate reconstruction of the complete stress tensor within the entire component.

Thin Film Coating Processing III

Wednesday PM Room: Plaza 4
 December 10, 2008 Location: Sofitel Centara Grand Bangkok

Session Chair: To Be Announced

2:45 PM

Hydroxyapatite Coating on Titanium Using Thermal Substrate Method in Aqueous Solution and the Evaluation of Osteoconductivity: *Kensuke Kuroda*¹; Ryoichi Ichino¹; Masazumi Okido¹; ¹Nagoya University

Hydroxyapatite (HAp) coatings were formed on titanium plates and rods by the thermal substrate method in an aqueous solution (pH = 8) that included 0.3 mM Ca(H₂PO₄)₂ and 0.7 mM CaCl₂. The coating experiments were conducted at 40~140 °C for 15 or 30 min. The properties for the coatings were studied using XRD, EDX, FT-IR, and SEM. All the specimens were covered with HAp, which had different surface morphology such as net-like, plate-like and needle-like. The coated samples were implanted in rats tibiae, the osteoconductivity were evaluated. Two weeks postimplantation,

new bone formed on the HAp coated in the cancellous bone and cortical bone, respectively. Bone-implant contact ratio, which was used for the evaluation of new bone formation, was significantly depended on the surface morphology of HAp, and the needle-like coated sample seems to promote rapid bone formation.

3:05 PM

Microstructure of Si-Al Diffused Coatings on an Advanced Nb Silicide Based Ultrahigh Temperature Alloy: *Xiping Guo*¹; Xiaodong Tian¹; Ping Guan¹; ¹Northwestern Polytechnical University

Al-modified silicide coatings were successfully prepared by both a two-stage and a co-deposition pack cementation process. The two-stage process coatings were prepared by firstly pack siliconizing at 1150° for 4h and then pack aluminizing at 800~1000° for 4h. The phase constituent of the pack siliconized coating was (Nb,X)Si₂. The mean content of Al in the firstly siliconized and then aluminized coating increased with the rising of aluminizing temperature. (Nb,Ti)₃Si₅Al₂ phase existed in the upper part of the coating when the aluminizing temperature reached to 860°. The co-deposition coatings were prepared by co-depositing Si and Al at 1000, 1050, 1100 and 1150° for 8h respectively. The co-deposition coatings had a multiple layer structure. The coating obtained by co-depositing Si and Al at 1050° possessed an upper layer with the phase constituents of (Nb,Ti)₃Si₅Al₂, (Nb,Ti)Al₃ and (Nb,X)Si₂, a (Nb,X)₅Si₃ mid layer and a lower layer composed of (Nb,Ti)Al₃ and (Cr,Al)₂(Nb,Ti).

3:25 PM

MWNT/SiC Coatings: Synthesis, Microstructure and Oxidation Resistance: *Yasuo Uchiyama*¹; Guo-Bin Zheng¹; Hideaki Sano¹; ¹Nagasaki University

MWNT/SiC coatings were developed for the application of antioxidation coatings of carbon materials and improving surface properties. Previous research showed the difficulty to control the structure of carbon nanotubes that were directly grown on C/C materials. In this study, the growth of MWNTs on C/C, graphite and other materials were extensively studied, with an emphasis on catalyst composition and the interaction between substrate and catalysts. The thickness and uniformity of MWNT layers were controlled by optimizing the synthesis parameters. Effect of pyrolytic carbon deposition to the integration of MWNTs and substrate was evaluated. MWNT/SiC coatings, which were prepared by deposition of SiC into MWNTs layer, were evaluated, focusing on the microstructure, interfacial bonding between MWNTs and SiC, and stress distribution in the coatings.

3:45 PM

Optical Characteristics of Reactively Sputtered Nitrogen Doped Chromium Oxide Thin Films: *Anurat Wisitsoraat*¹; P. Eiamchai¹; C. Oros²; M. Horpratum¹; V. Phatanasetkul¹; A. Tuantranont¹; P. Chindaudom¹; ¹National Electronics and Computer Technology Center; ²King Mongkut's University of Technology Thonburi

Chromium oxide is a transitional metal oxide with applications in optical coating, infrared sensors and hard coating. Recently, chromium oxide has been incorporated with different foreign atoms to modified its optical properties. Nevertheless, the optical characteristics of nitrogen doped chromium oxide materials have not been investigated. In this work, optical characteristics of nitrogen doped chromium oxide thin films prepared by reactive sputtering are characterized with different doping concentrations. The nitrogen doped chromium oxide was deposited on silicon substrates by reactive sputtering under a mixture of Ar, O₂ and N₂ gases. The nitrogen concentration in film is controlled by varying nitrogen flow rate from 0.5 to 8 sccm while the argon flow rate, oxygen flow rate, film thickness and radio frequency (rf) power are fixed at 4 sccm, 4 sccm, 200 W and 200 nm, respectively. The films were subsequently annealed in air at 300°C for 2 hours. The surface and chemical structure of the materials are characterized by means of scanning electron microscope (SEM), energy dispersive X ray spectroscopy (EDX) and X ray diffraction (XRD), respectively. The optical characteristics of the film were then characterized by spectroscopic ellipsometry (SE). It was found that as deposited films have amorphous crystal structure with smooth surface morphology and its nitrogen content is slowly increased as nitrogen flow rate increases. The optical constants of as deposited films

measured by SE show irregular behaviors and can not be fitted with standard ellipsometric models due to its non stoichiometry. After annealing, the films become polycrystalline with higher surface roughness and lower nitrogen content. The ellipsometric data of the annealed films can be well fitted with joint density of state parametric model. The calculated refractive index and extinction coefficient are considerably decreased as the nitrogen content increases. The results show that nitrogen doping can be a simple and useful mean for modulating optical constant of chromium oxide thin film in optical coating applications.

4:05 PM Break

4:30 PM

Structure and Property of Zr-Cu Binary Amorphous Films Deposited by Sputtering Process: *Junji Fujita*¹; Tadashi Serikawa¹; Katsuyoshi Kondoh¹; Hisamichi Kimura²; Akihisa Inoue²; ¹Osaka University; ²Tohoku University

Evaluation of structures and properties were carried out on Zr-Cu binary amorphous films via a glow discharge sputtering process, in employing the elemental composite target which consists of Zr or Cu chips on the other single plate. Film compositions were controlled by changing the number of each chip. Zr-Cu binary films had amorphous structures throughout almost all compositions, and indicated crystallized structures after annealing. The Zr₄₀Cu₆₀ film showed complete amorphous structure, and crystallizing temperature was higher than others. Film properties depended mainly on its compositions. For example, the higher Cu composition caused the lower corrosion resistance of the sputtered film. When employing 70%Ar-30%H₂ mixed gas as a sputtering gas, the structure of the fabricated film was more completely amorphous than that in using Ar gas. It suggests the addition of H₂ to Ar sputtering gas has an effect to form amorphous due to release residual stress in the deposited film.

4:50 PM

Thickness Effect on Phase Transformation Behavior of TiNiCu Thin Films for Bio- MEMS Applications: Yahya Sharabiani¹; *Ming Tan*¹; Christopher Shearwood¹; Weimin Huang¹; ¹Nanyang Technological University

TiNi shape memory alloy thin films formed by sputtering have attracted great interest as powerful actuators in micro-electro-mechanical systems (MEMS) such as microvalves, microfluid pumps, and microgrippers. Most studies have been concerned with films of a thickness of several microns while little work has been done thickness of a few hundred nanometers. Among TiNi-based alloys, Ti-Ni-Cu alloy is considered suitable for quick response actuation, since they show a narrow temperature hysteresis. In this study, TiNiCu thin films were prepared in different thicknesses (i.e. more than 1000 nm, sub-micron and nano scales) by magnetron sputtering deposition technique; and the effect of thickness on phase transformation behavior was studied. Curvature test, SEM, XRD, AFM and DSC were employed to characterize the thin films. Microstructural change, inter-diffusion layer and oxidation layer were also investigated with regards to the shape memory properties of the samples.

5:10 PM

The Effect of Substrate Location Arrangement in the PVD Deposition Chamber on the Mechanical Properties of the Coatings: Karuna Tuchinda¹; Chiya Damkam¹; *Waree Preechamongkit*¹; Rattanaporn Ratanabunlang¹; Nantaporn Wittayapairot¹; ¹King Mongkut's University of Technology Thonburi

Hard thin films, commonly called as hard coatings, have been successfully used to increase many engineering component life, especially forming dies and machining tools. PVD coating deposition process is one of the most popular process used for such purpose. However, the coatings properties obtained from PVD process have been found to vary significantly from one process to another process. Many researches have been carried out to investigate the effect of the deposition parameters, such as deposition current, voltage and pressure etc., on the coating properties. In this work, the effect of substrate location in a deposition chamber on the microstructure and the mechanical properties of the film being generated has been studied. The result could be very useful in the design of a substrate arrangement during PVD deposition process.

Closing Ceremony

Wednesday PM
December 10, 2008

Room: Auditorium B2, Bangkok Convention Centre
Location: Sofitel Centara Grand Bangkok

Session Chairs: Brajendra Mishra, Colorado School of Mines; Akio Fuwa, Waseda University; Paritud Bhandhubanyong, National Metal and Materials Technology Center

5:30 PM Closing Ceremony

Aqueous/Electrochemical Processing Poster Session

Mon AM-Wed PM
December 8, 2008

Room: Auditorium B2, Bangkok Convention Centre
Location: Sofitel Centara Grand Bangkok

Development of Noble Metal Oxide Electrode for Electrochemical Process: *Do-Won Chung*¹; Seong-Ho Son¹; Wonsik Lee¹; ¹Korea Institute of Industrial Technology

In electroplating and water treatment fields, demand and interest on development of electrode (DSE) with high productivity and efficiency have been increased. The purpose of this study is to produce noble metal oxide electrodes with good reactivity and durability, minimizing contents of the noble metals. For increase of durability, a micro porous oxide (TiO₂) layer was formed on surface of titanium substrate by anodizing process. During subsequent coating of metal oxide layer by thermal decomposition, the porous structures were filled with Ir, Pt and Ru oxides, etc. The formation of Ti-O layer improved adhesive property between noble metal oxide layer and titanium substrate, resulting in enhancement of durability. Also, due to addition of tantalum and/or a component, reactivity increased and an evolution of oxygen on the electrode decreased largely, improving durability, too. In field tests for sterilizing of swimming pool and power-plant cooling water, the electrode showed high efficiency in sodium-hypochlorite generation.

Effects of Surface Finishing Methods on Corrosion Resistance of Aluminum Alloy: *Kanokwan Saengkietiyut*¹; Pranee Rattanawaleedirojn¹; Weera Chukrachan¹; Adisak Thueploy¹; ¹Metallurgy and Materials Science Research Institute

The effects of surface finishing methods on corrosion resistance of aluminium alloy were investigated by polarization curve measurements using potentiometric methods. Specimens were prepared using surface finishings mechanical polishing, chemical polishing and electropolishing. For the mechanical polishing, specimens were ground with automatic grinding machine using silicon carbide papers. The chemical polishing, specimens were first prepared by mechanical polishing with silicon carbide papers 600 grit sizes and then immersed in an alkaline solution at 80°C for 20 minutes. The electropolishing, the specimens were also prepared by mechanical polishing with silicon carbide papers 600 grit sizes and then immersed in the same electrolyte as chemical polishing solution with applied voltage 15 volt for 20 minutes. All of the specimens were investigated by surface roughness measurement, optical microscope, scanning electron microscope and potentiodynamic technique in 3.5 wt.% NaCl solution.

Experimental E-pH Diagrams of AISI 316L Stainless Steel in 7100-ppm NaCl Aqueous Solution Containing Sulfate by Cyclic Polarisation Method: *Somrerak Chandra-ambhorn*¹; Wisarut Wachirasiri¹; ¹King Mongkut's University of Technology North Bangkok

An AISI 316L stainless steel was immersed in a de-aerated 7100-ppm NaCl aqueous solution containing Na₂SO₄ with the content from 0 to 3000 ppm at the solution pH from 3 to 11 at 27°C. The cyclic polarisation method was applied to construct the experimental E-pH diagram. When the content of Na₂SO₄ in the solution increased, the pitting-potential line in the diagram tended to shift to the noble direction. The less sensibility of the pitting potential on the solution pH particularly in acidic conditions was observed. However, the increase of Na₂SO₄ in the solution tended to lower the protection-potential line to the negative direction. This resulted in the widening of the imperfect passivation regime in the diagram. The chemical analysis was conducted to determine the types of ions dissolved from the metal into the solution.

Composites Processing Poster Session

Mon AM-Wed PM
December 8, 2008

Room: Auditorium B2, Bangkok Convention Centre
Location: Sofitel Centara Grand Bangkok

Characterization of Fiber Length Distribution in Short and Long-Glass-Fiber Reinforced Composites during Injection Molding Process: *Somjate Pacharaphun*¹; ¹Kasetsart University

The reduction in fiber length during injection molding of two commercial glass-fiber reinforced polypropylene (PP) granules was studied. The first containing 20 percent by weight (wt%) of short-glass-fibers with the average fiber length around 350 micron and the other filled with 40 wt% of relatively much longer fibers mostly around 7,000 micron. The fiber length distribution (FLD) was measured along the screw channels and after the molten composite is injected through a nozzle of an injection unit. The results indicated that the FLD moved to shorter fiber lengths along the screw channels further from the hopper. In both cases, fiber attrition occurs predominantly in the feed and compression zones, particularly in long-glass-fiber reinforced polypropylene. More severe fiber attrition in this finding can be assumed due to a higher fiber concentration and longer fiber length which result in a higher degree of fiber-fiber interaction and increased fiber-wall contacts.

Comparative Study of Ballistic Performance of High Strength Polyethylene Fiber Composite and Kevlar Composite: *Nuntikant Chaiwong*¹; Kuljira Sujirote¹; Kannigar Deteraksa¹; Taweechai Amornsakchai²; ¹National Metal and Materials Technology Center; ²Mahidol University

This research compares ballistic performance, at the same areal density or the same areal thickness, of 'Kevlar' composite to that of high strength polyethylene fiber composite developed from local materials. Hard armor plates with one square foot area, comprising 4 mm top ceramic layer and the polymer composite back plate, were prepared. According to NIJ standards, ballistic tests were conducted for protection levels 2A, 2, and 3A. Trauma depth and diameter left on witness clay were measured and compared. The result showed that on weight or areal density basis, the composite made of high strength polyethylene fiber performed better than the composite made of 'Kevlar' fiber. On the other hand, one thickness basis, 'Kevlar' composite performed slightly better than the composite made of polyethylene fiber when trauma depth is considered. However, considering the trauma diameter, high strength polyethylene fiber composite exhibited smaller diameter for both areal density and thickness comparison.

Effect of Precursor Preparation Conditions on Combustion Synthesis of Al-Ti Foams: *Norio Inoguchi*¹; Makoto Kobashi¹; Naoyuki Kanetake¹; ¹Nagoya University

Al-Ti foams were fabricated by combustion reaction of the blended powder compacts consisting of titanium and aluminum. The foaming agent (B₂C powder) was added to the blended powder to promote the foaming behavior by increasing the combustion temperature. The effect of the Al/Ti blending ratio, the amount of foaming agent and the size of elemental powders (aluminum and titanium) on the combustion foaming process were investigated. The uniform pore morphology was obtained only when the Al/Ti powder blending ratio was in an appropriate range. The adequate addition of the foaming agent increased the porosity and size of pores. The size of elemental powders was an important factor of combustion synthesis of Al-Ti foams, and will be discussed in the presentation.

Effects of Coupling Agents on the Mechanical Properties and Rheological Behaviors of the Nano-TiO₂ Filled Low Density Polyethylene (LDPE) Composite: *Chuanchom Aummate*¹; Jittiporn Kruenate¹; Thammarat Panyathanmaporn¹; Thammarak Sooksomsong¹; ¹National Metal and Materials Technology Center

Various concentrations of Tetrabutyl orthotitanate coupling agents were employed to investigate its effect on nano-TiO₂ particles filled low density polyethylene (LDPE). In this paper the nano-TiO₂ particles were prepared

by using surface treatment method before adding into the LDPE matrix. The coupling agents of Tetrabutyl orthotitanate type were used not only to overcome the agglomeration phenomenon of the additives in the matrix but also to improve the mechanical and rheological response of the composite. The mechanical properties and rheological behaviors of the composite were improved in a certain range. This is because the coupling agent might facilitate the link between the nano-TiO₂ particles and the LDPE matrix. The result from FTIR studies indicated a strong adhesion/bonding between the surface-modified nano-TiO₂ particles and the LDPE matrix. In addition, the SEM studies also revealed a better dispersion of surface-modified nano-TiO₂ particles.

Effects of Filler Characteristics and Filler Contents on Physical Properties of HA/PLA Composites: *Suriyan Rakmae*¹; *Yupaporn Ruksakulpiwat*¹; *Wimonlak Sutapan*¹; *Nitinat Suppakarn*¹; ¹*Suranaree University of Technology*

Biodegradable polymers have recently been introduced to various fields as alternatives to traditional materials. Among those polymers, poly(lactic acid) (PLA) is attracting attention as a biomaterial owing to its biocompatibility and absorbability. Mechanical properties of PLA are crucial properties that should be concerned for various applications e.g. orthopaedic applications. As another attempt to improve the mechanical properties of PLA, PLA composites can be prepared by combining it with hydroxyapatite (HA), a calcium phosphate similar to the inorganic content of bone. In this work, natural HA powders were produced from cattle bone, which is a natural and less expensive source for producing HA. Effects of filler characteristics and filler contents on morphology and mechanical properties of HA-PP composites were investigated.

Flame Retardant and Mechanical Properties of Glass fiber/PP Composites: *Rachasit Jeencham*¹; *Kasama Jarukumjorn*¹; *Nitinat Suppakarn*¹; ¹*Suranaree University of Technology*

Polypropylene (PP) composites have been widely used in various applications due to their inexpensive cost and acceptable properties. However, their high flammability limited their uses in several applications e.g. automotive parts, electronic devices. In this work, magnesium hydroxide (Mg(OH)₂) as a flame retardant was incorporated into milled-glass fiber/PP composites. Ratio of glass fiber to Mg(OH)₂ in each composite sample was varied. Maleic anhydride grafted polypropylene (MAPP) was used to improve the interface of polypropylene and fillers. Flammability and thermal behaviour of the composites were examined using a horizontal burning test and thermal gravimetric analyzer, respectively. Morphology and mechanical properties of the composites were also investigated. In addition, effect of flame retardants such as boric acid or zinc borate in combination with Mg(OH)₂ was also studied.

Formation and Characterization of Bulk Amorphous/Amorphous Composite Alloys by Mechanical Alloying and Vacuum Hot Pressing: *Pee-Yew Lee*¹; ¹*National Taiwan Ocean University*

In the present study, amorphous Ni₆₀Nb₂₀Zr₂₀ and Ti₅₀Cu₂₈Ni₁₅Sn₇ alloy powders were synthesized separately by using a mechanical alloying technique. The dual-amorphous-phased (Ti₅₀Cu₂₈Ni₁₅Sn₇)_{100-x}(Ni₆₀Nb₂₀Zr₂₀)_x (x = 0, 10, 20, and 30 vol %) powders were prepared by mixing the corresponding amorphous powders. The dual-amorphous-phased powders were then consolidated into bulk amorphous/amorphous composite (BA/AC) alloy discs. The amorphization status of as-prepared powders and bulk BA/AC composite discs was confirmed by X-ray diffraction and transmission electron microscopy. The microstructure of the BA/AC discs showed that the Ni₆₀Nb₂₀Zr₂₀ phase is distributed homogeneously within the Ti₅₀Cu₂₈Ni₁₅Sn₇ matrix. The (Ti₅₀Cu₂₈Ni₁₅Sn₇)₇₀(Ni₆₀Nb₂₀Zr₂₀)₃₀ BA/AC disc exhibited a relative density of 96.6% and its Vickers microhardness was 726 kg/mm².

Loading Zeolite as a Filler into the Unsaturated Polyester Resin: *Chuntip Kummuantip*¹; *Nattawut Lumkum*¹; *Suchat Dornthongdee*¹; *Nontipat Luengthongkum*¹; ¹*Rajamangala University of Technology Thanyaburi*

This work aimed to investigate the properties of the unsaturated polyester resin (UPR), which loaded with zeolite as the filler. The various contents of

zeolite, from 10 to 100 phr were loaded into the UPR. The zeolite loaded UPR samples were prepared by casting process at the room temperature. The properties of those samples were tested and compared with the calcium carbonate loaded UPR samples. The impact strength was tested according to ASTM D256 standard. The flexural strength was tested under condition of ASTM D790 standard. Hardness (Shore D) was tested depended on ASTM D2240 standard. The flame resistance was tested according to UL94 standard. The results suggested that the flexural modulus and hardness increased with the zeolite contents. However, the flexural strength decreased with the zeolite contents.

Mechanical Properties and Cure Characteristics of Natural Rubber Composites: Effect of Filler Types: *Kasama Jarukumjorn*¹; *Nitinat Suppakarn*¹; *Phakphum Sakuna*¹; *Wittawat Wongsorat*¹; ¹*Suranaree University of Technology*

Nowadays, materials from natural/renewal resources gain more attention in several applications due to environmental concerns. Among those kinds of materials, natural fibers can be alternative fillers for reinforcing natural rubber. In this study, natural rubber was reinforced with three types of fillers: carbon black, calcium carbonate, and sisal fiber. The filler content was 20 phr. Mechanical properties and cure characteristics of the composites were examined. In addition, the influence of fiber treatment(alkalization) on the mechanical properties and cure characteristics of the natural rubber-sisal fiber composites was investigated. The effect of sisal fiber and conventional fillers:carbon black and calcium carbonate on the mechanical properties of the composite was compared.

Preparation and Properties of Natural Rubber/Clay Nanocomposites: *Chalermpan Keawkumay*¹; *Kasama Jarukumjorn*¹; *Nitinat Suppakarn*¹; ¹*Suranaree University of Technology*

Natural rubber (NR) has many attractive properties including low cost, low hysteresis, high resilience, excellent dynamic properties, fatigue resistance and strain-induced crystallization. This work attempted to enhance mechanical properties of NR by preparing organoclay/NR nanocomposites. Moreover, epoxidized natural rubber (ENR) was also used to improve the interface between NR and organoclay. Effect of surface treatment of organoclay and effect of ENR on cure characteristics, morphology and mechanical properties of organoclay/NR nanocomposites were examined.

Energy Materials Processing Poster Session

Mon AM-Wed PM
December 8, 2008

Room: Auditorium B2, Bangkok Convention Centre
Location: Sofitel Centara Grand Bangkok

Evaluation of the Crofer 22 APU Stainless Steel Used as Interconnect in Solid Oxide Fuel Cells Oxidised in Dry and Humidified Cathode Atmospheres: *Somverk Chandra-ambhorn*¹; ¹*King Mongkut's University of Technology North Bangkok*

A new batch of Crofer 22 APU stainless steel (Fe-23Cr-0.43Mn-Ti-La) was evaluated in dry and humidified cathode atmospheres of solid oxide fuel cells (SOFCs). The cyclic oxidation at 800 to 1000°C was evaluated in dry air. The oxide scale on the sample did not spall in all studied conditions, but was suffered from the distortion of the steel plate due to the thermal cycles during the test, severely at 1000°C. The discontinuous isothermal oxidation was further conducted in pure oxygen and oxygen with 13% v/v water vapour. The spallation was not observed in all studied conditions. The oxidation rate of specimen oxidised in humidified oxygen seemed to be identical to that oxidised in the dry one. Oxidation kinetic parameters obtained in this work were discussed with those reported in the literature.

Influence of Annealing Conditions for Synthesized Powder on Grain Growth in GdPrS₃ Sintered Compact: *Hideito Sasaki*¹; Shinji Hirai¹; Michihiro Ohta²; Toshihiro Kuzuya¹; ¹Muroran Institute of Technology; ²National Institute of Advanced Industrial Science and Technology

Cubic Th₃P₄-type GdNdSe_{2.6} in which the carrier concentration is optimized due to Se deficiency and in which impurities are introduced to scatter phonons is known to have an excellent thermoelectric properties in the high-temperature range. In this study, a cubic Th₃P₄-type GdPrS₃ sintered compact was synthesized according to the following procedure. (1) A multiple oxide containing Gr and Pr was produced by the complex polymerization method. (2) Rhombic GdPrS₃ was produced from the multiple oxide by CS₂ gas sulfurization. And (3) the cubic Th₃P₄-type GdPrS₃ sintered compact was produced from the rhombic GdPrS₃ by annealing in a vacuum followed by pulsed electric current sintering. In particular, the influence of the annealing conditions on the oxygen and carbon impurity concentrations in the synthesis powder before sintering and the crystal grain size, composition, and thermoelectric property of the sintered compact was investigated.

Synthesis and Sintering of Single-Phase ReCuS₂ (Re: Nd, Pr, Sm, and Gd) Powders: *Massoud Omar*¹; Kohei Ohki¹; Michihiro Ohta²; Toshihiro Kuzuya¹; Shinji Hirai¹; ¹Muroran Institute of Technology; ²Advanced Industrial Science and Technology

Although rare-earth transition-metal sulfides have layered structures and excellent thermoelectric properties are expected similar to layered cobalt oxides, the thermoelectric properties of only a few sulfides have been reported. In this study, single-phase ReCuS₂ (Re: Nd, Pr, Sm, and Gd) powders were synthesized according to the following procedure. (1) Multiple oxides containing rare-earth elements and copper were produced by the complex polymerization method. (2) The produced multiple oxides were sulfurized by CS₂ gas. And (3) the single-phase sulfuration products were repeatedly pulverized and sulfurized for a maximum of three times. The sulfurization of the multiple oxide powders was confirmed to follow the unreacted core model. The sintered compacts were produced by pulsed electric current sintering at a sintering temperature just below their melting points, and the thermoelectric properties of these sintered compacts were compared.

Synthesis and Thermoelectric Property of Th₃P₄-Type SmEuGdS₄: *Taku Kawasaki*¹; Michihiro Ohta²; Shinji Hirai¹; Toshihiro Kuzuya¹; ¹Muroran Institute of Technology; ²National Institute of Advanced Industrial Science and Technology

EuGd₂S₄ is known to be a p-type semiconductor synthesized by the solid-phase reaction of EuS and Gd₂S₃, which are produced from rare-earth chlorides by H₂S gas sulfuration. Only a few Th₃P₄-type rare-earth sulfides have p-type electrical conductivity. In this study, Th₃P₄-type SmEuGdS₄ with stoichiometric composition and non-stoichiometric composition was synthesized according to the following procedure. (1) A multiple oxide containing Sm, Eu, and Gd was produced by the complex polymerization method. And (2) the produced multiple oxide was sulfurized by CS₂ gas. SmEuGdS₄ and EuGd₂S₄, which was produced by the same procedure as that of SmEuGdS₄, were annealed in order to increase their purity level. Subsequently, their sintered compacts were individually produced by pulsed electric current sintering, and their thermoelectric properties were compared.

Thermal Oxidation Kinetics during the Rotational Moulding of Polypropylene: *Sarrabi Salah*¹; Tcharkhtchi Abbas¹; ¹Laboratoire d'Ingénierie des Matériaux-Ecole Nationale Supérieure d'Arts et Métiers Paris

Rotational moulding is a polymer process method to create hollow plastics parts. This technique has a main disadvantage, a relative long cycle time which can cause a loss of final parts properties. Optimisation of rotational moulding conditions result in better understand thermal oxidation kinetic. This poster studies the thermal oxidation of polypropylene (PP) during its rotational moulding. In these conditions, a kinetic model has been derived from a realistic mechanistic scheme, in which Volatile Organic Compounds (V.O.Cs) and particularly Acetone is considered. We used this model to simulate the kinetic of polypropylene (PP) thermal oxidation in its molten state. Typically, for a temperature ramp from 170 to 250°C and 250 to 170°C with various heating rates. The validity of this model has been shown by

experimental results of mass loss and ketone groups build-up according to ageing time in a polypropylene film with a 40 µm thickness.

Environmental Protection Processing Poster Session

Mon AM-Wed PM
December 8, 2008

Room: Auditorium B2, Bangkok Convention Centre
Location: Sofitel Centara Grand Bangkok

Development of A Novel Impregnated Resin for High Selective Recovery of Lithium from Seawater: *Kenta Oonishi*¹; Yasuhiro Suzuka¹; Takahide Nakamura¹; Youhei Nishihama¹; Kazuharu Yoshizuka¹; ¹University of Kitakyushu

In recent years, the recovery of lithium from seawater has been developed, but it is difficult to recovery high-purity lithium due to the large amounts of contaminations such as sodium, magnesium, potassium etc. We have been developing a novel adsorbent having high selectivity toward lithium ions, that is, resin impregnated with β-diketone type extractant. Since the adsorption of lithium with impregnated resin increases with increase of pH value, the impregnated resin possesses the sufficient adsorption ability at high pH region. The impregnated resin also possesses high selectivity toward lithium ions in the presence of sodium and potassium. The impregnated resin is therefore suggested to be the most suitable separating material for using the separation process of lithium from seawater.

Novel Nano-Porous Adsorbent for Adsorptive Separation of Lithium from Geothermal Water: *Hideki Sato*¹; Yasuhiro Suzuka¹; Youhei Nishihama¹; Kazuharu Yoshizuka¹; ¹University of Kitakyushu

Novel nano-porous λ-MnO₂ adsorbent was developed specialized for adsorptive separation of lithium from geothermal water. The adsorption behavior was investigated at various temperatures, because the present adsorbent possesses the sufficient adsorption ability at high temperature as well as at high pH region. The adsorbent was then granulated by alumina-based binder to apply to the column operation of lithium recovery from geothermal water. Lithium could be selectively recovered by the granulated adsorbent, though arsenic and slight calcium were also adsorbed. The pre-treatment of arsenic prior to the lithium recovery has to be required, preventing from the arsenic adsorption.

Novel Zeolitic Adsorbents for Separation and Recovery of Tetramethyl Ammonium Hydroxide: *Kouhei Takatori*¹; Youhei Nishihama¹; Kazuharu Yoshizuka¹; ¹University of Kitakyushu

Separation and recovery of tetramethyl ammonium hydroxide (TMAH), which widely used in IC manufacturing industry and is quite toxic, has been investigated, employing zeolite A and zeolite X as adsorbents. The adsorption of TMAH with the zeolitic adsorbents increases with increase in pH value of aqueous solution. This indicates that the zeolitic adsorbents are suitable for the adsorptive removal of TMAH from the TMAH waste solution with alkaline region. When sodium ion in the zeolite was exchanged with several divalent cations such as calcium and strontium, the adsorption ability of TMAH increases due to the increase of the pore size of the adsorbent. Zeolitic adsorbent prepared with TMAH as a template has also high adsorption ability. Based on these fundamental results, the separation and recovery process of TMAH with column operation has been developed.

Recycling of Mg-Al-Zn Based Alloy by Vacuum Distillation: *Makoto Inoue*¹; Masashi Shima¹; Tetsuo Aida²; ¹Toyama National College of Technology; ²Toyama University

In this study, it examined recycling of a Mg-Al-Zn based alloy by vacuum distillation. The vacuum distillation used a vacuum distillation apparatus and I evacuated a vacuum and heated a Mg-Al-Zn based alloy to less than 1 Pa at 600°C. In making magnesium deposit got by the vacuum distillation method to be a billet for the extrusion, the extruding was carried out. There was no contamination of the impurity except for Zn on the chemical composition of extrusions. The corrosion resistance of extrusions was better than the AZ91D

magnesium base alloy die castings. The elongation of the extrusions was decreased a little from pure magnesium, and tensile strength, 0.2% proof stress and hardness of the extrusions increased.

Zeolitic Ion Exchanger for Adsorption of Molybdenum: *Syouhei Nishihama*¹; Kazuharu Yoshizuka¹; ¹University of Kitakyushu

Zeolitic ion exchangers were prepared for the adsorption of molybdenum, which is important material as the additive for ferroalloys. The adsorption of molybdenum with zeolitic ion exchanger increases with decrease in the pH value of the aqueous solution. This indicates cation species of the molybdenum is adsorbed via cation exchange. The adsorption also increases with increase in the pore size of the zeolite due to large ion size of the molybdenum. The column operation is applied using granulated zeolite with alumina-based binder for the adsorptive separation process of molybdenum.

Preparation of Bamboo Activated Carbon for the Recovery of Tetramethyl Ammonium Hydroxide: *Ayako Yamaguchi*¹; *Syouhei Nishihama*¹; Kazuharu Yoshizuka¹; ¹University of Kitakyushu

Activated carbon (AC) has been prepared from bamboo to apply as an adsorbent for the tetramethyl ammonium hydroxide (TMAH), which widely used in IC manufacturing industry and is corrosive compound. The AC prepared with the several conditions was characterized. The batchwise adsorption of TMAH with the AC revealed the adsorption increases with increase in the pH of the aqueous solution. This indicates the AC can be applied for recovering TMAH in waste solution. TMAH was also recovered by using AC column from the aqueous solution to develop treatment process for the waste solution.

Methanol crossover from anode to cathode is a main problem of commercial application. Our idea is to use nano silver particles stacked and sintered at low temperature to form small pore surface structure on the anode to increase the diffusion barrier. The principle is as the particle size decreases the pore size also decreases and hence the diffusion barrier increases. The firing of the nano silver coating is done at 150°C.

Casting of Intermetallic Alloy g-TiAl: *Li Sen Lin*¹; ¹Pratt and Whitney

This study will consider the casting.

Superplastic Deformation of Zr65Al10Ni10Cu15 Metallic Glass: *HaGuk Jeong*¹; ¹Korea Institute of Industrial Technology

Metallic glass alloys attract much attention due to their unique properties, such as superior strength, low elastic modulus, excellent corrosion resistance, low sliding friction and improved wear resistance. Besides these merits, some of them can exhibit superplasticity at elevated temperatures, allowing near-net-shape forming. They typically show the property in the specific temperature range so called supercooled liquid region defined by the difference between glass transition temperature (T_g) and crystalline temperature (T_x). The Zr65Al10Ni10Cu15 metallic glass is one of such alloys. The Zr65Al10Ni10Cu15 metallic glass sheet, which is fabricated by squeeze copper-mold casting, was deformed as a dome-shaped object by gas blowing technique at 696K. During the deformation some nanometer scale crystals appear in the alloy matrix. Furthermore a variation of crystallization degree was shown depending on deformed region, even though the sample was exposed at the same temperature during deformation. In the present work, the variation of crystallization in a sample is studied and discussed with a high resolution transmission electron microscopy.

Mechanical Behavior of Magnesium Alloy AZ31 Subjected to Consecutive Conventional Extrusion Followed by Equal Channel Angular Pressing (ECAP): *Sangmok Lee*¹; *Duk-Jae Yoon*¹; ¹Korea Institute of Industrial Technology

A new severe plastic deformation (SPD) process was developed by employing a combination of direct extrusion consecutively followed by Equal Channel Angular Pressing at the end of extrusion exit in attempting to refine microstructure of and enhance mechanical properties of Magnesium alloy AZ31. Microstructure after the process was observed by Optical and Electron microscope. Mechanical behavior was observed by tensile test at various strain rates. Finally, the results was compared with ones in other combined SPD processes.

Electrodeposition of Silver from Alkaline Bath on Ruthenium Substrate: *Seong-Ho Son*¹; *Hong-Kee Lee*¹; *Dae-Chol Kwon*¹; ¹Korea Institute of Industrial Technology

The purpose of this study is to investigate a rate determining step in electrodeposition of Ag in non-cyanide and alkaline solution. For this, rotating disk electrode system (RDE) was used. The effect of rotating speed on the electrodeposition rate of Ag was larger than that of temperature. The rate determining step of Ag electrodeposition was found out through activation energy of reaction. The activation energy of Ag in temperature range between 18°C and 32°C was 3.2kcal/mole and this implies that the electrodeposition rate of Ag is controlled by mass transport through a diffusion layer. Properties of Ag thin film and behavior of bottom-up filling were investigated with DC/pulse current conditions and species of additives. Also, the electrochemical behaviors in electrodeposition of Ag were examined with various organic additives.

Photochemical Activation Bonding of Cyclo-Olefin Polymer Plates: *Young-Jong Kim*¹; *Hiroyuki Sugimura*¹; *Yoshinao Taniguchi*²; *Yoshihiro Taguchi*²; ¹Kyoto University; ²Alps Electric

Vacuum ultra-violet (VUV) light and VUV-generated active oxygen species have been used to introduce polar functional groups on the surface of cycloolefin polymer (COP) substrates. COP substrates located in air were irradiated with VUV light at a wavelength of 172 nm. XPS analysis shows O1s and C1s spectra of the COP substrate surfaces when treated with VUV irradiation. The C1s spectra contain distinct signal components in the region of 286 - 290 eV. These components correspond to C-O, C=O and COO groups. Thus, COP substrate surface are proved to be oxidized with the VUV-

Materials Processing Poster Session

Mon AM-Wed PM
December 8, 2008

Room: Auditorium B2, Bangkok Convention Centre
Location: Sofitel Centara Grand Bangkok

Preliminary Study of the Synthesis of LaCoO₃ and LaNiO₃ Catalysts for Fuel Gas Conditioning: *Duangduen Atong*¹; *Siritha Ausadasuk*¹; *Viboon Sricharoenchaikul*²; ¹National Metal and Materials Technology Center; ²Chulalongkorn University

The product gas formed from biomass gasification for the production of fuels mainly contains CO, CO₂, H₂, CH₄ and other high molecular weight hydrocarbons, collectively known as tars. Production of tar free synthesis gas from gasification of biomass is seen as one of the greatest challenges for the successful development of efficient downstream fuel gas utilization processes. This present work reported the development of LaMnO₃ and LaCoO₃ catalysts which exhibit favorable activity for cracking of tar commonly found in biomass gasification process. Two methods were used in the preparation of perovskite type oxides which are co precipitation and sol-gel. Phase of prepared catalysts were determined by X ray diffraction (XRD). The specific surface area of the catalysts was evaluated using the BET technique. Scanning electron microscopy (SEM) and energy dispersion spectroscopy (EDS) were used to examine the morphology and elemental composition of obtained catalysts. Catalytic activity tests were performed with tar model compound under atmospheric pressure with different temperature of 400 800°C and partial oxidation conditions to confirm tar conversion efficiencies as well as study catalyst deactivation patterns.

Processing of Porous Silver Tape for Use as Direct Methanol Fuel Cell Electrode: *Mohammad Siddiqui*¹; *Yong Gao*¹; ¹Florida International University

The objective of this work is to design micro direct methanol fuel cells (DMFCs) by LTCC technique. LTCC structure can integrate many conductor, resistors and different active and passive components and can be manufactured in large scale comparing to current Si-based technology. In our LTCC-based DMFCs, the porous silver tape will be used to replace the traditional carbon electrode. The porous silver tape has been successfully studied in our lab.

generated active oxygen. Finally, COP plates with such an oxidized surface were successfully joined by compression bonding at a temperature below the glass transition temperature of COP.

Cationic Surfactant Modified Clay as Finishing Agent on Cotton Fabric: *Nantana Jiratumnukul¹; Siriwan Kitinawat¹; Narissara Koolpreechanan¹; ¹Chulalongkorn University*

Na-monomorillonite clay (Na-MMT) was modified by cationic surfactant using cationic exchange process. X-ray Diffraction pattern indicated that intercalation structure of modified clay was obtained. Cationic surfactant modified monmorillonite was incorporated to softening finishing formulation. Cotton fabric was finished using prepared finishing formulation by pad-dry cured method. Physical properties of finished cotton fabric were tested. The results showed that flame retardant property of finished cotton fabric increased when the amount of modified clay in the formulation increased. However, the softness of finished fabric decreased when the amount of modified clay in the formulation less than 5%. Nevertheless, incorporation of modified clay more than 5%, the softness of finished fabric increased. Moreover, it was found that the higher the amount of cationic surfactant modified clay was incorporated, the greater the reduction in whiteness of finished fabric. Tear strength of finished fabric was nearly the same level of those of unfinished cotton fabric.

Effect of Thermo-Mechanical Processing on Microstructure and Mechanical Properties of Ti-26Nb-Ge Alloys for Biomedical Application: *Won-Yong Kim¹; Han-Sol Kim¹; ¹Korea Institute of Industrial Technology*

Mechanical properties and elastic modulus were examined in order to clarify the influence on microstructures in Ti-26Nb-xGe, where $x=0.5\sim 1.5$ in atomic percent, prepared by arc melting, quenching, cold rolling and recrystallization heat treatment. On the basis of microstructural observations and phase analyses, it is evidently revealed that the microstructure of as-quenched sample appeared to mixture appearance consisting of mostly bcc-structured β -phase and small amount of orthorhombic-structured α'' -phase. Mixed features consisting of rotated cube and α -fiber components were characterized in cold rolled samples. Recrystallization heat treatment caused $\{111\}<110>$ fiber component to be markedly enhanced, while the intensity of rotated cube component decreased. The elastic modulus of cold rolled alloys exhibited higher values than those of recrystallized alloys in the chemical composition range investigated. The variation of elastic modulus values was interpreted in terms of changes in texture components depending on thermo-mechanical processing.

Impregnation of Ni-Al₂O₃ Catalyst for Methane Reforming: *Chartsak Chettapongsaphan¹; Navadol Laosiripojana¹; Sumittra Charojrochkul¹; Suttichai Assabumrungrat²; ¹National Metal and Materials Technology Center; ²Center of Excellence in Catalysis and Catalytic Reaction Engineering*

Hydrogen supply is the key factor for a fuel all commercialization in the future. There are many processes for hydrogen production from various sources of hydrocarbons i.e. steam reforming, partial oxidation. Ni-Al₂O₃ catalyst has been used in a steam reforming of methane in petrochemical industry. In our study, this type of catalyst has been fabricated via an impregnation process yielding comparable catalytic activity with commercially available catalyst. Our fabricated catalyst has been investigated using SEM, EDX for the morphology and elemental distribution of Ni. The main advantages of our process are simple, lime and cast effective technique.

Synthesis and the Lyotropic Liquid-Crystalline Behavior of Calamitic Liquid Crystals with a Coline Phosphate Moiety: *Junji Sekiguchi¹; Kiyoshi Kanie¹; Atsushi Muramatsu¹; ¹Institute of Multidisciplinary Research for Advanced Materials, Tohoku University*

Artificial phospholipids have been attracted a great deal of attentions, especially in the field of biochemistry, pharmacy and materials science, because design and synthesis of the amphiphilic phospholipids to form lipid bilayers would enable us to develop new artificial ion channels, biological sensors, and so on. In the present research, we focused our attention on the design and synthesis of new phospholipids having electro- or light-responsive calamitic mesogenic cores for the development of liquid-crystalline phospholipids. Introduction of such properties into artificial phospholipids

would be expected to develop electro- and light-responsive solid films controlling ion and/or material transportation-insulation. In the present report, the pH influence to the lyotropic liquid-crystalline phase behavior and the structure of phospholipids with calamitic cores in aqueous medium were examined by using POM, DSC, and SAXS. Furthermore, the electro-optical property of the liquid crystals was also investigated.

The Effect of Flow Condition in Electrolyte Bath on Anodic Film Thickness Produced on Extruded 6063 Aluminium Profile by Using Flow Analysis Simulation: *Thanaporn Korad¹; Umarin Phongsopititanan¹; Niphon Chumchery¹; ¹National Metal and Materials Technology Center*

In anodizing extruded 6063 aluminium profiles, anodic oxide film forming on the workpiece surface is sometime difficult to control uniformly. Applying current, suitable condition of electrolyte and the sufficient circulation in electrolyte bath are controlled to ensure that the correct electrochemical reaction of anodizing is presented. In this study, 3D flow analysis technique was applied to simulate flow of electrolyte in the electrolyte bath. Studying the effect of different flow in electrolyte bath was focusing on the representative areas, particularly the corners on the complicated designed profiles. Two extruded profiles were selected under the anodizing condition consisting of anodic film thickness of 8-10 microns, current density of 6,000-7,000 amp/m², a voltage of 19 Volt and anodizing temperature of 23°C for examination. The results obtained indicate that different flow character and different flow rates on different positions effected to anodic film thickness that was measured via optical microscope.

Alumina Ceramic Material for Compensate of the Blow Gate: *Piboon Kangtrakul¹; Kuljira Sujirote¹; ¹National Metal and Materials Technology Center*

The purpose of this research was to study Alumina Ceramics Material integration usage in part of sand pipeline for compression sand mould of the Aluminium Casting. The research presents comparison of Wear Resistance between Alumina Ceramics (Al₂O₃) and Tool Steels (SKD61). Wear Rate data gathering follow the DOE method (Design Of Experiment), to define variables, gather Wear Resistance data, Hardness and Young Modulus testing in the comparison of Alumina Ceramics (Al₂O₃) and Tool Steels (SKD61). The useful life of alumina ceramic material is a longer than tool steel therefore alumina ceramic can reduce cost and setup time. And also increase productivity

Wear Behavior of Alumina Nozzles by Sand Blasting: *Pattraporn Wichianrat¹; Kuljira Sujirote¹; Kannigar Dateraksa¹; ¹National Metal and Materials Technology Center (MTEC)*

Sand blasting as a cleaning method has been widely used for the application of paint or a sealant. This process is suitable for the treatment of metals, ceramic and can provide perfect surface treatment such as surface strengthening, surface modification, surface smoothing and surface clearing. The important process of sand blasting are the nozzles material because the abrasive particles are directed towards surface of the nozzles and it cause a surface fracture. In this paper, to study the wear rate of alumina nozzles by pressing technique and compare with commercial nozzles and used the nozzles 6 mm for our experiment. The erodent abrasives used in this study were of silica, silicon carbide and alumina powders under the same condition. The cumulative mass loss of the nozzles, fracture surface and hardness were investigated. It was found that the wear rate of alumina nozzles increased with increasing the hardness of erodent abrasives.

Study on Melt Spinning of Shaped Hollow Polypropylene Fibers: *Chureerat Prahsarn¹; Natee Srisawat²; ¹National Metal and Materials Technology Center; ²Rajamangala University of Technology Thanyaburi*

Hollow fibers have great advantages on insulation, high loft, and light weight. With non-circular cross-sectional shape, the hollow fibers can be expected to have some additional advantages on surface properties. In melt spinning of hollow fibers, there are many factors involving polymer properties and processing conditions that can affect fiber spinnability and fiber properties. It is important to understand the roles and effects of these influencing factors in order to produce hollow fibers with desired properties. In this study, round and triangular-shaped hollow fibers were melt-spun from

polypropylenes of two different melt viscosities (MFI = 12 and 60), under varied processing conditions including spinning temperatures, throughput rates, and fiber take-up speeds. Fiber properties such as fiber cross-sectional features, percent of hollow area in fiber, fiber fineness and luster will be characterized and discussed in relation to those varied parameters.

Fabrication and Organization of Copper-Based Complex Nanostructures: Danping Wang¹; Hua Chun Zeng¹; ¹National University of Singapore

Different structures of Cu₂O particles have been achieved via hydrothermal method. The synthetic parameters including reagent concentration, reaction time, surfactants and inorganic additives have been investigated to understand their effects on the crystal morphology. Sodium citrate, which is commonly used as a capping agent for the fabrications of noble metal particles, serves as the reducing agent to copper(II) nitrate in our experiments. Cetyltrimethylammonium bromide (CTAB), poly vinylpyrrolidone (PVP), and the novel combination of CTAB with polyoxyethylene (20) sorbitan trioleate (Tween-85) alkaline solution have been applied to control the structure and particle size. Inorganic salts such as sodium nitrate and ammonium nitrate also showed their capability to modify particle morphology. We were able to get hexa-pod frameworks, concaved cubes and pentagonal cross-section nanorods by a synergic work of habit growth and preference adsorption of surfactant or inorganic salts.

Optimization of Fabrication Process for High Strength and High Conductivity Cu-Ag Alloys: Hoon Cho¹; Byoung Lee¹; Hyung Jo¹; ¹Korea Institute of Industrial Technology

New trend of miniaturization in information technology device parts requires excellent strength Cu alloys with a satisfactory electric conductivity, simultaneously. The Cu-Ag alloy has been received as representative promising material because the Ag in Cu matrix has lowest electrical resistance. However, the mechanical properties for Cu alloys could be reduced with increasing electrical conductivity. Therefore the process during fabrication should be controlled in order to obtain higher electrical conductivity and mechanical properties, simultaneously. The present study has been carried out to examine the influence of fabrication process on the electrical and mechanical properties of Cu-Ag alloys with various Ag contents (1~12wt.%), and determining microstructure, mechanical properties and electrical conductivity during fabrication process.

Sequential Selective Separation System of Pd(II) and Pt(IV) from Strong HCl Solution by Novel SCN⁻-Retaining Tannin Gel (SCN-TG) Combined with Light on/off Device: Yeon-Ho Kim¹; Shinpei Yakuwa²; Yoshio Nakano³; ¹Tokyo Institute of Technology

Condensed-tannin gel particles with polyhydroxyphenyl groups have been investigated and recognized as a novel adsorbent for the hydrometallurgical recovery process of palladium and platinum from spent catalysts or scraps. However, high [HCl] of the leached solution causes the adsorbability to be decreased. To enhance the adsorption performance of tannin gel, SCN⁻, a softer ligand than Cl⁻, was introduced into the gel-network by electrostatic interaction with the hydroxyl groups protonated under the acidic condition. When SCN-TG (0.6 mmol-SCN/g-dry tannin gel) was used for Pd(II) and Pt(IV) recovery, their adsorption was successfully achieved even in concentrated HCl solution ([HCl] 1 to 5 M) with the adsorption capacity of about 55 mg-Pd/g-(dry SCN-TG) and 30 mg-Pt/g-(dry SCN-TG), respectively. Furthermore, the photosensitive Pt(IV) complexation suggested the light on/off system using SCN-TG: after selective adsorption of Pd(II) under dark condition (light off), the adsorbability of Pt(IV) can be enhanced by light irradiation (light on).

Preparation of Steam Reforming Catalyst via Combustion Synthesis Technique: Waraporn Nualpaeng¹; Navadol Laosiripojana¹; Suttichai Assabumrungrat²; Sumittra Charojrochkul³; ¹Joint Graduate School of Energy and Environment (JGSEE), King Mongkut's University of Technology; ²Department of Chemical Engineering, Faculty of Engineering, Chulalongkorn University; ³National Metal and Materials Technology Center

Hydrogen is a source of energy for the future but it rarely exists in its free form naturally. A reforming reaction is a widely used technique for

hydrogenation from hydrocarbon. A catalyst is needed to assist in the decomposition of hydrocarbon in this reaction. Ceria-based materials are selected to be used as catalyst in this study. They have been prepared via a combustion synthesis technique using metal nitrate and different fuel as an initial reactant. Phase and the crystallite size of the combusted products are determined using XRD. Particle sizes are measured using laser diffraction particle size analyzer. The specific surface area is determined using nitrogen adsorption isotherm (BET). Particle morphology and microstructure are examined using SEM. In the characteristic of catalytic activity, the stability and deactivation rate are investigated via the steam and dry reforming of methane, proven to have a good performance.

Zeolite – Silver Compound as Antimicrobial Agent in Ceramic Glazes: Sirithan Jiemsirilers¹; Latchanan Soparat¹; Wanida Wanaturaksawong¹; Kongrit Leesooksunt¹; Pornapa Sujaridworakun¹; Dujreutai Pongkao Kashima¹; ¹Chulalongkorn University

Nano and micro silver ions have been widely used as antibacterial agent in many commercial products for example wood, paint, filter, fabrics, and also ceramics. In normal ceramic production it is required a high temperature about 1100-200°C to fire the products. Silver as an element has a low melting point of 900°C. The compound of silver and zeolite was fabricated using impregnation method in order to entrap silver in zeolite structure and be able to withstand higher temperature. Zeolite was impregnated in AgNO₃ solution and then reduced with UV and NaBH₄ compared with non reduced one. As fabricated materials and fired specimens were characterized using XRD, SEM and EDS to identify the present of Ag and zeolite. Finally, the antibacterial activity test of selected samples was performed.

Effects of Heat Treatment on Strength and Ductility of Rolled and Forged Aluminum 6063 Alloy: Sanmbo Balogun¹; Samson Adeosun¹; David Esezobor¹; ¹University of Lagos

Current methods for improving strength and ductility (SaD) are SHT, quenching and age hardening, but data is scarce in the literature on the role of deformation processing of heat treatable (HT) alloys. This work examines the effect of HT on the SaD of rolled and forged AA6063. Cylindrical test samples were rolled, or forged at ambient temperature and then homogenized at 515°C for 22 hours. Some of the samples were HT at 525°C for 12 hours. Each sample was normalized, furnace cooled, water quenched with ageing at 210°C. The results show that the best combination of SaD can be achieved with rolled, solutionized at 525°C and water quenched. The SaD of forged and quenched sample at 525°C is superior to sample solutionized and water quenched. In both samples, the superior SaD are achieved by HT of the alloy at 525°C for 12 hours and water quenched.

Preparation of Ni-Alumina Membrane for Hydrogen Separation: Supawan Kasuriya¹; Duangduen Atong¹; ¹National Metal and Materials Technology Center

Dense ceramic-metal membrane (cermet membrane) was fabricated in order to separate hydrogen from syn-gas generated from gasification process. The hydrogen can further be utilized as fuel feed for highly anticipated energy production scheme of fuel cell. This preliminary work reports the preparation of Pd/Alumina and Pd/Zirconia membranes. Various amounts of palladium, 10 to 50 wt %, were prepared to form monolithic products by uniaxially pressing followed by cold isostatic pressing (CIP). Densification of the cermets were accomplished by pressureless or microwave sintering at temperatures of 1300 – 1400°C. The density of the sample was measured via Archimedes' principle. Phase composition and microstructure were examined by XRD and SEM. Mechanical properties including microhardness, flexural strength, and fracture toughness were also determined. These results were compared and discussed in terms of type of reactants, amount of palladium, heating method, and manufacturing route.

Preparation of Porous Tubular Ceramic Prepared by Extrusion Method for Hydrogen Separation Membrane: Mettaya Kittawan¹; Duangduen Atong¹; ¹National Metal and Materials Technology Center

Palladium-base membrane is known to have high selectivity and stability for hydrogen separation. In order to increase hydrogen permeation and separation factor, the membrane must be thinner and defect-free. Palladium

membrane supported on a porous alumina prepared by means of electroless plating is the promising method to provide good hydrogen permeability. The alumina tube substrate was pre-seeded by immersing in the palladium acetate solution and followed by reduction in the alkaline hydrazine solution. After that, the deposition of palladium membrane can be achieved from the plating bath containing EDTA stabilized palladium complex and hydrazine. The porous intermediate layer was introduced to surface of support. During the electroless plating process, the palladium growth from activation layer forming a structure of filled metal inside porous substrate. Therefore, the palladium membrane can be developed to have superior mechanical strength through the pore-filling process.

Modeling Material Processing Poster Session

Mon AM-Wed PM
December 8, 2008

Room: Auditorium B2, Bangkok Convention Centre
Location: Sofitel Centara Grand Bangkok

Computational Study of the Fatigue Behavior of Aluminum A356 Car Wheel: Karuna Tuchinda¹; Pimpon Dawan¹; Donlapa Kitkaew¹; Mantana Veerachinnapong¹; ¹King Mongkut's University of Technology Thonburi

Car wheel is one of the most important parts in the manufacturing industry of a car. Generally, car wheel failure is caused by mechanical fatigue which depends on many parameters, i.e. dimension and geometry, manufacturing process, material's properties and in-service conditions. The understanding in fatigue behavior of the part under real conditions would enhance the accuracy in predicting the service life of a wheel. In this work, the fatigue behavior of a car wheel made by cast aluminum (A356) will be studied using finite element techniques. The loading conditions experienced by a wheel during service will be simulated. The fatigue tests will also be carried out together with the microstructural examination. The finite element model will then be used to study the effect of in-service parameters, i.e. mean stress and car speed, on the life of a wheel.

Crack Monitoring for Metal Parts Using Digital Image Processing: Suparerk Sirivedin¹; Chatchawan Sonsiri²; Somchai Singto³; ¹King Mongkut's University of Technology North Bangkok; ²Srinakharinwirot University, Ongkarak; ³Chulachomklao Royal Military Academy

To prevent failure due to crack propagation in piping system, the development of crack monitoring system is essential. In practice, engineers have to go to the site to evaluate the cracks, which leads to an impact in overhead cost. At the present time, a handy digital camera can be exploited by taken the photographs of cracks and send them via internet to engineers. This work used digital image processing method to evaluate crack propagation in mechanical parts. The stress intensity factor, KI was calculated and compared with the fracture toughness of material, KIC. The strain energy release rate, G and toughness resistance, R were also calculated and compared with the result predicted by KIC method. The finite element analysis was also employed to compare the results with the experiment. It has been found that using digital image processing to monitor crack growth obtains better accuracy than measuring the displacement.

Modeling of the BOF Process Supported by Off-Gas Measurement: Noppon Jirathanakul¹; ¹Sirindhorn International Thai-German Graduate School of Engineering (TGGS)

This work will give an overview of the existing BOF process models and the results obtained with these models. In this work thermodynamic based concept will be used to develop the model. The development of model of a carbon balance for the BOF process by use of the CO- and CO₂-concentrations in the BOF off-gas as online input parameters to identify the tapping point. The other input parameters are: initial chemical composition and temperature of hot metal and scrap, volume flow of O₂, tapping carbon concentration and temperature and thermodynamic data. After finishing the model, the determination of concentration and temperature curves with the

Technical Program

developed model for lab scale experiments will be done. Comparison of the results between the model and experiment will be discussed.

Nanomaterials Processing Poster Session

Mon AM-Wed PM
December 8, 2008

Room: Auditorium B2, Bangkok Convention Centre
Location: Sofitel Centara Grand Bangkok

Hydrothermally-Induced Gold Sponges via Self-Assembly of Au Nanoparticles: Zhang Yu Xin¹; Zeng Hua Chun¹; ¹Minerals, Metals and Materials Technology Center

In this work, we present a self-assembly approach for generation of nanostructured Au sponges by virtue of Au nanoparticles as starting building blocks. It is found that the hydrothermal condition is essential to detach DDT and TOAB surfactants and thus trigger the self-assembly of Au nanoparticles. The resultant Au sponges are comprised of finely branched nanowires whose diameters can be selected in the range of 15-150 nm. The sponge morphology can be further tuned by manipulating surfactant population, concentration of metallic nanoparticles, amount and type of alcohol solvent, process temperature and time, etc. In principle, this template-free approach can also be extended to large-scale 3D organizations of other surfactant-capped transition/noble metal nanoparticles.

Carbon Nanostructures Synthesized by Rapid Quenching of Red-Hot Graphite Rod in Ethanol: Xiaoping Zou¹; ¹Research Center for Sensor Technology, Beijing Information Technology Institute

A number of methods have been developed for the synthesis of carbon nanotubes. However, these methods typically require high temperatures, complex procedures, and metallic catalyst particles. Here, we demonstrate that it is possible to make multi-walled carbon nanotubes directly from red-hot graphite rods. We heated the graphite rods in air until they were red hot (above 800°C) and then plunged them into ethanol at room temperature. After a weak explosion, the ethanol became a little bit muddy solution. We suggest that the rapid quenching and the thermal gradient across the graphite layers cause them to curve and crimp, allowing the edges to bond to each other. The nanotubes have an inner diameter between 1 and 5 nm, and an outer diameter between 10 and 20 nm, and appear to be straight and a few of defects.

Carbon Nanotubes Synthesized by Catalytic Combustion Technique with M(NO₃)_n as Catalyst Precursor: Hongdan Zhang¹; Xiaoping Zou¹; ¹Research Center for Sensor Technology, Beijing Information Technology Institute

Carbon nanotubes have been synthesized by catalytic combustion technique with M(NO₃)_n as catalyst precursor, where M = Fe, Co and Ni. The morphology and microstructure of the obtained materials were measured and analyzed by scanning electron microscope (SEM), transmission electron microscope (TEM) and the graphitized structures were confirmed by Raman spectra. The result shows that better quality CNTs can be achieved with iron nitrate as catalyst precursor, and helical carbon nanofibers were produced with nickel nitrate. Carbon nanotubes with disordered structure were obtained when the catalyst precursor is cobalt nitrate. It is considered that catalyst has important effect on the morphology and quality of CNTs. The growth mechanism of CNTs with different catalyst precursor was also discussed in this paper.

Direct Loading of Metallic Ni Nanoparticle on Titanium Dioxide Photocatalyst through Reductive Deposition at Vapor-Solid Interface: Masaki Yoshinaga¹; Kiyoshi Kanie¹; Nobuaki Sato¹; Atsushi Muramatsu¹; ¹Institute of Multidisciplinary Research for Advanced Materials, Tohoku University

Photocatalytic processes in titanium dioxide has been devoted much effort for practical utilization because titanium dioxide has high oxidation activity. Indeed producible potential of hydrogen as new energy source has been also attracted. However, titanium dioxide requires loading of transition metals or

metal oxides such as Pt, RuO_x, Ni or NiO_x in order to enhance the hydrogen evolution activity, which shows quite low activity without any loading. The conventional method like impregnation often involves processes such as drying up and thermal treatment under hydrogen atmosphere, resulting in agglomeration of particles and then leading to the loss of catalytic performance. Here we propose a novel technique, CVRD (Chemical Vapor Reductive Deposition) method, for metallic nanoparticle preparation directly on either a particle or a thin film surface without aggregation. Metallic nickel nanoparticles loaded by CVRD method successfully promoted photocatalytic activity for hydrogen evolution of titanium dioxide, compared with the nickel-free material.

Effects of Temperature on the Synthesis of Well-Aligned Carbon Nanotube Arrays by Floating Catalyst Chemical Vapor Deposition: Xiaoping Zou¹; Jin Cheng¹; ¹Research Center for Sensor Technology, Beijing Information Technology Institute

In this paper, we discussed the effects of synthesis temperature on the synthesis of carbon nanotubes by ethanol catalytic chemical vapor deposition. To investigate the effects of temperature on the synthesis of CNTs, we have synthesized CNTs at 650°, 700°, 750°, 800°, 850°, and 900° on quartz plates. Our results indicated that aligned carbon nanotubes arrays preferred to grow at higher synthesis temperature. And we also found that the synthesis temperature could affect not only on the aligned growth of carbon nanotubes but also on the graphitization degree and the diameter of carbon nanotubes.

Influence of Stability of Flames on Carbon Nanofibers Prepared by Ethanol Combustion: Jin Cheng¹; Xiaoping Zou¹; ¹Research Center for Sensor Technology, Beijing Information Technology Institute

Various carbon products, such as carbon nanotubes, nanocoils, non-coiled carbon nanofibers, Y-shaped carbon nanofibers, etc., were symbiotic in deposits synthesized by flames. It is difficult to obtain single-type products because there are many factors that could influence on carbon products prepared by flames. Here, we report that the influence of stability of ethanol flames on carbon nanofibers prepared by ethanol catalytic combustion process. Controlled experiments were performed to investigate the influence of stability of flames on carbon nanofibers. The results revealed that carbon nanofibers were affected by the stability of flames.

Mechanical Synthesis of Barium Titanate from Nanocrystalline BaCO₃ and TiO₂: Akira Kondo¹; Hirofumi Shimoda¹; Kazuyoshi Sato¹; Satoshi Ohara¹; Hiroya Abe¹; Makio Naito¹; ¹Osaka University

Mechanochemical synthesis of fine barium titanate (BaTiO₃) nanoparticles using an attrition type milling apparatus was investigated. During the milling, mechanical forces such as compression and shear stress were repeatedly applied on a mixture of BaCO₃ and TiO₂ with no media balls. The formation of BaTiO₃ was observed in the subsequent milling, and its synthesis was completed after only 15 min without external heating. The particle size of the synthesized BaTiO₃ was mostly of several 10 nm.

Organic-Inorganic Hybrid Liquid Crystals: Hybridization of CO₂H-Substituted Spherical Monodispersed Gold Nanoparticles with Organic Liquid-Crystalline Dendrons with an Amino-Group: Kiyoshi Kanie¹; Masaki Matsubara¹; Hiroshi Nakamura²; Atsushi Muramatsu¹; ¹Tohoku University; ²Toyota Centeal Research and Development Laboratories

A novel organic-inorganic hybrid thermotropic liquid crystal with thermotropic cubic mesophases has been developed by the hybridization of organic dendrons having an amino-group with CO₂H-modified spherical gold nanoparticles with narrow size distribution through ionic interaction or formation of covalent bonding. Small angle X-ray scattering and DSC measurements revealed that the hybrids showed thermotropic cubic mesophases in a wide range of temperatures. Effect of the generation of the dendrons, the particle size, and the monodispersity on the formation of the thermotropic mesophases has also been investigated. This technique may lead to the development of novel and dynamically functional materials with light insulating-transmitting property.

Photocatalytic Activities of TiO₂ from Different Origins: Supatra Jinawath¹; ¹Chulalongkorn University

Two types of TiO₂ powder synthesized from different precursors, TiOSO₄ and TiCl₃ by different hydrolysis routes, were characterized for mineral phase, particle morphology, specific surface area and surface charge by XRD, SEM, BET and zetasizer, respectively. Their potential for photocatalysis under UV-irradiation was comparatively assessed through the decolorization of both cationic dye (Methylene Blue) and anionic azo dye (Drimarene Red X-RN) at the natural pH of the aqueous dye solution.

Preparation and Characterization of Silica Nanorods: Guang Zhu¹; ¹Beijing Information Technology Institute

A simple method is presented for the preparation of silica nanorods with a diameter of about 400nm with smooth surface. The silica nanorods were synthesized by physical vapor deposition method at 1300°. The synthesized samples were characterized by means of scanning electron microscopy, transmission electron microscopy and Raman spectroscopy. The results show that synthesized silica nanorods have a uniform size, well-defined shape, and smooth surface, and the morphology and microstructure of silica nanorods are affected by synthesis conditions, such as synthesis temperature, synthesis time, and protection of gas flow rate etc. The possible growth mechanism of silica rods in this process is proposed, and a possible multiple-reaction model was proposed to explain the formation of silica nanorods. The present method has some advantages such as simple experiment set-up, flexible synthesis conditions, and large area synthesis of silica nanorods.

Rare Earth Chalcogenide Fine Particles Derived from Various Rare Earth-Ligand Complexes: Toshihiro Kuzuya¹; Shinji Hirai¹; Michihiro Ohta²; ¹Muroran Institute of Technology; ²National Institute of Advanced Industrial Science and Technology

Transition metal chalcogenide nanoparticles have been synthesized using various metal and chalcogen sources. Especially, metal-thiole or -aliphatic amine complexes enable us to use sulfur powder as chalcogen source for the synthesis of metal chalcogenide nanoparticles. Also thiol and amine molecules serve as surface modifiers to control the crystal growth of nanoparticles and eliminate the surface dangling bonds. Last decade, highly monodispersed nanoparticles with high quantum yield have been synthesized via the reaction between these complexes and sulfur source. On the other hand, thermal decomposition of metal - thiole and - xanthate complexes can provide us an alternative way. Therefore, it is believed that these synthesis strategies can be applied to the synthesis of monodispersed rare earth chalcogenide nanoparticles. In this report, the synthesis of rare earth sulfide fine particle was examined using various rare earth - ligand complexes such as rare earth - thiole, - xanthate and - aliphatic amine.

Synthesis and Characterization of Nanozeolite Microporous Titanosilicate ETS-10 Assisted by Surfactants: Yu Wang¹; Hua Chun Zeng¹; ¹Minerals, Metals, and Materials Technology Center

Microporous titanosilicate, ETS-10, is widely used in ion exchange, and catalytic studies because of its high surface area. This structure comprises of corner-sharing SiO₄ tetrahedra and TiO₆ octahedra linked through bridging oxygen atoms, that constitute from SiO₄ and AlO₄ tetrahedra giving rise to one negative charge for whole framework. The disorder arises from structural faulting along planes parallel to the 12-ring channel directions, and it is allowable to describe the structure in terms of an intergrowth of two ordered polymorphs with tetragonal and monoclinic symmetry, respectively. This work focuses on the synthesis and characterization of nanozeolite ETS-10 by using Tween-85, CTAB, and PVP as surfactant, respectively. Experiments indicate that it is useful to increase the quality of crystal by adding CTAB into gel as surfactant. It is helpful to adjust the size of nanozeolites in order to meet for potential applications in the industry. Further investigation is in progress.

Synthesis and Morphology Control of ITO Nanoparticles by Precious pH Control in Liquid Phase System: *Yosuke Endo*¹; *Kiyoshi Kanie*²; *Kimitaka Sato*³; *Atsushi Muramatsu*²; ¹Institute of Multidisciplinary Research for Advanced Materials; ²Institute of Multidisciplinary Research for Advanced Materials, Tohoku University; ³Dowa Electronics Company

Sputter-deposited ITO (Indium Tin Oxide) thin films have been widely used as a transparent electrode for display devices and touch panels. However, the tedious sputtering processes prevent us the future application of such transparent electrodes. In the present study, we have prepared ITO nanoparticles by precisely pH-controlled hydrothermal method from highly viscous suspension, followed by calcination at relatively low temperatures (~ 300°C). The morphology and the size of the resulting indium hydroxide depended on the initial pH of the highly viscous solution. By the calcination of the indium hydroxide nanoparticles in the presence of Sn source afforded ITO nanoparticles without any changing of the morphology.

Synthesis of Naturally Nanocomposite by Rapid Solidified Al-Mg-Cu Alloys: *Hossein Shokrvash*¹; ¹University of Maragheh

In later investigate on Al50Mg35Cu15 alloy melt-spun ribbons; X-ray and microscopic experiments shows, the amorphous phase resembles FCI quasicrystal. Also very useful accurate crystallized phase manifestation, star form and directionally arranged. Therefore Al50Mg35Cu15 in rapid solidification transform to a novel homogeny multiphase (HMP) structure; as we noted Naturally NanoComposite (NNC). This nano-composite matrix is microcrystalline Al-rich phase as star form, and reinforcement is quasicrystals with particle size 20-40°. The proposed mechanism of NNC materials, for instance Al-Mg-Cu alloys that are trend a intermetallic compounds; in rapid solidification tendency to nucleation of quasicrystals in microcrystalline matrix.

Synthesis of Flower-Like Silica Nanowires: *Guang Zhu*¹; ¹Beijing Information Technology Institute

A novel flower-like silica nanowires was synthesized by using silicon and silica mixed powder as Si source using thermal evaporation method at 1050°. The as-grown product was characterized by scanning electron microscopy, transmission electron microscopy, energy-dispersive X-ray spectroscopy. The results indicated silica nanowires had a flower-like microstructure with smooth surface, and had no metal contaminations. A possible growth model based on vapor–solid mechanism is suggested.

Synthesis of Mono-Sized Silica Nanoparticles by Combustion Technique: *Guang Zhu*¹; ¹Beijing Information Technology Institute

A simple combustion technique is presented for the preparation of mono-sized silica nanoparticles by employing tetraethyl orthosilicates as precursor. The as-grown white sample was characterized by means of scanning electron microscopy. The results showed the size and structure of silica nanoparticles were relative to the unique synthesis conditions. According to the observation and analysis of the scanning electron microscopy images, the possible growth mechanism of silica nanoparticles in this process is proposed.

Synthesis of Nanosized Precipitated Calcium Carbonate: *Nooririnah Bt Omar Irinah*¹; ¹Universiti Teknologi Mara

Precipitated calcium carbonate consists of relatively pure calcium carbonate compared to ground natural calcium carbonate. Important properties of precipitated calcium carbonate are its non-toxicity, low intrinsic colour, weather resistance, low abrasiveness, low electrolyte content and the pH stabilizing effect. Every different kind of crystal is suitable for a particular application and only the right PCC can boost the quality of the end products. Spray method is one of the alternative that we can used to control of crystal size and to produce small particle size. In this study spray gun was used to produce mist milk of lime and will be spray together with CO₂ at the same time but from different nozzle into a chamber. TEM results show particle size of PCC range from 80-250nm. In this study, parameter that been controlled were initial flow rate of CO₂, Calcination temperature and concentration of initial milk of lime.

Synthesize of Silica Nanowires by a Simple versus Reaction: *Guang Zhu*¹; ¹Beijing Information Technology Institute

Silica amorphous nanowires with diameters of 40–100 nm have been synthesized by heating Si/SiO₂/C mixtures with Fe catalyst at 1050° at ambient pressure. The as-grown product was characterized by scanning electron microscopy, transmission electron microscopy, and energy-dispersive X-ray spectroscopy. The results reveal that the obtained silica nanowires had no metal contaminations, and these nanowires are amorphous structure covered by graphite layer. The growth mechanism is assumed to be a vapor–liquid–solid process.

Powder Preparation/Processing Poster Session

Mon AM-Wed PM
December 8, 2008

Room: Auditorium B2, Bangkok Convention Centre
Location: Sofitel Centara Grand Bangkok

Application of Micro Metal Injection Molding Process in Manufacturing Micro Mold: *Wonsik Lee*¹; *Jin Man Jang*¹; *Se-Hyun Ko*¹; *Il-Ho Kim*¹; ¹Korea Institute of Industrial Technology

In this work, manufacturing technologies of micro mold were studied by micro injection molding process, which was perceived from the fact that volume and size of green bodies molded are reduced after sintering. The first metal mold with gear cavity of 1.2 mm in diameter was prepared by wire EDM and a kind of polymer was injected into the cavity, resulting in a tiny polymer gear. Then, stainless steel feedstock was again injected/compressed on the polymer gear and debinded together with polymer gear followed by sintering. As a result, another metal mold with gear cavity reduced to about 20% and through repetition of this process chain, gear mold with cavity below 500µm was finally obtained. In reduction of size, height of gear tooth was shrunk larger and roughness and precision of cavity were not changed almost in respect of size.

Feedstock Infiltration for Manufacturing Open Celled Ti Foam in Metal Injection Molding Technology: *Il-Ho Kim*¹; *Wonsik Lee*¹; *Se-Hyun Ko*¹; *Jin Man Jang*¹; ¹Korea Institute of Industrial Technology

For manufacture of open celled Ti foams, some technologies have developed such as powder-space holder injection method, gel casting and slurry coating on open celled polyurethane foam, etc. However, it seems that most of these techniques are not economical or it is difficult to obtain homogeneous cell structures by them. In this work, new method for manufacture of open celled Ti foam was tried: fabrication of polymer precursor with thin path network and infiltration of feedstock into the path by injection molding method followed by debinding and sintering. Polymer precursor was fabricated by stacking and compressing spherical polymer balls and binder system for feedstock was devised newly to increase flowability at low temperature. In infiltration of feedstock, increase of injection speed caused segregation of binder and powders and after debinding and sintering, open celled Ti foam with porosity of above 70% was obtained.

Manufacture of Micro Two Step Gear by Micro Powder Injection Molding: *Jin Man Jang*¹; *Wonsik Lee*¹; *Seong-Ho Son*¹; *Se-hyun Ko*¹; *Il-Ho Kim*¹; *Jin Mo Lee*²; ¹Korea Institute of Industrial technology; ²P.I.M. Korea

In present work, manufacturing technologies of micro 2 step gear by micro powder injection molding (µ-PIM) were studied with stainless steel(average size of 4µm in diameter) and zirconia (a few tens nm in diameter) powders. Sizes of gears were about 500µm and 2 mm in diameter, respectively. For molding, precision micro mold with roughness below Ra 100 nm was produced by micro electroforming. Injection pressure and temperature were varied to obtained green bodies filled entirely into micro mold. Optimum pressure and temperature in nano zirconia powders were higher than those in micron stainless steel powders, resulting from lower flowability in nano zirconia feedstock. In debinding process, removal of binder was more difficult in nano zirconia feedstock and longer debinding time was required.

After sintering in vacuum, densities of stainless steel and zirconia gears were measured to above 99% and 97%, respectively.

Preparation of Titanium MIM-Feedstock Using a PEG/PMMA Binder: *Nutthita Chuankrerkkul*¹; Wen Xu²; Muhammad Ismail²; Alfred Sidambe²; Iain Todd²; ¹Chulalongkorn University; ²Innovative Metal Processing Centre (IMPC)

Titanium and its alloys are well-known for their unique properties such as relatively low density, excellent corrosion resistance, high strength and biocompatible. They are widely used in aerospace or biomedical applications. Metal injection moulding (MIM) is a cost effective process for a fabrication of small, complex-shaped components for high performance applications. In this work, a binder system, composed of polyethylene glycol (PEG) and polymethyl methacrylate (PMMA), was developed for the preparation of feedstock of titanium for MIM. The processing parameters and the rheological behaviour have been investigated. Feedstocks, containing 69 vol% of powder, can be successfully prepared and extruded with a small plunger-typed injection moulding machine. They exhibited shear thinning behaviour over the range of shear rates tested. The preliminary study showed that the PEG/PMMA binder system can be employed in the preparation of the feedstock for MIM.

Synthesis of Silica Hollow Particles Using Escherichia Coli as Templates: *Toshiyuki Nomura*¹; Yoshio Morimoto¹; Yasuhiro Konishi¹; ¹Osaka Prefecture University

Inorganic hollow particles have attracted great interests in recent years because of their various applications such as catalysis, drug delivery and thermal insulator. Many techniques have been employed to produce hollow particles such as spray drying, emulsion-interfacial polymerization and self-assembly method. In this study, silica hollow particles were prepared using a gram-negative bacterium *Escherichia coli* as a biological template. Silica hollow particles were synthesized by controlling hydrolysis of tetraethyl orthosilicate (TEOS) in the presence of ammonia following the so-called Stöber process. The generated particles were calcined at 873K. The calcined particles were then observed by scanning electron microscopy (SEM). They kept the morphology of biological cells and possessed a hollow structure. The thickness was ca. 50 µm. This result indicates that this bacteria-templating technique using various bacteria enables the synthesis of hollow spheres, rods, wires, and other three dimensional structures with the morphology of bacterium.

Enhancing the Antibacterial Activity of Ceramic Tile by Silver Nanoparticles Intercalated Kaolinite: *Dujreutai Kashima*¹; Natechanok Chitvoranund¹; Chanin Areewattanakul¹; Pornapa Sujaridworakun¹; Sirithan Jiemsirilers¹; ¹Chulalongkorn University

Silver shows melting point at 960°C so it is not capable to appear on the surface of ceramic tile after once firing at 1200°C. To overcome this problem, silver nanoparticles were trapped in the interlamellar space of a layered kaolinite which is one of the raw materials used in ceramic glaze. Disaggregation of the lamellae of kaolinite was achieved by the intercalation of dimethyl sulfoxide (DMSO), then it was suspended in aqueous AgNO₃ solution and finally the adsorbed Ag⁺ ions were reduced by UV irradiation. The obtained 1%Ag nanoparticles in kaolinite were added into ceramic glaze by varying the weight added from 1g to 10 g, then sprayed on the green tile, finally sintered at 1200°C, soaking time 15 min. Color shade and surface of as-sintered specimen was inspected by UV-VIS spectrophotometry and SEM, respectively. The antibacterial activity test was performed in comparison with the standard tile without Ag/kaolinite addition.

Fabrication and Sintering of Silicon Nitride Sheets by Tape Casting with Y2O3-SiO2-MgO Addition: *Thanakorn Wasanapiampong*¹; Yuthana Kaewtabut²; Siripan Nilpairach³; ¹Research Unit of Advanced Ceramics, Department of Materials Science, Faculty of Science, Chulalongkorn University; ²Chulalongkorn University; ³Metallurgy and Materials Science Research Institute, Chulalongkorn University

Tape casting is the most famous method for the manufacturing of ceramic substrate for integrated circuit components. Silicon nitride is a reference material for high strength, high electrical resistivity, and moderate thermal conductivity which meet the requirements of the substrate. In this work, controlling the total binder and plasticizer content on rheological behavior on non-aqueous silicon nitride slip for tape casting was investigated. In order to obtain sinterable compacts at low temperature and pressureless sintering, Y₂O₃, SiO₂ and MgO were used as sintering aid. The effect of the sintering aid on the rheological behavior, the green and sintered cast tape characteristics was also studied.

Physical and Mechanical Properties of Sintered Clay Ceramic-Containing MSW Incineration Bottom Ash: *Supawan Kasuriya*¹; Parjaree Tavorniti¹; Sirithan Jiemsirilers²; ¹National Metal and Materials Technology Center; ²Chulalongkorn University

Incineration is a treatment process for municipal solid waste (MSW) in Thailand and the bottom ash which is a by-product from municipal solid waste incinerator are nowadays landfilled. The feasibility of re-use this ash as a raw material in production of ceramics was studied. Firstly, the chemical composition of the bottom ash was characterized and based on this result; batches containing bottom ash and traditional clay were prepared. The samples were pressed and sintered at a range of temperatures 1000 to 1125°C. The physical and mechanical properties of the resultant materials were studied. Phase formation and microstructure were also examined.

Preparation and Photocatalytic Activity Study of Energy Storage WO3-TiO2 Photocatalyst: *Sitthisunton Supothina*¹; *Ramida Rattanakam*¹; ¹National Metal and Materials Technology Center

Titanium oxide (TiO₂) has been reported as the most active photocatalyst. However, the TiO₂ suffers from a charge recombination. In addition, it cannot be used in dark condition. Modification of TiO₂ by coupling of another oxide that could reduce the charge recombination and to store electrons during illumination has been proposed. These stored electrons could subsequently be released back to the TiO₂ in dark thus continuing photocatalytic activity. Based on this principle, WO₃-TiO₂ is expected to be served to such condition because such back and forth switching of electrons is possible because of the multivalence of tungsten. In this present work, the WO₃-TiO₂ photocatalyst was prepared by high speed ball milling. The obtained WO₃-TiO₂ photocatalyst was characterized by using an XRD, SEM, TEM and a UV-VIS diffused reflection spectrometer. Photocatalytic activity in the dark was also performed in order to study the capability of WO₃-TiO₂ as antibacterial agents.

Processing of Ceramics Poster Session

Mon AM-Wed PM
December 8, 2008

Room: Auditorium B2, Bangkok Convention Centre
Location: Sofitel Centara Grand Bangkok

Dielectric Properties of Glasses: *Jirapan Dutchaneephet*¹; Pisutti Dararutana¹; Narin Sirikulrat¹; ¹Chiang Mai University

Effects of Processing Parameters on Templated Grain Growth Parameters of Bi0.5Na0.5TiO3 with Bi4Ti3O12 Seed Crystals: *Paisan Setasuwon*¹; ¹National Metal and Materials Technology Center

Na_{0.5}Bi_{0.5}TiO₃ (BNT) is one of the potential candidates for non-lead piezoelectric materials to replace existing lead-based ones. Properties of BNT could be enhanced by templated grain growth technique (TGG) through induction of grain orientation with crystal seeds. Crystals with anisotropic shape are able to be arranged with shear forces into orientation. Platelet and needle are typical shapes of seeds. BNT structure is cubic and therefore, its crystals are isotropic. Earlier, two compatible seed materials, Bi₄Ti₃O₁₂ and SrTiO₃, were successfully synthesized as anisotropic seed crystals for BNT. However, results of TGG with Bi₄Ti₃O₁₂ are of mixed successes and failures. Effects of processing parameters were studied to identify the condition for success.

Templated Grain Growth of $\text{Bi}_0.5\text{Na}_0.5\text{TiO}_3$ with Novel Seeds of $\text{Na}_0.5\text{Bi}_4.5\text{Ti}_4\text{O}_{15}$ Crystals: *Paisan Setasuwon*¹; ¹National Metal and Materials Technology Center

$\text{Na}_0.5\text{Bi}_0.5\text{TiO}_3$ (BNT) is one of the potential candidates for non-lead piezoelectric materials to replace existing lead-based ones. Properties of BNT could be enhanced by templated grain growth technique (TGG) through induction of grain orientation with crystal seeds. Crystals with anisotropic shape are able to be arranged with shear forces into orientation. Platelet and needle are typical shapes of seeds. BNT structure is cubic and therefore, its crystals are isotropic. Earlier, two compatible seed materials, $\text{Bi}_4\text{Ti}_3\text{O}_{12}$ and SrTiO_3 , were successfully synthesized as anisotropic seed crystals for BNT. Just recently, $\text{Na}_0.5\text{Bi}_4.5\text{Ti}_4\text{O}_{15}$ (NBT15) crystals were studied as a candidate for alternative seeds for TGG of BNT. Thin platelet-shaped NBT15 crystals were synthesized in molten NaCl. Templated grain growth of BNT with NBT15 seed crystals was studied and electrical properties were characterized.

Two-Stage Sintering of Ferroelectric Ceramics: *Wanwilai Chaisan*¹; ¹Department of Physics, Faculty of Science, Chaing Mai University

The potential of a two-stage sintering technique as a low cost and simple ceramic fabrication was demonstrated in this study. The relationships between conditions of fabricating process, structural characteristic and electrical property of the two selected ferroelectric ceramics, i.e., lead based PZT and non-lead based BT were examined via X-ray diffraction (XRD), scanning electron microscope (SEM) and dielectric measurement, respectively. A sintering time of 2 h at 1000°C followed by a second step in the temperature range of 1000-1400°C for 2 h was employed to the all samples and compared to the one-step sintering process. The results lead to the conclusion that, under suitable two-stage sintering conditions, the dense BT ceramics with fine grain can be successfully achieved with good dielectric properties whereas PZT samples exhibit poor densification with low dielectric properties.

Processing of Electronic Materials and Devices Poster Session

Mon AM-Wed PM
December 8, 2008

Room: Auditorium B2, Bangkok Convention Centre
Location: Sofitel Centara Grand Bangkok

Effect of Fluorine Content and Deposition Temperature on the Optical, Structural and Electrical Properties of Spray Pyrolysis SnO_2 Thin Films: *Chanipat Euvananont*¹; *Thamrong Chansawang*²; *Sirichai Supapon*³; *Chanchana Thanachayanont*¹; ¹National Metal and Materials Technology Center; ²Kasetsart University; ³Mahanakorn University of Technology

FTO or fluorine-doped tin oxide ($\text{SnO}_2:\text{F}$) is widely used as a transparent conducting oxide especially in dye-sensitized solar cell industries. In this investigation, thin films of FTO were prepared on glass substrates using ultrasonic spray pyrolysis technique. Air zero gas was used as a carrier gas. Solution of SnCl_2 in methanol 90% and 10% of DI water were used as precursors. Fluorine doping was achieved by adding NH_4F . The effect of fluorine doping concentration was investigated by varying F:Sn molar ratios of 0:1, 0.5:1 and 1:1, respectively. All of FTO films with the varied molar ratios were deposited at temperatures of 300, 400 and 500°C. The effect of doping concentration and substrate temperature were related to morphologies and micro-structural information characterized using GAXRD, SEM. The 4-point probe measurement and UV-VIS spectrophotometer were used to identify electrical and optical properties of all films, respectively.

Thin Film Coating Processing Poster Session

Mon AM-Wed PM
December 8, 2008

Room: Auditorium B2, Bangkok Convention Centre
Location: Sofitel Centara Grand Bangkok

Carbon Films Deposited on Copper Plate by Ethanol Chemical Vapor Deposition: *Jin Cheng*¹; *Xiaoping Zou*¹; ¹Research Center for Sensor Technology, Beijing Information Technology Institute

In this paper, we present carbon films deposited on copper plate by ethanol chemical vapor deposition. We employed scanning electron microscopy, transmission electron microscopy, and Raman spectroscopy to characterize the deposits. The thick of the film was a few micrometers. According to Raman spectrum, we know the films exhibit low graphitization. According to SEM observation, we find there are many protuberances on the film surface. Due to directly grow on metal substrate and possess protuberances on film surface, it is fit for application as electron source.

Dielectric Reliability of Organic Materials: *Teresa Oh*¹; ¹Cheongju University

Common dielectric layer was widely used with SiO_2 . Spin-on-glass (SOG) and chemical vapor deposition (CVD) O_3 -TEOS processes for SiO_2 have been used in the semiconductor industry. However, general for the application in ultra large scale integration inter-metal dielectric (IMD), the current gate silicon dioxide (SiO_2) film will need to be replaced with a material possessing a low dielectric constant (low-k) material. The dielectric constant and the leakage current of SiOC film was measured according to the various past annealing temperature. The pore structure increased the leakage current because of the charge scattering at the boundary or polarization, in spite of low dielectric constant 1.75 owing to the porosity. Moreover, the leakage current decreased according to the annealing temperature after deposition.

Optical Property of Thermal Barrier Coating at High Temperature: *Geunsik Lim*¹; *Aravinda Kar*¹; ¹University of Central Florida

A radiative component in thermal barrier coatings and other ceramic oxides becomes significant at high temperature. Low radiative absorption and high scattering properties of thermal barrier coating play in reducing the temperature gradient. The dielectric constant, refractive index, and extinction coefficient are determined for improvements in turbine blade performance at high temperature. Optical properties of zirconia containing 7wt% Y_2O_3 will be discussed both for the conductive and the radiative components in the temperature range 1000-1873 K. The effect of various influencing parameters, i.e., radiation-conduction parameter, surface emissivity, single scattering albedo and optical thickness has been illustrated.

Parameter Optimization by Using a Taguchi's Method for Deposition of Water-Repellent Film on Glass Substrate: *Sithisuntorn Supothina*¹; *On-uma Nimittrakoolchai*¹; *Nithi Atthi*²; ¹National Metal and Materials Technology Center; ²National Electronics and Computer Technology Center

A silicone-based water-repellent film having strong adhesion and good optical transparency has been deposited onto glass surface by dip coating method. To find optimum condition for film deposition, parameters including amount of silicone base, oxide particulate, Pt catalyst, semifluorinated silane and curing time as well as type of oxide particulate were varied at 3 levels for each parameter. By using a Taguchi method of experimental design, the experimental condition was reduced from 729 to only 16 runs. The optimum condition (silicone = 0.2 ml, Pt catalyst = 10 ml, SiO_2 nanoparticle = 0.005 g, semifluorinated silane = 1.0 ml and curing time = 120 min) gave a water-repellent film having water contact angle of 160°, film loss of only 0.75 % based on tape test and 84% optical transparency.

Processing Route of Pulsed-Pressure MOCVD in the Deposition of Thin TiO₂ Films on Si Substrates Using TTIP: *Vilailuck Siriwoongrungson¹; Susan Krumdieck¹; Maan Alkaisi¹; ¹University of Canterbury*

The processing parameters for thin TiO₂ deposition on Si substrates using titanium tetra-isopropoxide (TTIP) by pulsed-pressure MOCVD (PP-MOCVD) was investigated. The temperature was varied between 400°C and 600°C under base pressure of 50-200 Pa with relaxation time in the range of 10-20 sec. The surface morphology and thicknesses of the films were examined using a scanning electron microscope (SEM), while energy dispersive x-ray spectroscopy (EDS) was used to qualitatively identify the films composition. The thicknesses of TiO₂ films were in the range of 200-400 nm. The principal composition of the films was TiO₂. The growth rate, morphology, and grain size were examined as functions of processing parameters. The films showed rutile phase and columnar growth with minor effects of pressure and relaxation time. The grain sizes in the range of 50-100 nm were almost the same with the variation of relaxation time but decreased as the base pressure increased.

The Improvement of Water Resistance Property of Paperboard by Low Temperature Plasma: *Suchada Thawornwiriyanan¹; Amporn Sane¹; Pornchai Rachtanapun²; Dheerawan Boonyawan²; Tunyarut Jinkarn¹; ¹Kasetsart University; ²Chiangmai University*

Paper and boards are considered one of the most practical packaging materials. However, one critical drawback of paperboard is its hydrophilic nature. Absorption of moisture reduces physical and mechanical strength of paper and paperboard, causing corruption of packages during storage and distribution. This study aims to improve water resistance property of paperboard by low temperature plasma treatment. In the study, SF₆ is used as a plasma source and treatment conditions are studied to determine optimal setting conditions. At optimal condition, effects of treatment time on water resistance property are investigated. The paperboard selected for this study is an uncoated duplex board with a basis weight of 300 g/m². After SF₆ plasma treatment, contact angle measurement and surface morphology analysis are conducted. According to the result, treated duplex boards show significant improvement on water resistance properties over the control. This is due to the C-F bond generated on the paperboard surface.

Notes

A

Abbas, T	56
Abd Aziz, N	35
Abdul Azis, S	14
Abe, H	29, 61
Abe, K	13
Adachi, K	15
Adeosun, S	20, 22, 59
Ahchawarattaworn, J	41
Ahniyaz, A	29
Aida, T	56
Aikawa, T	45
Akagi, S	19
Akatsuka, M	28
Akedo, J	29
Akkarapattanaoogon, N	50
Alam, M	16
Alkaisi, M	65
Amaranan, S	16
Amin, M	33
Amin, N	33
Amornsakchai, T	54
Andoh, K	27
Andronie, A	12
Angkaew, S	19
Ankem, S	42
Anzai, K	21
Aoki, T	19
Araki, S	23
Arase, T	48
Araujo, E	18
Areerat, S	37
Areewattanakul, C	63
Asao, H	37
Assabumrungrat, S	58, 59
Atong, D	57, 59
Atthi, N	64
Auechalitanukul, C	41
Aummate, C	54
Ausadasuk, S	57
Aussawasathien, D	30
Awakura, Y	13, 27, 42, 48
Awang, R	25

B

Bade, K	23
Balogun, S	20, 22, 59
Bansiddhi, A	43
Barakat, N	30
Bau, N	36
Benke, S	51
Bhandhubanyong, P	12, 18, 53
Binraheem, A	36
Bleck, W	51
Bonifazi, G	39
Boochatham, P	21
Boonme, S	50
Boonpoke, A	13
Boonthongkong, Y	45
Boonyawan, D	65
Boonyongmaneerat, Y	21, 29
Borhani Haghighi, S	46
Borrisuthhekul, R	50
Bowen, P	38
Brody, H	26, 31
Buggakupta, W	35
Bunnaul, P	30

C

Cannon, W	41
Cao, L	39
Chaikittiratana, A	39
Chaisan, W	64
Chaiwong, N	54
Chaiyakot, C	17
Chakrabarti, S	14
Chakthin, S	36
Chalermkarnnon, P	25
Chandra-ambhorn, S	13, 21, 23, 42, 54, 55
Chang, S	37
Chansawang, T	64
Charit, I	28
Charojrochkul, S	25, 51, 58, 59
Chen, F	51
Chen, H	51
Chen, Q	38
Chen, Y	34
Chen, Z	27
Cheng, J	61, 64
Chepushtanova, T	49
Cheruvu, N	13, 36
Chetpattananondh, K	30
Chettapongsaphan, C	50, 58
Chiarakorn, S	13
Chidthaisong, A	13
Chindaudom, P	52
Chino, Y	35
Chitvoranund, N	63
Chmielus, M	21
Cho, H	59
Chonan, T	15
Choypan, W	21
Chuankrerkkul, N	29, 63
Chukrachan, W	54
Chumchery, N	58
Chung, D	54
Chungchoo, C	38
Correa, O	16, 18
Cui, J	17, 26
Cui, Y	36
Cunha, C	16
Cvelbar, U	15

D

Dahle, A	26
Dai, L	15
Damkam, C	53
Dararutana, P	63
Dateraksa, K	29, 43, 58
Dawan, P	60
Deteraksa, K	54
Dheeradhada, V	52
Dittanet, P	15
Dobatkin, S	24
Dodbiba, G	22, 39, 48, 50
Dornthongdee, S	55
Duengkratok, C	23
Dulyapraphant, P	39
Dunand, D	21, 43
Dunne, D	47
Dunne, F	34
Dutchaneephet, J	63
Dzegan, J	24

E

Edwards, P	21
Eiad-ua, A	43
Eiamchai, P	52
Eidhed, W	23
Endo, Y	62
Engstrom, A	38
Esaka, H	26, 31
Esezobor, D	20, 22, 59
Euvananont, C	45, 64
Evans, W	51

F

Fallahian, S	45
Fang, Z	44
Fu, H	17, 31
Fugetsu, B	16
Fuji, M	24, 43
Fujii, T	35
Fujisawa, T	28, 44
Fujita, F	27
Fujita, J	53
Fujita, K	15
Fujita, M	31
Fujita, T	13, 22, 39, 48, 50
Fujiwara, M	25
Fujiwara, T	40
Fukuda, H	16, 30
Fukuda, M	17
Fukushima, H	33
Fukuyama, H	16, 45
Fukuzawa, D	48
Funaoka, M	19
Furukawa, N	13
Fuwa, A	18, 27, 31, 33, 53

G

Galerie, A	13
Galeyev, R	34
Gallage, R	40
Gandy, D	13
Gao, Y	57
Gao, Z	45
Ghazali, C	33
Girish, B	12, 27
Glazunov, A	38
Gollapudi, S	28
Goto, Y	40
Gourlay, C	26
Grigoryev, E	25
Guan, P	52
Guo, X	52
Gupta, A	47
Gupta, M	12, 16, 17, 31, 36
Gupta, S	21

H

Hagisawa, K	29
Haiki, K	33
Hakamada, M	47
Hanada, Y	51
Haruyama, W	28
Haseeb, A	23
Hashemi, S	35
Hata, H	33
Hattori, Y	39, 44

Hayashi, S.....	37
Hayashibe, Y.....	33
Heilig, M.....	20
Henein, H.....	20, 48
Hideyuki, M.....	14
Higashino, K.....	48
Hing, P.....	41
Hino, J.....	19
Hiraga, K.....	41, 45
Hirai, A.....	28
Hirai, S.....	42, 56, 61
Hiramoto, T.....	18
Hirano, M.....	37
Hirato, T.....	15, 33, 34
Hiroyoshi, N.....	28
Holehonnur, S.....	27
Hori, K.....	28
Horpratun, M.....	52
Hoshi, M.....	48
Hoshino, T.....	40
Hu, X.....	36
Hua Chun, Z.....	60
Huang, D.....	16
Huang, T.....	17
Huang, W.....	53
Huang, X.....	17
Huang, Y.....	29
Hurduc, N.....	12
Hwang, K.....	44

I

Ibrahim, R.....	25
Ichii, T.....	46
Ichino, R.....	46, 52
Iida, O.....	37
Imai, A.....	49
Imai, H.....	16, 30
Imai, M.....	43
Imashuku, S.....	13
Imasyuku, S.....	42
Inoguchi, N.....	54
Inoue, A.....	53
Inoue, K.....	19
Inoue, M.....	56
Inprasit, T.....	42
Intarasakda, S.....	42
Irinah, N.....	62
Ishibashi, N.....	32
Ishida, T.....	18
Ismail, M.....	63
Itagaki, K.....	14
Itamura, M.....	21
Ito, A.....	46
Ito, M.....	28
Itou, H.....	51
Izaki, H.....	30
Izumi, K.....	32

J

Jang, J.....	44, 62
Jaritgnam, S.....	28
Jarukumjorn, K.....	55
Jauhari, I.....	14, 35
Jayaram, K.....	36
Jeencham, R.....	55
Jeong, H.....	57
Jha, A.....	37, 50

Jianzhong, C.....	22
Jiemsirilers, S.....	59, 63
Jinawath, S.....	15, 61
Jinkarn, T.....	65
Jiratthanakul, N.....	60
Jiratticharoean, W.....	25
Jiratumnukul, N.....	58
Jittaseno, N.....	49
Jo, H.....	59
Joo, H.....	32
Joshi, S.....	36
Jun, T.....	52
Jung, J.....	32
Junin, C.....	25

K

Kaewtabut, Y.....	63
Kaewthip, P.....	45
Kajikawa, K.....	34
Kakihana, M.....	18, 30, 32
Kakimoto, S.....	33
Kamada, K.....	44
Kamegai, T.....	35
Kanetake, N.....	12, 34, 54
Kangtrakul, P.....	58
Kanie, K.....	58, 60, 61, 62
Kanlayasiri, K.....	14, 30
Kano, J.....	37
Kano, Y.....	33
Kaowphong, S.....	30
Kar, A.....	64
Karabasappa, B.....	27
Kasemsuwan, K.....	13
Kashima, D.....	59, 63
Kaspin, S.....	48
Kasuriya, S.....	59, 63
Kawamura, T.....	43
Kawasaki, M.....	48
Kawasaki, T.....	56
Keawkumay, C.....	55
Keul, C.....	51
Khaleghi, E.....	28
Khan, K.....	14
Khomnotai, C.....	17
Khongwong, W.....	43
Khumsuk, P.....	46
Khunathai, K.....	19
Kijboon, W.....	25
Kikuchi, M.....	21
Kikuchi, S.....	27
Kikuchi, T.....	33
Kim, B.....	41, 45
Kim, H.....	30, 58
Kim, I.....	44, 62
Kim, S.....	15
Kim, W.....	58
Kim, Y.....	57, 59
Kimura, H.....	43, 53
Kimura, Y.....	37
Kinjyo, M.....	33
Kitamura, T.....	46
Kitinawarat, S.....	58
Kitiwan, M.....	59
Kitkaew, D.....	60
Kitkamthorn, U.....	50
Ko, S.....	44, 62
Kobashi, M.....	34, 54
Kobatake, H.....	45

Kobayashi, K.....	40
Kobayashi, M.....	18
Koesuko, K.....	17
Kojima, R.....	29
Komoda, M.....	33
Komoda, Y.....	17
Kon, T.....	19
Kondo, A.....	29, 61
Kondoh, K.....	16, 30, 53
Konishi, Y.....	15, 24, 63
Koolprechanan, N.....	58
Korad, T.....	58
Korsunsky, A.....	52
Koshy, P.....	21
Kovarik, T.....	24
Koyama, K.....	18, 23, 24, 28, 29, 30, 33, 34, 39, 44, 45, 52
Kraus, L.....	49
Kritboonyarit, P.....	39
Kruenate, J.....	54
Krumdieck, S.....	65
Kuboyama, H.....	33
Kuma, J.....	31
Kume, Y.....	34
Kumnuantip, C.....	55
Kunioshi, C.....	18
Kunishige, S.....	34
Kupparavalli, P.....	12
Kuroda, K.....	52
Kurokawa, K.....	49
Kusuda, H.....	34
Kuwayama, Y.....	28
Kuzuya, T.....	56, 61
Kwon, D.....	57

L

Lahiri, A.....	37
Laksanacharoen, S.....	22
Laosiripojana, N.....	13, 58, 59
Larpiattaworn, S.....	44
Laukli, H.....	26
Lavernia, E.....	38
Lawsuriyonta, M.....	12
Lee, B.....	59
Lee, H.....	21, 57
Lee, J.....	62
Lee, K.....	32
Lee, P.....	55
Lee, S.....	21, 57
Lee, W.....	44, 54, 62
Leesooksunt, K.....	59
Lertloykulchai, B.....	48
Li, J.....	15
Li, L.....	44
Liang, Y.....	22
Lim, G.....	64
Lima, N.....	16
Limpitpanich, P.....	27
Limthongkul, P.....	25, 42
Lin, L.....	57
Lin, Y.....	49
Liu, C.....	40
Liu, F.....	51
Liu, L.....	17, 31
Liu, Y.....	45
Lraorprasertsuk, K.....	23
Lu, X.....	38
Luengthongkum, N.....	55

Luganov, V..... 49
Lumkum, N..... 55

M

Mabuchi, M..... 34, 35
Maeda, T..... 21
Mallick, A..... 44
Manonukul, A..... 16, 24, 25
Martinelli, J..... 16
Maruoka, S..... 39
Maruyama, T..... 18
Marya, M..... 20
Matsubara, M..... 61
Matsuda, M..... 50
Matsufumi, T..... 32
Matsuo, A..... 40
Matsuo, S..... 40
Matsushita, N..... 40
Matsuura, D..... 19
Matsuura, H..... 36
Matsuura, K..... 32, 47, 49
Matsuzaki, K..... 34
Mazumdar, D..... 14
Menbangpong, L..... 30
Mishima, K..... 27
Mishra, B..... 20, 22, 42, 47, 49, 53
Mitarai, Y..... 14
Miura, H..... 39
Miyachi, A..... 42
Miyachi, Y..... 26
Mizuta, Y..... 33, 34
Montenegro, V..... 28
Morimoto, Y..... 63
Morino, K..... 43
Morita, K..... 41, 45
Mozetic, M..... 15
Muangjunburee, P..... 36
Muenya, N..... 24
Muhamad, S..... 25
Mujumdar, A..... 14, 19
Müllner, P..... 21
Muramatsu, A..... 50, 58, 60, 61, 62
Murase, K..... 46
Murayama, N..... 14
Murty, K..... 28

N

Nagamine, S..... 40
Naganuma, T..... 48
Nagaumi, H..... 17, 26, 31
Nagira, T..... 31, 41
Nai, M..... 12, 16, 31
Nai, S..... 17
Naito, M..... 29, 61
Naixiang, F..... 22
Nakae, H..... 26
Nakajima, H..... 12
Nakamura, H..... 61
Nakamura, K..... 16
Nakamura, T..... 15, 56
Nakano, H..... 33, 34
Nakano, Y..... 59
Nakashima, K..... 30
Nakatsuka, N..... 31
Nakayama, H..... 25
Nakayama, T..... 13
Nakazawa, H..... 28

Nakmoto, Y..... 34
Naoki, H..... 32
Narisako, M..... 19
Narita, H..... 29
Narita, M..... 18
Nawathe, S..... 16
Nemecek, S..... 49
Ngampungpis, K..... 46
Ngernbamrung, S..... 29
Nihei, T..... 28
Nilpairach, S..... 63
Nilsonthi, T..... 13
Nimittrakoolchai, O..... 64
Niranatlumpong, P..... 38
Niranjana Rao, K..... 12
Nishihama, S..... 19, 32, 56, 57
Nishimura, T..... 20
Nishizaki, Y..... 46
Nithi-Uthai, N..... 22
Niyama, E..... 21
Niyomwas, S..... 47
Nomura, T..... 24, 63
Nooklay, B..... 30
Nor, I..... 12
Northwood, D..... 50
Nose, K..... 40
Nose, Y..... 13, 42, 48
Nozawa, T..... 28
Nualpaeng, W..... 59
Nukaya, T..... 50
Nunwong, P..... 38

O

Oberson, P..... 42
Ochulor, F..... 22
Ogasawara, D..... 23
Ogawa, A..... 28
Ogawa, N..... 44
Ogi, T..... 24
Ogibayashi, S..... 31
Oh, T..... 64
Ohara, S..... 61
Oharu, K..... 48
Ohashi, N..... 40
Ohki, K..... 56
Ohnaka, I..... 31
Ohsasa, K..... 17, 32, 47, 49
Ohshima, M..... 40
Ohta, M..... 42, 56, 61
Ohtsu, H..... 33
Oi, T..... 22
Oida, M..... 18
Okabe, T..... 21, 22, 42, 48
Okada, M..... 14, 44
Okane, T..... 35
Okano, S..... 13
Okido, M..... 46, 52
Okumura, Y..... 42
Okura, T..... 14
Oladoye, A..... 22
Olevsky, E..... 28, 39
Olson, D..... 20, 35, 42
Omar, M..... 56
Omata, T..... 40
Omran, A..... 30
Ono, T..... 17
Oohashi, H..... 40
Oonishi, K..... 56

Oros, C..... 52
Oshita, H..... 39
Otaka, S..... 31
Otarawanna, S..... 26
Otsuka, I..... 30
Otsuka-Yao-Matsuo, S..... 40
Ouampan, S..... 46
Oue, S..... 33

P

Padijal, A..... 16
Pakdeesathaporn, S..... 45
Pandit, K..... 26
Pang, J..... 32
Pang, M..... 24
Panpa, W..... 15
Panyakaew, S..... 12
Panyathanmaporn, T..... 54
Parajuli, D..... 19
Park, H..... 37, 39
Park, Y..... 32
Patcharaphun, S..... 54
Pavarajarn, V..... 13
Peng, H..... 34
Petrova, R..... 20
Petrykin, V..... 18, 30, 32
Phalakornkule, C..... 39
Phatanasettakul, V..... 52
Phiriyawirut, M..... 48
Phongsophtanan, U..... 58
Pillis, M..... 18, 19
Piyamanocha, P..... 37
Pongkao, D..... 29
Pongsaksawad, W..... 46
Poolthong, N..... 22, 25, 36
Popa, S..... 12
Powell, A..... 39, 51
Prahl, U..... 51
Praharn, C..... 58
Pratoomwan, P..... 45
Preechapongkit, W..... 53
Prombut, P..... 47
Pumwongpitak, P..... 44

R

Rachtanapun, P..... 65
Rakmae, S..... 55
Ramanathan, L..... 16, 18, 19
Rao, G..... 13
Ratanabunlang, R..... 53
Rattanakam, R..... 63
Rattanakornkan, K..... 51
Rattanawaleedirojn, P..... 54
Reddy, R..... 29, 43, 47
Ruksakulpiwat, Y..... 55
Rungseesantivanon, W..... 22
Ryoshi, K..... 39
Ryu, T..... 44

S

Sadaki, J..... 22
Saengkiattiyut, K..... 54
Safi, S..... 45
Safullin, R..... 34
Sahajwalla, V..... 21
Sahasithiwat, S..... 19, 30
Saiki, Y..... 29

Saito, F	50	Soma, Y	40	Termsuksawad, P	49
Saito, N	47	Son, S	54, 57, 62	Tewari, S	25, 26
Saitoh, N	24	Songsiri, K	25	Thanachayanont, C	13, 25, 45, 64
Sakai, T	39, 48	Sonohara, E	19	Thavarungkul, N	22, 36
Sakairi, M	33	Sonsiri, C	60	Thawornwiriyanan, S	65
Sakamoto, D	14	Sooksomsong, T	54	Thiemsorn, W	45
Sakamoto, N	23	Soparat, L	59	Thirathipviwat, P	17
Sakata, M	33	Sricharoenchaikul, V	57	Thomson, R	14
Sakuna, P	55	Sridhar, B	36, 49	Thongruang, W	30
Salah, S	56	Srimuang, K	25	Thongtem, S	30
Salishchev, G	40	Srisawat, N	49, 58	Thongwichean, T	39
Salman, S	46	Sritharan, T	46	Thueploy, A	54
Sandu, E	12	Stamatin, I	12	Thumsorn, S	49
Sandu, V	12	Strandlund, H	38	Tian, X	52
Sane, A	65	Stratton, P	20, 42	Tikasakul, P	28
Sangchay, W	29	Suchiva, K	18	Toda, K	48
Sano, H	28, 52	Suehiro, K	42	Todd, I	63
Sansernnivet, M	25	Sugimura, H	46, 57	Tofuku, A	15
Sasaki, H	56	Sugiyama, A	31	Tomita, K	18
Satish, B	12, 27	Sugiyama, S	18	Tongsri, R	22, 25, 36
Sato, D	22	Sujaridworakun, P	29, 59, 63	Tonnayopas, D	28
Sato, F	37	Sujirote, K	29, 43, 54, 58	Towprayoon, S	13
Sato, H	56	Suksangpanomrung, A	51	Tsukihashi, F	36
Sato, K	61, 62	Sumida, I	18	Tsunekawa, M	28
Sato, N	28, 50, 60	Supapon, S	64	Tuantranont, A	52
Sato, S	28, 35	Supcharoen, D	19	Tuchinda, K	53, 60
Satter, M	23	Supothina, S	63, 64		
Schoenung, J	27, 38	Suppakam, N	55	U	
Sekiguchi, J	58	Supradist, M	17, 35	Ubonchonlakat, K	24
Sekimoto, H	48	Sutapan, W	55	Uchiyama, Y	46, 52
Sergiienko, R	15	Suwanpinij, P	51	Uda, S	17
Serikawa, T	53	Suwattananont, N	20	Uda, T	13, 42, 48
Serranti, S	39	Suzuka, Y	56	Udomphol, T	38
Setasuwon, P	63, 64	Suzuki, M	36	Ueda, S	40
Shagiev, M	34, 40	Suzuki, R	19, 20	Uesugi, K	31
Sharabiani, Y	53	Suzuki, S	12, 31	Umeda, T	17, 35
Shearwood, C	32, 53	Suzuki, T	36	Umetani, K	31
Sheikh, H	35, 51	Suzuki, Y	49	Usami, N	48
Shibata, J	14, 33			Utara, S	21
Shima, M	56	T		Utsunomiya, S	49
Shimanaka, S	24	Tachimi, T	24		
Shimizu, T	34	Taguchi, Y	57	V	
Shimizu, Y	35	Tahara, S	34	Valiakhmetov, O	34
Shimoda, H	61	Takada, K	45	Vedantam, S	44
Shimokawa, K	18	Takagi, M	18	Veerachinnapong, M	60
Shin, S	44	Takahashi, M	24, 43	Viehland, D	15
Shinohe, T	28	Takahashi, N	36	Viriyarattanasak, P	21
Shirayama, S	48	Takasu, T	38, 51	Viyani, E	46
Shivakumar, B	27	Takatori, K	56	Vizhian, S	36
Shokrvash, H	62	Takeda, T	27	Voisin, L	14
Shpigunova, O	38	Takeharu, K	41		
Shunichiro, K	32	Takenaka, K	34	W	
Sidambe, A	63	Takeyasu, H	48	Wachirasiri, W	54
Siddesh, H	27	Tamagawa, H	36	Wagata, H	40
Siddiqui, M	57	Tan, M	32, 53	Wananuraksawong, W	59
Sikong, L	24, 29	Tanahashi, M	44	Wang, C	31, 36
Singh, R	14, 37	Tanaka, F	35, 37	Wang, D	59
Singto, S	60	Tanaka, M	29	Wang, H	50
Sirikulrat, N	63	Tanaka, Y	40	Wang, L	22
Sirinukulwattana, K	19	Tane, M	12	Wang, Y	61
Sirivedin, S	38, 60	Tanespolake, W	21	Wangyao, P	49
Siriwongrungsom, V	65	Taniguchi, K	40	Wasanapiampong, T	63
Sithilor, W	35	Taniguchi, Y	57	Watanabe, H	24, 43
Smith, G	22	Tanimura, Y	50	Watanabe, K	49
Smithmaitrie, P	30	Tanno, H	22	Watanabe, M	37
Smugersky, J	38, 44	Tavormiti, P	63	Watanabe, T	23, 29, 40
Soda, R	37	Tawkaew, S	20	Watanabe, Y	44
Sohn, H	44	Taya, M	36		
Solihin	50				

Wei, R	13	Zheng, G	52
West, G	14	Zhong, J.....	49
Wichianrak, R.....	22	Zhong, X.....	17
Wichianrat, P.....	58	Zhonghua, W.....	14, 19
Wiraseranee, C.....	49	Zhou, J	16
Wisitsoraat, A.....	52	Zhu, G	29, 61, 62
Witchanantakul, T.....	50	Zou, X	60, 61, 64
Wittayapairot, N.....	53	Zrnik, J	24, 49
Wiwattanadate, D.....	49	Zuo, Y	26
Wolfe, T.....	20	Zuyao (T.Y.), X.....	50
Wong, E.....	16		
Wongkasemjit, S	42		
Wong On, J.....	49		
Wongpinkaew, K.....	46		
Wongsorat, W.....	55		
Wora-uaychai, N.....	25		
Wu, X	26		

X

Xiaodong, W.....	50
Xiong, Y.....	38
Xu, R	45
Xu, W	63

Y

Yakuwa, S	59
Yamabe, H.....	34
Yamaguchi, A.....	14, 57
Yamaguchi, K.....	19, 35
Yamakawa, T.....	43
Yamamoto, Y.....	31
Yamashita, S.....	33
Yamashita, Y.....	40
Yamauchi, A.....	49
Yang, Y	15
Yanli, J	22
Yano, T	43
Yao, K	24
Yasuda, H.....	31, 41
Yasuda, Y	48
Yazdanfar, H.....	21
Yeomans, J.....	35
Yoichi, Y.....	33
Yokoyama, T.....	49
Yoneda, J.....	19
Yonezu, K.....	49
Yonghua, R.....	50
Yoon, D.....	57
Yoshida, H.....	41, 45
Yoshida, K.....	43
Yoshikawa, H.....	40
Yoshimura, M.....	23, 29, 40
Yoshinaga, M.....	50, 60
Yoshiya, M.....	31, 41
Yoshizuka, K.....	19, 32, 56, 57
Yuasa, M	34
Yukihiro, S	32
Yuse, F	13
Yu Xin, Z.....	60

Z

Zen, H	18
Zeng, H	24, 59, 61
Zhang, D	32
Zhang, H	17, 26, 60
Zhang, J.....	17, 31
Zhang, Q	50

PMP III

Conference Proceedings

The complete PMP-III proceedings has been produced in CD-ROM format. Each attendee paying the full conference registration fee receives one free CD-ROM. Students and others may purchase the CD-ROM at the conference registration desk.



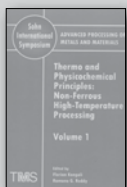
**TMS KNOWLEDGE
RESOURCE CENTER**

Purchase these related titles from the TMS Knowledge

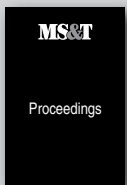
Resource Center:



TMS 2008 Annual Meeting Supplemental Proceedings,
Volume 1: Materials Processing and Properties



Advanced Processing of Metals and Materials (9-volume set)



Proceedings from the Materials Science & Technology Conference (MS&T)

For additional details and to purchase these publications, visit the
Knowledge Resource Center online at <http://knowledge.tms.org>.

	Mon AM	Mon PM	Tues AM	Tues PM	Wed AM	Wed PM
Auditorium B2, BCC	Opening Ceremony and Monday Plenary Lecture Poster Session	Monday Keynote Lecture Poster Session	Tuesday Plenary Lecture Poster Session	Tuesday Keynote Lecture Poster Session	Wednesday Plenary Lecture Poster Session	Wednesday Keynote Lecture Poster Session Closing Ceremony
Plaza 1	Energy Materials Processing I	Aqueous/ Electrochemical Processing I	Energy Materials Processing II	Aqueous/ Electrochemical Processing II	Energy Materials Processing III	Materials Processing IX
Plaza 2	Solidification Processing I	Solidification Processing II	Solidification Processing III	Processing of Ceramics I	Processing of Ceramics II	
Plaza 3	Materials Processing I	Materials Processing II	Processing of Electronic Materials and Devices: Processing of Electronic Materials and Devices II	Materials Processing V	Materials Processing VIII	Materials Processing X
Plaza 4	Processing of Electronic Materials and Devices: Processing of Electronic Materials and Devices I	Materials Processing III	Thin Film Coating Processing I	Materials Processing VI	Thin Film Coating Processing II	Thin Film Coating Processing III
Plaza 5	Composites Processing I	Materials Processing IV	Composites Processing II	Composites Processing III	Processing of Electronic Materials and Devices: Processing of Electronic Materials and Devices III	Composites Processing IV
Plaza 6	Environmental Protection Processing I	Environmental Protection Processing II	Environmental Protection Processing III	Materials Processing VII		
Plaza 7	Nanomaterials Processing I	Nanomaterials Processing II	Nanomaterials Processing III	Nanomaterials Processing IV	Nanomaterials Processing V	Materials Processing XI
Plaza 8	Powder Preparation/ Processing I	Powder Preparation/ Processing II	Powder Preparation/ Processing III	Modeling Material Processing I	Powder Preparation/ Processing IV	Modeling Material Processing II